USC
UNIVERSIDADE DE SANTIAGO DE COMPOSTELA

ESCUELA DE DOCTORADO INTERNACIONAL EN CIENCIAS DE LA SALUD DE LA USC

Jesús
Álvarez Trabado

*Tesis doctoral*

# *Sorbitan ester nanoparticles as a novel tool for the treatment of ocular surface diseases*

Santiago de Compostela, 2018

PD en Investigación y Desarrollo de Medicamentos

USC
UNIVERSIDADE
DE SANTIAGO
DE COMPOSTELA

CENTRO INTERNACIONAL DE ESTUDOS
DE DOUTORAMENTO E AVANZADOS
DA USC (CIEDUS)

TESE DE DOUTORAMENTO

# SORBITAN ESTER NANOPARTICLES AS A NOVEL TOOL FOR THE TREATMENT OF OCULAR SURFACE DISEASES

Jesús Álvarez Trabado

**ESCOLA DE DOUTORAMENTO INTERNACIONAL**

**PROGRAMA DE DOUTORAMENTO EN INVESTIGACIÓN E DESENVOLVEMENTO DE MEDICAMENTOS**

SANTIAGO DE COMPOSTELA

2018

USC
UNIVERSIDADE
DE SANTIAGO
DE COMPOSTELA

CENTRO INTERNACIONAL DE ESTUDOS DE DOUTORAMENTO E AVANZADOS DA USC (CIEDUS)

# DECLARACIÓN DO AUTOR DA TESE

## SORBITAN ESTER NANOPARTICLES AS A NOVEL TOOL FOR THE TREATMENT OF OCULAR SURFACE DISEASES

D. Jesús Álvarez Trabado

Presento a miña tese, seguindo o procedemento axeitado ao Regulamento, e declaro que:

1) A tese abarca os resultados da elaboración do meu traballo.
2) De selo caso, na tese faise referencia ás colaboracións que tivo este traballo.
3) A tese é a versión definitiva presentada para a súa defensa e coincide coa versión enviada en formato electrónico.
4) Confirmo que a tese non incorre en ningún tipo de plaxio doutros autores nin de traballos presentados por min para a obtención doutros títulos.

*En Santiago de Compostela, 18 de setembro de 2018*

Asdo. Jesús Álvarez Trabado

USC
UNIVERSIDADE
DE SANTIAGO
DE COMPOSTELA

CENTRO INTERNACIONAL DE ESTUDOS DE DOUTORAMENTO E AVANZADOS DA USC (CIEDUS)

# AUTORIZACIÓN DOS DIRECTORES DA TESE

## SORBITAN ESTER NANOPARTICLES AS A NOVEL TOOL FOR THE TREATMENT OF OCULAR SURFACE DISEASES

D. Alejandro Sánchez Barreiro
Dna. Yolanda Diebold Luque

INFORMAN:

*Que a presente tese, correspóndese co traballo realizado por D.* ***Jesús Álvarez Trabado****, baixo a miña dirección, e autorizo a súa presentación, considerando que reúne os requisitos esixidos no Regulamento de Estudos de Doutoramento da USC, e que como director desta non incorre nas causas de abstención establecidas na Lei 40/2015.*

*En Santiago de Compostela, 18 de setembro de 2018.*

Asdo. Alejandro Sánchez

Asdo. Yolanda Diebold

USC
UNIVERSIDADE
DE SANTIAGO
DE COMPOSTELA

# DECLARACIÓN DE AUSENCIA DE CONFLITO DE INTERESES

*De acordo coas directrices da Escola de Doutoramento Internacional (EDI) en Ciencias da Saúde da Universidade de Santiago de Compostela (USC) (acordo de 3 de maio de 2018), o doutorando Jesús Álvarez Trabado declara non ter ningún posible conflito de intereses en relación coa presente tese doutoral.*

*En Santiago de Compostela, a 18 de setembro de 2018*

Asdo. Jesús Álvarez Trabado

USC
UNIVERSIDADE
DE SANTIAGO
DE COMPOSTELA

*En memoria de Begoña Seijo*

USC
UNIVERSIDADE
DE SANTIAGO
DE COMPOSTELA

## Acknowledgments / Agradecimientos

Este trabajo no habría sido posible sin todo el apoyo recibido por parte de las personas que han formado parte de mi vida a lo largo de estos últimos cuatro años, y a las que brevemente me gustaría agradecer su contribución.

Sin duda el agradecimiento más emotivo se lo dedico a Begoña Seijo, no solo por haber sido desde el principio mi guía en el mundo de la investigación, sino por todos los consejos recibidos y por los valores éticos y profesionales aportados a lo largo de estos años.

Agradecer a mis directores de tesis, Alejandro Sánchez y Yolanda Diebold, la confianza depositada así como todos los valiosos consejos recibidos que sin duda me han ayudado al crecimiento personal y profesional, y que en definitiva han hecho posible esta tesis.

Agradecer a mis compañeros del Instituto de Oftamobiología Aplicada (IOBA) la cálida acogida desde el primer momento. A los integrantes del Grupo de Superficie Ocular, en especial Laura, Antonio y Mario, agradecerles su dedicación y ayuda prestada así como todas las vivencias y buenos momentos que pasamos juntos.

Agradecer a mis compañeros de laboratorio de Santiago, especialmente a Inés, Rafa, Andrea, Fany, Cristina y Rita los buenos ratos compartidos. A todos mis compañeros de departamento y doctorado, en especial a Antón, Jorge, Helena, Víctor y Lorena su apoyo y amistad.

Agradecer a todos los profesores del Departamento de Farmacología, Farmacia y Tecnología Farmacéutica, en especial a Francisco Otero y Carmen Álvarez su dedicación y valiosos consejos que sin duda fueron claves en este trabajo.

*I would like to thank Proffessor Sharmila Masli for giving me the opportunity to work as a part of her resarch group at the Boston University. I would also to thank Dr. Tatfong Ng for his warm welcome and the scientific support provided during my stay.*

Finalmente, quiero dedicar este trabajo a mi familia, especialmente a mis padres por la comprensión, el afecto y el apoyo recibido durante estos años, y a Natalia por haber sido mi pilar fundamental y por haberme soportado en los momentos más complicados.

USC
UNIVERSIDADE
DE SANTIAGO
DE COMPOSTELA

## Table of contents / Índice

USC
UNIVERSIDADE
DE SANTIAGO
DE COMPOSTELA

## List of abbreviations / Listado de abreviaturas

| | | |
|---|---|---|
| **ACN** | Acetonitrile | Acetonitrilo |
| **ANOVA** | Analysis of variance | Análisis de varianza |
| **BCA** | Bicinchoninic acid | Ácido bicinconínico |
| **BZK** | Benzalkonium chloride | Cloruro de benzalconio |
| **CFS** | Corneal fluorescein score | Puntuación de la tinción con fluoresceína |
| **CN** | Corneal neovascularization | Neovascularización corneal |
| **CsA** | Cyclosporine A | Ciclosporina A |
| **CTAB** | Cetyltrimethylammonium bromide | Bromuro de cetiltrimetilamonio |
| **DED** | Dry eye disease | Enfermedad de ojo seco |
| **DL** | Drug loading | Capacidad de carga |
| **DLS** | Dynamic light scattering | Espectroscopía de correlación fotónica |
| **DMEM** | Dulbecco´s Modified Eagle Medium | Medio de cultivo Eagle modificado de Dulbecco |
| **DMSO** | Dimethylsulfoxide | Dimetilsulfóxido |
| **DPBS** | Dulbecco's phosphate buffered saline | Tampón fosfato salino de Dulbecco |
| **DSC** | Differential scanning calorimetry | Calorimetría diferencial de barrido |
| **EE** | Entrapment efficiency | Eficiencia de encapsulación |
| **EPCs** | Conjuntival epithelial primary cultures | Cultivos primarios de conjunctiva humana |
| **FBS** | Fetal bovine serum | Suero fetal bovino |
| **H&E** | Hematoxilin and eosin | Hematoxilina y eosina |
| **HA** | Hyaluronic acid | Ácido hialurónico |
| **HCE** | Human corneal epithelial cell line | Línea celular de epitelio corneal humano |
| **HPLC** | High performance liquid chromatography | Cromatografía líquida de alta resolución |
| **IL** | Interleukin | Interleuquina |
| **IOBA-NHC** | Normal human conjunctiva cell line | Línea cellular de epitelio de conjuntiva humana normal |
| **LDA** | Laser doppler anemometry | Anemometría de dispersion láser |
| **MGD** | Meibomian gland dysfunction | Disfunción de las glándulas de Meibomio |

| | | |
|---|---|---|
| **MMPs** | Matrix metalloproteinases | Metaloproteinasas de matriz |
| **NMR** | Nuclear magnetic resonance | Resonancia magnética nuclear |
| **NPs** | Nanoparticles | Nanopartículas |
| **ODD** | Ocular drug delivery | Administración ocular de fármacos |
| **OPT** | Optimized | Optimizado |
| **OS** | Ocular surface | Superficie ocular |
| **PAS/AA** | Periodic acid-Schiff/Alcian blue | Ácido periódico de Schiff/azul alcián |
| **PBMC** | Peripheral blood mononuclear cells | Células sanguíneas mononucleares periféricas |
| **PdI** | Polidispersity index | Índice de polidispersión |
| **PEG** | Polyethylenglycol | Polietilénglicol |
| **Rapa** | Rapamycin | Rapamicina |
| **RT** | Room temperature | Temperatura ambiente |
| **RT-PCR** | Reverse transcription polymerase chain reaction | Reacción en cadena de la polimerasa con retrotranscripción |
| **SD** | Standard deviation | Desviación estándar |
| **SENS** | Sorbitan ester nanoparticles | Nanopartículas de éster de sorbitan |
| **SLF** | Simulated lachrymal fluid | Fluido lagrimal simulado |
| **Span® 80** | Sorbitan monooleate | Monooleato de sorbitán |
| **TEM** | Transmission electron microscopy | Microscopía electrónica de transmission |
| **TGF** | Transforming growth factor | Factor de crecimiento transformante |
| **TNF-α** | Tumoral necrosis factor alpha | Factor de necrosis tumoral alfa |
| **TPGS** | D-alpha-tocopheryl-polyethylene glycol 1000 succinate | D-alfa-tocoferol-polietilenglicol 1000 succinato |
| **TSP-1** | Thrombospondin-1 | Trombospondina-1 |
| **UPW** | Ultrapure water | Agua ultrapura |
| **VEGF** | Vascular endothelial growth factor | Factor de crecimiento del endotelio vascular |
| **XRD** | X-Ray powder diffraction | Difracción de rayos X de polvo |
| **XTT** | 2,3-bis(2-methoxy-4-nitro-5-sulfophenyl)-2H-tetrazolium-5-carboxanilide | 2,3-bis(2-metoxi-4-nitro-5-sulfonil)-2H-tetrazolio-5-carboxianilida |

# *Abstract/Resumen*

USC
UNIVERSIDADE
DE SANTIAGO
DE COMPOSTELA

**Abstract**

The main objective of this Doctoral Thesis work was the design and development of a new nanoparticle-based therapeutic strategy for the topical treatment of diseases affecting ocular surface, including dry eye disease and corneal neovascularization.

For this purpose, we modified our previously patented sorbitan ester nanoparticles (SENS) to obtain two types of nanosystems capable to target ocular surface structures: a cationic nanoparticle variety and its hyaluronic acid (HA)-coated version. The first step was to obtain optimized nanoparticle formulations using cyclosporine A as drug model. Both types of nanoparticles (NPs) showed adequate physicochemical properties for topical administration, adequate physical and biological stability and adequate *in vitro* biocompatibility. Nonetheless, the HA-coated NPs exhibited higher targeting potential than that of the uncoated NPs, which is related to the enhanced cellular uptake by corneal cells through specific receptor-mediated endocytosis. Both types of cyclosporine-loaded NPs showed same immunosuppressant effect in *ex vivo* stimulated human lymphocytes than the commercial formulation, confirming that the drug maintained its biological activity after entrapment inside NPs. Next step was to assess their *in vivo* therapeutic efficacy using an experimental dry eye mouse model. *In vivo* studies showed that HA-coated cyclosporine-loaded NPs presented higher therapeutic efficacy than the uncoated NPs reversing main dry eye-associated signs. In addition, the HA-coated blank NPs might have some therapeutic effect probably because to the additional benefits provided by HA. Finally, we developed and preliminarily characterized rapamycin-loaded NPs for the topical treatment of corneal neovascularization. Both types of NPs showed adequate physicochemical properties for topical ophthalmic administration and adequate *in vitro* biocompatibility. Both types of rapamycin-loaded NPs showed same *in vitro* antiangiogenic efficacy than the drug solution, confirming maintenance of biological activity after drug entrapment.

Overall, our results confirm the suitability and clinical potential of SENS as drug delivery systems for the topical treatment of ocular surface pathologies. Particularly, the beneficial effects of HA-coating on the physicochemical and biopharmaceutical properties, and therapeutic efficacy of NPs were elucidated.

**Resumen**

El objetivo principal de esta Tesis Doctoral ha sido el diseño y desarrollo de una nueva estrategia terapéutica basada en nanopartículas para el tratamiento tópico de enfermedades que afectan la superficie ocular, incluidas el ojo seco y la neovascularización corneal.

Con este propósito, modificamos nuestras previamente patentadas nanopartículas de ésteres de sorbitán (SENS) para obtener nanosistemas capaces de dirigirse específicamente a las estructuras de la superficie ocular. Se desarrollaron dos formulaciones optimizadas para administración tópica ocular usando ciclosporina A (CsA) como fármaco modelo: una variedad de nanopartículas catiónicas y su versión recubierta con ácido hialurónico (HA). Ambos tipos de nanopartículas (NPs) mostraron propiedades fisicoquímicas adecuadas para la administración tópica, buena estabilidad física y biológica y adecuada biocompatibilidad *in vitro*. Las NPs recubiertas con HA exhibieron una capacidad de direccionamiento mayor que las NPs no recubiertas. Ambos tipos de NPs cargadas con CsA mostraron el mismo efecto inmunosupresor en linfocitos humanos activados que la formulación comercial, lo que confirma que el fármaco mantuvo su actividad biológica después de la encapsulación en las NPs. Los estudios *in vivo* en un modelo murino experimental de ojo seco mostraron que las NPs cargadas con CsA recubiertas con HA presentaban una mayor eficacia terapéutica que las NPs sin recubrimiento. Además, se comprobó que las NPs blancas recubiertas de HA podrían tener algún efecto terapéutico probablemente debido a los beneficios adicionales que proporciona HA. Finalmente, desarrollamos y caracterizamos preliminarmente NPs cargadas con rapamicina para el tratamiento tópico de la neovascularización corneal. Ambos tipos de NPs mostraron propiedades fisicoquímicas adecuadas y una adecuada biocompatibilidad *in vitro*. Ambos tipos de NP cargadas con rapamicina mostraron la misma eficacia antiangiogénica *in vitro* que la solución del fármaco, confirmando que su actividad biológica se mantuvo después la encapsulación.

En resumen, nuestros resultados confirman la idoneidad y el potencial clínico de las SENS como sistemas de administración de fármacos para el tratamiento tópico de las patologías de la superficie ocular. Particularmente, se puso de manifiesto el efecto beneficioso del recubrimiento con HA en las propiedades fisicoquímicas y biofarmacéuticas así como en la eficacia terapéutica de las NPs.

# *Thesis organization/*

# *Organización de la tesis*

USC
UNIVERSIDADE
DE SANTIAGO
DE COMPOSTELA

**Thesis organization**

This Doctoral Thesis is presented as a compendium of three original research articles and one review article, two of which (Chapter I and review) are already published in peer-reviewed scientific journals. This thesis has been organized to comply with the regulations of the International Doctorate School at the University of Santiago de Compostela, Santiago de Compostela (Spain) regarding thesis structure, languages used, and ethical and intellectual property issues.

Experiments from Chapters I, II and III are the result of a close collaboration between the Ocular Surface Research Group from the Institute of Applied Ophthalmo-Biology (IOBA-University of Valladolid, Valladolid, Spain) and the Department of Pharmacology, Pharmacy and Pharmaceutical Technology from the Faculty of Pharmacy of Santiago de Compostela (University of Santiago de Compostela, Santiago de Compostela, Spain). Experiments from Chapter II are also the result of an international collaboration with the Department of Ophthalmology from the Faculty of Medicine at Boston University (Boston, MA, USA), where I have been for three months, which has also given me the opportunity to fulfill the requirements to apply for the International-awarded Doctoral Thesis Degree.

The thesis report organization (**Figure 1**) was defined by its main objective: the design and development of a nanoparticle-based therapeutic alternative to existing topical treatments for dry eye disease and corneal neovascularization. To this end, we first performed an extensive review, enclosed as **Annex I**, analyzing main factors that affect topical ocular administration. This review was published as an article entitled ***Designing lipid nanoparticles for topical ocular drug delivery*** **(**Alvarez-Trabado et al., International Journal of Pharmaceutics, 2017 Sep; 532: 204-217).

With this information, we designed and optimized nanoparticles for topical ocular drug delivery, which is described in **Chapter I**. We evaluated their biocompatibility, targeting ability and biological activity. These results were published in an article entitled ***Sorbitan ester nanoparticles (SENS) as a novel topical ocular drug delivery system: Design, optimization, and in vitro/ex vivo evaluation*** **(**Alvarez-Trabado et al., International Journal of Pharmaceutics, 2018 May; 546: 20-30).

In **Chapter II**, we evaluated the efficacy of the optimized formulations in an experimental model of dry eye disease. We monitored disease progression during the treatment and, at the end of the study, performed complete histopathological and molecular analyses.

Lastly, in **Chapter III**, we developed a nanoparticle-based therapeutic approach for the treatment of corneal neovascularization using an *in vitro* model and the optimized parameters from Chapter I. We preliminarily characterized the formulations in terms of their physicochemical properties, biocompatibility and *in vitro* therapeutic efficacy.

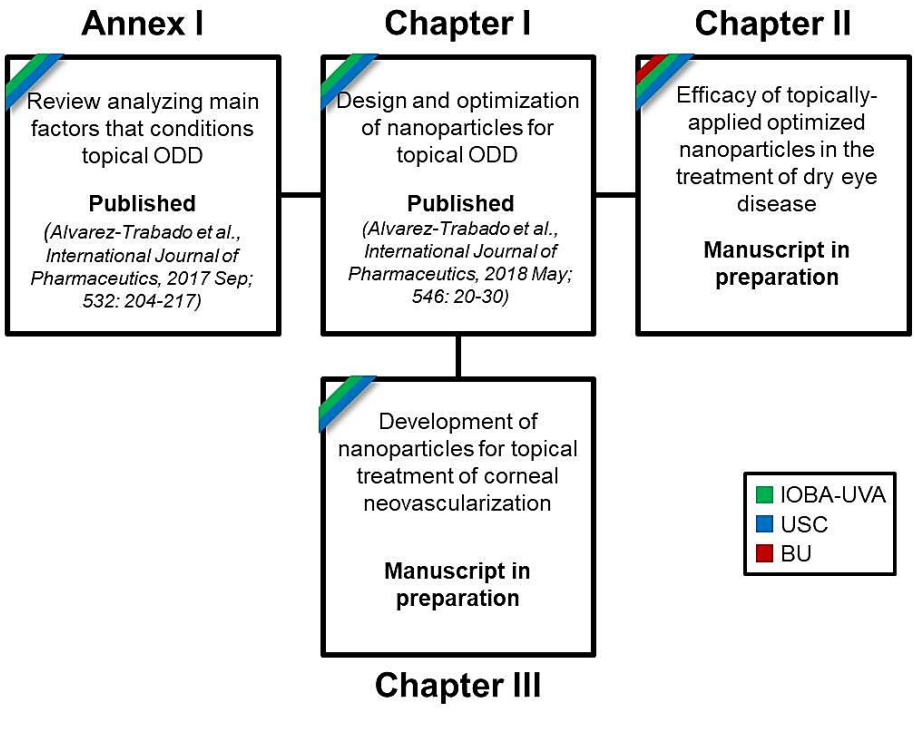


**Figure 1.** Diagram showing the thesis organization with the three chapters and the annex. IOBA-UVA, Institute of Applied Ophthalmo-Biology–University of Valladolid; USC, University of Santiago de Compostela; and BU, Boston University.

**Organización de la tesis**

Esta Tesis Doctoral se presenta como un compendio de tres artículos de investigación y un artículo de revisión, dos de los cuales (Capítulo I y revisión) ya están publicados en revistas científicas revisadas por pares. Esta tesis ha sido organizada para cumplir con las normas de la Escuela Internacional de Doctorado de la Universidad de Santiago de Compostela, Santiago de Compostela (España) con respecto a la estructura de la tesis, los idiomas utilizados y los aspectos éticos y de propiedad intelectual.

Los experimentos de los Capítulos I, II y III son el resultado de una estrecha colaboración entre el Grupo de Investigación de Superficie Ocular del Instituto de Oftalmobiología Aplicada (IOBA-Universidad de Valladolid, Valladolid, España) y el Departamento de Farmacología, Farmacia y Tecnología Farmacéutica de la Facultad de Farmacia de Santiago de Compostela (Universidad de Santiago de Compostela, Santiago de Compostela, España). Los experimentos del Capítulo II son también el resultado de una colaboración internacional con el Departamento de Oftalmología de la Facultad de Medicina de la Universidad de Boston (Boston, MA, EE. UU.), donde estuve de estancia durante tres meses, lo que me ha dado la oportunidad de cumplir los requisitos para solicitar el Grado de Tesis Doctoral con Mención Internacional.

La organización de la tesis (**Figura 1**) se definió por su objetivo principal: el diseño y desarrollo de una alternativa terapéutica basada en nanopartículas a los tratamientos tópicos existentes para el ojo seco y la neovascularización corneal. Con este propósito, se realizó una extensa revisión, incluida como **Anexo I**, analizando los principales factores que condicionan la administración tópica ocular. Esta revisión se publicó como un artículo titulado ***Designing lipid nanoparticles for topical ocular drug delivery*** (Alvarez-Trabado et al., International Journal of Pharmaceutics, 2017 Sep; 532: 204-217).

Con esta información, diseñamos y optimizamos dos tipos de nanopartículas para la administración tópica ocular de fármacos (**Capítulo I**). Evaluamos su biocompatibilidad, capacidad de direccionamiento y actividad biológica. Estos resultados se publicaron en un artículo titulado ***Sorbitan ester nanoparticles (SENS) as a novel topical ocular drug delivery system: Design, optimization, and in vitro/ex vivo evaluation*** (Alvarez-Trabado et al., International Journal of Pharmaceutics, 2018 May; 546: 20-30).

En el **Capítulo II**, evaluamos la eficacia de las formulaciones optimizadas en un modelo experimental de ojo seco. Monitorizamos la progresión de la enfermedad durante el tiempo que duró el tratamiento y, al final del estudio, realizamos un completo análisis histopatológico y molecular de los tejidos de interés.

Por último, en el **Capítulo III**, empleando los parámetros optimizados del **Capítulo I**, desarrollamos una aproximación terapéutica basada en nanopartículas cargadas con rapamicina para el tratamiento de la neovascularización corneal**.** Las formulaciones fueron caracterizadas preliminarmente en términos de sus propiedades fisicoquímicas, biocompatibilidad y eficacia terapéutica *in vitro*.

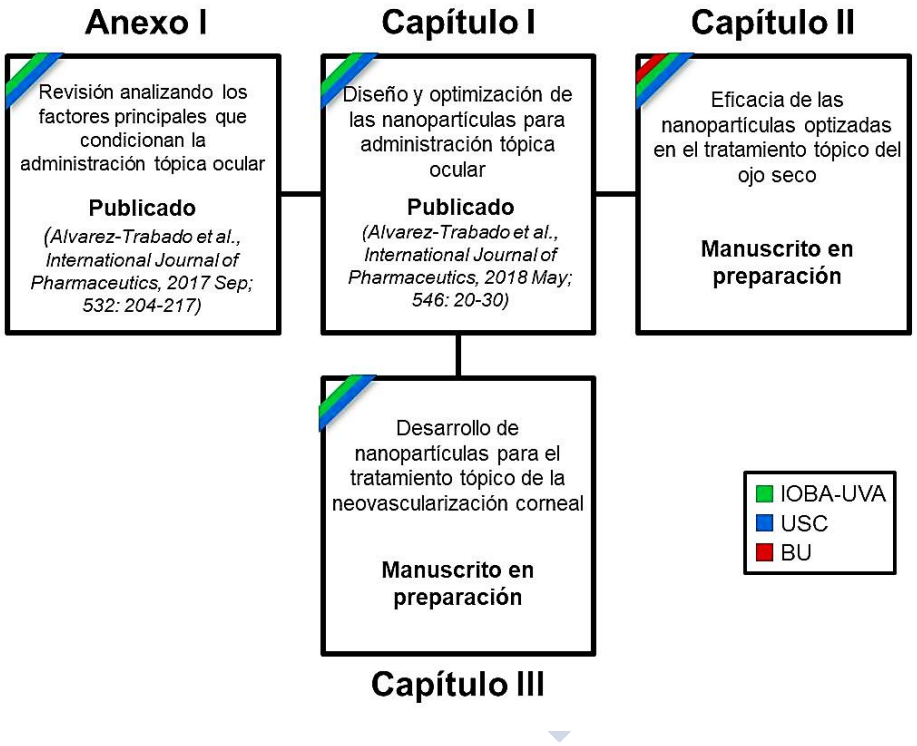


**Figura 1.** Diagrama de la organización de las tesis incluyendo los tres capítulos y el anexo. IOBA-UVA, Instituto de Oftalmobiología Aplicada-Universidad de Valladolid; USC, Universidad de Santiago de Compostela; y BU, Universidad de Boston.

# *Resumen en español*

USC
UNIVERSIDADE
DE SANTIAGO
DE COMPOSTELA

# 1. Introducción

## 1.1. El ojo y la superficie ocular

El ojo es el órgano principal del sistema visual y es el responsable de transformar los estímulos lumínicos que percibimos de nuestro entorno en señales eléctricas que puedan ser interpretadas por el cerebro. Es un órgano complejo formado por diferentes estructuras y tejidos que pueden ser clasificados en los segmentos anterior y posterior. El segmento anterior incluye la córnea, el limbo, la conjuntiva, el humor acuoso, el iris y el cristalino, mientras que el segmento posterior incluye el humor vítreo, la retina y el nervio óptico. A su vez, los epitelios corneal, limbar y conjuntival forman parte de una estructura funcional denominada superficie ocular (SO). Esta estructura, junto con las diferentes glándulas oculares (glándulas lagrimales principales y accesorias, glándulas de Meibomio y glándulas de Moll y Zeis), y la película lagrimal se integran en una unidad fisiopatológica que se conoce como unidad funcional lagrimal. La presencia de conexiones neuronales, hormonas y mecanismos inmunitarios contribuye a la función homeostática de esta unidad, cuyo objetivo final es preservar la transparencia corneal y en consecuencia la visión.

## 1.2. La SO como barrera biofarmacéutica.

La SO proporciona un entorno de protección que no sólo previene la entrada de patógenos en el ojo, sino que también actúa como una auténtica barrera biofarmacéutica condicionando la biodisponibilidad de substancias terapéuticas administradas por vía tópica. Los principales elementos que constituyen esta barrera biofarmacéutica son la película lagrimal, la córnea y la conjuntiva. La película lagrimal es un entorno dinámico en continuo recambio con un elevado contenido en enzimas y proteínas que favorece la eliminación e inactivación de los fármacos. La córnea es una estructura altamente organizada formada por cinco capas de diferente naturaleza que actúan como barreras selectivas al paso de substancias. Particularmente, el epitelio (capa más externa) presenta uniones intercelulares estrechas que dificultan seriamente la penetración de los fármacos. La conjuntiva, que normalmente se asocia con la absorción no productiva, también se considera una barrera biofarmacéutica cuando el objetivo terapéutico se pretende alcanzar a través de la ruta transconjuntival-esclerótica. Aunque presenta mayor superficie y permeabilidad que la córnea, el tamaño molecular constituye el principal factor limitante para el paso de los fármacos.

## 1.3. Patologías de la SO

### 1.3.1. El papel de la inflamación en la SO

La SO puede verse afectada por patologías de muy diversa naturaleza (ej. infecciones, lesiones, enfermedades autoinmunes) no obstante, la mayoría de estas patologías presentan una condición patológica común: la inflamación. Aunque la inflamación es una respuesta fisiopatológica beneficiosa que ayuda a restaurar la homeostasis de la zona afectada, también puede convertirse en una respuesta perjudicial si se produce de forma descontrolada o si no resuelve adecuadamente. La presencia de inflamación crónica en la SO puede inducir cambios estructurales en los tejidos, que se traducen en procesos patológicos como la neovascularización o la fibrosis, que deterioran seriamente la visión y calidad de vida del paciente.

### 1.3.2. El ojo seco, una patología inflamatoria.

El ojo seco es una de las enfermedades oculares más comunes. Se estima que su prevalencia varía entre 5-50% a nivel mundial, y se sitúa en torno al 18.4% en España. Es una patología de origen multifactorial que se asocia con alteraciones en la composición y estabilidad de la película lagrimal, disfunción de las glándulas lagrimales y presencia de inflamación en la SO. En este contexto también se produce un incremento en la osmolaridad de la lágrima y la sobreexpresión de diversas citoquinas y quimiocinas proinflamatorias.

La concepción actual del ojo seco, describe a esta patología como un "círculo vicioso" que se desconecta progresivamente de sus causas iniciales y que se puede convertir en una enfermedad crónica si no existe una intervención terapéutica adecuada. En este "círculo vicioso", la inflamación juega un papel fundamental. Ciertos estímulos externos (ej. entornos con mucha evaporación), cambios en la composición de la película lagrimal (ej. disfunción de las glándulas de Meibomio) o alteraciones en la función fisiológica lagrimal pueden inducir un estado inflamatorio subyacente en la SO. Este estado se puede agravar en pacientes con enfermedades autoinmunes, tales como el síndrome de Sjögren, debido a fallos en los mecanismos de autorregulación del sistema inmune. La presencia de mediadores pro-inflamatorios en la SO tales como citoquinas (ej. interleuquina (IL)-1 y factor de necrosis tumoral alfa (TNF-α)) o metaloproteinasas de matriz extracelular (MMPs), se relaciona con la amplificación de la cascada inflamatoria, disfunción de las glándulas secretoras y alteraciones en la proliferación de las células epiteliales. Además, ciertas citoquinas pueden inducir la expresión de moléculas de adhesión en las células endoteliales de los vasos de la conjuntiva,

facilitando la extravasación de linfocitos T que participan en la perpetuación de la respuesta inflamatoria. De hecho, la respuesta inflamatoria crónica puede inducir una reacción autoinmune en la que linfocitos T autorreactivos se dirigen a la SO donde deterioran más aún la condición homeostática.

### 1.3.3. La neovascularización corneal.

La neovascularización corneal es una de las patologías oculares más incapacitantes. El crecimiento de vasos desde el plexo vascular limbal hacia la córnea compromete gravemente la transparencia corneal y en consecuencia la función visual del paciente. Existen diversas causas que pueden propiciar el desarrollo de neovascularización corneal, tales como los trasplantes corneales, las infecciones crónicas, las lesiones por agentes químicos o mecánicos, la deficiencia de células madre limbares o el uso prolongado de lentes de contacto. Aunque los mecanismos exactos de esta patología no están totalmente claros, se cree que la inflamación juega un papel fundamental en su etiología. En condiciones fisiológicas la córnea mantiene su transparencia debido al equilibrio existente entre los factores antiangiogénicos y los proangiogénicos, sin embargo, en determinadas circunstancias patológicas como las mencionadas anteriormente se produce una respuesta inflamatoria que puede decantar el balance a favor de los factores proangiogénicos. Uno de los principales factores proangiogénicos es el factor de crecimiento del endotelio vascular (VEGF). Este péptido no sólo participa en la activación, la migración y la proliferación de las células vasculares endoteliales, sino que además actúa como una quimiocina que atrae células del sistema inmune, principalmente macrófagos, que a su vez son capaces de producir más VEGF amplificando así la cascada angiogénica. Por otro lado, las citoquinas pro-inflamatorias (ej. IL-1, IL-6) y las MMPs liberadas en el proceso inflamatorio participan en el proceso angiogénico directa o indirectamente favoreciendo la sobreexpresión de VEGF.

## 1.4. Administración tópica ocular.

### 1.4.1. Formas de dosificación convencionales.

La administración tópica es la vía de administración preferida y más utilizada en el tratamiento de las enfermedades del segmento anterior del ojo. Ventajas como la facilidad de aplicación, el efecto rápido y local del fármaco administrado así como el bajo costo de producción contribuyen a que las formas de dosificación tópicas representen alrededor del 90% de las formulaciones oftálmicas comercializadas. No obstante, las formas de dosificación convencionales (soluciones, suspensiones,

ungüentos y emulsiones) presentan ciertas limitaciones tales como la necesidad de administración frecuente para mantener los niveles terapéuticos en el sitio de acción o la aparición de molestias oculares que en última instancia repercute en la adherencia del paciente al tratamiento. Sin embargo, la mayor desventaja de estas formas farmacéuticas es la baja biodisponibilidad del fármaco que se obtiene en el tejido diana, que normalmente es menor del 5%. Se han propuesto diversos enfoques tecnológicos para mejorar las propiedades biofarmacéuticas de estas formulaciones tales como el empleo de agentes viscosificantes y promotores de la penetración en soluciones y suspensiones; la reducción del tamaño de partícula en las suspensiones; o el empleo de surfactantes catiónicos en el caso de las emulsiones.

### 1.4.2. Nuevas formas de dosificación.

Los principales esfuerzos en el diseño de nuevas formas de dosificación se centran en incrementar la biodisponibilidad de los fármacos incrementando el tiempo de residencia de la formulación en el área precorneal y promoviendo su penetración a través de la SO. Con este propósito se han desarrollado diversas formulaciones incluyendo sistemas de gelificación *in situ*, insertos oculares, lentes de contacto medicadas o nanosistemas. Los sistemas de gelificación *in situ* incrementan considerablemente el tiempo de permanencia de los fármacos en el área precorneal, sin embargo, su elevada viscosidad puede llegar a comprometer el confort ocular. Los insertos oculares permiten la liberación controlada y sostenida de los fármacos, no obstante, su característica solidez se asocia con la sensación de cuerpo extraño en el ojo. Las lentes de contacto, aparte de su acción correctora de la función visual, también permiten la cesión controlada y sostenida de los fármacos. Sin embargo, su uso prolongado está relacionado con la aparición de diversas patologías de la SO. Los nanosistemas (ej. nanomicelas, liposomas, dendrímeros y nanopartículas (NPs)) permiten la administración de fármacos con problemas de solubilidad o estabilidad incrementando tanto su tiempo de residencia como su penetración intraocular. Además, dada su naturaleza coloidal, estos sistemas pueden ser fácilmente formulados en colirios de base acuosa facilitando así su aplicación y aceptación por parte del paciente. La principal desventaja de los nanosistemas radica en su limitada estabilidad fisicoquímica y biológica.

***Nanopartículas para administración tópica ocular de fármacos***

Uno de los nanosistemas más prometedores para administración ocular de fármacos son las NPs. Estos sistemas, que destacan por su versatilidad, pueden ser específicamente diseñados para adaptarse al objetivo terapéutico tanto en lo que a su composición como a sus características fisicoquímicas se refiere. En su preparación se emplean diversos materiales biocompatibles, tales como polímeros naturales o sintéticos (ej. gelatina, albúmina, ácido poliláctico) o lípidos (ej. triglicéridos, ácidos grasos, esteroides). También se emplean polímeros de recubrimiento que ayudan a maximizar la interacción de las NPs con las estructuras oculares, tales como el quitosano o el ácido hialurónico. El recubrimiento con quitosano favorece la retención precorneal de las NPs así como la penetración corneal de los fármacos, que en última instancia se traduce en un incremento de su biodisponibilidad. Este efecto positivo del quitosano se debe no sólo a su carga positiva, que facilita la interacción electrostática de las NPs con la capa mucosa precorneal -cargado negativamente-, sino a su habilidad para alterar transitoriamente la permeabilidad del epitelio corneal, favoreciendo así la penetración de los fármacos. En el caso del recubrimiento con ácido hialurónico, se ha demostrado que las NPs recubiertas con este polisacárido favorecen una mayor penetración corneal del fármaco que sus homólogas no recubiertas. Este efecto positivo del ácido hialurónico se debe, por un lado, a sus propiedades mucoadhesivas que incrementan la retención precorneal de las NPs y, por otro, a su habilidad para interaccionar con los receptores de ácido hialurónico -ampliamente distribuidos por la superficie del epitelio corneal- que favorecen la endocitosis de las NPs y en consecuencia la penetración del fármaco.

A pesar de que las NPs han demostrado su eficacia preclínica en el tratamiento de diferentes patologías de la SO, tales como el ojo seco o la neovascularización corneal, su potencial terapéutico todavía no ha podido ser explotado en el ámbito clínico. Esta situación probablemente se deba a la combinación de varios factores, entre los que destaca la necesidad de más evidencias sobre la seguridad del uso prolongado de los tratamientos a base de NPs. Además, hay que tener en cuenta que desde el punto de vista industrial existen ciertos aspectos críticos, como la relación coste-beneficio, la facilidad de escalado de la producción o la reproducibilidad entre lotes, en los que fracasan muchos de los nanosistemas desarrollados.

# 2. Hipótesis y objetivos

## 2.1. Hipótesis

Es posible desarrollar un sistema de administración tópica ocular de fármacos a base de nanopartículas de éster de sorbitán (SENS), capaz de dirigirse específicamente a las estructuras de la SO y maximizar la eficacia terapéutica del fármaco sin comprometer la biocompatibilidad ocular.

## 2.2. Objetivos

***Objetivo general***

Diseñar y desarrollar SENS como una alternativa terapéutica a los tratamientos tópicos existentes para dos tipos de enfermedades: ojo seco y neovascularización corneal.

***Objetivos específicos:***

i. Diseñar y optimizar dos tipos de SENS cargadas con fármacos para terapia ocular tópica: una variedad de NPs catiónicas y su versión recubierta con ácido hialurónico (Anexo I y Capítulo I).
ii. Caracterizar las NPs desarrolladas con respecto a sus propiedades fisicoquímicas y su estabilidad (Capítulos I, II y III).
iii. Evaluar la biocompatibilidad *in vitro* y la capacidad de direccionamiento *in vitro* y *ex vivo* de las NPs (Capítulos I y III).
iv. Evaluar la actividad biológica *in vitro* y *ex vivo* de las NPs cargadas con fármacos (Capítulos I y III).
v. Evaluar la eficacia terapéutica de las NPs cargadas con ciclosporina en el tratamiento del ojo seco en un modelo animal (Capítulo II).

## 3. Materiales y métodos

### 3.1. Elaboración de las NPs

Para la elaboración de las NPs catiónicas, todos los componentes del sistema incluyendo el monoleato de sorbitan (Span® 80), el d-alfa-tocoferol-polietilenglicol 1000 succinato (TPGS), el bromuro de cetiltrimetilamonio (CTAB), y la ciclosporina (CsA) o la rapamicina (Rapa) –para las formulaciones cargadas con fármaco- se disolvieron en 30 ml de etanol absoluto. Las NPs se formaron espontáneamente tras verter esta fase orgánica sobre una fase acuosa (agua ultrapura, 60 mL) bajo agitación magnética continua (500 rpm, 15 minutos). La fracción de etanol se eliminó mediante rotavapor y la formulación se concentró hasta un volumen final de 10 mL.

Para preparar las NPs recubiertas con ácido hialurónico (HA), se mezclaron dos volúmenes de NPs catiónicas recién preparadas con un volumen de una solución acuosa de HA. Las NPs resultantes se colocaron en un agitador orbital (75 rpm, 20 minutos) para asegurar la correcta adsorción del HA.

### 3.2. Caracterización fisicoquímica de las NPs

El tamaño de las NPs y el potencial zeta se determinaron mediante espectroscopía de correlación fotónica y anemometría de dispersión laser, respectivamente. Las muestras fueron previamente diluidas con KCl 0,1 mM.

La eficacia de encapsulación y la capacidad de carga de las NPs se determinaron por cromatografía líquida de alta resolución tras separar por filtración (0,22 μm) la fracción de fármaco atrapado en las NPs de la fracción libre en forma de cristales.

La morfología de las NPs se evaluó mediante microscopía electrónica de transmisión tras la tinción de las muestras con ácido fosfotúngstico.

### 3.3. Análisis estructural de las NPs

Para realizar el análisis estructural de las NPs se utilizaron tres técnicas complementarias: la resonancia magnética nuclear se usó para estudiar la estructura de las NPs en estado líquido (dispersión acuosa); y la calorimetría diferencial de barrido y la difracción de rayos X de polvo se utilizaron para estudiar la estructura de las NPs en estado sólido (sistemas liofilizados).

### 3.4. Estudios de estabilidad física y biológica

La estabilidad física de las NPs se analizó tanto en su estado líquido (dispersión acuosa) como en su estado sólido (sistemas liofilizados). Para preparar los sistemas liofilizados, se testaron tres agentes crioprotectores: sacarosa, glucosa y trehalosa (5-20% w/v). Las NPs recién preparadas y las NPs liofilizadas se almacenaron a 4ºC, a temperatura ambiente y a 37ºC durante tres meses. Al comienzo y al final de los estudios, se midieron el tamaño y el potencial zeta de las NPs.

La estabilidad biológica de las NPs se determinó incubando las formulaciones con fluido lagrimal simulado enriquecido en proteínas (5 horas, 37ºC). Como en el caso anterior, al comienzo y al final del estudio se midieron el tamaño y el potencial zeta de las NPs.

### 3.5. Esterilización de las formulaciones

Las formulaciones empleadas para los experimentos *in vitro*, *ex vivo* e *in vivo* fueron previamente esterilizadas por filtración empleando filtros de 0,22 µm de diámetro de poro. Asimismo se estudió la aplicabilidad de la esterilización a altas temperaturas evaluando las alteraciones en las propiedades fisicoquímicas de las NPs tras un ciclo de autoclavado (121ºC, 20 minutos).

### 3.6. Biocompatibilidad *in vitro* de las NPs

Para determinar la biocompatibilidad de las formulaciones desarrolladas se emplearon dos líneas celulares derivadas de los epitelios de la superficie ocular: la línea de epitelio corneal humano (HCE) y la línea de epitelio conjuntival normal humano (IOBA-NHC).

Para evaluar la potencial citotoxicidad de las NPs se realizaron dos series de experimentos. En una serie, las células HCE fueron expuestas durante 30 minutos a concentraciones crecientes de NPs blancas y cargadas con CsA. En la otra serie, las células HCE e IOBA-NHC fueron expuestas durante 24 horas a concentraciones crecientes de NPs blancas y cargadas con Rapa. Transcurridos estos periodos se realizó el ensayo XTT de acuerdo con las instrucciones del fabricante y se determinó la viabilidad celular.

En otro estudio, se evaluó la proliferación celular de las células HCE tras la exposición durante 30 minutos a diferentes concentraciones de NPs. Al finalizar el período de

incubación se retiraron las formulaciones y se realizó el ensayo Alamar Blue® a las 0, 24 y 48 horas para determinar el porcentaje de proliferación.

### 3.7. Estudio de la internalización de las NPs en células corneales

La capacidad de los nanosistemas desarrollados para dirigirse a las células corneales se investigó en la línea celular HCE. Para poder realizar el seguimiento de las NPs, el fármaco se reemplazó por el marcador fluorescente Nile Red cuya señal puede ser fácilmente monitorizada por técnicas de fluorescencia.

Tras el bloqueo selectivo de cada uno de los diferentes mecanismos de internalización, las células se incubaron durante 30 minutos con las NPs. Al final de este período, las células se despegaron de los pocillos -usando el tampón del ensayo de radioinmunoprecipitación- y se determinó el contenido en proteína total mediante el método de ácido bicinconínico (BCA) y la señal fluorescente de cada lisado celular -mediante fluorometría-. Los valores de internalización se obtuvieron al normalizar la señal fluorescente con respecto al contenido en proteína de cada muestra.

Para observar la distribución de las NPs en las células HCE se empleó la técnica de microscopía de fluorescencia. Se tomaron imágenes bidimensionales a diferentes tiempos de exposición (5-30 minutos) y se realizó un escaneado del eje Z a los 30 minutos de exposición.

### 3.8. Estudio *ex vivo* de la interacción de las NPs con la córnea porcina

Se realizaron dos estudios diferentes para evaluar la interacción de las NPs con la córnea porcina. Por un lado se realizó un estudio para determinar la biodistribución de las NPs marcadas con Nile Red y, por otro lado, se realizó un estudio con NPs cargadas con CsA para determinar cuantitativamente la penetración del fármaco.

Para estudiar la biodistribución de las NPs se colocó un anillo de silicona de 12 mm sobre la córnea central de los globos oculares, y se aplicaron 300 µL de las formulaciones durante 30 minutos. Posteriormente se retiraron las formulaciones y se procesaron los tejidos para su posterior análisis por microscopia de fluorescencia.

La penetración de la CsA se midió usando córneas de cerdo *ex vivo* aisladas a partir de ojos enucleados en un matadero local y procesadas en el laboratorio, las cuales fueron montadas entre el compartimento donador y el receptor de células de difusión vertical de Franz. El compartimento receptor se llenó con SLF sin proteínas y se mantuvo bajo

agitación magnética continua. En el compartimento donador se colocaron las formulaciones. Tras 30 minutos de incubación a 37ºC, se retiraron las formulaciones, se pesaron las córneas y se extrajo la fracción de fármaco que penetró para su posterior cuantificación por HPLC.

### 3.9. Evaluación *ex vivo/in vitro* de la actividad biológica de las NPs

La actividad inmunosupresora de las NPs cargadas con CsA se evaluó mediante un ensayo funcional *ex vivo* de linfocitos humanos activados. Los linfocitos, que se extrajeron en el momento del ensayo de un donante sano, fueron expuestos a las formulaciones y a la concanavalina -agente estimulante- durante 24 horas. Tras este período de incubación, se separaron las células de los sobrenadantes -mediante centrifugación-, y éstos últimos se almacenaron a -80ºC para posteriormente determinar el contenido en IL-2 mediante el correspondiente enzimoinmunoensayo.

La actividad antiangiogénica de las NPs cargadas con Rapa se evaluó mediante dos ensayos *in vitro* diferentes basados en la monitorización de la producción de VEGF. En uno de los ensayos se estudió el efecto antiangiogénico de las formulaciones en cultivos primarios de epitelio de conjuntiva humana previamente estimulados con IL-6 (citoquina proangiogénica). En otro ensayo se determinó el potencial antiangiogénico de las formulaciones en la línea celular IOBA-NHC. En este caso se usó una combinación de TNF-α e IL-1β para estimular la producción de VEGF. Al final de ambos ensayos se obtuvieron los sobrenadantes y se almacenaron a -80ºC para posteriormente determinar el contenido en VEGF-A mediante el correspondiente enzimoinmunoensayo.

### 3.10. Evaluación *in vivo* de la eficacia de las NPs cargadas con CsA

Para la evaluación de la eficacia terapéutica de las NPs cargadas con CsA se empleó un modelo animal de enfermedad inflamatoria ocular: ratones deficientes en trombospondina-1 (TSP-1). Estos animales, con la edad, desarrollan un proceso inflamatorio en la SO similar al que se da en el ojo seco de tipo Sjögren. Los animales se dividieron en cuatro grupos según el tratamiento recibido: el grupo 1 recibió NPs catiónicas cargadas con CsA (tratamiento 1), el grupo 2 recibió NPs catiónicas blancas (control del tratamiento 1), el grupo 3 recibió NPs recubiertas de HA cargadas con CsA (tratamiento 2), y el grupo 4 recibió NPs recubiertas de HA blancas (control del tratamiento 2). Tanto los tratamientos como los controles se administraron diariamente de forma tópica (5 µL/ojo) durante 21 días.

La eficacia de los tratamientos se monitorizó evaluando dos de los principales signos asociados con el ojo seco: la integridad corneal y la función secretora. La integridad corneal se evaluó mediante la tinción corneal con fluoresceína y su correspondiente gradación (CFS), y la función secretora se evaluó midiendo los niveles de MUC5AC en lágrima. Al cabo de los 21 días, se practicó la eutanasia a todos los animales y se procesaron los tejidos de interés -globos oculares y ganglios cervicales- para su posterior análisis histopatológico y molecular. Para el análisis histopatológico, los globos oculares se fijaron, cortaron y tiñeron con hematoxilina-eosina y ácido periódico de Schiff-azul alcián. Para el análisis molecular, primero se procesaron los ganglios para extraer el contenido de ARN, luego éste se convirtió en el correspondiente ADNc y finalmente se llevó a cabo la reacción en cadena de la polimerasa para cuantificar de forma relativa la expresión de las citoquinas IL-6, IL-1β y TNF-α.

## 4. Resultados y discusión

### *4.1. Nanopartículas de éster de sorbitán (SENS) como un nuevo sistema de administración tópica ocular de fármacos: diseño, optimización y evaluación in vitro/ex vivo*

Para el diseño de las NPs se tuvieron en cuenta tanto las propiedades tecnológicas de cada uno de los componentes como su estatus regulatorio y su biocompatibilidad. Todos los componentes empleados en la preparación de las formulaciones cuentan con la aprobación de las agencias regulatorias europeas y americanas, y son comúnmente empleados por las industrias farmacéutica y alimentaria.

La primera etapa del desarrollo de las NPs consistió en obtener una formulación catiónica optimizada, cuyas propiedades fisicoquímicas fuesen las más apropiadas para administración tópica ocular (Anexo I). Con este objetivo se realizó un diseño experimental Box-Behnken en el que se evaluó la influencia de la concentración de los diferentes componentes en las propiedades fisicoquímicas de las NPs (Capítulo I, Tabla 2). En base a la matriz de datos generada se llevó a cabo un proceso de optimización estadística tras el cual la formulación optimizada presentó la siguiente composición (p/v): Span® 80 2%, TPGS 0,22%, CTAB 0,03%, CsA 0,65%. Esta formulación presentó un tamaño de partícula de 170,5 nm, potencial zeta de +33,9 mV, eficiencia de encapsulación de 83,95% y capacidad de carga del fármaco de 19,66%. Usando como

base esta formulación se desarrolló un segundo tipo de NPs recubiertas con HA (0,015% p/v) cuyo tamaño se incrementó ligeramente (177,6 nm) y cuyo potencial zeta viró a negativo (–20,6 mV) debido a la adsorción del polímero. El análisis de las formulaciones por microscopía electrónica de transmisión mostró que ambos tipos de NPs presentaban morfología esférica con una distribución homogénea de tamaño partícula (Capítulo I, Figura 2). En el caso de las NPs recubiertas con HA se apreció una zona periférica menos opaca debido a la adsorción del polisacárido. El análisis estructural de las formulaciones por resonancia magnética confirmó la presencia de una estructura sólida con cierta flexibilidad hacia la periferia de la nanopartícula (Capítulo I, Figura 3). Asimismo, se observó que la encapsulación del fármaco no modificó la estructura de las NPs, sugiriendo que éste se encontraba disuelto a nivel molecular en su interior. Las formulaciones presentaron estabilidad adecuada tras tres meses de almacenamiento a 4ºC, temperatura ambiente y 37ºC (Capítulo I, Figura 4a). Las formulaciones también fueron estables en presencia de fluido lagrimal simulado enriquecido con proteínas (Capítulo I, Figura 4b).

La biocompatibilidad de las NPs fue evaluada en una línea de epitelio corneal mediante dos estudios *in vitro* complementarios. Por un lado el ensayo XTT demostró que ambos tipos de NPs mantuvieron niveles adecuados de viabilidad celular en todo el rango de concentraciones testado (Capítulo I, Figura 5a). Concretamente, la concentración de NPs de 0,2% (p/v) que equivale a un contenido en CsA del 0,05% (p/v) en las formulaciones cargadas con el fármaco –misma dosis que Restasis®- no mostró diferencias significativas con respecto al control negativo (células con medio de cultivo). Por otro lado, el estudio de proliferación celular confirmó la seguridad de las NPs en todo el rango de concentraciones testado (Capítulo I, Figura 5b). En este caso no hubo diferencias significativas entre las NPs y el control negativo.

Los estudios de internalización de las NPs en la línea de epitelio corneal demostraron que ambos tipos de NPs entraron en las células por mecanismos dependientes de energía (Capítulo I, Figura 6a). En el caso de las NPs catiónicas la endocitosis estuvo mediada por caveolas, mientras que en el caso de las NPs recubiertas con HA el principal mecanismo de internalización fue la endocitosis mediada por receptores de HA. Precisamente, este direccionamiento específico a través de los receptores de HA puede explicar la mayor señal fluorescente observada en las células corneales (Capítulo I, Figura 6b,c). Las diferencias entre ambos tipos de NPs también se

plasmaron en su distribución intracelular. Mientras que las NPs catiónicas se acumularon principalmente entorno al núcleo (cargado negativamente), las NPs recubiertas con HA se distribuyeron uniformemente por todo el citoplasma.

El patrón de distribución observado *in vitro* en las células corneales también se observó en el estudio *ex vivo* de la distribución de las NPs a través de la córnea porcina (Capítulo I, Figura 7). Las NPs catiónicas se acumularon principalmente en la parte apical del epitelio y entorno a los núcleos celulares, presumiblemente debido a la carga negativa de ambas estructuras. Por el contrario, las NPs recubiertas con HA se distribuyeron ampliamente a través de las capas del epitelio y alcanzaron el estroma corneal. Además, la penetración corneal de la CsA con las NPs catiónicas y las NPs recubiertas con HA (Capítulo I, Figura 8) fue 1,3 veces y 2,1 veces superior a la formulación comercial, respectivamente.

Finalmente, el estudio *ex vivo* de la actividad biológica de las NPs en linfocitos humanos activados, confirmó que ambos nanosistemas mantuvieron inalterada la actividad biológica del fármaco, y su potencia inmunosupresora fue similar a la de la formulación comercial usada como referencia.

### *4.2. Las nanopartículas de éster de sorbitán (SENS) cargadas con ciclosporina mejoran los signos del ojo seco en ratones deficientes en TSP-1.*

En este trabajo las NPs catiónicas cargadas con ciclosporina presentaron un tamaño de 176,9 nm, potencial zeta de +33,6 mV y eficiencia de encapsulación de 84,4%. Tras el recubrimiento con HA, el tamaño de las NPs se incrementó hasta 188,2 nm, y el potencial zeta descendió a -24,5 mV. Ambas formulaciones fueron isotonizadas con sacarosa y el pH ajustado con NaOH para mejorar la tolerancia ocular. Se investigó la liofilización de las formulaciones con el propósito de incrementar la estabilidad de las NPs y facilitar su transporte. De los tres agentes crioprotectores evaluados, la sacarosa fue el que mejores resultados ofreció (Capítulo II, Figura 3). Las NPs crioprotegidas con sacarosa mostraron una estabilidad adecuada tras tres meses de almacenamiento a 4ºC y temperatura ambiente. Las NPs almacenadas a 37ºC experimentaron un incremento en el tamaño de partícula probablemente debido a un fenómeno de aglomeración. El análisis estructural de las formulaciones liofilizadas por calorimetría diferencial de barrido y difracción de rayos X de polvo confirmaron que el fármaco interacciona a

nivel molecular con los componentes de las NPs y que se encuentra disuelto a nivel molecular en el interior de las nanoestructuras (Capítulo II, Figura 4). El estudio de esterilización de las formulaciones por autoclave determinó que el recubrimiento con HA previene la desestabilización de las NPs a altas temperaturas, probablemente debido al efecto estérico adicional que proveen las cadenas de este polisacárido (Capítulo II, Figura 5).

La eficacia terapéutica de las formulaciones se evaluó monitorizando los diversos signos asociados a la inflamación de la SO. La integridad corneal y la función secretora evolucionaron de forma diferente dependiendo del tratamiento administrado (Capítulo II, Figura 6). Las NPs recubiertas con HA cargadas con ciclosporina fueron capaces de revertir el daño corneal, disminuyendo la puntuación de la tinción con fluoresceína a valores similares a los de un ratón sano (reducción del CFS en un 70,5%). Aunque no fue significativo, también se apreció una ligera recuperación del daño corneal en los ratones tratados con las NPs blancas recubiertas de HA (reducción del CFS en un 26,0%). Estos resultados se pueden explicar por un probable mecanismo sinérgico entre las propiedades terapéuticas del HA, que promueven la curación del epitelio corneal, y la actividad inmunosupresora de la CsA, que reduce la inflamación de la SO. Además, la mayor captación corneal de las NPs recubiertas con HA puede contribuir a su mayor eficacia (Capítulo I, Figura 6b,c). La función secretora se monitorizó midiendo los niveles de MUC5AC en lágrima, teniendo en cuenta que la inflamación de la SO está asociada a la disfunción de las células caliciformes conjuntivales que se traduce en una menor producción de esta mucina. Los resultados obtenidos indican que ambos tipos de NPs cargadas con CsA son capaces de incrementar los niveles de MUC5AC, mejorando así la función secretora (Capítulo II, Figura 7). De los animales tratados con las NPs blancas, sólo se apreció mejoría en el grupo de los ratones tratados con las NPs recubiertas con HA. Este curioso resultado probablemente se deba a la habilidad del HA para incrementar la densidad de células caliciformes.

El análisis histopatológico no mostró diferencias en la morfología de la córnea y la conjuntiva de los ratones de los cuatro grupos experimentales, con respecto a la integridad tisular o la presencia de infiltrados de células inflamatorias (Capítulo II, Figura 8a). No obstante, sí que se observaron diferencias en la densidad de células caliciformes conjuntivales (Capítulo II, Figura 8a,b). Los ratones tratados con las NPs cargadas con CsA y los ratones tratados con las NPs blancas recubiertas con HA

mostraron una mayor densidad de células caliciformes que sus homólogos tratados con las NPs blancas catiónicas. Estos resultados se correlacionan con los niveles de MUC5AC encontrados en lágrima, lo que indica que las NPs cargadas con CsA y las NPs blancas recubiertas con HA ejercen efectos beneficiosos en la recuperación de la densidad de células caliciformes, aumentando consecuentemente la secreción de MUC5AC a la película lagrimal.

Para determinar la eficacia de los tratamientos, también se realizó un análisis molecular de las tres principales citoquinas proinflamatorias asociadas al ojo seco. Niveles elevados de IL-6, IL-1β y TNF-α en la SO están relacionados con la presencia de un estado inflamatorio subyacente que contribuye al deterioro de la función homeostática y al daño tisular. El análisis molecular de las citoquinas presentes en los nódulos linfáticos cervicales determinó que ambos tipos de NPs cargadas con CsA fueron capaces de disminuir los niveles de las tres citoquinas proinflamatorias, en comparación con las formulaciones control -NPs blancas- (Capítulo II, Figura 9). Concretamente la reducción en los niveles de TNF-α puede explicar el efecto positivo de las NPs cargadas con CsA en la recuperación de la función secretora, puesto que niveles elevados de TNF-α se relacionan con atrofia y/o apoptosis de las células caliciformes.

### *4.3. Nanopartículas de éster de sorbitán (SENS) cargadas con rapamicina como nuevas herramientas para el tratamiento de la neovascularización corneal: caracterización fisicoquímica preliminar y eficacia antiangiogénica in vitro.*

Para preparar las NPs cargadas con Rapa se usó el mismo método y la misma composición que fueron empleados para preparar las NPs cargadas con CsA (Capítulo I), con la salvedad de que la concentración de Rapa fue diferente. De este modo, las NPs catiónicas presentaron la siguiente composición (p/v): Span® 80 2%, TPGS 0,22%, CTAB 0,03%, Rapa 0,2%. Asimismo, para la preparación de las NPs recubiertas con HA, las NPs catiónicas se incubaron con una solución de HA 0,015% (p/v). Tal y como refleja la Tabla 1 (Capítulo III) las NPs presentaron un tamaño nanométrico, con baja polidispersión y potenciales zeta alejados de la electroneutralidad (>|19| mV). La incorporación de la Rapa (eficiencia de encapsulación del 78%) no alteró significativamente el tamaño de partícula de los sistemas sugiriendo que el fármaco se encontraba disuelto a nivel molecular en el interior de las nanoestructuras. Considerando que la solubilidad en agua de la Rapa es de 2,6 µg/mL, la encapsulación

del fármaco por las NPs incrementó 600 veces su solubilidad. El análisis de la distribución de tamaños y las microfotografías de microscopía electrónica de transmisión (Capítulo III, Figura 2) confirmaron que ambos tipos de NPs presentaban un tamaño de partícula homogéneo, sin diferencias apreciables entre la morfología de las NPs blancas y las cargadas. Como en el Capítulo I, también se observó el efecto corona en las formulaciones recubiertas con HA, sinónimo de la correcta adsorción del polisacárido. El análisis estructural de las formulaciones liofilizadas por calorimetría diferencial de barrido y difracción de rayos X de polvo confirmaron que la Rapa interacciona a nivel molecular con la matriz de las NPs (Capítulo III, Figura 3a) y que no existe una formación cristalina del fármaco en las formulaciones (Capítulo III, Figura 3b). El compendio de ambos estudios sugiere que el fármaco se encontraba solubilizado a nivel molecular en el interior de las NPs.

La biocompatibilidad de las formulaciones fue evaluada en dos líneas celulares derivadas de la SO: la línea de epitelio corneal y la línea de epitelio conjuntival. En general se observaron diferentes perfiles de citotoxicidad en función tanto del tipo de nanopartícula como de la línea celular utilizada (Capítulo III, Figura 4). Observamos una disminución de la viabilidad dependiente de la concentración de Rapa en ambas líneas celulares, que fue más acentuada en la línea celular del epitelio conjuntival. Probablemente esta toxicidad superior se deba a la mayor sensibilidad al daño de las células conjuntivales. No obstante, la dosis NPs de 75 µg/mL -equivalente a 500 ng/mL de Rapa para las NPs cargadas con fármaco- mantuvo la viabilidad celular por encima del 70% y, en consecuencia, esta dosis se usó en los experimentos de eficacia adicionales. Cabe destacar que, aunque no fue significativo, las NPs recubiertas con HA mostraron menor toxicidad probablemente al efecto citoprotector del HA.

Finalmente, se evaluó la eficacia de las NPs en dos ensayos funcionales *in vitro* de producción de VEGF. Tanto en el ensayo realizado en los cultivos primarios de epitelio de conjuntiva humana estimulados con IL-6, como en el ensayo realizado en las células IOBA-NHC estimuladas con TNF-α y IL-1β, las formulaciones cargadas con Rapa fueron capaces de reducir la expresión de VEGF a niveles similares a los que obtuvo la Rapa disuelta en DMSO. En vista de estos resultados, suponemos que las NPs fueron eficazmente internalizadas y metabolizadas por las células, provocando la liberación de la Rapa al citosol y consecuentemente se produjo la reducción en la expresión de VEGF. Además, las microfotografías tomadas a las células IOBA-NHC durante los

experimentos demostraron que ninguno de los tratamientos comprometió la morfología celular, lo que garantizó que las variaciones en los niveles de VEGF fueron debidas exclusivamente a la regulación de los mecanismos moleculares celulares y no a alteraciones en la viabilidad celular.

## 5. Conclusiones

Teniendo en cuenta todos los resultados presentados en este trabajo, se puede concluir lo siguiente.

i. Se ha demostrado que las SENS pueden ser desarrolladas y optimizadas como un sistema de administración tópica ocular de fármacos. Las NPs también pueden ser decoradas superficialmente con HA con el propósito de obtener un direccionamiento específico a estructuras de la SO, tales como la córnea.

ii. Las NPs desarrolladas mostraron propiedades fisicoquímicas adecuadas para la administración tópica ocular. Particularmente, la elevada carga de CsA, que provocó un aumento notable en la solubilidad en agua de este fármaco, no comprometió la estabilidad física de la dispersión acuosa de NPs.

iii. Las NPs desarrolladas mostraron un perfil de seguridad adecuado en la línea celular corneal y las líneas conjuntivales. Las NPs recubiertas de HA mostraron una mayor capacidad de direccionamiento a la córnea en comparación con las NPs no recubiertas, tanto *in vitro* como *ex vivo*.

iv. El proceso de producción de las NPs no afectó la actividad biológica de la CsA y la Rapa, y ambos fármacos pudieron liberarse de la matriz de las NPs en sus formas bioactivas para ejercer sus efectos terapéuticos.

v. Se ha demostrado que las NPs recubiertas con HA mejoraron la eficacia terapéutica de la CsA aplicada tópicamente en el tratamiento del ojo seco. Estos resultados probablemente se deben a un mecanismo sinérgico entre la eficacia antiinflamatoria de CsA y los beneficios terapéuticos y tecnológicos proporcionados por el HA. Esta prueba de concepto puede ayudar en el diseño de sistemas de administración tópica ocular de fármacos basados en NPs más eficientes.

# *Introduction*

USC
UNIVERSIDADE
DE SANTIAGO
DE COMPOSTELA

## 1. The eye

The eye is the main organ of the visual system and is the responsible of the sense of sight. It allows the transduction of the light signals proceeding from environment into electric stimuli that can be interpreted by the brain [1]. Due to its relevant role, this organ possesses particular anatomical and physiological characteristics to protect and preserve its function.

### 1.1. Eye anatomy and physiology

The eye globe is a highly organized structure constituted by three adjacent layers called sclera, uvea and retina. The sclera is the outermost layer and is composed mainly by collagen and elastic fibers that protects and gives mechanical stability to the eye [2]. It is bounded to the cornea through the corneal limbus. The uvea is the intermediate layer and is formed by iris, ciliary body and choroid. It is a vascularized layer whose main roles are to provide nutrients to eye tissues and to maintain the homeostasis of the aqueous humor [3]. The retina is the innermost layer of the eye and is formed by a complex structure combining layers of pigmented epithelium cells and light-sensitive cells (photoreceptors). It is a neural tissue that is responsible of light reception and its nervous transmission [4].

The eye is also formed by different tissues and structures that can be classified into anterior and posterior segments. Anterior segment includes cornea, limbus, conjunctiva, aqueous humor, iris and lens whereas posterior segment includes vitreous humor, retina, and optic nerve.

Corneal, limbal and conjunctival epithelia are commonly named the ocular surface (OS). This structure along with different glands (main and accessory lacrimal glands, meibomian glands and eyelid-associated Moll and Zeis glands, are integrated in a pathophysiological unit that also includes the tear film, namely the lacrimal functional unit [5]. The presence of neural connections, hormones and immune mechanisms contributes to the homeostatic function of this unit, whose ultimate role is to preserve corneal transparency and consequently, eye sight [6].

## 1.2. Biopharmaceutical barriers in the eye

The eye is an isolated and highly protected organ that have numerous anatomical and physiological barriers that prevent not only the entrance of pathogens but also therapeutic substances [7]. Ocular drug delivery focuses on placing the therapeutic agent in the target tissue in the eye by overcoming these barriers, maximizing treatment efficacy without compromising patient safety and compliance. For this purpose, different administration routes have been used including topical, periocular, intravitreal, systemic (parenteral) and oral [8]. Administered drug by each route has to face specific tissue constrains before accessing the therapeutic target (**Figure 1**). These barriers are the OS and the scleral barriers for the topical and periocular administrations, and the blood-ocular barriers system including aqueous and retinal barriers, for the systemic and oral administrations (**Table 1**). Intravitreal administration presents the advantage that drugs are directly injected into the ocular cavity overcoming main biological barriers. Nevertheless, diffusion of drug or drug vehicles (i.e. nanoparticles) in the vitreous is conditioned by its size and net charge [9,10]. In addition, the high risk of occurrence of serious complications, such as endophthalmitis or intraocular inflammation, limits the use of intravitreal injections [11].

### 1.2.1. The OS barrier

The OS barrier mainly affects drugs administered topically, and is the result of the combination of the precorneal tear film with the static barriers formed by the cornea and the conjunctiva by itself. This protective environment seriously conditions ocular drug bioavailability obtained with conventional topical dosage forms which is usually below 5% [12,13].

#### *The tear film*

The tear film, which is a three-phasic lipid-aqueous-mucus layer, not only acts as a drug solubility-limiting barrier but also present a variety of enzymes and proteins that can contribute to the drug metabolism or inactivation [14,15]. In normal conditions tear volume (6-8 µL) is renewed at rate of 16% of total tear volume per minute thanks to the physiological blinking (15-20 blinks/min) [16]. Drug instillation usually triggers the blinking reflex increasing blinking rate and also inducing tear production. This combined effect facilitates formulation drainage through the nasolacrimal system meaning that a fraction of the administered dose will be lost [17]. This aspect has

particular relevance taking into account that instilled volume of conventional dosage forms (i.e. eye drops) is in the range of 25-50 µL, and the exceeding dose is quickly washed-out from the OS without exert any therapeutic effect being responsible of undesirable systemic effects [18].

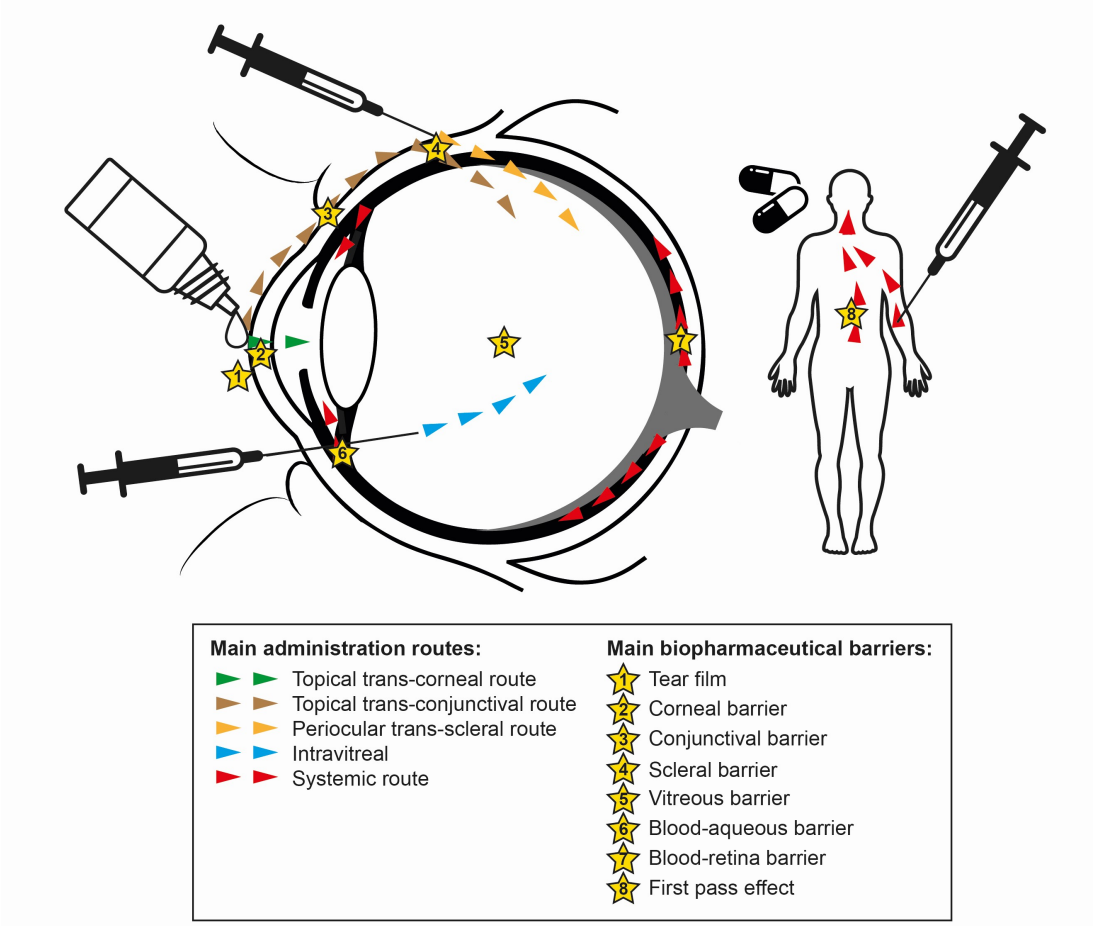


**Figure 1. Main ocular administration routes.** Schematic created by Jesús Álvarez-Trabado.

### *The corneal barrier*

The cornea is an avascular and transparent tissue that has a twofold function: first, the cornea has a central role in the vision process due to its refractive power and second, it acts as a biological barrier to prevent intraocular entrance of pathogens and chemicals [19]. The Cornea is composed by five layers namely epithelium, the Bowman's layer, stroma, the Descemet's membrane, and endothelium. The epithelium is the outermost layer consisting in 5-6 cells layers tightly bounded by tight junctions (or *zonula*

*occludens*) and firmly attached to the Bowman's layer through a basal membrane. It is a highly hydrophobic layer that allows the passage of lyophilic substances (by transcellular route) and prevents entrance of hydrophilic ones [20]. The corneal stroma represents about 90% of the thickness of the cornea and is composed by highly organized collagen fibers, proteoglycans, glycoproteins and water. This tissue provides transparency and structural support to the cornea [21]. Due to its aqueous nature and opened structure it allows the diffusion of large hydrophilic molecules, but avoids the diffusion of lipophilic ones [20]. The endothelium is the innermost layer of cornea and is constituted by a porous single cell layer that is attached to the stroma by Descemet's membrane. Its main function is to regulate corneal hydration and nutrition by facilitating the passage of water from the stroma and the diffusion of nutrients from the aqueous humor [22]. For this reason, it constitutes a weak barrier to the passage of drugs.

***The conjunctival barrier***

The conjunctiva is a highly vascularized mucous membrane that covers the inner part of eyelids (palpebral or tarsal conjunctiva) and one-third of anterior eye globe (bulbar conjunctiva) joining both portions in the area referred as the fornix (forniceal conjunctiva). The conjunctiva plays different roles including the protection and homeostasis of the ocular surface and the production of different components of the tear film [23]. This tissue is formed by a layer of epithelial cells and its underlying stroma that is attached to the sclera in the bulbar portion. Conjunctiva has a 17-fold [24] and 2-30 fold [25] larger surface and higher permeability than the cornea, respectively. For instance, drug penetration through the conjunctiva is higher than through the cornea, especially for hydrophilic molecules, being reported penetration of molecules with high molecular weight [26]. Although conjunctiva can be a target tissue for drug delivery to the posterior segment of the eye by the underlying trans-scleral diffusion [27,28], and so act as a biopharmaceutical barrier, it is often considered a tissue related with non-productive drug absorption that can lead to systemic side effects due to its high vascularization [8,29].

### 1.2.2. The scleral barrier

The sclera is a fibrous tissue that covers four-fifths of eye globe having an approximate surface area of 16.3 $cm^2$ [30]. It constitutes a biopharmaceutical barrier for the ocular penetration of topically administered drugs that access through the conjunctiva and for drugs administered by periocular injection in the subconjunctival, subtenonian, retrobulbar and peribulbar spaces. Due to absence of an epithelial cell covering it is more permeable to solutes than the cornea and the conjunctiva; nonetheless the intricate matrix that forms sclera, which is mainly composed by collagen fibers and negatively charged proteoglycans, acts as a barrier that retains molecules depending on its physicochemical properties. Hence, drug diffusion is highly conditioned by particular physicochemical properties of the drug including molecular weight, radius, shape, net charge and charge distribution [7,31].

### 1.2.3. The blood-ocular barriers system

The blood-ocular barriers system is formed by the blood-aqueous barrier in the anterior segment and the blood-retinal barrier in the posterior segment. Both structures maintain the eye as a quite impermeable organ preventing the entrance of substances from systemic circulation.

***The blood-aqueous barrier***

The blood-aqueous barrier is formed by the tight junctions present in the endothelium of vessels vascularizing iris and ciliary body, in the non-pigmented epithelium of ciliary body and in the inner wall of endothelium of Schlemm's canal [32,33]. Combination of both structures prevent the entrance of solutes in the intraocular environment, such as the aqueous humor [34]. It is also reported the presence of transporters (i.e. multidrug resistance-associated proteins) in the iris and ciliary body that limit drug permeation from blood to the aqueous humor and that actively eliminate drug from aqueous humor to blood [35].

***The blood-retinal barrier***

The blood-retinal barrier is formed by an outer and an inner barriers [36,37]. The outer barrier is constituted by the retinal pigment epithelium and prevents the diffusion of solutes from the choroid to the sub-retinal space [37]. The inner barrier comprises the intercellular tight junctions present in the endothelium of retinal microvasculature and

strictly controls the diffusion of molecules from the systemic circulation to the retina [37]. Molecular weight and lipophilicity are the major factors affecting drug permeability through this barrier [38]. Small and lipophilic molecules can easily cross the retinal pigmentary endothelium trough the transcellular route, whereas hydrophilic molecules only can diffuse through the paracellular pathway, being crucial that have a reduced molecular weight [38].

**Table 1. Summary of main ocular administration routes and associated biopharmaceutical barriers, emphasizing the most relevant physicochemical properties that determine ocular drug delivery.**

| Administration route | | Biopharmaceutical barriers | Related physicochemical properties | Ref. |
|---|---|---|---|---|
| Topical | Trans-corneal | Tear film<br>Corneal barrier | Small and fairly lipophilic substances (log D of 2-3) can easily penetrate cornea.<br>Only hydrophilic substances with MWs <100 Da can diffuse through paracellular route. | [39,40]<br>[20] |
| | Trans-conjunctival | Tear film<br>Conjunctival barrier<br>Scleral barrier | Hydrophilic substances with medium size (up to 20-40 KDa) can diffuse trough conjunctiva. However small MWs are desirables. | [26,41] |
| Periocular | | Scleral barrier | Large and hydrophilic substances (up to 70-150 KDa) can diffuse trough sclera, although small MWs are preferred.<br>Globular shaped substances with small molecular radius have higher penetration than linear molecular shaped ones.<br>Negatively charged molecules can easily diffuse. | [42,43]<br>[44]<br>[45] |
| Intravitreal | | Vitreous | Negatively charged molecules (150 KDa) and PEGylated negatively charged particles, with particle size of 200-510 nm can freely penetrate the vitreous. | [9,46] |
| Systemic/oral | | Blood-aqueous barrier | Slightly lipophilic drugs better diffuse across blood-aqueous barrier and obtains the higher aqueous humor uptake index (AHUI) | [47] |
| | | Blood-retina barrier | Cationic lipophilic molecules and aminoacid-mimetic drugs can overcome blood-retina barrier | [48] |

## 2. Diseases affecting the OS

As mentioned before, the lacrimal functional unit works as a complex network to maintain OS homeostasis. Any alteration in the physiological function of this unit may lead to an OS disease. Diseases affecting the OS include a broad spectrum of pathologies that may differ from each other regarding their etiology, but generally present a common pathological condition: The presence of inflammation [49].

In this work, we studied one of the most prevalent OS inflammatory disorders: the dry eye disease (DED). We also studied a less prevalent but more disabling condition that may arise secondary to chronic inflammation: the corneal neovascularization (CN). For a better understanding of both pathologies, we studied their pathological mechanisms from their general pathophysiology to their local effects at the OS.

### 2.1. Pathophysiology of inflammation

Inflammation is an adaptive response caused by noxious stimuli and conditions such as infection and tissue injury. It is generally accepted that a controlled inflammatory response is beneficial because it contributes to restoring tissue homeostasis, but may become harmful if dysregulated or prolonged over time [50].

The acute inflammatory response involves a coordinated cascade of events that begins with the extravasation of plasma components and leukocytes (mainly neutrophils) to the injured tissue. In microbial infections, this initial event is triggered by the tissue-resident macrophages and mast cells that produce different pro-inflammatory mediators (e.g. chemokines, cytokines and eicosanoids) after the pathogen recognition. Those mediators provoke the extravasation of blood components (exudate) that normally are restricted to the blood vessels. Endothelium of the blood vessels plays an active role during this initial stage because it participates in the selective extravasation of neutrophils preventing the leakage of erythrocytes. This selectivity is achieved by the induced endothelial cell expression of surface selectins that specifically bind to integrins and chemokine receptors of leukocytes [51]. Neutrophils, that become activated by direct contact with pathogens or when are exposed to the surrounding cytokines, release the toxic contents of their granules to eliminate the pathogen [52]. The released substances do not discriminate between pathogens and host targets, so it may induce collateral damage to host tissues [53]. An effective acute inflammatory response results in the elimination of the pathogenic agent followed by a resolution and tissue-repair phase. In this phase a shift in the lipid mediators occurs, from pro-inflammatory

eicosanoids to anti-inflammatory lipoxins. Lipoxins, that precludes the recruitment of neutrophils, promotes the recruitment of monocytes and the subsequent tissue remodeling [54]. Other substances such as resolvins, protectins or transforming growth factor-β (TGF-β) contributes to the resolution of the inflammatory status [54]. If the acute inflammatory response is unable to eradicate the pathogen, the inflammation persists and acquires new characteristics. The neutrophils are replaced by macrophages and T lymphocytes. If this response is still insufficient, inflammation may become chronic. Chronic inflammation can result not only from the presence of persistent pathogens, but also from other causes of tissue injury such as autoimmune responses, in which the persistent noxious stimulus are self-antigens [50].

The continuous presence of a stressful stimulus on the OS may contribute to the development of a chronic inflammatory response, as occurs in DED [55]. Pro-inflammatory cytokines, which are secreted by epithelial and endothelial cells in response to the noxious stimulus, promotes the migration of immune cells to the injured tissue [55]. Dendritic cells present in the conjunctiva capture the antigens and migrates to peripheral lymph nodes where they process and present antigenic peptides to T cells. Antigenic presentation in combination with costimulatory molecules result in T cell activation. Activated T lymphocytes migrate from lymph nodes to the inflamed tissue transforming the acute inflammation into a chronic response [55]. If there is no appropriate therapeutic intervention, chronic inflammation of the OS may induce tissue-associated changes, such as edema, neovascularization and fibrosis that seriously deteriorate the patient vision and quality of life [56].

### 2.1.1. Dry eye, an inflammatory OS disease.

Dry Eye Disease (DED) is one of the most common ocular disorders affecting patients worldwide. According to a recent report of the International Dry Eye Workshop (DEWS) [57], the prevalence of symptomatic DED range from 5 to 50%, depending on the criteria of the study. The same report concludes that disease prevalence was higher in women than men, and age and Asian ethnicity are risk factors for suffering this disorder. Studies in Spain and USA using similar criteria revealed that prevalence of symptomatic DED was 18.4% and 14.5%, respectively [57]. The DEWS defines DED as “a multifactorial disease of the tears and ocular surface that results in symptoms of discomfort, visual disturbance, and tear film instability with potential damage to the ocular surface. It is accompanied by increased osmolarity of the tear film and

inflammation of the ocular surface" [58]. Historically, DED was divided in two types: aqueous-deficient dry eye and evaporative dry eye.

***Aqueous-deficient dry eye***

Aqueous-deficient dry eye results from a failure of lacrimal gland secretion due to gland destruction or dysfunction that leads to an altered function of OS epithelia and tear film. Events such as increase in tear osmolarity and production of inflammatory molecules (interleukin (IL)-1β, tumor necrosis factor (TNF-α) and matrix metalloproteinases (MMPs) among many others) happen in this context [59]. This type of DED can be subdivided in two subtypes: Sjögren's syndrome-associated dry eye and non-Sjögren's syndrome dry eye. In Sjögren's syndrome, which is an autoimmune systemic disease that primarily affects function of endocrine glands, both lacrimal and salivary glands are infiltrated by activated T cells causing acinar and duct cell dead and gland hyposecretion [58]. The non-Sjögren's syndrome dry eye is related with other causes of lacrimal system failure such as age-related gland dysfunction, cicatrizing diseases such as trachoma or pemphigoid, and chemical or thermal burns. Certain pathologic conditions such as diabetes mellitus, may cause reflex lacrimal hyposecretion and reduced blinking rate leading to non-Sjögren's syndrome dry eye [60]. It is reported that some systemically administered drugs (i.e. anticholinergic, betablockers) may also induce this type of dry eye [61].

***Evaporative dry eye***

Evaporative dry eye occurs when there is a noticeable loss of the tear film water content in the presence of a normal secretory function of the lacrimal gland system. Causes of evaporative dry eye can be further divided into intrinsic and extrinsic causes. Intrinsic causes include alterations of the lid aperture such as lagophthalmos; reduced blinking rates as occurs in the work environment or in pathologic situations as can be in Parkinson's disease; and Meibomian gland dysfunction (MGD), which is the most common cause of evaporative dry eye [60]. MGD is defined as an abnormal function of Meibomian glands and is correlated either with low- or high-meibum-delivery to the tear film. Alterations in the lipid composition of tear film may result in eye irritation and underlying inflammation [49]. Extrinsic causes of DED include OS diseases such as allergic conjunctivitis or vitamin A deficiency [62]. Other extrinsic factors related with

evaporative dry eye are contact lens wearing [63], or the chronic use of preservative-containing eyedrops [64].

Stern and Pflugfelder propose a holistic conception of DED as a "vicious circle" in which inflammation has the pivotal role (**Figure 2**) [65]. External stimulus (e.g. desiccating environmental stress); changes in tear fluid composition (e.g. MGD); and alterations in the physiologic lacrimal function may result in OS inflammation. These pro-inflammatory stimuli may be exacerbated in patients with autoimmune diseases, such as Sjögren syndrome, because of dysfunction of their immunoregulatory pathways. Exposure of corneal epithelial cells to hyperosmolar conditions results in the activation of stress-induced signaling pathways that ultimately results in the production of pro-inflammatory cytokines (e.g. IL-1 and TNF-α) and MMPs. These mediators can initiate the inflammatory cascade leading to the dysfunction of tear-secreting glands, altered epithelial cell proliferation and ocular surface disease. The presence of certain pro-inflammatory cytokines in the conjunctiva triggers the production of adhesion molecules by vascular and endothelial cells that may lead to extravasation of T lymphocytes that further aggravate the disease. Furthermore, the pro-inflammatory cytokines IL-1, TNF-α and transforming growth factor-β (TGF-β) significantly increase the production of MMPs that, apart from its noxious proteolytic action (degrade tight junctions of corneal epithelium), may activate latent IL-1β, TNF-α and TGF-β. This interaction between pro-inflammatory cytokines and MMPs is capable of creating a cycle of escalating inflammation on the OS. Further advances in the knowledge of this pathology suggest that inflammation and subsequent dysfunction of the lacrimal functional unit triggers an autoimmune reaction in which autoreactive T cells are targeted to the OS where they release pro-inflammatory cytokines that further deteriorate the homeostatic condition [66]. This conception considers DED as an autonomous self-sustaining disease state that is progressively disconnected from its initial causes and may become chronic if there is no appropriate therapeutic intervention.

Given the key role of inflammation in the pathogenesis of DED, the most successful therapeutic approaches are focused in lowering the inflammatory status of OS [65]. Therapies that hydrate ocular surface, such as artificial tears or secretagogues, may exert an indirect anti-inflammatory effect by lowering the tear osmolarity and by reducing the shear forces from blinking. Corticosteroids are often used in acute inflammatory

episodes, but should not be chronically used due to their multiple side effects [67]. Instead, cyclosporine A is commonly used for chronic treatment. This immunosuppressant drug that precludes T lymphocyte activation may decrease apoptosis of epithelial cells on the lacrimal gland and ocular surface [65]. It is also related with increased tear production and corneal barrier reparation [67].

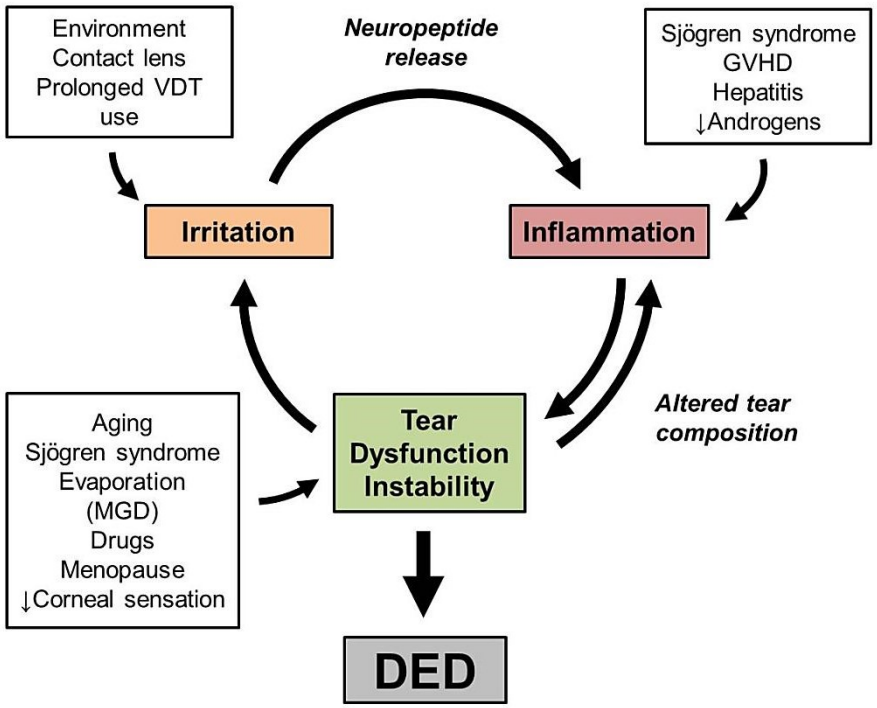


**Figure 2. The vicious circle theory of DED.** Adapted from Stern et al. with permission of Elsevier. DED, dry eye disease; VDT, video display terminal; GVHD, graft vs host disease; MGD, Meibomian gland dysfunction.

## 2.2. Pathophysiology of neovascularization

The development of new blood vessels is essential for life. During the embryonic phase, *de novo* development of blood vessels (vasculogenesis) allows embryo development and growth. In the adult life, the formation of new blood vessels from pre-existing ones (angiogenesis) is essential for repairing processes such as wound healing and post-ischemic tissue restoration. However, when this physiological process is dysregulated, the abnormal development of new blood vessels (neovascularization) may lead to several pathophysiological processes [68].

Angiogenesis is essential in the post-embryonic stage, because tissue growth needs to be accompanied with parallel vasculature expansion. This process involves the differentiation, proliferation and organization of endothelial cells into capillary tubes. Cytokines, cell adhesion molecules and vascular endothelial growth factors contributes to the development of vessel architecture [69]. Angiogenic growth factors, such as vascular endothelial growth factor (VEGF), fibroblast growth factor (FGF) and angiopoietin, control the initiation and regulate the rate and extent of the angiogenic process. Particularly, VEGF is considered the key mediator of angiogenesis. It is a polyvalent peptide capable of promoting endothelial cell proliferation, migration and capillary tube formation [70]. In the mature organism, VEGF expression is limited and there is balance between proangiogenic and antiangiogenic factors. After tissue injury, a combination of cytokines, growth factors and other molecules is released stimulating angiogenesis directly or indirectly via VEGF. This process is essential for tissue repairing. It is reported that certain cytokines such as platelet derived growth factor, TNF-α, TGF-β or IL-1 may stimulate VEGF production [71,68]. However, in some pathologic circumstances such as cancer and diabetes mellitus, the upregulated VEGF expression result in pathological consequences [68]. It is reported that VEGF production is upregulated in chronic wounds or in chronic inflammatory disorders such as rheumatoid arthritis and lupus erythematosus [72,73].

Ocular neovascularization is one of the main causes of severe vision loss. It can affect different eye structures including the retina, choroid and cornea. CN is a serious clinical problem arising from chronic pathologic processes such as hypoxia or inflammation. As occurs with other angiogenic processes, it is known the active participation VEGF in CN [72]. It is demonstrated that VEGF stimulation potently induces CN whereas VEGF inhibition potently reduces CN [74,75]. It is also demonstrated the presence of elevated levels of VEGF in patients with CN [76,77]. These evidences together, point to the central role of VEGF in the pathogenesis of this disease.

### 2.2.1. Corneal neovascularization (CN)

The cornea is an avascular and transparent structure, but under certain pathologic circumstances the ingrowth of blood vessels from the limbal vascular plexus may occur. This angiogenic process, referred as corneal neovascularization (CN), seriously compromises the patient visual function, leading to total vision loss in the worst-case scenario [78,79]. Although the global epidemiology of CN is difficult to know, a report of the General Eye Service of the Massachusetts Eye and Ear Infirmary (1996)

estimates its prevalence in 4.14% [80]. CN may be propitiated by variety of causes including corneal allograft rejection, chronic infection, chemical/mechanical injury, limbal stem cell deficiency and extended contact lens wearing [78].

Although the exact mechanisms of CN are not clear yet, it is considered that inflammation plays a crucial role in its etiopathogenesis (**Figure 3**) [74,81,82]. In physiological conditions, cornea remains avascular due to the balance between antiangiogenic and proangiogenic factors. Pathological circumstances such as those mentioned above, provoke an inflammatory response that may lead to unbalance in behalf to proangiogenic factors. Corneal stromal keratocytes, epithelial cells, and inflammatory cells release proangiogenic factors such as VEGF that promote the activation, migration and proliferation of vascular endothelial cells [83]. Conjunctival fibroblasts and epithelial cells also showed upregulation of VEGF production in the presence of pro-inflammatory stimulus [84]. VEGF may act as a chemoattractant for immune cells, particularly macrophages. Once at the site of injury, these cells are able to amplify the angiogenic cascade by secreting more VEGF [74,85]. Other substances that actively participate in the CN are the MMPs. These proteolytic enzymes allow the angiogenic process by degrading the extracellular matrix surrounding the new sprouting capillaries. During this process, they release matrix-bound cytokines, growth factors and latent signaling molecules that magnify the angiogenic process [83]. It is documented that MMP-2 and MMP-9 were significantly elevated in a mouse model of neovascularization, showing direct interdependence between their levels and the underlying inflammatory status [81]. Other inflammatory mediators that participate in the CN process are cytokines such as IL-1 and IL-6. IL-1 is a pleiotropic cytokine involved in the acute inflammatory response. It facilitates immune cell activation, upregulation of cell adhesion molecules and chemoattraction [86]. It is reported that the blockade of IL-1 after corneal injury, translate into a significantly reduced angiogenic response [87]. IL-6 is also a multifunctional cytokine that plays a central role in host defense. It participates in immune and hematopoietic activities and is also a potent inductor of the acute inflammatory phase [88]. It is though that the angiogenic properties of IL-6 are mediated through a VEGF-dependent pathway. This is because IL-6 experimentally induced CN can be precluded by using VEGF antagonists [89].

Treatment of CN is focused in eliminating existing vessels and preventing the formation of new vasculature. Non-steroidal anti-inflammatory drugs and corticosteroids are commonly used to reduce inflammation and neovascularization [90,91]; laser and fine

needle diathermy are used to obliterate the invading vessels [92,93]; and amniotic membrane transplantation may reverse the conjunctival-like phenotype of vascularized areas to a cornea-like phenotype [94]. In addition, the recent use of anti-VEGF agents and immunosuppressant drugs with antiangiogenic properties may help to treat CN from its inner core [95].

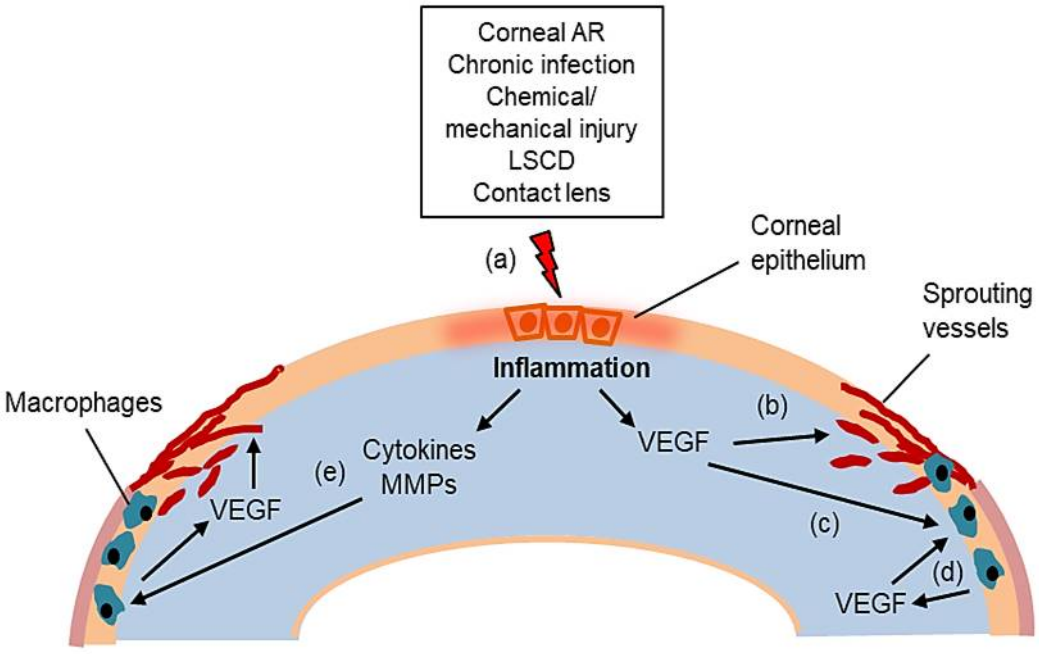


**Figure 3. Inflammatory ethiopathogenesis of CN.** (a) Some pathologic circumstances can trigger an inflammatory response in the cornea that leads to the release of pro-inflammatory and pro-angiogenic mediators. (b) The key pro-angiogenic mediator, VEGF, directly activate vascular endothelial cell activation and proliferation. (c) VEGF also acts as a chemoattractant for macrophages, which release more VEGF amplifying the angiogenic cascade. (e) Pro-inflammatory cytokines and MMPs participate in the recruitment inflammatory cells via direct and indirect VEGF-pathway. AR, allograft rejection; LSCD, limbal stem cell deficiency; VEGF, vascular endothelial growth factor; MMPs, matrix metalloproteinases. Schematic created by Jesús Álvarez-Trabado.

## 3. Topical ocular drug delivery

Topical administration is the preferred and most used ocular drug delivery route for the treatment of anterior segment diseases. Advantages such as ease of application, rapid and local effect of the administered drug, and low cost of production allow topical dosage forms represent around 90% of the marketed ophthalmic formulations [96,97]. Nonetheless conventional topically-applied formulations, such as solutions, suspensions, ointments and emulsions, present inherent disadvantages such as the need for frequent dose administration (which has an impact in patient adherence to treatment), associated ocular discomfort and a major common concern: The low drug bioavailability at the site of action. As mentioned above, ocular drug bioavailability obtained with conventional dosage forms is less than 5%. Efforts in designing novel topical drug delivery systems are focused in enhancing this parameter by two complementary technological approaches: first, by increasing the formulation residence time in the precorneal area and second, by promoting drug penetration through OS structures [97-99]. Main approaches in the development of conventional and novel topically-applied drug delivery systems are briefly summarized below.

### 3.1. Conventional drug delivery systems

#### 3.1.1. Eye drops solutions

Conventional eye drops in form of solution represents around 76% of the approved ophthalmic products in the US [100]. From a pharmacokinetic perspective, eye drop solutions provoke a pulse of drug penetration through cornea immediately after instillation. Then, drug concentration quickly declines due to the formulation clearance by the physiological precorneal factors [97]. In this regard, various additives had been used to ameliorate formulations biopharmaceutical properties. Viscosity enhancers, such as natural gums, cellulose derivatives (i.e. hydroxypropyl methylcellulose) or polyvinyl alcohols [101] are used to extend the formulation contact time with the precorneal area, minimizing drug clearance. Penetration promotors such as benzalkonium chloride or polyoxyethylene glycol-derived surfactants are used to enhance the trans-corneal drug penetration [102]. In a lesser extent, cyclodextrins are used to formulate poor water-soluble drugs such as corticosteroids in an aqueous vehicle that can be administered drop-wise [103].

### 3.1.2. Eye drops suspensions

Eye drops in form of *suspension* are the more pragmatic approach to topically-administer water insoluble drugs, representing nearly the 10% of approved ophthalmic dosage forms [100]. In this case, the insoluble drug is finely divided into particles which can be dispersed into an aqueous or non-aqueous vehicle. Particle size is the main physicochemical aspect that determine the biopharmaceutical properties of suspensions [104]. Larger particles (30-40 μm) are better retained in the precorneal area but are often associated with eye irritation and discomfort, while smaller particles present a faster drug dissolution rate but the reduced size allows its quickly clearance from the OS [104]. Thus, an optimum particle size might be determined in each case.

One representative example of the importance of the physicochemical optimization is the commercialized formulation ILEVRO™ (2012; Alcon Research, Ltd., Fort Worth, TX). It is a 0.3% nepafenac eye drop suspension approved in USA and Europe for the treatment of pain and inflammation after cataract surgery. ILEVRO™ is a reformulation of the previously marketed 0.1% NEVANAC® ophthalmic suspension (2005; Alcon Research, Ltd., Fort Worth, TX) with the objective of enhancing ocular nepafenac bioavailability [105][106]. This optimized formulation consists in higher drug concentration, reduction in drug particle size, and incorporation of guar gum and carboxymethyl cellulose as viscosity enhancers [105].

### 3.1.3. Ointments

Ophthalmic ointments represent around the 10% of ophthalmic dosage forms in the USA market [100]. Ointment-based formulations consist in mixtures of semisolid hydrocarbon bases that have the melting point at physiological temperature. The oleaginous white petrolatum is the most commonly used semisolid base in ophthalmic drug delivery. Ophthalmic ointments are commonly used for administration of water insoluble drugs, such as corticosteroids, antibiotics or combinations of both [107]. These formulations contribute to ameliorate drug bioavailability either by increasing its residence time or providing a sustained drug release from the ointment to the ocular structures [107]. However, ointments present low patient acceptance due to the administration-associated ocular discomfort and blurred vision.

### 3.1.4. Emulsions

Emulsions represent approximately the 1% of total approved ophthalmic dosage forms [100]. Although two main types of emulsion are used in drug delivery, namely oil-in-water (O/W) and water-in-oil emulsions (W/O), o/w emulsions are preferred for

ocular drug delivery because of its better ocular tolerability and less irritancy [97]. In (O/W) emulsions, the drug is dissolved in the oil phase which is simultaneously dispersed and stabilized in the surrounding aqueous phase. This biphasic composition allows the easy drop-wise administration of the drug.

One of the most well-known ophthalmic emulsion systems is Restasis® (Allergan, Irvine, CA, USA) that was approved by FDA in 2002 for the treatment of dry eye disease [108]. This o/w formulation is formed by a cyclosporine-loaded castor oil organic phase that is dispersed and stabilized in an aqueous phase containing surfactants and other polymers. In the EU, an alternative CsA emulsion system is commercialized under the name of Ikervis® (Santen Inc, Emeryville, CA, USA) [108]. This cationic nanoemulsion is composed by medium chain triglycerides acting as the cyclosporine solubilizing agent. This organic phase is dispersed and stabilized in an aqueous phase containing a mixture of different surfactants, including cetalkonium chloride that provides positive surface charge to the emulsion particles. The positive surface charge may increase the formulation contact time due to electrostatic interactions with the negatively charged precorneal area [109].

## 3.2. Novel drug delivery systems

### 3.2.1. *In situ* gelling systems

*In situ* gelling systems are formed by natural, semisynthetic or synthetic polymers that can undergo a sol-gel transition in the presence of specific environment stimuli such as temperature, pH or ionic strength [110]. Main goal of these systems is to increase drug bioavalability by increasing drug retention time in the precorneal area [111]. Thermoresponsive gelling systems contains polymers such as poly (N-isopropylacrilamide), poloxamers (Pluronics®) or cellulose derivatives such as methylcellulose, carboxymethylcellulose and hydroxypropyl methylcellulose, that experience gelation when formulation reaches physiologic ocular temperature.[110]. pH-responsive gelling systems are formed by polymers such as cellulose acetate phthalate or carbomers (polyacrilic acid derivatives) that experience the sol-gel transition after formulation reaches the physiological pH. The underlying changes in the ionization state leads to changes in polymer conformation and solubility [110]. Ionic-responsive gelling systems contain natural polymers such as gellan or xanthan gum that undergo gelation in the presence of monovalent or divalent cations found in the tear film [110].

### 3.2.2. Ocular inserts

Ocular inserts are solid or semisolid drug-loaded devices that are placed into the conjunctival sac, presenting size and shape specifically designed for ophthalmic application. These devices offer several advantages over conventional formulations such as the extended ocular residence time and the controlled cession of the therapeutic substance [112]. The major drawback of inserts is the poor patient acceptance due to the foreign body sensation [112]. Ophthalmic inserts can be classified as soluble or insoluble [112]:

***Soluble inserts***

Soluble inserts are the oldest class of ophthalmic inserts, in which whole system is dissolved in the presence of tears. The main advantage of soluble inserts is that they not need to be removed from the application site. The main drawback is related with their limited time of action, which usually is less than 24 hours [113]. The unique soluble insert nowadays commercialized is Lacrisert® (Aton Pharma, Lawrenceville, NJ, USA) a hydroxypropyl cellulose device approved for the treatment of dry eye disease [114]. NOSD® (Smith and Nephew Pharmaceuticals, Harlow, Essex, UK) is another soluble device made of water-soluble polyvinyl-alcohol that only was approved for diagnostic uses [114].

***Insoluble inserts***

Insoluble inserts are made by water insoluble polymers forming different device architectures (e.g. oval- or ring-shaped) that allow the controlled release of the entrapped drug. Drug cession from insert can be driven either by diffusion as by osmotic mechanisms [113]. Ocusert® (Alza Corporation, Mountain View, CA, USA) was the first commercialized insoluble device. It consisted in two ethylene-vinyl acetate membranes filled with pilocarpine and surrounded by a titanium dioxide ring. Although this device extended the anti-glaucoma action for a week, the frequent foreign body sensation perceived by patients caused its drop out from the market [114]. Other insoluble ophthalmic inserts are Mydrasert® (Thea Laboratories, Clermont-Ferrand, France), a tropicamide/phenylephrine-loaded ethyl cellulose rod-shaped device used in clinic to induce mydriasis before surgery, and Helios™ (ForSight Vision5 Inc., Menlo Park, CA, USA) a bimatoprost-loaded ring-shaped device used in the glaucoma treatment, currently in phase III of clinical trials [114].

### 3.2.3. Medicated contact lenses

Contact lenses are curved-shape devices which are placed over cornea to correct refractive errors of the eye. Apart from its primary function, those devices can be also used as drug delivery systems [115]. Due to its opened structure (often a hydrogel) those devices can be easily drug-loaded by simply soaking in a drug solution. Once drug-loaded contact lens is placed onto the eye, drug slowly diffuses into the post-lens tear film being available to penetrate trough the trans-corneal route. However this "soak and release" approach is related with short drug release times. Alternative solutions such as entrapment of drug-laden nanoparticles and molecular imprinting are promising approaches to extend drug release [115].

### 3.2.4. Nanotechnology-based systems

The main objective of nanotechnology-based ocular systems is to enhance drug therapeutic efficacy by increasing its bioavailability without compromising patient safety and compliance [116]. In addition, targeted delivery, controlled drug release and reduced dose frequency are key features that any novel drug nanosystem might accomplish. In the last decades, multiple nanosystems have been developed for ocular drug delivery [117] being nanomicelles, liposomes, dendrimers and nanoparticles the most studied systems (**Figure 4**).

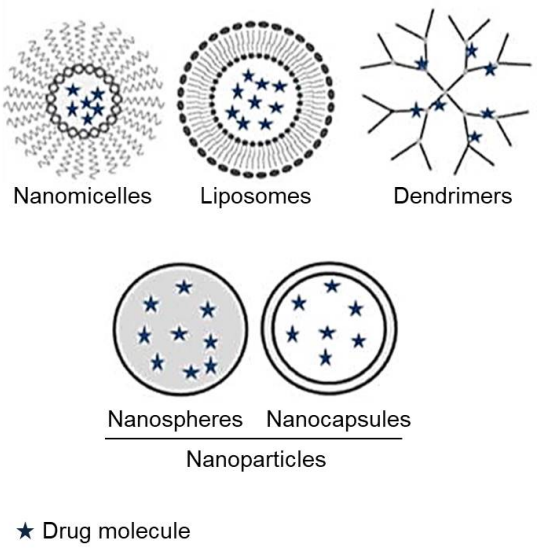


**Figure 4. Schematic representation of main nanotechnology-based ocular drug delivery systems.** Adapted from Patel et al. [97] with permission of Baishideng Publishing Group Inc.

***Nanomicelles***

Nanomicelles are one of the most commonly used carrier systems for ophthalmic administration. They are simply structures made of amphiphilic substances (i.e. surfactants) presenting a hydrophobic core and a hydrophilic shell. This conformation allows dissolving poor water soluble drugs such as corticoids [118] or immunosupressants [119] into a clear aqueous formulation. Cationic chitosan-coated nanomicelles were developed as a strategy for extend dexamethasone permanence into the precorneal area [120]. These nanosystems showed a 1.7-fold increase in ocular drug biovailability compared with eye drops.

***Liposomes***

Liposomes are vesicular structures that comprise one or more phospholipid bilayers enclosing one or more aqueous compartments. Depending on their dimension and number of lipid bilayers they can be classified as single-, multi- or unilamellar liposomes. Liposomes present the advantage that can encapsulate either hydrophilic or lipophilic molecules due its biphasic aqueous/lipid nature [116]. Nonetheless technological issues such as poor loading capacity and physical stability or the impossibility of sterilization by autoclaving, seriously limit its commercial viability. As occurred in the case of nanomicelles, the use of cationic surface-modified liposomes was reported as an effective strategy to enhance ocular drug bioavailability [121].

***Dendrimers***

Dendrimers are polymeric highly-branched nanosized structures that can be used for ocular drug delivery purposes. These nanosystems are highly tunable carriers that can entrap both lipophilic and hydrophilic drugs [122]. *In vivo* studies showed that poly(amidoamine) dendrimers enhanced fluorescein residence time and ocular bioavailability of pilocarpine and tropicamide [123]. Posterior work demonstrated that those type of dendrimers can strongly interact with tear film mucins confirming their potential to extend drug contact time with the OS, and hence its bioavailability [124].

***Nanoparticles***

Nanoparticles are colloidal structures with size ranging from 10 to 1000 nm that can be made of a great variety of materials. For ophthalmic use, nanoparticles are generally composed of natural or synthetic polymers (e.g. chitosan, gelatin, albumin,

poly(lactic acid), poly(epsilon-caprolactone) and lipids (e.g. triglycerides, fatty acids, steroids). In both cases, drug can be homogeneously distributed through the nanoparticle matrix (i.e. nanospheres) or enclosed inside a polymeric shell (i.e. nanocapsules).

Composition and physicochemical characteristics of nanoparticles can be specifically tuned to obtain the most appropriate carrier system. Technological approaches such as nanoparticle coating (second generation of nanoparticles) or specific ligand functionalization (third generation of nanoparticles) can be used to maximize interaction with ocular structures [125].

One of the most followed strategies is the nanoparticle coating with positively charged substances such as chitosan [126-128] (**Figure 5a**). Calvo et al. observed that chitosan-coated poly-epsilon-caprolactone nanoparticles showed higher indomethacin corneal penetration than its poly-l-lysine-coated version, having both nanosystems similar physicochemical characteristics [129]. They attributed this difference to the specific nature of chitosan that increased contact time with negatively charged corneal surface and enhanced nanoparticles uptake by corneal cells. It is reported that chitosan acts not only as a mucoadhesive polymer, but also alters transcorneal permeability by opening the tight junctions present between epithelial cells [130].

Alternatively to the paradigm of cationic chitosan coating, other natural polymers have been evaluated to enhance biopharmaceutical properties of nanoparticles, as can be the case of hyaluronic acid (**Figure 5b**). Hyaluronic acid is a natural polymer that consists in repeating units of D-glucuronic acid and N-acetyl-D-glucosamine. This polysaccharide possesses strong mucoadhesive properties that can be exploited in ocular drug delivery [131]. Hyaluronic acid-coated polycaprolactone nanospheres developed by Barbault-Foucher et al. were the first attempt to hyaluronic acid-coating [132]. Hyaluronic acid was electrostatically adsorbed onto nanoparticle surface thanks to the presence of cationic surfactants forming the nanostructures. Further studies with these nanosystems demonstrated that hyaluronic coating enhanced *in vivo* cyclosporine corneal penetration in comparison with the same uncoated nanoparticles [133]. Although this enhancement was first exclusively attributed to mucoadhesive properties of hyaluronic acid, further studies demonstrated that hyaluronic acid-coated nanosystems can specifically interact with hyaluronic acid receptors present in corneal cells favoring nanoparticles uptake [134,135].

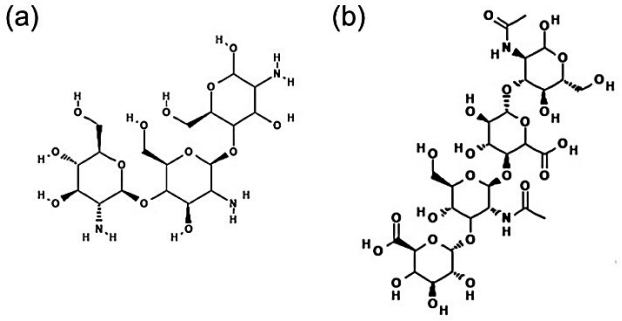


**Figure 5. Molecular structures of (a) deacetylated chitosan and (b) hyaluronic acid.** Structures were obtained from the PubChem database [136][137]. Permitted by PubChem**.**

## Nanoparticles in the treatment of OS diseases

### *Inflammation*

As already mentioned, chronic inflammation is the most common pathologic condition present in different OS diseases. Majority of nanoparticle-based research therapies are focused in enhancing ocular bioavailability of anti-inflammatory substances such as corticoids or non-steroidal anti-inflammatory drugs. Nanoparticles containing hydrocortisone [138], dexamethasone [139], indomethacin [140] or flurbiprofen [141], were successfully developed showing promising results. Sharma et al. developed poly-epsilon-caprolactone nanoparticles loaded with the anti-inflammatory agent celecoxib [142]. Those nanosystems showed particle size under 200 nm, high drug entrapment efficiency (~97%) and controlled (zero-order release kinetics) and sustained (<75% released after 8 hours) drug release. Developed nanoparticles were also more effective in the treatment of an *in vivo* model of arachidonic acid-induced ocular inflammation than the aqueous suspension. Corneal hydration level after treatment was found within the permissible ranges suggesting acceptable ocular tolerability.

### *Dry eye disease (DED)*

DED is one of the most challenging OS diseases due its multifactorial etiology and high prevalence. Therapeutic efforts are focused in the treatment of key pathophysiologic conditions such as inflammation or tear film instability. In this respect, the most promising nanoparticle-based therapeutic approaches includes cyclosporine-loaded [143,144] and genetic material-loaded nanoparticles [145,146]. Liu

et al. developed cyclosporine-loaded poly(lactic acid)-dextran nanoparticles modified with phenylboronic acid [147]. This grafting moiety provided nanoparticles with intense mucoadhesive properties extending its OS residence time beyond 24 hours. Therapeutic efficacy of nanoparticles was evaluated in an experimentally induced *in vivo* mouse model of dry eye. Once-a-week dosing of 0.005% to 0.01% CsA in nanoparticles demonstrated elimination of inflammation signs and recovery of OS goblet cells numbers after a month treatment, while thrice daily administration of reference formulation Restasis® (0.05% CsA) only showed elimination of inflammation without goblet cell numbers recovery.

***Corneal neovascularization***

Corneal neovascularization is a highly disabling disease that seriously jeopardizes patient's quality of life. The disequilibrium between antiangiogenic and proangiogenic factors at the OS causes the ingrowth of blood vessels from conjunctiva into the cornea that dramatically alters visual function even leading to total corneal blindness. Different antiangiogenic drugs have been formulated into nanoparticle formulations including anti-VEGF molecules such as bevacizumab [148] or apatinib [149]; natural compounds such as curcumin [150] or epigalloccatechin-gallate [151]; and genetic material [152]. Chang et al. developed epigalloccatechin-gallate-loaded gelatin nanoparticles functionalized with a hyaluronic acid-peptide conjugate for targeting vascular endothelial cells [151]. Nanoparticles presented size under 200 nm, positive zeta potential, high epigalloccatechin-gallate entrapment efficiency and sustained drug release beyond 30 hours. *In vitro* studies demonstrated that functionalized nanoparticles inhibited proliferation of human umbilical vein endothelial cells at low drug concentrations when compared with the free drug or the non-functionalized nanoparticles. When functionalized nanoparticles were topically administered to a corneal neovascularization mouse model, fewer and thinner vessels were observed demonstrating the efficacy and targeting capacity of these nanoparticles.

Despite these nanotechnology-based advances, the therapeutic potential of NPs has not yet been exploited in clinic, probably due to the combination of safety concerns that still arise in the nanotechnology field and the need for more consensus on the most appropriate technological properties that need to gather the new NP-based ocular drug delivery systems.

**References**

[1] R.A. Armstrong, R.P. Cubbidge, The Eye and Vision, in: V.R. Preedy (Ed.), Handb. Nutr. Diet Eye, Elsevier, San Diego, 2014: pp. 3–9. doi:10.1016/B978-0-12-401717-7.00001-0.

[2] K. Trier, The Sclera, in: J. Fischbarg (Ed.), Biol. Eye, Elsevier, 2005: pp. 353–373. doi:10.1016/S1569-2590(05)10013-5.

[3] L.A. Remington, Uvea, in: L.A. Remington (Ed.), Clin. Anat. Physiol. Vis. Syst., Third Edit, Elsevier, Saint Louis, 2012: pp. 40–60. doi:10.1016/B978-1-4377-1926-0.10003-7.

[4] R.G. Gregg, M.A. McCall, S.C. Massey, Function and Anatomy of the Mammalian Retina, in: S.J. Ryan, S.R. Sadda, D.R. Hinton, A.P. Schachat, S.R. Sadda, C.P. Wilkinson, P. Wiedemann, A.P. Schachat (Eds.), Retina, Fifth Edit, Elsevier, London, 2013: pp. 360–400. doi:10.1016/B978-1-4557-0737-9.00015-1.

[5] M.E. Stern, R.W. Beuerman, R.I. Fox, J. Gao, A.K. Mircheff, S.C. Pflugfelder, The pathology of dry eye: the interaction between the ocular surface and lacrimal glands, Cornea. 17 (1998) 584–9.

[6] S. Barabino, Y. Chen, S. Chauhan, R. Dana, Ocular surface immunity: Homeostatic mechanisms and their disruption in dry eye disease, Prog. Retin. Eye Res. 31 (2012) 271–285. doi:10.1016/j.preteyeres.2012.02.003.

[7] D. Huang, Y.-S. Chen, I.D. Rupenthal, Overcoming ocular drug delivery barriers through the use of physical forces, Adv. Drug Deliv. Rev. (2017). doi:10.1016/j.addr.2017.09.008.

[8] R. Gaudana, H.K. Ananthula, A. Parenky, A.K. Mitra, Ocular Drug Delivery, AAPS J. 12 (2010) 348–360. doi:10.1208/s12248-010-9183-3.

[9] B.T. Käsdorf, F. Arends, O. Lieleg, Diffusion Regulation in the Vitreous Humor, Biophys. J. 109 (2015) 2171–2181. doi:10.1016/j.bpj.2015.10.002.

[10] H. Kim, S.B. Robinson, K.G. Csaky, Investigating the Movement of Intravitreal Human Serum Albumin Nanoparticles in the Vitreous and Retina, Pharm. Res. 26 (2009) 329–337. doi:10.1007/s11095-008-9745-6.

[11] K.G. Falavarjani, Q.D. Nguyen, Adverse events and complications associated with intravitreal injection of anti-VEGF agents: a review of literature., Eye (Lond). 27 (2013) 787–94. doi:10.1038/eye.2013.107.

[12] S. Reimondez-Troitino, N. Csaba, M.J. Alonso, M. de la Fuente, Nanotherapies for the treatment of ocular diseases, Eur. J. Pharm. Biopharm. 95 (2015) 279–293. doi:10.1016/j.ejpb.2015.02.019.

[13] J. Alvarez-Trabado, Y. Diebold, A. Sanchez, Designing lipid nanoparticles for topical ocular drug delivery, Int. J. Pharm. 532 (2017). doi:10.1016/j.ijpharm.2017.09.017.

[14] S. Duvvuri, S. Majumdar, A.K. Mitra, Role of metabolism in ocular drug delivery., Curr. Drug Metab. 5 (2004) 507–515. doi:10.2174/1389200043335342.

[15] T.J. Mikkelson, S.S. Chrai, J.R. Robinson, Altered bioavailability of drugs in the eye due to drug-protein interaction., J. Pharm. Sci. 62 (1973) 1648–1653. doi:10.1002/jps.2600621014.

[16] M.S. Norn, Tear secretion in normal eyes, Acta Ophthalmol. 43 (2009) 567–573. doi:10.1111/j.1755-3768.1965.tb03693.x.

[17] R. Agarwal, I. Iezhitsa, P. Agarwal, N.A. Abdul Nasir, N. Razali, R. Alyautdin, N.M. Ismail, Liposomes in topical ophthalmic drug delivery: an update, Drug Deliv. 23 (2014) 1–17. doi:10.3109/10717544.2014.943336.

[18] L.G. Martini, J.K. Embleton, R.J. Malcolmson, C.G. Wilson, The use of small volume ocular sprays to improve the bioavailability of topically applied ophthalmic drugs, Eur. J. Pharm. Biopharm. 44 (1997) 121–126. doi:10.1016/S0939-6411(97)00071-4.

[19] A.O. Eghrari, S.A. Riazuddin, J.D. Gottsch, Overview of the Cornea, in: J.F. Hejtmancik, J.M. Nickerson (Eds.), Mol. Biol. Eye Dis., Academic Press, 2015: pp. 7–23. doi:10.1016/bs.pmbts.2015.04.001.

[20] M. Malhotra, D.K. Majumdar, Permeation through cornea., Indian J. Exp. Biol. 39 (2001) 11–24.

[21] K.M. Meek, C. Knupp, Corneal structure and transparency, Prog. Retin. Eye

Res. 49 (2015) 1–16. doi:10.1016/j.preteyeres.2015.07.001.

[22] A.J. Hertsenberg, J.L. Funderburgh, Stem Cells in the Cornea, in: J.F. Hejtmancik, J.M. Nickerson (Eds.), Mol. Biol. Eye Dis., Academic Press, 2015: pp. 25–41. doi:10.1016/bs.pmbts.2015.04.002.

[23] K. Hosoya, V.H.L. Lee, K.-J. Kim, Roles of the conjunctiva in ocular drug delivery: a review of conjunctival transport mechanisms and their regulation, Eur. J. Pharm. Biopharm. 60 (2005) 227–240. doi:10.1016/j.ejpb.2004.12.007.

[24] M.A. Watsky, M.M. Jablonski, H.F. Edelhauser, Comparison of conjunctival and corneal surface areas in rabbit and human, Curr. Eye Res. 7 (1988) 483–486. doi:10.3109/02713688809031801.

[25] W. Wang, H. Sasaki, D.S. Chien, V.H. Lee, Lipophilicity influence on conjunctival drug penetration in the pigmented rabbit: a comparison with corneal penetration., Curr. Eye Res. 10 (1991) 571–579. doi:10.3109/02713689109001766.

[26] A.J. Huang, S.C. Tseng, K.R. Kenyon, Paracellular permeability of corneal and conjunctival epithelia, Invest. Ophthalmol. Vis. Sci. 30 (1989) 684–9.

[27] Y. Shikamura, Y. Yamazaki, T. Matsunaga, T. Sato, A. Ohtori, K. Tojo, Hydrogel Ring for Topical Drug Delivery to the Ocular Posterior Segment, Curr. Eye Res. 41 (2016) 653–661. doi:10.3109/02713683.2015.1050738.

[28] I. Ahmed, T.F. Patton, Importance of the noncorneal absorption route in topical ophthalmic drug delivery, Invest. Ophthalmol. Vis. Sci. 26 (1985) 584–7.

[29] D. Achouri, K. Alhanout, P. Piccerelle, V. Andrieu, Recent advances in ocular drug delivery, Drug Dev. Ind. Pharm. 39 (2013) 1599–1617. doi:10.3109/03639045.2012.736515.

[30] T.W. Olsen, S.Y. Aaberg, D.H. Geroski, H.F. Edelhauser, Human sclera: thickness and surface area., Am. J. Ophthalmol. 125 (1998) 237–41.

[31] M.A. Grimaudo, E. Tratta, S. Pescina, C. Padula, P. Santi, S. Nicoli, Parameters affecting the transscleral delivery of two positively charged proteins of comparable size, Int. J. Pharm. 521 (2017) 214–221. doi:10.1016/j.ijpharm.2017.02.044.

[32] J.G. Cunha-Vaz, The blood-ocular barriers: past, present, and future, Doc. Ophthalmol. 93 (1997) 149–57.

[33] M. Coca-Prados, The Blood-Aqueous Barrier in Health and Disease, J. Glaucoma. 23 (2014) S36–S38. doi:10.1097/IJG.0000000000000107.

[34] J. Barar, A.R. Javadzadeh, Y. Omidi, Ocular novel drug delivery: impacts of membranes and barriers, Expert Opin. Drug Deliv. 5 (2008) 567–581. doi:10.1517/17425247.5.5.567.

[35] J. Lee, R.M. Pelis, Drug Transport by the Blood-Aqueous Humor Barrier of the Eye, Drug Metab. Dispos. 44 (2016) 1675–1681. doi:10.1124/dmd.116.069369.

[36] E.A. Runkle, D.A. Antonetti, The blood-retinal barrier: structure and functional significance, Methods Mol. Biol. 686 (2011) 133–48. doi:10.1007/978-1-60761-938-3_5.

[37] M. Campbell, P. Humphries, The blood-retina barrier: tight junctions and barrier modulation, Adv. Exp. Med. Biol. 763 (2012) 70–84.

[38] L. Pitka¨nen, V.-P. Ranta, H. Moilanen, A. Urtti, Permeability of Retinal Pigment Epithelium: Effects of Permeant Molecular Weight and Lipophilicity, Investig. Opthalmology Vis. Sci. 46 (2005) 641. doi:10.1167/iovs.04-1051.

[39] N.M. Davies, Biopharmaceutical considerations in topical ocular drug delivery, Clin. Exp. Pharmacol. Physiol. 27 (2000) 558–62.

[40] A. Edward, M.R. Prausnitz, Predicted permeability of the cornea to topical drugs, Pharm. Res. 18 (2001) 1497–508.

[41] M.R. Prausnitz, J.S. Noonan, Permeability of cornea, sclera, and conjunctiva: a literature analysis for drug delivery to the eye, J. Pharm. Sci. 87 (1998) 1479–88.

[42] T.W. Olsen, H.F. Edelhauser, J.I. Lim, D.H. Geroski, Human scleral permeability. Effects of age, cryotherapy, transscleral diode laser, and surgical thinning, Invest. Ophthalmol. Vis. Sci. 36 (1995) 1893–903.

[43] J. Ambati, C.S. Canakis, J.W. Miller, E.S. Gragoudas, A. Edwards, D.J. Weissgold, I. Kim, F.C. Delori, A.P. Adamis, Diffusion of high molecular weight

compounds through sclera., Invest. Ophthalmol. Vis. Sci. 41 (2000) 1181–5.

[44] D.H. Geroski, H.F. Edelhauser, Transscleral drug delivery for posterior segment disease, Adv. Drug Deliv. Rev. 52 (2001) 37–48. doi:10.1016/S0169-409X(01)00193-4.

[45] N.P.S. Cheruvu, U.B. Kompella, Bovine and Porcine Transscleral Solute Transport: Influence of Lipophilicity and the Choroid–Bruch's Layer, Investig. Opthalmology Vis. Sci. 47 (2006) 4513. doi:10.1167/iovs.06-0404.

[46] Q. Xu, N.J. Boylan, J.S. Suk, Y.-Y. Wang, E.A. Nance, J.-C. Yang, P.J. McDonnell, R.A. Cone, E.J. Duh, J. Hanes, Nanoparticle diffusion in, and microrheology of, the bovine vitreous ex vivo, J. Control. Release. 167 (2013) 76–84. doi:10.1016/j.jconrel.2013.01.018.

[47] R. Toda, K. Kawazu, M. Oyabu, T. Miyazaki, Y. Kiuchi, Comparison of Drug Permeabilities Across the Blood–Retinal Barrier, Blood–Aqueous Humor Barrier, and Blood–Brain Barrier, J. Pharm. Sci. 100 (2011) 3904–3911. doi:10.1002/jps.22610.

[48] K. Hosoya, M. Tomi, M. Tachikawa, Strategies for therapy of retinal diseases using systemic drug delivery: relevance of transporters at the blood–retinal barrier, Expert Opin. Drug Deliv. 8 (2011) 1571–1587. doi:10.1517/17425247.2011.628983.

[49] J.M. Biber, Classification of Ocular Surface Disease, in: E.J. Holland, M.J. Mannis, W.B. Lee (Eds.), Ocul. Surf. Dis. Cornea, Conjunctiva Tear Film, Elsevier, London, 2013: pp. 35–44. doi:10.1016/B978-1-4557-2876-3.00006-7.

[50] R. Medzhitov, Origin and physiological roles of inflammation, Nature. 454 (2008) 428–435. doi:10.1038/nature07201.

[51] J.S. Pober, W.C. Sessa, Evolving functions of endothelial cells in inflammation, Nat. Rev. Immunol. 7 (2007) 803–815. doi:10.1038/nri2171.

[52] C. Nathan, Neutrophils and immunity: challenges and opportunities, Nat. Rev. Immunol. 6 (2006) 173–182. doi:10.1038/nri1785.

[53] C. Nathan, Points of control in inflammation, Nature. 420 (2002) 846–852. doi:10.1038/nature01320.

[54] C.N. Serhan, J. Savill, Resolution of inflammation: the beginning programs the

end, Nat. Immunol. 6 (2005) 1191–1197. doi:10.1038/ni1276.

[55] M.E. Stern, K.F. Siemasko, J. Gao, M. Calonge, J.Y. Niederkorn, S.C. Pflugfelder, Evaluation of ocular surface inflammation in the presence of dry eye and allergic conjunctival disease., Ocul. Surf. 3 (2005) S161-4.

[56] M. Friedlander, Fibrosis and diseases of the eye, J. Clin. Invest. 117 (2007) 576–586. doi:10.1172/JCI31030.

[57] F. Stapleton, M. Alves, V.Y. Bunya, I. Jalbert, K. Lekhanont, F. Malet, K.-S. Na, D. Schaumberg, M. Uchino, J. Vehof, E. Viso, S. Vitale, L. Jones, TFOS DEWS II Epidemiology Report, Ocul. Surf. 15 (2017) 334–365. doi:10.1016/j.jtos.2017.05.003.

[58] DEWS, The definition and classification of dry eye disease: report of the Definition and Classification Subcommittee of the International Dry Eye WorkShop (2007)., Ocul. Surf. 5 (2007) 75–92.

[59] A. Enríquez-de-Salamanca, S. Bonini, M. Calonge, Molecular and cellular biomarkers in dry eye disease and ocular allergy, Curr. Opin. Allergy Clin. Immunol. 12 (2012) 523–533. doi:10.1097/ACI.0b013e328357b488.

[60] C. Vitali, S. Bombardieri, R. Jonsson, H.M. Moutsopoulos, E.L. Alexander, S.E. Carsons, T.E. Daniels, P.C. Fox, R.I. Fox, S.S. Kassan, S.R. Pillemer, N. Talal, M.H. Weisman, European Study Group on Classification Criteria for Sjögren's Syndrome, Classification criteria for Sjögren's syndrome: a revised version of the European criteria proposed by the American-European Consensus Group, Ann. Rheum. Dis. 61 (2002) 554–8.

[61] S.E. Moss, Incidence of Dry Eye in an Older Population, Arch. Ophthalmol. 122 (2004) 369. doi:10.1001/archopht.122.3.369.

[62] J.C. Sherwin, M.H. Reacher, W.H. Dean, J. Ngondi, Epidemiology of vitamin A deficiency and xerophthalmia in at-risk populations, Trans. R. Soc. Trop. Med. Hyg. 106 (2012) 205–214. doi:10.1016/j.trstmh.2012.01.004.

[63] M.A. Lemp, L. Bielory, Contact Lenses and Associated Anterior Segment Disorders: Dry Eye Disease, Blepharitis, and Allergy, Immunol. Allergy Clin. North Am. 28 (2008) 105–117. doi:10.1016/j.iac.2007.11.002.

[64] C. Baudouin, A. Labbé, H. Liang, A. Pauly, F. Brignole-Baudouin, Preservatives in eyedrops: The good, the bad and the ugly, Prog. Retin. Eye Res. 29 (2010) 312–334. doi:10.1016/j.preteyeres.2010.03.001.

[65] M.E. Stern, S.C. Pflugfelder, Inflammation in dry eye, Ocul. Surf. 2 (2004) 124–30.

[66] M.E. Stern, C.S. Schaumburg, R. Dana, M. Calonge, J.Y. Niederkorn, S.C. Pflugfelder, Autoimmunity at the ocular surface: pathogenesis and regulation, Mucosal Immunol. 3 (2010) 425–442. doi:10.1038/mi.2010.26.

[67] S.C. Pflugfelder, Antiinflammatory therapy for dry eye, Am. J. Ophthalmol. 137 (2004) 337–342. doi:10.1016/j.ajo.2003.10.036.

[68] D.C. Felmeden, A.D. Blann, G.Y.H. Lip, Angiogenesis: basic pathophysiology and implications for disease., Eur. Heart J. 24 (2003) 586–603.

[69] J. Folkman, P.A. D'Amore, Blood vessel formation: what is its molecular basis?, Cell. 87 (1996) 1153–1155.

[70] J.S. Penn, A. Madan, R.B. Caldwell, M. Bartoli, R.W. Caldwell, M.E. Hartnett, Vascular endothelial growth factor in eye disease, Prog. Retin. Eye Res. 27 (2008) 331–371. doi:10.1016/j.preteyeres.2008.05.001.

[71] N. Asano-Kato, K. Fukagawa, N. Okada, T. Kawakita, Y. Takano, M. Dogru, K. Tsubota, H. Fujishima, TGF-beta1, IL-1beta, and Th2 cytokines stimulate vascular endothelial growth factor production from conjunctival fibroblasts, Exp. Eye Res. 80 (2005) 555–560. doi:10.1016/j.exer.2004.11.006.

[72] M. Grunewald, I. Avraham, Y. Dor, E. Bachar-Lustig, A. Itin, S. Yung, S. Chimenti, L. Landsman, R. Abramovitch, E. Keshet, VEGF-Induced Adult Neovascularization: Recruitment, Retention, and Role of Accessory Cells, Cell. 124 (2006) 175–189. doi:10.1016/j.cell.2005.10.036.

[73] E. Robak, A. Wozniacka, A. Sysa-Jedrzejowska, H. Stepien, T. Robak, Serum levels of angiogenic cytokines in systemic lupus erythematosus and their correlation with disease activity., Eur. Cytokine Netw. 12 (2001) 445–452.

[74] C. Cursiefen, L. Chen, L.P. Borges, D. Jackson, J. Cao, C. Radziejewski, P.A.

D'Amore, M.R. Dana, S.J. Wiegand, J.W. Streilein, VEGF-A stimulates lymphangiogenesis and hemangiogenesis in inflammatory neovascularization via macrophage recruitment., J. Clin. Invest. 113 (2004) 1040–1050. doi:10.1172/JCI20465.

[75] C.M. Lai, M. Brankov, T. Zaknich, Y.K. Lai, W.Y. Shen, I.J. Constable, I. Kovesdi, P.E. Rakoczy, Inhibition of angiogenesis by adenovirus-mediated sFlt-1 expression in a rat model of corneal neovascularization., Hum. Gene Ther. 12 (2001) 1299–1310. doi:10.1089/104303401750270959.

[76] C. Cursiefen, C. Rummelt, M. Kuchle, Immunohistochemical localization of vascular endothelial growth factor, transforming growth factor alpha, and transforming growth factor beta1 in human corneas with neovascularization., Cornea. 19 (2000) 526–533.

[77] W. Philipp, L. Speicher, C. Humpel, Expression of vascular endothelial growth factor and its receptors in inflamed and vascularized human corneas., Invest. Ophthalmol. Vis. Sci. 41 (2000) 2514–2522.

[78] P. Lee, C.C. Wang, A.P. Adamis, Ocular neovascularization: an epidemiologic review., Surv. Ophthalmol. 43 (1998) 245–69.

[79] S. Resnikoff, D. Pascolini, D. Etya'ale, I. Kocur, R. Pararajasegaram, G.P. Pokharel, S.P. Mariotti, Global data on visual impairment in the year 2002., Bull. World Health Organ. 82 (2004) 844–851. doi:/S0042-96862004001100009.

[80] K.A. Colby, A.P. Adamis, Prevalence of corneal neovascularization in a general eye service population, Investig. Opthalmology Vis. Sci. 37 (1996) S593.

[81] W. Shi, J. Liu, M. Li, H. Gao, T. Wang, Expression of MMP, HPSE, and FAP in stroma promoted corneal neovascularization induced by different etiological factors, Curr. Eye Res. 35 (2010) 967–977. doi:10.3109/02713683.2010.502294.

[82] Y. Gong, D.-R. Koh, Neutrophils promote inflammatory angiogenesis via release of preformed VEGF in an in vivo corneal model., Cell Tissue Res. 339 (2010) 437–448. doi:10.1007/s00441-009-0908-5.

[83] J.L. Clements, R. Dana, Inflammatory corneal neovascularization:

etiopathogenesis, Semin. Ophthalmol. 26 (2011) 235–245. doi:10.3109/08820538.2011.588652.

[84] C.N. Nagineni, A. William, A. Cherukuri, W. Samuel, J.J. Hooks, B. Detrick, Inflammatory cytokines regulate secretion of VEGF and chemokines by human conjunctival fibroblasts: Role in dysfunctional tear syndrome, Cytokine. 78 (2016) 16–19. doi:10.1016/j.cyto.2015.11.016.

[85] Z. Li, Y. Li, M. Lin, W. Su, W.-X. Zhang, Y. Zhang, L. Yao, D. Liang, Activated macrophages induce neovascularization through upregulation of MMP-9 and VEGF in rat corneas, Cornea. 31 (2012) 1028–1035. doi:10.1097/ICO.0b013e31823f8b40.

[86] C.A. Dinarello, Immunological and inflammatory functions of the interleukin-1 family, Annu. Rev. Immunol. 27 (2009) 519–550. doi:10.1146/annurev.immunol.021908.132612.

[87] M.R. Dana, S.N. Zhu, J. Yamada, Topical modulation of interleukin-1 activity in corneal neovascularization, Cornea. 17 (1998) 403–409.

[88] R.J. Simpson, A. Hammacher, D.K. Smith, J.M. Matthews, L.D. Ward, Interleukin-6: structure-function relationships, Protein Sci. 6 (1997) 929–955.

[89] Q. Ebrahem, A. Minamoto, G. Hoppe, B. Anand-Apte, J.E. Sears, Triamcinolone Acetonide Inhibits IL-6– and VEGF-Induced Angiogenesis Downstream of the IL-6 and VEGF Receptors, Investig. Opthalmology Vis. Sci. 47 (2006) 4935. doi:10.1167/iovs.05-1651.

[90] Y. Monnier, J. Zaric, C. Ruegg, Inhibition of angiogenesis by non-steroidal anti-inflammatory drugs: from the bench to the bedside and back., Curr. Drug Targets. Inflamm. Allergy. 4 (2005) 31–38.

[91] C. Cursiefen, H. Wenkel, P. Martus, A. Langenbucher, N.X. Nguyen, B. Seitz, M. Kuchle, G.O. Naumann, Impact of short-term versus long-term topical steroids on corneal neovascularization after non-high-risk keratoplasty., Graefes Arch. Clin. Exp. Ophthalmol. 239 (2001) 514–521.

[92] K.J. Lim, W.R. Wee, J.H. Lee, Treatment of corneal neovascularization with

argon laser, Korean J. Ophthalmol. 7 (1993) 25–27. doi:10.3341/kjo.1993.7.1.25.

[93] C.T. Pillai, H.S. Dua, P. Hossain, Fine needle diathermy occlusion of corneal vessels., Invest. Ophthalmol. Vis. Sci. 41 (2000) 2148–2153.

[94] J.C. Kim, S.C. Tseng, The effects on inhibition of corneal neovascularization after human amniotic membrane transplantation in severely damaged rabbit corneas, Korean J. Ophthalmol. 9 (1995) 32–46. doi:10.3341/kjo.1995.9.1.32.

[95] X. Liu, S. Wang, X. Wang, J. Liang, Y. Zhang, Recent drug therapies for corneal neovascularization, Chem. Biol. Drug Des. 90 (2017) 653–664. doi:10.1111/cbdd.13018.

[96] J.C. Lang, Ocular drug delivery conventional ocular formulations, Adv. Drug Deliv. Rev. 16 (1995) 39–43. doi:10.1016/0169-409X(95)00012-V.

[97] A. Patel, K. Cholkar, V. Agrahari, A.K. Mitra, Ocular drug delivery systems: An overview, World J. Pharmacol. 2 (2013) 47–64. doi:10.5497/wjp.v2.i2.47 [doi].

[98] A. LUDWIG, The use of mucoadhesive polymers in ocular drug delivery, Adv. Drug Deliv. Rev. 57 (2005) 1595–1639. doi:10.1016/j.addr.2005.07.005.

[99] M. Ali, M.E. Byrne, Challenges and solutions in topical ocular drug-delivery systems, Expert Rev. Clin. Pharmacol. 1 (2008) 145–161. doi:10.1586/17512433.1.1.145.

[100] X. Xu, M. Al-Ghabeish, Z. Rahman, Y.S.R. Krishnaiah, F. Yerlikaya, Y. Yang, P. Manda, R.L. Hunt, M.A. Khan, Formulation and process factors influencing product quality and in vitro performance of ophthalmic ointments, Int. J. Pharm. 493 (2015) 412–425. doi:10.1016/j.ijpharm.2015.07.066.

[101] G. MESEGUER, P. BURI, B. PLAZONNET, A. ROZIER, R. GURNY, Gamma Scintigraphic Comparison of Eyedrops Containing Pilocarpine in Healthy Volunteers, J. Ocul. Pharmacol. Ther. 12 (1996) 481–488. doi:10.1089/jop.1996.12.481.

[102] M.F. Saettone, P. Chetoni, R. Cerbai, G. Mazzanti, L. Braghiroli, Evaluation of ocular permeation enhancers: In vitro effects on corneal transport of four β-blockers, and in vitro/in vivo toxic activity, Int. J. Pharm. 142 (1996) 103–113. doi:10.1016/0378-5173(96)04663-7.

[103] T. Loftsson, E. Stefansson, Cyclodextrins in eye drop formulations: enhanced topical delivery of corticosteroids to the eye, Acta Ophthalmol. Scand. 80 (2002) 144–150. doi:10.1034/j.1600-0420.2002.800205.x.

[104] M.F. Saettone, B. Giannaccini, D. Monti, Ophthalmic emulsions and suspensions, J. Toxicol. Cutan. Ocul. Toxicol. 20 (2001) 183–201. doi:10.1081/CUS-120001857.

[105] S.S. Modi, R.P. Lehmann, T.R. Walters, R. Fong, W.C. Christie, L. Roel, D. Nethery, D. Sager, A. Tsorbatzoglou, B. Philipson, C.E. Traverso, H. Reiser, Once-daily nepafenac ophthalmic suspension 0.3% to prevent and treat ocular inflammation and pain after cataract surgery: Phase 3 study, J. Cataract Refract. Surg. 40 (2014) 203–211. doi:10.1016/j.jcrs.2013.07.042.

[106] J.E. Chastain, M.E. Sanders, M.A. Curtis, N. V Chemuturi, M.E. Gadd, M.A. Kapin, K.L. Markwardt, D.C. Dahlin, Distribution of topical ocular nepafenac and its active metabolite amfenac to the posterior segment of the eye, Exp. Eye Res. 145 (2016) 58–67. doi:10.1016/j.exer.2015.10.009.

[107] Q. Bao, R. Jog, J. Shen, B. Newman, Y. Wang, S. Choi, D.J. Burgess, Physicochemical attributes and dissolution testing of ophthalmic ointments, Int. J. Pharm. 523 (2017) 310–319. doi:10.1016/j.ijpharm.2017.03.039.

[108] F. Lallemand, M. Schmitt, J.-L. Bourges, R. Gurny, S. Benita, J.-S. Garrigue, Cyclosporine A delivery to the eye: A comprehensive review of academic and industrial efforts, Eur. J. Pharm. Biopharm. 117 (2017) 14–28. doi:10.1016/j.ejpb.2017.03.006.

[109] F. Lallemand, P. Daull, S. Benita, R. Buggage, J.-S. Garrigue, Successfully improving ocular drug delivery using the cationic nanoemulsion, novasorb., J. Drug Deliv. 2012 (2012) 604204. doi:10.1155/2012/604204.

[110] A.A. Al-Kinani, G. Zidan, N. Elsaid, A. Seyfoddin, A.W.G. Alani, R.G. Alany, Ophthalmic gels: Past, present and future, Adv. Drug Deliv. Rev. (2017). doi:10.1016/j.addr.2017.12.017.

[111] M. Zignani, C. Tabatabay, R. Gurny, Topical semi-solid drug delivery: kinetics and tolerance of ophthalmic hydrogels, Adv. Drug Deliv. Rev. 16 (1995) 51–60. doi:10.1016/0169-409X(95)00015-Y.

[112] M.F. Saettone, L. Salminen, Ocular inserts for topical delivery, Adv. Drug Deliv. Rev. 16 (1995) 95–106. doi:10.1016/0169-409X(95)00014-X.

[113] A. Kumari, P. Sharma, V. Garg, G. Garg, Ocular inserts - Advancement in therapy of eye diseases, J. Adv. Pharm. Technol. Res. 1 (2010) 291. doi:10.4103/0110-5558.72419.

[114] C.J.F. Bertens, M. Gijs, F.J.H.M. van den Biggelaar, R.M.M.A. Nuijts, Topical drug delivery devices: A review, Exp. Eye Res. 168 (2018) 149–160. doi:10.1016/j.exer.2018.01.010.

[115] F.A. Maulvi, T.G. Soni, D.O. Shah, A review on therapeutic contact lenses for ocular drug delivery., Drug Deliv. 23 (2016) 3017–3026. doi:10.3109/10717544.2016.1138342.

[116] L. Lalu, V. Tambe, D. Pradhan, K. Nayak, S. Bagchi, R. Maheshwari, K. Kalia, R.K. Tekade, Novel nanosystems for the treatment of ocular inflammation: Current paradigms and future research directions, J. Control. Release. 268 (2017) 19–39. doi:10.1016/j.jconrel.2017.07.035.

[117] D.R. Janagam, L. Wu, T.L. Lowe, Nanoparticles for drug delivery to the anterior segment of the eye, Adv. Drug Deliv. Rev. 122 (2017) 31–64. doi:10.1016/j.addr.2017.04.001.

[118] S. Patel, C. Garapati, P. Chowdhury, H. Gupta, J. Nesamony, S. Nauli, S.H.S. Boddu, Development and Evaluation of Dexamethasone Nanomicelles with Potential for Treating Posterior Uveitis After Topical Application, J. Ocul. Pharmacol. Ther. 31 (2015) 215–227. doi:10.1089/jop.2014.0152.

[119] C. Guo, Y. Zhang, Z. Yang, M. Li, F. Li, F. Cui, T. Liu, W. Shi, X. Wu, Nanomicelle formulation for topical delivery of cyclosporine A into the cornea: in vitro mechanism and in vivo permeation evaluation, 5 (2015) 12968. http://dx.doi.org/10.1038/srep12968.

[120] I. Pepić, A. Hafner, J. Lovrić, B. Pirkić, J. Filipović-Grččić, A Nonionic Surfactant/Chitosan Micelle System in an Innovative Eye Drop Formulation, J. Pharm. Sci. 99 (2010) 4317–4325. doi:10.1002/jps.22137.

[121] G. Tan, S. Yu, H. Pan, J. Li, D. Liu, K. Yuan, X. Yang, W. Pan, Bioadhesive chitosan-loaded liposomes: A more efficient and higher permeable ocular delivery platform for timolol maleate, Int. J. Biol. Macromol. 94 (2017) 355–363. doi:10.1016/j.ijbiomac.2016.10.035.

[122] M.A. Kamaleddin, Nano-ophthalmology: Applications and considerations, Nanomedicine Nanotechnology, Biol. Med. 13 (2017) 1459–1472. doi:https://doi.org/10.1016/j.nano.2017.02.007.

[123] T.F. Vandamme, L. Brobeck, Poly(amidoamine) dendrimers as ophthalmic vehicles for ocular delivery of pilocarpine nitrate and tropicamide, J. Control. Release. 102 (2005) 23–38. doi:10.1016/j.jconrel.2004.09.015.

[124] I. Bravo-Osuna, M. Noiray, E. Briand, A.M. Woodward, P. Argüeso, I.T.M. Martínez, R. Herrero-Vanrell, G. Ponchel, Interfacial Interaction between Transmembrane Ocular Mucins and Adhesive Polymers and Dendrimers Analyzed by Surface Plasmon Resonance, Pharm. Res. 29 (2012) 2329–2340. doi:10.1007/s11095-012-0761-1.

[125] A. Sanchez, M.J. Alonso, Nanoparticular Carriers for Ocular Drug Delivery, in: Nanoparticulates as Drug Carriers, PUBLISHED BY IMPERIAL COLLEGE PRESS AND DISTRIBUTED BY WORLD SCIENTIFIC PUBLISHING CO., 2006: pp. 649–673. doi:10.1142/9781860949074_0027.

[126] A. Fabiano, R. Bizzarri, Y. Zambito, Thermosensitive hydrogel based on chitosan and its derivatives containing medicated nanoparticles for transcorneal administration of 5-fluorouracil, Int. J. Nanomedicine. Volume 12 (2017) 633–643. doi:10.2147/IJN.S121642.

[127] Ameeduzzafar, S.S. Imam, S.N. Abbas Bukhari, J. Ahmad, A. Ali, Formulation and optimization of levofloxacin loaded chitosan nanoparticle for ocular delivery: In-vitro characterization, ocular tolerance and antibacterial activity, Int. J. Biol. Macromol. 108 (2018) 650–659. doi:10.1016/j.ijbiomac.2017.11.170.

[128] S. Natesan, S. Pandian, C. Ponnusamy, R. Palanichamy, S. Muthusamy, R. Kandasamy, Co-encapsulated resveratrol and quercetin in chitosan and peg modified chitosan nanoparticles: For efficient intra ocular pressure reduction, Int. J. Biol.

Macromol. 104 (2017) 1837–1845. doi:10.1016/j.ijbiomac.2017.04.117.

[129] P. Calvo, J.L. Vila-Jato, M.J. Alonso, Evaluation of cationic polymer-coated nanocapsules as ocular drug carriers, Int. J. Pharm. 153 (1997) 41–50. doi:10.1016/S0378-5173(97)00083-5.

[130] D. Vllasaliu, R. Exposito-Harris, A. Heras, L. Casettari, M. Garnett, L. Illum, S. Stolnik, Tight junction modulation by chitosan nanoparticles: comparison with chitosan solution., Int. J. Pharm. 400 (2010) 183–193. doi:10.1016/j.ijpharm.2010.08.020.

[131] M. Guter, M. Breunig, Hyaluronan as a promising excipient for ocular drug delivery, Eur. J. Pharm. Biopharm. 113 (2017) 34–49. doi:10.1016/j.ejpb.2016.11.035.

[132] S. Barbault-Foucher, R. Gref, P. Russo, J. Guechot, A. Bochot, Design of poly-epsilon-caprolactone nanospheres coated with bioadhesive hyaluronic acid for ocular delivery., J. Control. Release. 83 (2002) 365–375.

[133] İ. Yenice, M.C. Mocan, E. Palaska, A. Bochot, E. Bilensoy, İ. Vural, M. İrkeç, A. Atilla Hıncal, Hyaluronic acid coated poly-ε-caprolactone nanospheres deliver high concentrations of cyclosporine A into the cornea, Exp. Eye Res. 87 (2008) 162–167. doi:10.1016/j.exer.2008.04.002.

[134] L. Contreras-Ruiz, M. de la Fuente, J.E. Párraga, A. López-García, I. Fernández, B. Seijo, A. Sánchez, M. Calonge, Y. Diebold, Intracellular trafficking of hyaluronic acid-chitosan oligomer-based nanoparticles in cultured human ocular surface cells., Mol. Vis. 17 (2011) 279–90.

[135] M. de la Fuente, B. Seijo, M.J. Alonso, Novel Hyaluronic Acid-Chitosan Nanoparticles for Ocular Gene Therapy, Investig. Opthalmology Vis. Sci. 49 (2008) 2016. doi:10.1167/iovs.07-1077.

[136] PubChem, Hyaluronic acid molecular structure, (n.d.). https://pubchem.ncbi.nlm.nih.gov/compound/24728612 (accessed July 10, 2018).

[137] PubChem, Chitosan molecular structure, (n.d.). https://pubchem.ncbi.nlm.nih.gov/compound/129662530 (accessed July 10, 2018).

[138] A.K. Zimmer, P. Maincent, P. Thouvenot, J. Kreuter, Hydrocortisone delivery to healthy and inflamed eyes using a micellar polysorbate 80 solution or albumin

nanoparticles, Int. J. Pharm. 110 (1994) 211–222. doi:10.1016/0378-5173(94)90243-7.

[139] M.A. Kalam, Development of chitosan nanoparticles coated with hyaluronic acid for topical ocular delivery of dexamethasone, Int. J. Biol. Macromol. 89 (2016) 127–136. doi:10.1016/j.ijbiomac.2016.04.070.

[140] A.A. Badawi, H.M. El-Laithy, R.K. El Qidra, H. El Mofty, M. El dally, Chitosan based nanocarriers for indomethacin ocular delivery, Arch. Pharm. Res. 31 (2008) 1040–1049. doi:10.1007/s12272-001-1266-6.

[141] E. Vega, M.A. Egea, O. Valls, M. Espina, M.L. García, Flurbiprofen Loaded Biodegradable Nanoparticles for Ophtalmic Administration, J. Pharm. Sci. 95 (2006) 2393–2405. doi:10.1002/jps.20685.

[142] A.K. Sharma, P.K. Sahoo, D.K. Majumdar, A.K. Panda, Topical ocular delivery of a COX-II inhibitor via biodegradable nanoparticles, Nanotechnol. Rev. 5 (2016) 435–444. doi:10.1515/ntrev-2016-0004.

[143] K. Hermans, D. den Plas, E. Schreurs, W. Weyenberg, A. Ludwig, Cytotoxicity and anti-inflammatory activity of cyclosporine A loaded PLGA nanoparticles for ocular use, Pharmazie. 69 (2014) 32–37. doi:10.1691/ph.2014.2206.

[144] P. Aksungur, M. Demirbilek, E.B. Denkbaş, J. Vandervoort, A. Ludwig, N. Ünlü, Development and characterization of Cyclosporine A loaded nanoparticles for ocular drug delivery: Cellular toxicity, uptake, and kinetic studies, J. Control. Release. 151 (2011) 286–294. doi:10.1016/j.jconrel.2011.01.010.

[145] L. Contreras-Ruiz, G.K. Zorzi, D. Hileeto, A. López-García, M. Calonge, B. Seijo, A. Sánchez, Y. Diebold, A nanomedicine to treat ocular surface inflammation: performance on an experimental dry eye murine model, Gene Ther. 20 (2013) 467–477. doi:10.1038/gt.2012.56.

[146] G. Konat Zorzi, L. Contreras-Ruiz, J.E. Párraga, A. López-García, R. Romero Bello, Y. Diebold, B. Seijo, A. Sánchez, Expression of MUC5AC in Ocular Surface Epithelial Cells Using Cationized Gelatin Nanoparticles, Mol. Pharm. 8 (2011) 1783–1788. doi:10.1021/mp200155t.

[147] S. Liu, M.D. Dozois, C.N. Chang, A. Ahmad, D.L.T. Ng, D. Hileeto, H. Liang,

M.-M. Reyad, S. Boyd, L.W. Jones, F.X. Gu, Prolonged Ocular Retention of Mucoadhesive Nanoparticle Eye Drop Formulation Enables Treatment of Eye Diseases Using Significantly Reduced Dosage, Mol. Pharm. 13 (2016) 2897–2905. doi:10.1021/acs.molpharmaceut.6b00445.

[148] I. Luis de Redín, C. Boiero, M.C. Martínez-Ohárriz, M. Agüeros, R. Ramos, I. Peñuelas, D. Allemandi, J.M. Llabot, J.M. Irache, Human serum albumin nanoparticles for ocular delivery of bevacizumab, Int. J. Pharm. 541 (2018) 214–223. doi:10.1016/j.ijpharm.2018.02.003.

[149] J.E. Lee, K.L. Kim, D. Kim, Y. Yeo, H. Han, M.G. Kim, S.H. Kim, H. Kim, J.H. Jeong, W. Suh, Apatinib-loaded nanoparticles suppress vascular endothelial growth factor-induced angiogenesis and experimental corneal neovascularization, Int. J. Nanomedicine. Volume 12 (2017) 4813–4822. doi:10.2147/IJN.S135133.

[150] N. Pradhan, R. Guha, S. Chowdhury, S. Nandi, A. Konar, S. Hazra, Curcumin nanoparticles inhibit corneal neovascularization, J. Mol. Med. 93 (2015) 1095–1106. doi:10.1007/s00109-015-1277-z.

[151] C.-Y. Chang, M.-C. Wang, T. Miyagawa, Z.-Y. Chen, F.-H. Lin, K.-H. Chen, G.-S. Liu, C.-L. Tseng, Preparation of arginine-glycine-aspartic acid-modified biopolymeric nanoparticles containing epigalloccatechin-3-gallate for targeting vascular endothelial cells to inhibit corneal neovascularization, Int. J. Nanomedicine. Volume 12 (2016) 279–294. doi:10.2147/IJN.S114754.

[152] H. Han, S. Son, S. Son, N. Kim, J.Y. Yhee, J.H. Lee, J.-S. Choi, C.-K. Joo, H. Lee, D. Lee, W.J. Kim, S.H. Kim, I.C. Kwon, H. Kim, K. Kim, Reducible Polyethylenimine Nanoparticles for Efficient siRNA Delivery in Corneal Neovascularization Therapy, Macromol. Biosci. 16 (2016) 1583–1597. doi:10.1002/mabi.201600051.

USC
UNIVERSIDADE
DE SANTIAGO
DE COMPOSTELA

# *Motivation*

USC
UNIVERSIDADE
DE SANTIAGO
DE COMPOSTELA

The eye is one of the most protected organs in the body, having many anatomical and physiological barriers that not only protect it from the entrance of pathogens but also make access to therapeutic substances difficult. In the case of topical ocular drug delivery, the barrier that constitutes the ocular surface itself severely limits the bioavailability and efficacy of topically applied formulations. Ocular surface pathologies such as dry eye disease or corneal neovascularization require prolonged treatments with frequent administration to maintain therapeutic drug levels at the site of action, which ultimately compromise patient safety and adherence to the treatment.

Nanoparticles (NPs) have shown potential for years as ocular drug delivery systems. These systems can both increase drug residence times on the ocular surface as well as their intraocular penetration, resulting in higher drug bioavailability. In this sense, providing nanosystems with positive charges that favor interactions with the negatively charged mucus layer of the tear film that covers the corneal tissue, therefore extending drug residence times and penetration, has been the dominant paradigm in the design of nanoparticles for topical ocular administration. Alternatively, some authors have studied the possibility of specifically targeting the cornea using targeting molecules such as hyaluronic acid, whose receptors are present in corneal epithelial cells. This strategy allows for specific interactions and favors receptor-mediated endocytosis and the subsequent corneal penetration.

In this work, we used our recently patented sorbitan ester NPs (SENS), which previously demonstrated safety and efficacy as drug delivery systems. The design and development of these NPs as topical ocular drug delivery systems was focused on obtaining two nanosystems with different technological properties as follows: an optimized cationic nanosystem and its hyaluronic acid-coated version. This approach allowed us to perform a comparative analysis between the physicochemical and biopharmaceutical properties of both nanosystems throughout the thesis.

This thesis work is the result of a close collaboration with the following two research groups that have extensive experience in the development of NPs for ocular drug delivery: the Ocular Surface Group from the Institute of Applied Ophthalmo-Biology at the University of Valladolid (Valladolid, Spain), particularly the research team led by Dr. Yolanda Diebold, and the research group from the Department of Pharmacology, Pharmacy and Pharmaceutical Technology of the Faculty of Pharmacy

at the University of Santiago de Compostela (Santiago de Compostela, Spain), particularly the research team led by Dr. Alejandro Sánchez. The collaboration with both groups has been highly fruitful over the past 15 years, as shown by multiple joint projects and the abundant joint scientific results and publications.

Finally, the need to perform a proof-of-concept to determine the therapeutic efficacy of the developed NPs in a relevant animal model of ocular disease was considered. To this end, we contacted the research group led by Dr. Sharmila Masli at Boston University (Boston, MA, USA) because they have experience with an experimental disease model of dry eye.

This explains the approach of this research work to identify the most appropriate NP-based therapeutic alternative to conventional treatments for dry eye disease and corneal neovascularization. We consider the extensive experience together with the multidisciplinary aspects of all parts implicated in this project as one of the major strengths of this work.

# *Hypothesis and objectives*

USC
UNIVERSIDADE
DE SANTIAGO
DE COMPOSTELA

**Hypothesis**

It is possible to develop a topically applied sorbitan ester-based nanoparticulated drug delivery system able to specifically target ocular surface structures and maximize drug therapeutic efficacy without compromising ocular biocompatibility.

**General Objective**

To design and develop sorbitan ester nanoparticles (SENS) as a therapeutic alternative to existing topical treatments for dry eye disease and corneal neovascularization.

Specific objectives:

1. To design and optimize two types of drug-loaded SENS for topical ocular therapy: a cationic nanoparticle variety and its hyaluronic acid-coated version (Annex I and Chapter I).

2. To characterize the developed nanoparticles regarding their physicochemical properties and stability (Chapters I, II and III).

3. To evaluate the *in vitro* biocompatibility and *in vitro* and *ex vivo* targeting ability of the nanoparticles (Chapters I and III).

4. To evaluate the *in vitro* and *ex vivo* biological activity of drug-loaded nanoparticles (Chapters I and III).

5. To evaluate the therapeutic efficacy of cyclosporine-loaded nanoparticles for the treatment of dry eye disease in an animal model (Chapter II).

USC
UNIVERSIDADE
DE SANTIAGO
DE COMPOSTELA

# *Chapter I*

## *Sorbitan ester nanoparticles (SENS) as a novel topical ocular drug delivery system: Design, optimization, and in vitro/ex vivo evaluation*

USC
UNIVERSIDADE
DE SANTIAGO
DE COMPOSTELA

**Abstract**

We explored the potential of two types of sorbitan ester nanoparticles (SENS) as novel tools for topical ocular drug delivery. The optimized SENS formulation (SENS-OPT) consisted of nanoparticles (NPs) of 170.5 nm, zeta potential +33.9 mV, and cyclosporine loading of 19.66%. After hyaluronic acid (HA) coating, the resulting SENS-OPT-HA NPs had a particle size of 177.6 nm and zeta potential of -20.6 mV. The NPs were stable during 3 months of storage at different temperatures and did not aggregate in the presence of protein-enriched simulated lacrimal fluid. There was no toxicity to cultured human corneal epithelial (HCE) cells when exposed to NPs up to 0.4% (w/v). Both NPs were effectively internalized by HCE cells through active mechanisms. Endocytosis of SENS-OPT NPs was caveolin-dependent whereas SENS-OPT-HA NP endocytosis was mediated by HA receptors. HA-receptor-mediated endocytosis may be responsible for the higher cellular uptake of SENS-OPT-HA NPs. After cyclosporine incorporation into the NPs, corneal penetration of this immunosuppressive drug by loaded SENS-OPT NPs was 1.3-fold higher than the commercial reference formulation Sandimmun®. For cyclosporine-loaded SENS-OPT-HA NPs, the penetration was 2.1-fold higher than for Sandimmun®. In *ex vivo* stimulated lymphocytes, both formulations demonstrated the same reduction in IL-2 levels as Sandimmun®.

USC
UNIVERSIDADE
DE SANTIAGO
DE COMPOSTELA

## 1. Introduction

Most drugs used in ocular therapies are formulated as topically-applied dosage forms (i.e., eyedrops) because topical administration is a simple and non-invasive route that achieves high levels of patient compliance. However, conventional dosage forms present several pharmaceutical issues that limit therapeutic efficacy due to low drug bioavailability, the most evident drawback. The underlying reason is that the eye is a highly protected organ composed of numerous nearly impermeable anatomical and physiological barriers that prevent access of foreign substances such as drugs [1]. In fact, intraocular drug bioavailability achieved with conventional topical dosage forms is generally less than 5% [2].

One of the most studied drugs in ocular drug delivery (ODD) is the immunosuppressive agent cyclosporine A (CsA). This cyclic undecapeptide is effective in the treatment of various ocular surface disorders in which the immune system is activated as occurs in dry eye disease [3] or after corneal graft transplantation [4]. However, the choice of an appropriate vehicle for topical administration of CsA represents a big challenge for scientists due the unfavorable physicochemical (poor water solubility) and biopharmaceutical properties (low permeability) [5].

In the recent decades, multiple CsA formulations have been developed, including emulsions, microparticles, *in situ* gelling systems, drug-loaded contact lenses, and nanotechnology-based systems [5]. The colloidal nature of nanocarriers not only improves the solubility of CsA, it also improves key biopharmaceutical properties such as formulation residence time and drug penetration through cornea. Li et al. reported that in rabbit corneas cationic chitosan-coated liposomes had prolonged drug retention and higher levels of CsA compared to uncoated liposomes [6]. Polymeric chitosan-coating of CsA-loaded lipid and polymeric nanoparticles (NPs) also showed promising results by improving the intraocular availability of this drug [7–10]. Other cationic nanosystems that have been evaluated for ODD include cationic Eudragit® polymers, sterylamine, didecyldimethylammonium bromide, and cetyltrimethylammonium bromide (CTAB) [11–14]. As alternatives to cationic nanosystems, other mucoadhesive formulations have been proposed. Hyaluronic acid (HA)-coated colloidal systems have gained attention lately for topical administration because of their technological features. In addition to its mucoadhesiveness, HA coating enhances nanoparticle uptake by corneal cells due to specific targeting of HA-receptors [15]. In a recent study, Kalam

observed that dexamethasone ocular bioavailability obtained with chitosan NPs and HA-coated chitosan NPs was 1.83- and 2.14-fold higher respectively than with the drug solution alone [16]. This author attributed this difference to the presence of the HA coating that may allow a targeted receptor-mediated endocytosis by corneal cells.

Recently, our group patented novel types of NPs based on the cheapest available materials in the pharmaceutical market, sorbitan esters [17]. Based on our patented NPs, the objective of the present work was to optimize and evaluate two novel NP formulations specifically designed for topical ODD. As a drug model, we selected CsA because of its proven anti-inflammatory efficacy in the treatment of common eye diseases. We employed a Box-Behnken experimental design to optimize the physicochemical properties of the initial prototype formulations. According to the design outcome, we selected a cationic optimized formulation (SENS-OPT) for further study. Additionally, an anionic optimized formulation was prepared based upon the SENS-OPT by coating it with HA (SENS-OPT-HA). The developed NPs were characterized physicochemically and evaluated in terms of biocompatibility, cellular uptake, corneal penetration, and immunosuppressant activity.

## 2. Materials and methods

### 2.1. Materials

Sorbitan monooleate (Span® 80), d-α-tocopheryl polyethylene glycol 1000 succinate (TPGS), CTAB, HA, Nile red, filipin, chlorpromazine, concanavalin A (Con A), NaOH, benzalkonium chloride (BZK), 2,3-bis[2-methoxy-4-nitro-5-sulfophenyl]-2H-tetrazolium-5-carboxyanilide inner salt (XTT), and simulated lacrimal fluid (SLF) components were purchased from Sigma-Aldrich (Madrid, Spain). High performance liquid chromatography (HPLC)-grade acetonitrile (ACN) was from VWR (Barcelona, Spain). Cyclosporine A (CsA) was obtained from LC Laboratories (Woburn, MA, USA). Sandimmun® was obtained from the local hospital pharmacy. Alamar Blue® reagent was from Bio-Rad (Madrid, Spain). Dulbecco's Phosphate Buffered Saline (DPBS), DMEM/F12 culture medium and other cell culture reagents were purchased from Invitrogen-Gibco (Inchinnan, UK). Pierce® BCA Protein Assay Kit was from Thermo Fisher Scientific (Waltham, MA, USA), and IL-2 enzyme-linked immunosorbent assay (ELISA) kit was purchased from Diaclone (Besançon, France).

### 2.2. Preparation of SENS

NPs were prepared according to our previously patented method [17]. Briefly, all NP components, including Span® 80, TPGS, and CTAB, were dissolved in 30 mL of absolute ethanol. For drug-loaded preparations, CsA was added to this mixture. This organic phase was then poured steadily over an aqueous phase (ultrapure water, 60 mL) under continuous magnetic stirring (500 rpm, 15 minutes), leading to the spontaneous formation of SENS. Immediately, the ethanol was removed by a rotating evaporator, and the formulation was subsequently concentrated to a final volume of 10 mL.

### 2.3. SENS optimization by Box-Behnken experimental design

A three-factor, three-level Box-Behnken experimental design was performed to develop an optimized formulation for topical ODD. A design matrix was built with combinations of three factors (independent variables, **Table 1**) consisting of low, medium, and high concentrations of Span® 80, TPGS, and CsA. These concentration ranges were selected by evaluating the results of preliminary experiments. In those experiments, critical formulation parameters were considered, such as a preferred particle size under 200 nm, zeta potential as far as possible from electroneutrality, and the highest drug payloads that did not compromise nanosystem stability. The cationic agent CTAB was constantly kept at the lowest possible level in all formulations to avoid potential biocompatibility issues. Fixed objectives (dependent variables, **Table 1**) were selected to minimize particle size at the same time as maximizing zeta potential, entrapment efficiency, and final drug loading.

**Table 1. Variables of Box-Behnken experimental design.**

| Independent variables | Levels under study | | |
|---|---|---|---|
| | Low | Medium | High |
| Span® 80 amount (% w/v) | 2.00 | 2.50 | 3.00 |
| TPGS amount (% w/v) | 0.10 | 0.20 | 0.30 |
| CsA amount (% w/v) | 0.30 | 0.48 | 0.65 |
| Dependent variables | Established constraints | | |
| Particle size (nm) | Minimize | | |
| Zeta potential (mV) | Maximize | | |
| Entrapment efficiency (%) | Maximize | | |
| Drug loading (%) | Maximize | | |

Span® 80, sorbitan monooleate; TPGS, d-α-tocopheryl polyethylene glycol 1000 succinate; CsA, cyclosporine A.

The design matrix was constructed using Statgraphics® Centurion XVI (Statpoint Technologies, Inc., Warrenton, VA, USA) software, according to which a total of 15 experimental runs, including 12 factorial points and 3 center points, were required. The composition of these formulations and the corresponding experimental responses observed for each variable were recorded (**Table 2)**. Statgraphics® software statistically fitted each response to the most appropriate polynomial model and provided response surface plots where the relationships between factors and responses were graphically represented. A one-way analysis of variance (ANOVA) determined if each observed response could be attributed to significant ($p \leq 0.05$) individual effects or interaction effects of the three factors.

As a final step in experimental design, a multiple variable optimization process was implemented. The resulting optimized formulation was identified as SENS-OPT. To demonstrate design validity, a SENS-OPT formulation and two checkpoint formulations (SENS-HIGH and SENS-LOW) were prepared in triplicates. The predicted and experimental values of responses were compared, and the percentage of prediction error was determined as follows:

$$Bias\ (\%) = \frac{\text{Experimental value} - \text{Predicted Value}}{\text{Predicted Value}} \times 100$$

### 2.4. Preparation of SENS-OPT-HA

An anionic optimized formulation was prepared by the surface coating of SENS-OPT with HA. The positive surface charge provided by CTAB allowed polymer adsorption. SENS-OPT-HA was prepared by mixing two volumes of SENS-OPT with one volume of HA (1,600 KDa) solution, giving a final HA concentration of 0.015% (w/v). The total HA adsorption occurred after placing the NPs in an orbital shaker at 75 rpm for 20 minutes.

### 2.5. Physicochemical characterization of NPs

Sample particle size (Z-average) and particle distribution (polydispersity index) were determined by dynamic light scattering (DLS) after appropriate dilution with 0.1 mM KCl. Analyses were carried out at 25ºC with a detection angle of 173º. Otherwise, the NP zeta potential (mean electrophoretic mobility) was quantified by laser doppler anemometry. Both analyses were run with a Zetasizer® 3000HS (Malvern Instruments, Malvern, UK).

Morphology of the NPs was assessed by transmission electron microscopy (CM 12 Phillips, Eindhoven, Netherlands). Samples were placed onto Formvar® coated copper supports and subsequently treated with 2% (w/v) phosphotungstic acid solution before imaging.

CsA entrapment efficiency was directly determined by measuring the NP drug content. Samples were passed through a 0.22 μm filter, as proposed by Guo et al., to remove crystals of unentrapped CsA [18]. The NPs were then disrupted and the drug extracted by mixing 1:4 (v/v) with ACN. CsA was quantified by HPLC using a KromaPhase C18 reverse phase column (250×4.6 mm, 5 μm diameter). The HPLC system (Merck-Hitachi, Darmstadt, Germany) was composed of an L-6200 pump model, an AS-4000 automatic injector, an L-5025 column oven, and an L-4500 UV-detector coupled to a computer by a D-6000 interface. The mobile phase consisted of ACN and ultrapure water mixed in a gradient mode ranging from 80:20 (v/v) to 100:00 (v/v) over a period of 5 minutes followed by 100:00 (v/v) isocratic mode for 3 minutes. Then, the gradient was progressively returned to 80:20 (v/v) at the end of the run. The flow rate was 1 mL/min. Injection volume was 20 μL and the column oven temperature was 70ºC. The CsA detection was at 220 nm. Under these conditions CsA retention time was 6.8 minutes. Entrapment efficiency (EE%) and drug loading (DL%) were determined by the following equations:

$$EE(\%) = \frac{Weig \quad of\ CsA\ recovered\ from\ nanoparticles}{Wei \quad of\ CsA\ initially\ added} \times 100 \qquad (1)$$

$$DL(\%) = \frac{Weig \quad of\ CsA\ recovered\ from\ nanoparticles}{Weight\ of\ nanoparticles} \times 100 \qquad (2)$$

**2.6. NP structural analysis by nuclear magnetic resonance (NMR)**

NMR was employed for studying the structure of SENS-OPT and SENS-OPT-HA NPs. An unloaded formulation was included as a placebo (SENS-BLK). The identification of spectrum peaks corresponding to raw materials was done using the $^{1}H$ NMR technique while the identification of the spectrum of NP peaks was done using the $^{1}H$-wg NMR technique. Additionally, a $^{1}H$ diffusion filter spectrum was measured for each NP sample (data not shown). In this spectrum the (sharp) peaks of low molecular weight species such as impurities or solvents were eliminated (or strongly attenuated), thus enabling identification of the specific NP peaks.

### 2.7. Physical and biological stability of the developed NPs

To determine the physical stability of the NPs, freshly prepared formulations were placed into sealed vials and stored at either 4ºC, room temperature (RT), or 37ºC. For each condition, three different vials were analyzed. NP size and zeta potential were monitored by DLS at month 0 (RT, immediately after preparation) and after 3 months to detect possible destabilization.

In addition, the biological stability of the NPs was assessed *in vitro*. The NPs were mixed with a protein-enriched SLF 4.3:1 (v/v) and incubated for 5 hours at 37ºC. This proportion was selected based upon the instilled volume of conventional eyedrops, around 30 µL, and the permanent tear volume, 7 µL. The protein-enriched SLF (pH 7.4) was composed of 0.268% (w/v) bovine serum albumin, 0.268% (w/v) lysozyme, 0.134% (w/v) globulin, 0.008% (w/v) $CaCl_2 \cdot 2H_2O$, 0.650% (w/v) D-glucose, 0.658% (w/v) NaCl, and ultrapure water [19]. Possible changes in particle size and polydispersity were assessed at predetermined intervals by DLS measurements. Four samples were evaluated for each time point.

### 2.8. Cell line and culture conditions

A human corneal epithelial cell line (HCE) [20] was used in passages 32-40. Cells were cultured in DMEM/F-12 medium supplemented with 10% fetal bovine serum, 5000 U/mL penicillin/streptomycin, 10 ng/mL epidermal growth factor, and 5 µg/mL insulin. The cultures were maintained at 37ºC in a 5% $CO_2$ humidified atmosphere.

### 2.9. Cell viability assay

To assess cell viability, corneal cells were seeded onto 96-well plates ($2x10^4$ cells/well) and grown until 80% confluence. The cells were then incubated for 30 minutes with NP dilutions (prepared in phenol red-free DMEM) at the following concentrations (w/v): 0.1%, 0.2%, and 0.4%, that were equivalent to 0.025%, 0.05%, and 0.1% CsA for the drug-loaded NPs. Negative controls consisted of cells exposed to phenol red-free DMEM. Positive controls consisted of cells exposed to 0.01% (w/v) BZK and cells exposed to 0.003% (w/v) CTAB. Finally, all formulations were washed out, and the XTT cell viability assay was performed according to the manufacturer's instructions. The percentage of living cells was calculated based upon the negative control. Three independent experiments were performed.

### 2.10. Cell proliferation assay

Cell proliferation was evaluated using the Alamar Blue® assay. Corneal cells were seeded onto 24-well plates ($2x10^4$ cells/well) and grown until 60% confluence. The cells were then incubated for 30 minutes with NP dilutions and controls. Cell proliferation was measured at 0, 24, and 48 hours after exposure, according to the manufacturer's instructions. The percentage of cell proliferation was based upon the negative control at 0 hours. Three independent experiments were performed.

### 2.11. Cellular uptake of NPs

Uptake of NPs by HCE cells was studied using Nile red-loaded NPs. CsA was replaced by this fluorescent dye during preparation of the NPs. In all studies, the NP concentration was adjusted with phenol red-free DMEM to 0.2% (w/v), which was equivalent to 6.67 µg/mL of Nile red. Cellular uptake was qualitatively monitored by fluorescence microscopy and semi-quantitatively by fluorometry.

NP internalization mechanisms were studied as previously reported, with minimum modifications [15]. HCE cells were seeded at a density of $8x10^5$ cells/well and grown until 80% confluence. Different internalization blocking conditions (**Table 3**) were applied for an hour to each well, except for the controls. Then, inhibitors were removed and 300 µL of diluted NPs were added to all wells and incubated for 30 minutes. Afterwards, the cells were washed three times with DPBS to remove extracellular NPs and then disrupted with 300 µL of radioimunoprecipitation assay buffer. Then, 200 µL of the lysate were used for fluorescence analysis, and the protein content of the remaining volume was determine with the Pierce® BCA Protein Assay Kit. Fluorescence values were normalized to the total protein content of each well. Relative internalization was calculated based on the control with no cellular uptake inhibition. Four independent experiments were performed.

To determine the NP intracellular distribution in living cells, HCE cells were seeded in 8-well multichamber Permanox® slides ($5x10^5$ cells/well) and grown until confluent. Afterwards, 100 µL of diluted NPs were added to each well and incubated for 5, 15, and 30 minutes. Then the formulations were removed, and the wells were washed three times with DPBS. Cell nuclei were counterstained with Hoesch dye, and images were taken with an inverted fluorescence microscope (Leica DMI 6000B, Wetzlar, Germany) at 40x magnification.

The fluorescence of cell-associated NPs over time was also analyzed. Confluent HCE cells ($2x10^5$ cells/well) were incubated with NPs for 30 minutes. Then the formulations were withdrawn, the cells were washed with DPBS. Phenol red-free DMEM was added to each well, and the fluorescence corresponding to 0 hours was determined (Spectramax® M5; $\lambda_{Excitation}$ = 559 nm, $\lambda_{Emission}$ = 629 nm). Then, at 2, 4, and 6 hours after NP exposure, the surrounding medium was replaced with freshly prepared medium and the fluorescence was subsequently measured.

**2.12. Nanoparticle distribution and CsA penetration through ex vivo pig cornea**

Porcine eye balls were obtained from a local slaughterhouse and used within one hour after sacrifice. Nile red-loaded NPs were used for qualitative analysis of NP distribution. CsA-loaded NPs were used for measurement of CsA penetration. In both cases, the NP concentration was 0.2 % (w/v).

For qualitative analysis, a 12-mm silicon ring was placed over the central cornea of the pig eyeballs, and 300 µL of NPs or controls (Nile red in olive oil) were applied for 30 minutes. The eyeballs were then washed with DPBS and placed in 2.5% buffered paraformaldehyde. The central cornea was harvested, embedded in optimal cutting temperature medium, and frozen. Tissue sections of 5 µm thickness were obtained by cryostat cutting and subsequently observed by fluorescence microscopy. Representative images of two independent experiments were taken.

CsA penetration was measured using excised pig corneas (n = 4) mounted between the donor and receptor compartment of vertical Franz diffusion cells (VidraFoc, Valencia, Spain). The receptor compartment was filled with SLF without proteins and kept under continuous stirring. Formulations were applied to each donor compartment and incubated at 37ºC for 30 minutes. In this experiment, the commercial formulation Sandimmun®, a microemulsion commonly used in hospital-made CsA preparations [21], was used as the reference. After 30 minutes, the corneas were removed, and the diffusion zone was carefully trimmed and weighed. The corneas were digested using 500 µL of 0.5 M NaOH for 12 hours at 37ºC [22]. The fraction of CsA that penetrated was extracted using 500 µL of ACN and quantified by HPLC. The penetration of CsA was normalized based on each corneal weight. Relative CsA penetration was calculated with regard to the reference formulation.

### 2.13. Inhibition of IL-2 production by Con A-stimulated human lymphocytes

The immunosuppressive activity of the NPs was assessed *ex vivo* on freshly isolated human lymphocytes. Peripheral blood mononuclear cells (PBMC) including monocytes and lymphocytes were isolated from a sample of human venous blood from a healthy donor following the "Basic Protocol 3" reviewed by Dagur et al. [23], after a signed informed consent was obtained. The PBMCs were transferred to a 25-$cm^2$ culture flask containing DMEM/F-12 medium supplemented with 10% fetal bovine serum and 1% (v/v) penicillin/streptomycin. The cells were incubated for 4 hours at 37ºC to facilitate monocyte adhesion to flask walls. Then, lymphocytes remaining in suspension were withdrawn and seeded onto a 96-well plate at a density of $4x10^5$ cells/well. Blank NPs, CsA-loaded NPs, and Sandimmun® were added to wells at a CsA concentration of 25 ng/mL [24]. The concentration of blank NPs was adjusted to the equivalent of the CsA NP concentration. Later, Con A was added to all wells at a final concentration of 20 µg/mL with the exception of negative control wells [24]. After 24 hours of incubation at 37ºC in a 5% $CO_2$ humidified atmosphere, the 96-well plate was centrifuged at 1,000 rpm for 10 minutes and supernatants collected and stored at -80ºC until analysis. IL-2 content was measured using a specific ELISA kit following manufacturer instructions. Three independent experiments were performed.

### 2.14. Statistical analysis

All experimental data were expressed as means ± standard deviations (SD). Comparison of data groups was performed by a one-way ANOVA followed by pairwise comparisons (Tukey test) using Statistical Procedures for the Social Sciences software (SPSS 20.0; SPSS Inc., Chicago, USA). Significant differences were considered when the *p*-value was $\leq 0.05$.

## 3. Results and discussion

Several considerations must be accounted for when designing a novel formulation. Selection of formulation components must clearly focus on technological properties, but also on the regulatory status and biocompatibility. All of the formulation components used in this study were approved by European and American regulatory agencies according to their safety and biocompatibility profiles. The major NP component was Span® 80, a widely used excipient in the food industry and oral pharmaceutical formulations [25]. Other components were CTAB, a quaternary ammonium derivative

commonly used as a preservative in eyedrops, and TPGS, a vitamin E derivative present in various commercialized ophthalmic formulations [26,27]. We previously reported the use of TPGS for the development of SENS intended for topical ocular cyclosporine delivery [28]. Indeed, the use of TPGS has recently attracted the interest of some authors for the development of other nanosystems also designed for topical ocular delivery [29]. In addition, HA, a frequent component of artificial tears, was selected as a NP surface modifier.

### 3.1. SENS optimization by Box-Behnken experimental design and subsequent coating with HA

After adequate selection of materials, we focused on obtaining formulations with the most appropriate physicochemical properties by using a Box-Behnken experimental design. The experimental results obtained for particle size, zeta potential, entrapment efficiency, and drug loading of each formulation are summarized in **Table 2.**

**Table 2. Box-Behnken design matrix and corresponding observed responses.**

| Run | Independent variables* | | | Observed responses in dependent variables | | | | |
|---|---|---|---|---|---|---|---|---|
| | Span® (% w/v) | TPGS (% w/v) | CsA (% w/v) | PS (nm) | PdI | ZP (mV) | EE (%) | DL (%) |
| 1[c] | 2.50 | 0.20 | 0.48 | 178.4 | 0.095 | +30.73 | 80.63 | 12.30 |
| 2 | 3.00 | 0.30 | 0.48 | 181.1 | 0.095 | +28.87 | 80.63 | 10.32 |
| 3 | 2.50 | 0.30 | 0.65 | 169.5 | 0.062 | +30.27 | 81.71 | 15.80 |
| 4[c] | 2.50 | 0.20 | 0.48 | 179.6 | 0.060 | +31.60 | 80.93 | 12.34 |
| 5 | 3.00 | 0.20 | 0.30 | 185.5 | 0.036 | +28.13 | 82.64 | 7.13 |
| 6 | 2.00 | 0.30 | 0.48 | 157.6 | 0.064 | +31.23 | 76.99 | 13.57 |
| 7 | 3.00 | 0.10 | 0.48 | 185.8 | 0.039 | +32.13 | 79.31 | 10.74 |
| 8[c] | 2.50 | 0.20 | 0.48 | 180.3 | 0.076 | +31.63 | 82.28 | 12.52 |
| 9 | 2.00 | 0.20 | 0.65 | 171.2 | 0.055 | +33.67 | 85.62 | 19.97 |
| 10 | 3.00 | 0.20 | 0.65 | 185.0 | 0.079 | +31.97 | 82.64 | 14.26 |
| 11 | 2.00 | 0.20 | 0.30 | 168.1 | 0.073 | +33.20 | 72.02 | 8.83 |
| 12 | 2.50 | 0.10 | 0.65 | 185.8 | 0.027 | +36.73 | 86.31 | 17.58 |
| 13 | 2.50 | 0.30 | 0.30 | 175.5 | 0.060 | +29.70 | 76.28 | 7.48 |
| 14 | 2.50 | 0.10 | 0.30 | 177.5 | 0.034 | +33.07 | 76.51 | 8.03 |
| 15 | 2.00 | 0.10 | 0.48 | 171.7 | 0.037 | +35.63 | 75.04 | 14.33 |

*The CTAB concentration was 0.03% (w/v) in all experimental runs; [c]center points of design; Span®, sorbitan monooleate; TPGS, d-α-tocopheryl polyethylene glycol 1000 succinate; CsA, cyclosporine A; PS, particle size; ZP, zeta potential; EE, entrapment efficiency; DL, drug loading PdI, polydispersity index.

The optimization of particle size was focused on minimizing it because it is generally accepted that smaller NPs are more suitable for topical ocular administration than larger ones. This may be attributed to the fact that smaller NPs can travel faster through the precorneal mucus layer of the tear film [30] and are easily internalized by corneal epithelial cells [31]. Also, for particle sizes under 200 nm, the formulations can be easily sterilized by filtration. While Span® 80 increases particle size ($p \leq 0.001$, **Figure 1a)**, probably due to the inclusion of more molecules within the NP matrix, TPGS has the opposite effect ($p \leq 0.001$, **Figure 1a)**. We attribute this decrease in size to the distribution of TPGS over the NP surface and the resulting decrease in the interfacial tension between water and the NPs. Consequently, the increased amount of surfactant contributes to the reduction in particle size. This effect was also observed by McCall et al. in the preparation of poly(lactic-co-glycolic acid) NPs [32]. CsA did not significantly affect particle size, probably because it was distributed within the NP matrix (**Figure 1a**).

Our primary goal in zeta potential optimization was to maximize it. It is generally accepted that positively charged NPs can easily interact with the negatively charged corneal surface, thus enabling extended residence times. In addition, zeta potentials far away from electroneutrality contribute to the stability of nanosystems [33,34]. The zeta potential was in the range of +28.13 to +36.73 mV and varied as a function of the TPGS and CsA concentrations (**Figure 1b**). TPGS exerts a negative effect on the zeta potential ($p \leq 0.001$, **Figure 1b**) due to the presence of the NP polyethylene-glycol moieties oriented towards the surrounding medium. These moieties provoke the displacement of the surface shear plane, resulting in lower zeta potentials [35]. Interestingly, our findings suggest that CsA concentration positively affects zeta potential ($p \leq 0.01$, **Figure 1b**). This is surprising because of the neutral nature of CsA, but other authors also reported this effect [36]. The underlying reason may be attributed to the reorganization of the molecules on the NP surface secondary to the entrapment of CsA. This effect was more explicit at low TPGS concentrations (**Figure 1b**), which can be explained by the absence of shear plane displacement. This hypothesis is consistent with outcomes obtained for EE% (75.04%~86.31%) (**Figure 1c**) and DL% (7.13%~19.97%) (**Figure 1d**), where increasing CsA concentration resulted in higher values of EE% and DL% ($p<0.001$). As foreseen, apart from the drug proper, the EE% was also positively affected by the amount of Span® 80, the main NP matrix component ($p \leq 0.05$).

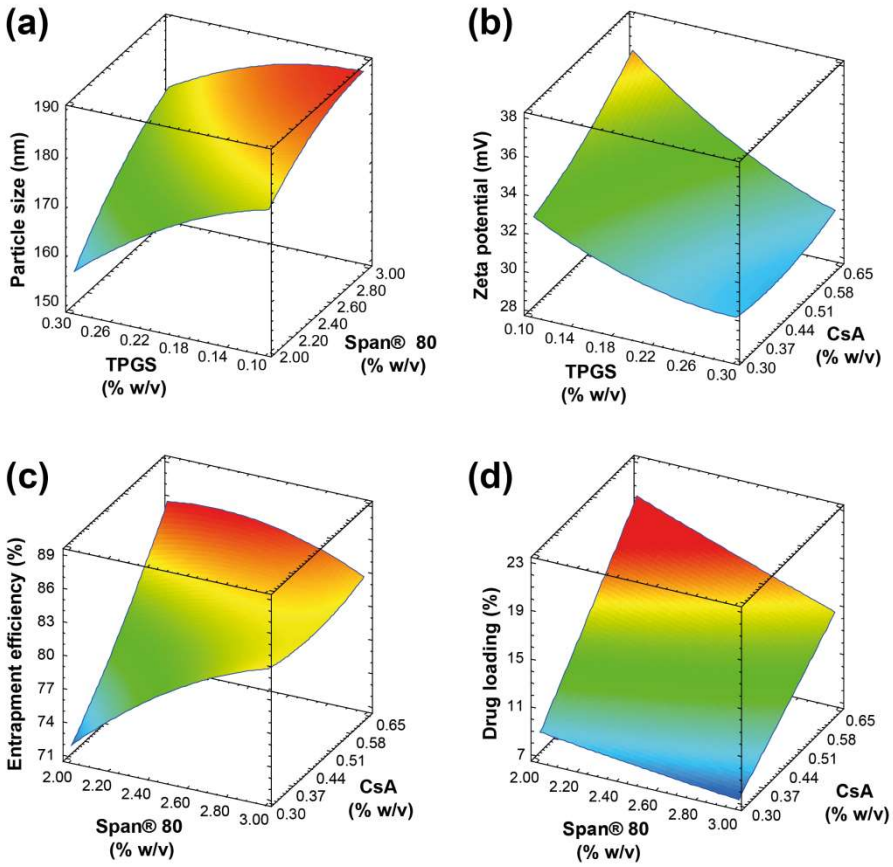


**Figure 1. Response surface graphs showing particle size, zeta potential, entrapment efficiency, and drug loading as functions of Span 80, TPGS, and CsA concentrations.** (a) Particle size was mainly determined by the concentrations of Span® 80 (positive effect, $p \leq 0.001$) and TPGS (negative effect, $p \leq 0.001$). (b) The zeta potential was mainly determined by the concentrations of TPGS (negative effect, $p \leq 0.001$) and CsA (positive effect, $p \leq 0.01$). (c) The entrapment efficiency was mainly determined by the concentrations of Span® 80 and CsA (both positive effect, $p \leq 0.05$). (d) Drug loading was mainly determined by the concentration of CsA positive effect, $p \leq 0.001$) and Span® 80 (negative effect, $p < 0.001$).

The resulting optimized formulation, SENS-OPT (**Table 4**), had a particle size under 200 nm, zeta potential above +30 mV, and high values of entrapment efficiency and drug loading, all of which are suitable properties for topical ODD. The Box-Behnken design was also validated by comparison between predicted and observed values in the four response variables considered. Accounting for the low bias (< |3.11|%) obtained in the three formulations evaluated (**Table 4)**, the results demonstrated the validity and predictive ability of this design.

**Table 4. Validation table with predicted values, experimental values, and prediction errors for optimized formulation (SENS-OPT) and two additional checkpoint formulations (SENS-HIGH and SENS-LOW)**.

| Code | Composition (% w/v) | | | | Dependent variable | Predicted value | Experimental value | | Bias (%) |
|---|---|---|---|---|---|---|---|---|---|
| | Span | TPGS | CTAB | CsA | | | Mean | SD | |
| SENSHIGH | 2.75 | 0.25 | 0.03 | 0.56 | PS (nm) | 179.9 | 177.2 | 5.8 | -1.50 |
| | | | | | ZP (mV) | +30.3 | +29.6 | 2.0 | -2.31 |
| | | | | | EE (%) | 82.19 | 81.77 | 2.14 | -0.51 |
| | | | | | DL (%) | 13.22 | 13.19 | 0.30 | -0.23 |
| SENSOPT | 2.00 | 0.22 | 0.03 | 0.65 | PS (nm) | 168.4 | 170.5 | 5.0 | +1.26 |
| | | | | | ZP (mV) | +33.0 | +33.9 | 0.5 | +2.82 |
| | | | | | EE (%) | 85.53 | 83.95 | 2.11 | -1.85 |
| | | | | | DL (%) | 19.69 | 19.66 | 0.40 | -0.15 |
| SENSLOW | 2.25 | 1.5 | 0.03 | 0.39 | PS (nm) | 175.4 | 176.3 | 6.8 | +0.48 |
| | | | | | ZP (mV) | +33.0 | +33.4 | 1.7 | +1.21 |
| | | | | | EE (%) | 76.78 | 79.16 | 3.28 | +3.10 |
| | | | | | DL (%) | 10.86 | 11.17 | 0.44 | +2.85 |

Span® 80, sorbitan monooleate; TPGS, d-α-tocopheryl polyethylene glycol 1000 succinate; CTAB, cetyltrimethylammonium bromide; CsA, cyclosporine A; SD, standard deviation; PS, particle size; ZP, zeta potential; EE, entrapment efficiency; DL, drug loading.

In addition to SENS-OPT, we developed an optimized HA-coated formulation. The underlying objective was to determine if HA surface tailoring improves the biopharmaceutical properties of SENS. An HA of 1,600 KDa was selected because high molecular weight HA exhibits greater affinity for HA receptors than does the low molecular weight variety [37]. Different HA concentrations were previously evaluated (data not show) to determine how they affected the physicochemical properties of the NPs (i.e., particle size, zeta potential, and HA association efficacy). The most adequate HA concentration was 0.015%, which we selected for preparing SENS-OPT-HA. In the preparation of HA-coated NPs, the particle size increased from 165.5 ± 5.8 to 177.6 ± 5.1 nm, whereas the zeta potential decreased from +27.1 ± 0.5 to –20.6 ± 0.7 mV, indicating polymer adsorption onto the surface of SENS-OPT.

### 3.2. Physicochemical characterization of SENS-OPT and SENS-OPT-HA

Transmission electron microscopy showed homogeneous populations of SENS-OPT and SENS-OPT-HA NPs (**Figure 2a, b respectively**), with spherical shapes and particle sizes in accordance with DLS measurements. SENS-OPT-HA presented a less opaque corona, probably because of the disposition of HA molecules on the NP surface, confirming the adsorption of HA.

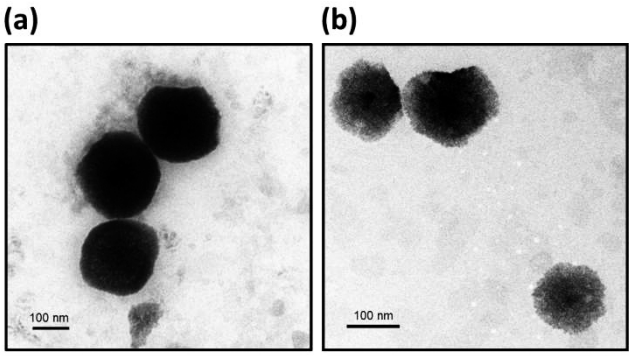


**Figure 2. Transmission electron microscopy of SENS-OPT and SENS-OPT-HA.** (a) SENS-OPT and (b) SENS-OPT-HA presented spherical shapes and the particle size distribution was homogeneous. SENS-OPT-HA had a less opaque corona surrounding because of the HA coating.

Liquid NMR can provide useful structural insights regarding molecular mobility of the NP components. Typically, when the molecular mobility decreases, as in the case of the formation of nanostructures, the relaxation time also decreases and causes a broadening in the NMR spectrum line. There can even be a total loss of the peak if the molecules are incorporated into a rigid local environment and occluded from bulk water [38]. Structural analysis of formulations by NMR (**Figure 3f-h)** showed that all formulation components form nanostructures, as indicated by the loss or broadening of peaks observable in the $^{1}$H-wg NMR spectrum of the NPs. Also, the visibility of peaks from the Span® 80, the polyethylene glycol (PEG) residues of TPGS, and the $NMe_3$ group of CTAB indicates that these molecules had some mobility or "flexibility" in the surrounding water environment. This means that there is a fraction of these components that form part of the surface of the NPs and therefore are exposed to the bulk water. These results are in agreement with our previously published data about the general structure of Span® NPs, in which they presented a flexibility gradient from an inner rigid core towards a more flexible region located at the surface [39].

The absence of visible peaks of CsA in the drug-loaded formulations indicates a restricted mobility of this molecule because of the effective entrapment inside the NPs. In comparing the drug loaded formulations with the placebo control formulation, it was evident that the incorporation of CsA did not disturb the NP structure. Nonetheless, CsA slightly affects reorganization of molecules at the NP surface because the $NMe_3$ group of CTAB was absent when the drug was present. This is consistent with the zeta potential variations observed in the Box-Behnken design. On the other hand, the spectrum of HA peaks in the SENS-OPT-HA were not discerned, probably because of the combined effect of the low HA intensity and the complete peak overlapping with other components.

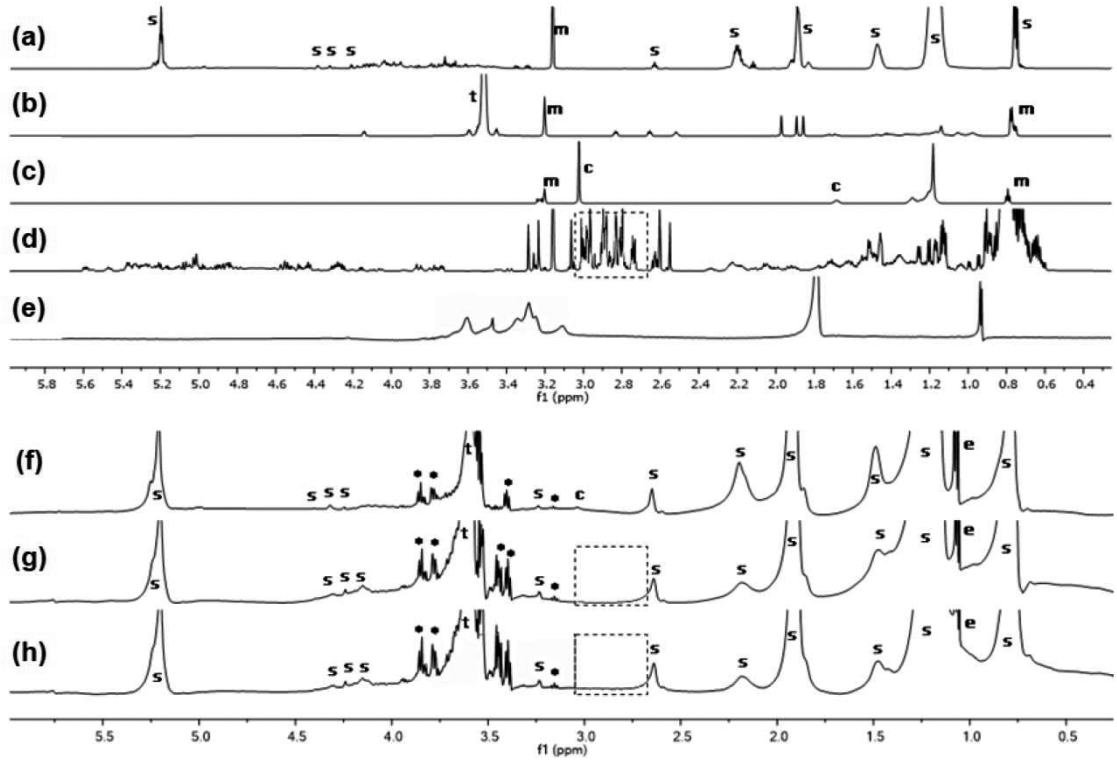


**Figure 3. NMR spectra. (Upper) $^1$H NMR spectrum of raw materials used in the preparation of nanoparticles.** (a) Span®80, (b) TPGS, (c) CTAB, (d) CsA, and (e) HA; (Lower) $^1$H-wg NMR spectrum of NPs (f) SENS-BLK, (g) SENS-OPT, and (h) SENS-OPT-HA. s, Span®80; t, polyethylene glycol (PEG) of TPGS; c, trimethyl amino ($NMe_3$) peak of CTAB; e, ethanol; m, methanol; *, low molecular weight impurity. Peak broadening occurred in (f), (g), and (h), indicating all of the raw materials detailed above formed NPs. There were no differences between the spectra of (f) placebo and (g, h) CsA-loaded NPs, with the exception of loss of the "c" peak in the presence of CsA.

Another important consideration when developing a new formulation is to evaluate the physical and biological stability because it can directly determine the technological viability. The developed NPs exhibited adequate physical stability after storage for 3 months under three different temperature conditions **(Figure 4a)**. There were minor but statistically significant variations in particle size ($p \leq 0.05$) and zeta potential over time ($p \leq 0.05$). We do not consider that these variations were of any technological significance relative to the stability of the NPs. In addition, both NPs showed zadequate biological stability after incubation with protein-enriched SLF (**Figure 4b**). Only SENS-OPT-HA underwent a minor, but statistically significant, increase in particle size ($p \leq 0.05$ at hours 2 and 5), probably due to protein opsonization secondary to the hydrogen bonding between HA and surrounding proteins. This good stability can be attributed to the electro-steric stabilization provided by zeta potentials far away from electroneutrality and to the steric hindrance provided by PEG residues of TPGS.

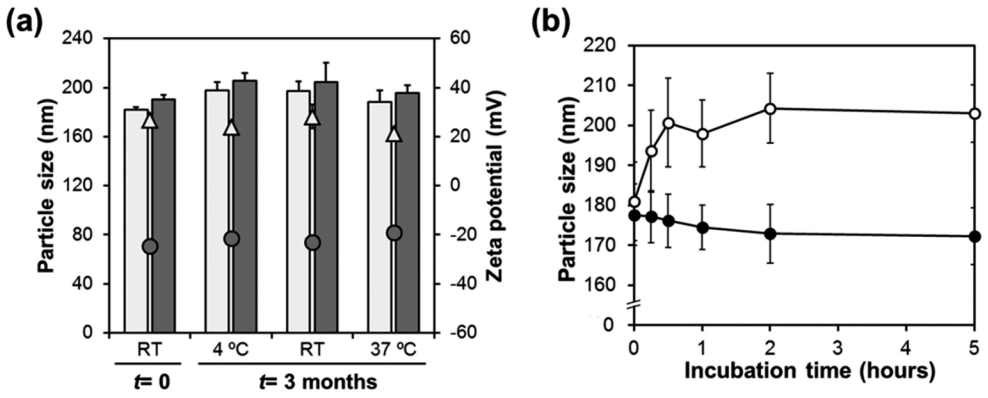


**Figure 4. Physical and biological stability of SENS-OPT and SENS-OPT-HA after storage for 3 months at different temperatures.** (a) Size and zeta potential of the SENS-OPT NPs (white bars and triangles) and SENS-OPT-HA NPs (grey bars and circles). Both types of NPs exhibited minor variations in size and zeta potential after 3 months ($p \leq 0.05$). (b) Biological stability of the SENS-OPT (black circles) and SENS-OPT-HA (white circles) NPs. Lines indicate the size evolution of the NPs during five hours of incubation with protein-enriched SLF. Only SENS-OPT-HA NPs experienced minor but significant increases in particle size after 2 hours of incubation ($p \leq 0.05$).

### 3.3. In vitro evaluation of biocompatibility of developed NPs

The biocompatibility of NPs was assessed *in vitro* with HCE cells using two complementary assays. The acute toxicity of the formulations after 30 minutes of exposure was determined using the XTT cell viability assay. Neither the SENS-OPT nor the SENS-OPT-HA reduced cell viability, even up to 0.2% (w/v) (**Figure 5a)**. These concentrations were equivalent to 0.05% (w/v) CsA, which is the drug concentration in the commercial formulation Restasis®. Only the highest concentration tested, 0.4%, slightly reduced viability ($p \leq 0.01$). As expected, both positive controls, BZK and CTAB, induced a marked reduction ($p \leq 0.001$) in cell viability. CTAB (0.003% [w/v]) was included as a control because it is the same cationic agent concentration present in the 0.2% (w/v) NPs. The biggest difference observed between cell viability of both samples can be attributed to the efficient incorporation of CTAB by SENS-OPT, which excludes the presence of free molecules of this surfactant that can cause cell damage. This effect was previously reported by Sznitowska et al. with different quaternary ammonium derivatives in the presence of emulsions [40].

In addition to the cell viability assay, cell proliferation assays were performed to determine if cell replication was compromised after nanoparticle exposure. Only the positive control with CTAB irreversibly inhibited cell proliferation ($p \leq 0.001$, **Figure 5b**). After the 30 minute exposure to the NPs, cell recovery and proliferation were unaffected.

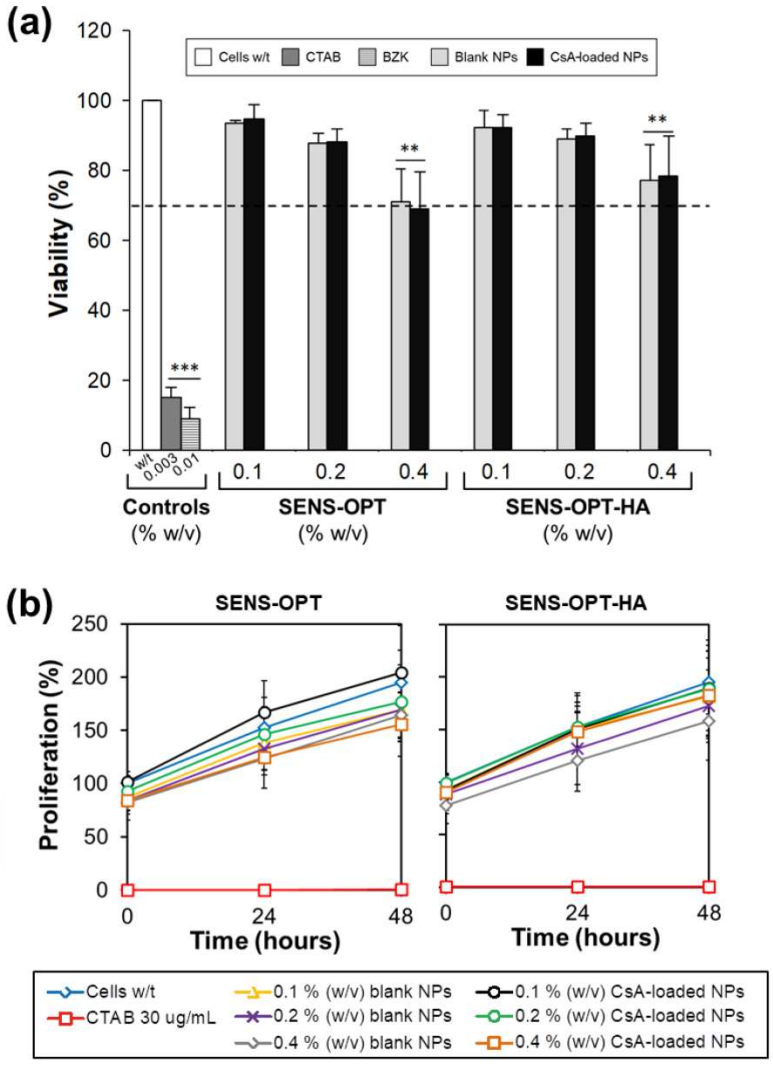


**Figure 5. HCE cell line viability and proliferation results for SENS-OPT and SENS-OPT-HA.** (a) Only the highest NP concentration significantly reduced (**$p \leq 0.01$) cell viability in comparison with control cells without treatment (w/t). Positive controls cetyltrimethylammonium bromide (CTAB) and benzalkonium chloride (BZK) drastically reduced cell viability (***$p \leq 0.001$). (b) Only the positive control CTAB significantly inhibited cell proliferation (***$p \leq 0.001$). There were no significant differences among the proliferation profiles of cells without treatment and cells treated with NPs.

### 3.4. Cellular uptake of NPs and interaction with ex vivo porcine cornea

Nanosystems, unlike conventional formulations that deliver drug content through passive diffusion mechanisms, have the advantage of accessing target cells by active mechanisms. This implies that a drug can be specifically directed to a target and that adverse effects could be minimized while efficacy could be maximized.

Uptake by corneal epithelial cells of the NP formulations that we developed was efficiently driven through energy-dependent active transport mechanisms ($p \leq 0.001$ for each type of NP, **Figure 6a)** as suggested by uptake inhibition at 4°C. For SENS-OPT, the main cell uptake mechanism was caveolin-mediated endocytosis as shown by inhibition with filipin ($p \leq 0.05$). For SENS-OPT-HA, the mechanism was receptor-mediated endocytosis as shown by inhibition with excess HA ($p \leq 0.05$). This active targeting through HA receptors could be responsible for the higher fluorescence signal observed in corneal epithelial cells (**Figure 6b**). It is reported that HA receptors present on corneal cells would enhace and speed up NP internalization [15,16]. The observed differences in the intracellular distribution of the two types of NPs (**Figure 6b**) may be explained by the net difference in charge. The positive surface charge of SENS-OPT could allow an electrostatic interaction with the negatively charged nucleus of the cell, facilitating accumulation. In contrast, the negative surface charge of HA-coated NPs could provoke a repulsion effect from the cell nucleus, leading to a broad distribution in the cytosol. Although SENS-OPT-HA presented higher cellular uptake than the uncoated NP version ($p \leq 0.001$, **Figure 6c**) the intracellular presence of both types of NPs diminished in a similar extent with time, suggesting that both formulations were easily degraded by the corneal cells.

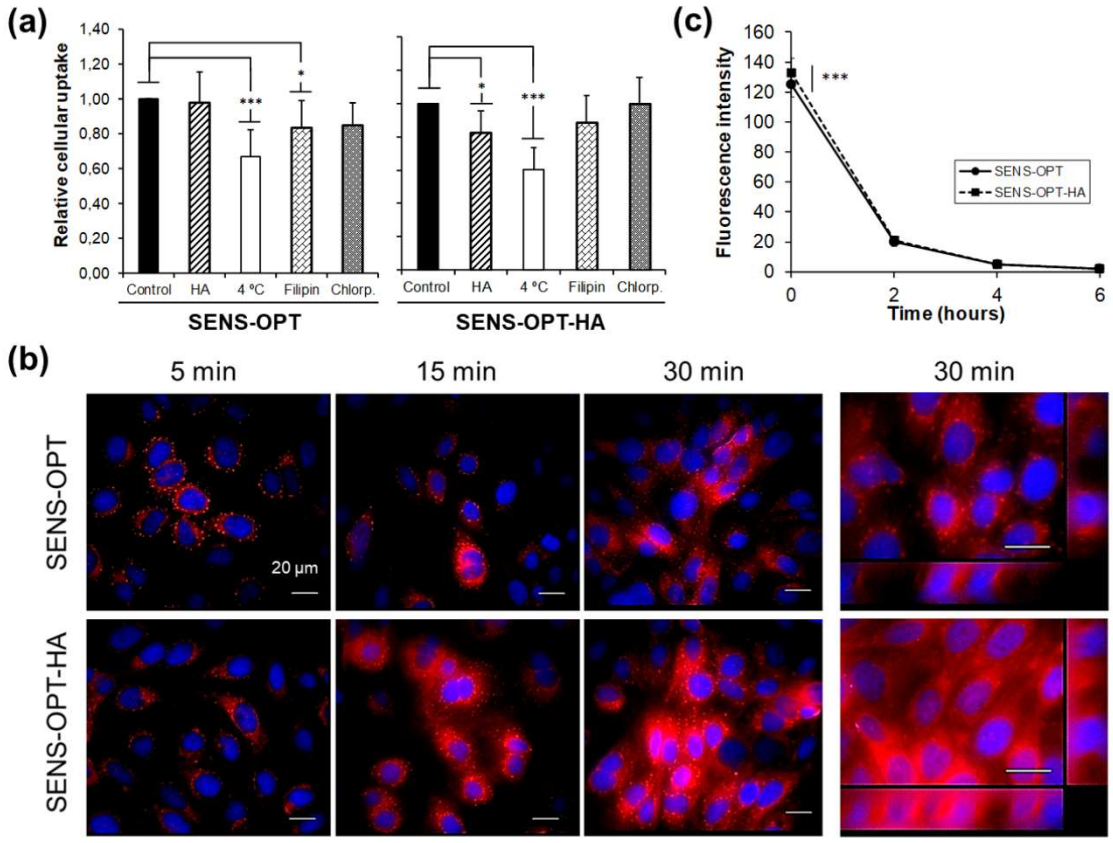


**Figure 6. NP cellular uptake by HCE cells.** (a) Different blocking conditions were applied for inhibition of specific cellular uptake mechanisms. SENS-OPT cellular uptake was significantly reduced by low temperature (*$p \leq 0.001$) and filipin (*$p \leq 0.05$), an inhibitor of caveolin-mediated endocytosis. SENS-OPT-HA uptake was significantly reduced by low temperature (*$p \leq 0.001$) and excess HA (*$p \leq 0.05$). Chlorpromazine (Chlorp), an inhibitor of clathrin-mediated endocytosis, did not affect either SENS-OPT or SENS-OPT-HA NP uptake. (b) Fluorescence microscopy of HCE cells after exposure for 5, 15, and 30 minutes to Nile red-loaded SENS-OPT and SENS-OPT-HA NPs. Cationic SENS-OPT NPs were accumulated mostly around the cell nuclei. In contrast, anionic SENS-OPT-HA NPs were broadly distributed in the cytosol. Both types of NPs were located inside cells as shown in Z-scan images (upper and lower right panels) obtained after NP exposure for 30 minutes. (c) Over a two-hour exposure period, the fluorescence of both NPs was reduced by 85%.

The distribution pattern observed *in vitro* in corneal cells was also observed in the *ex vivo* study of NP distribution through porcine cornea (**Figure 7a-c)**. SENS-OPT were accumulated mostly in the apical part of epithelium and surrounding cell nuclei, presumably due to the negative charge of both structures (**Figure 7b**). In contrast, SENS-OPT-HA were broadly distributed through the epithelium layers and reached the corneal stroma (**Figure 7c**).

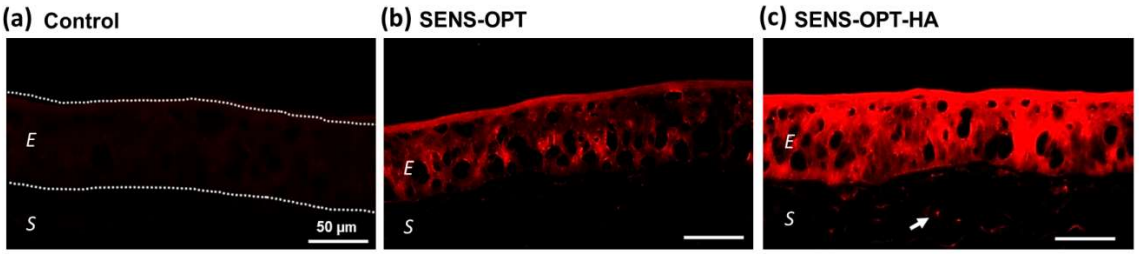


**Figure 7. Fluorescence microscopy of porcine cornea after topical application of Nile red dissolved in olive oil, Nile red-loaded SENS-OPT, and Nile red-loaded SENS-OPT-HA NPs.** (a) Nile red dissolved in olive oil had minimal penetration into the corneal epithelium. The corneal epithelium, which was nearly invisible due to the limited Nile red uptake, was highlighted with a dotted line at the anterior and posterior surfaces. (b) SENS-OPT NPs accumulated mostly in the apical part of the epithelium (E) and surrounding cell nuclei. (c) SENS-OPT-HA NPs were broadly distributed through epithelial layers and reached the corneal stroma (S) (white arrow).

In addition, results from the CsA penetration study (**Figure 8**) confirmed that SENS-OPT and SENS-OPT-HA promoted a 1.3-fold increase and a 2.1-fold increase respectively in drug penetration compared to commercial formulation ($p \leq 0.05$).

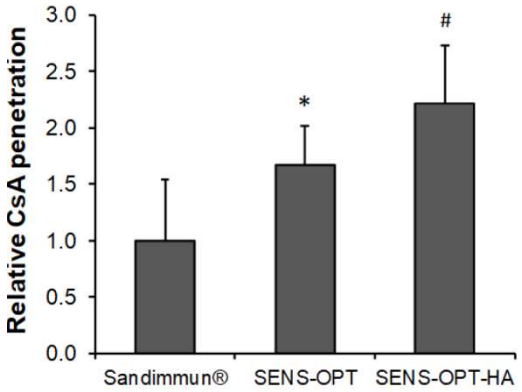


**Figure 8. Relative CsA penetration through excised pig cornea.** SENS-OPT and SENS-OPT-HA promoted a 1.3-fold increase and a 2.1-fold increase respectively in drug penetration compared to reference formulation Sandimmun®. SENS-OPT-HA promote higher CsA penetration than the uncoated NPs. Significant differences are represented by: $*p \leq 0.05$ compared to Sandimmun and SENS-OPT-HA; and $\#p \leq 0.05$ compared to Sandimmun and SENS-OPT.

### 3.5. Ex vivo evaluation of the immunosuppressive activity of CsA-loaded NPs

The immunosuppressive activity of the NPs was confirmed using a functional *ex vivo* assay of lymphocyte activation. CsA specifically inhibits T-lymphocyte activation by blocking the calcineurin pathway, which ultimately results in the suppression of IL-2 production [41]. We evaluated the biological activity of the NPs by measuring IL-2 production after activation with Con A of human lymphocytes freshly obtained from peripheral blood.

IL-2 basal production in lymphocytes was very low but increased significantly when Con A was added ($p \leq 0.001$, **Figure 9**). Both CsA-loaded SENS-OPT and SENS-OPT-HA NPs decreased IL-2 levels ($p \leq 0.001$) to a similar extent as the commercial formulation Sandimmun® used as reference. This means that CsA maintained biological activity after entrapment inside the NPs, and the immunosuppressive effect was as high as that provided by the commercial formulation. Interestingly, our findings suggest that blank SENS-OPT-HA might have some immunosuppressant activity (**Figure 9**). However, we attribute this effect to an experimental artifact secondary to the interaction of HA with IL-2 [42]. Our interpretation is that IL-2 was adsorbed onto the NP surface, and therefore, after the NP withdrawal step, the IL-2 levels inside the well plate were lowered.

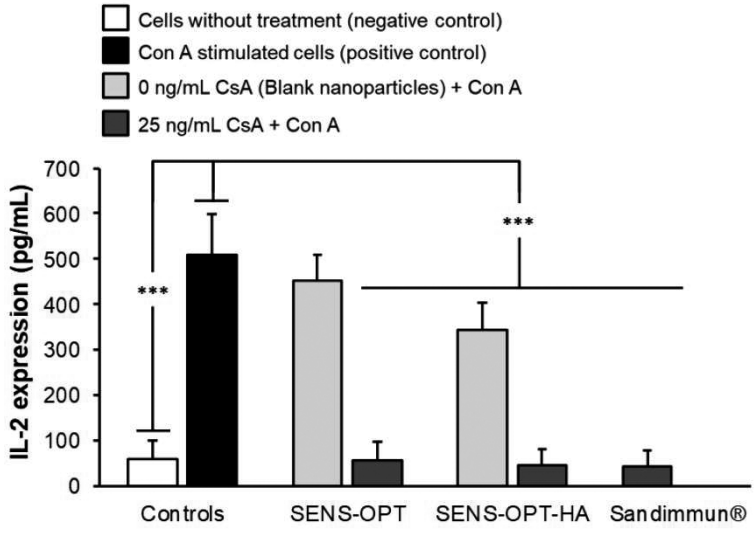


**Figure 9. Inhibitory effect of blank and CsA-loaded NPs on IL-2 production by freshly isolated human lymphocytes stimulated with Con A.** IL-2 production was stimulated by the addition of Con A. In cells previously treated with CsA-loaded SENS-OPT or SENS-OPT-HA NPs, the basal levels were maintained after Con A exposure (***$p \leq 0.001$). This effect was the same as observed for the commercial formulation Sandimmun®. IL-2 reduction induced by blank SENS-OPT-HA was attributed to an experimental artifact.

## 4. Conclusions

In this study, two types of NPs were successfully developed as novel tools for topical CsA administration. Both formulations showed adequate physicochemical properties, including particle size in the nanometric range, high drug loading, and good physical and biological stability. Biocompatibility studies showed that both SENS-OPT and SENS-OPT-HA could be considered safe in the concentration range evaluated. Also, *ex vivo* evaluation of biological activity revealed that both NPs exhibited the same immunosuppressive efficacy as the commercial formulation Sandimmun®. Additionally, the HA-coating of SENS-OPT, i.e., SENS-OPT-HA, induced a higher cellular uptake by cultured HCE cells and penetration across porcine corneal tissues than the uncoated SENS-OPT formulation. Our results are consistent with the active targeting of the HA-coated NPs to corneal HA-receptors that then facilitated NP internalization as reported by others. For these reasons, although further studies are necessary, we consider SENS-OPT-HA as a promising formulation that will improve the efficacy of topically-applied CsA. This enhanced delivery system may even allow the use of lower CsA concentrations than those required in the currently available commercial formulations.

## 5. Acknowledgments

This work was supported by grants from the Ministry of Economy and Competitiveness of Spain (MAT2013-47501-C02-R), Agencia Estatal y del Fondo Estrutural (FEDER), Xunta de Galicia (Competitive Reference Groups-FEDER Funds, Ref. 2017-PG101), and FPI Scholarship Program (BES-2014-069437).

**References**


[1] A. Patel, K. Cholkar, V. Agrahari, A.K. Mitra, Ocular drug delivery systems: An overview, World J. Pharmacol. 2 (2013) 47–64. doi:10.5497/wjp.v2.i2.47

[2] S. Reimondez-Troitino, N. Csaba, M.J. Alonso, M. de la Fuente, Nanotherapies for the treatment of ocular diseases, Eur. J. Pharm. Biopharm. 95 (2015) 279–293. doi:10.1016/j.ejpb.2015.02.019.

[3] M.K. Rhee, F.S. Mah, Clinical utility of cyclosporine (CsA) ophthalmic emulsion 0.05% for symptomatic relief in people with chronic dry eye: a review of the literature, Clin. Ophthalmol. 11 (2017). doi:10.2147/OPTH.S113437.

[4] M. Ziaei, B. Manzouri, Topical Cyclosporine in Corneal Transplantation, Cornea. 34 (2015) 110–115.

[5] F. Lallemand, M. Schmitt, J.-L. Bourges, R. Gurny, S. Benita, J.-S. Garrigue, Cyclosporine A delivery to the eye: A comprehensive review of academic and industrial efforts, Eur. J. Pharm. Biopharm. 117 (2017) 14–28. doi:10.1016/j.ejpb.2017.03.006.

[6] N. Li, C.-Y. Zhuang, M. Wang, C.-G. Sui, W.-S. Pan, Low molecular weight chitosan-coated liposomes for ocular drug delivery: In vitro and in vivo studies, Drug Deliv. 19 (2012) 28–35. doi:10.3109/10717544.2011.621994.

[7] L. Battaglia, I. D'Addino, E. Peira, M. Trotta, M. Gallarate, Solid lipid nanoparticles prepared by coacervation method as vehicles for ocular cyclosporine, J. Drug Deliv. Sci. Technol. 22 (2012) 125–130. doi:10.1016/S1773-2247(12)50016-X.

[8] G. Sandri, M.C. Bonferoni, E.H. Gokce, F. Ferrari, S. Rossi, M. Patrini, C. Caramella, Chitosan-associated SLN: in vitro and ex vivo characterization of cyclosporine A loaded ophthalmic systems., J. Microencapsul. 27 (2010) 735–746. doi:10.3109/02652048.2010.517854.

[9] K. Hermans, D. Van den Plas, A. Everaert, W. Weyenberg, A. Ludwig, Full factorial design, physicochemical characterisation and biological assessment of cyclosporine A loaded cationic nanoparticles, Eur. J. Pharm. Biopharm. 82 (2012) 27–35. doi:10.1016/j.ejpb.2012.05.003.

[10] A.M. De Campos, A. Sánchez, M.J. Alonso, Chitosan nanoparticles: a new vehicle for the improvement of the delivery of drugs to the ocular surface. Application to cyclosporin A, Int. J. Pharm. 224 (2001) 159–168. doi:10.1016/S0378-5173(01)00760-8.

[11] P. Aksungur, M. Demirbilek, E.B. Denkbaş, J. Vandervoort, A. Ludwig, N. Ünlü, Development and characterization of Cyclosporine A loaded nanoparticles for ocular drug delivery: Cellular toxicity, uptake, and kinetic studies, J. Control. Release. 151 (2011) 286–294. doi:10.1016/j.jconrel.2011.01.010.

[12] X. Li, S. Nie, J. Kong, N. Li, C. Ju, W. Pan, A controlled-release ocular delivery system for ibuprofen based on nanostructured lipid carriers., Int. J. Pharm. 363 (2008) 177–182. doi:10.1016/j.ijpharm.2008.07.017.

[13] A. Leonardi, C. Bucolo, F. Drago, S. Salomone, R. Pignatello, Cationic solid lipid nanoparticles enhance ocular hypotensive effect of melatonin in rabbit, Int. J. Pharm. 478 (2015) 180–186. doi:10.1016/j.ijpharm.2014.11.032.

[14] J.F. Fangueiro, A.C. Calpena, B. Clares, T. Andreani, M.A. Egea, F.J. Veiga, M.L. Garcia, A.M. Silva, E.B. Souto, Biopharmaceutical evaluation of epigallocatechin gallate-loaded cationic lipid nanoparticles (EGCG-LNs): In vivo, in vitro and ex vivo studies, Int. J. Pharm. 502 (2016) 161–169. doi:10.1016/j.ijpharm.2016.02.039.

[15] L. Contreras-Ruiz, M. de la Fuente, J.E. Párraga, A. López-García, I. Fernández, B. Seijo, A. Sánchez, M. Calonge, Y. Diebold, Intracellular trafficking of hyaluronic acid-chitosan oligomer-based nanoparticles in cultured human ocular surface cells., Mol. Vis. 17 (2011) 279–90.

[16] M.A. Kalam, The potential application of hyaluronic acid coated chitosan nanoparticles in ocular delivery of dexamethasone., Int. J. Biol. Macromol. 89 (2016) 559–568. doi:10.1016/j.ijbiomac.2016.05.016.

[17] A. Sanchez, B. Seijo, G.K. Zorzi, E.S. Carvalho, A. Pensado, Nanoparticulate systems prepared from Sorbitan esters, WO2013068625 A1, 2013.

[18] C. Guo, Y. Zhang, Z. Yang, M. Li, F. Li, F. Cui, T. Liu, W. Shi, X. Wu, Nanomicelle formulation for topical delivery of cyclosporine A into the cornea: in vitro mechanism and in vivo permeation evaluation, 5 (2015) 12968. doi:10.1038/srep12968.

[19] S. Cohen, E. Lobel, A. Trevgoda, Y. Peled, A novel in situ-forming ophthalmic drug delivery system from alginates undergoing gelation in the eye, J. Control. Release. 44 (1997) 201–208. doi: 10.1016/S0168-3659(96)01523-4.

[20] K. Araki-Sasaki, Y. Ohashi, T. Sasabe, K. Hayashi, H. Watanabe, Y. Tano, H. Handa, An SV40-immortalized human corneal epithelial cell line and its characterization., Invest. Ophthalmol. Vis. Sci. 36 (1995) 614–621.

[21] F. Lallemand, O. Felt-Baeyens, K. Besseghir, F. Behar-Cohen, R. Gurny, Cyclosporine A delivery to the eye: a pharmaceutical challenge., Eur. J. Pharm. Biopharm. 56 (2003) 307–318.

[22] A.M. De Campos, A. Sánchez, R. Gref, P. Calvo, M.J. Alonso, The effect of a PEG versus a chitosan coating on the interaction of drug colloidal carriers with the ocular mucosa, Eur. J. Pharm. Sci. 20 (2003) 73–81. doi: 10.1016/S0928-0987(03)00178-7.

[23] P.K. Dagur, J.P. McCoy, Collection, Storage, and Preparation of Human Blood Cells, in: Curr. Protoc. Cytom., John Wiley & Sons, Inc., Hoboken, NJ, USA, 2015: p. 5.1.1-5.1.16. doi:10.1002/0471142956.cy0501s73.

[24] M.J. Blanco-Prieto, M. Guada, V. Sebastian, S. Irusta, E. Feijoo, M. del C. Dios-Vieitez, Lipid nanoparticles for cyclosporine A administration: development, characterization, and in vitro evaluation of their immunosuppression activity, Int. J. Nanomedicine. 10 (2015) 6541. doi:10.2147/IJN.S90849.

[25] K. Kato, P. Walde, N. Koine, S. Ichikawa, T. Ishikawa, R. Nagahama, T. Ishihara, T. Tsujii, M. Shudou, Y. Omokawa, T. Kuroiwa, Temperature-Sensitive Nonionic Vesicles Prepared from Span 80 (Sorbitan Monooleate), Langmuir. 24 (2008) 10762–10770. doi:10.1021/la801581f.

[26] A. Fernández-Ferreiro, M. Barcia, F. Otero-Espinar, M. Lamas, Lubricantes oculares en el tratamiento del ojo seco, Panor. Actual Del Medicam. 38 (2014) 350–356.

[27] K. Gumus, Topical Coenzyme Q10 Eye Drops as an Adjuvant Treatment in Challenging Refractory Corneal Ulcers: A Case Series and Literature Review., Eye Contact Lens. 43 (2017) 73–80. doi:10.1097/ICL.0000000000000229.

[28] J. Alvarez-Trabado, A. López-García, A. Sánchez, Y. Diebold, Sorbitan ester nanoparticles (SENS) as topical ocular cyclosporine delivery systems, Invest. Ophthalmol. Vis. Sci. 58 (2017) 4116.

[29] M.A. Grimaudo, S. Pescina, C. Padula, P. Santi, A. Concheiro, C. Alvarez-Lorenzo, S. Nicoli, Poloxamer 407/TPGS Mixed Micelles as Promising Carriers for Cyclosporine Ocular Delivery., Mol. Pharm. 15 (2018) 571–584. doi:10.1021/acs.molpharmaceut.7b00939.

[30] S.K. Lai, Y.-Y. Wang, J. Hanes, Mucus-penetrating nanoparticles for drug and gene delivery to mucosal tissues, Adv. Drug Deliv. Rev. 61 (2009) 158–171. doi: 10.1016/j.addr.2008.11.002.

[31] J.-H. Park, H. Jeong, J. Hong, M. Chang, M. Kim, R.S. Chuck, J.K. Lee, C.-Y. Park, The Effect of Silica Nanoparticles on Human Corneal Epithelial Cells, Sci. Rep. 6 (2016) 37762. doi:10.1038/srep37762.

[32] R.L. McCall, R.W. Sirianni, PLGA nanoparticles formed by single- or double-emulsion with vitamin E-TPGS., J. Vis. Exp. (2013) 51015. doi:10.3791/51015.

[33] L. Wu, J. Zhang, W. Watanabe, Physical and chemical stability of drug nanoparticles, Adv. Drug Deliv. Rev. 63 (2011) 456–469. doi: 10.1016/j.addr.2011.02.001.

[34] B. Heurtault, P. Saulnier, B. Pech, J.-E. Proust, J.-P. Benoit, Physico-chemical stability of colloidal lipid particles, Biomaterials. 24 (2003) 4283–4300. doi: 10.1016/S0142-9612(03)00331-4.

[35] A.A. Abdelbary, X. Li, M. El-Nabarawi, A. Elassasy, B. Jasti, Effect of fixed aqueous layer thickness of polymeric stabilizers on zeta potential and stability of aripiprazole nanosuspensions, Pharm. Dev. Technol. 18 (2013) 730–735. doi:10.3109/10837450.2012.727001.

[36] Z. Urban-Morlan, A. Ganem-Rondero, L.M. Melgoza-Contreras, J.J. Escobar-Chavez, M.G. Nava-Arzaluz, D. Quintanar-Guerrero, Preparation and characterization of solid lipid nanoparticles containing cyclosporine by the emulsification-diffusion method., Int. J. Nanomedicine. 5 (2010) 611–620. doi:10.2147/IJN.S12125.

[37] S. Mizrahy, S.R. Raz, M. Hasgaard, H. Liu, N. Soffer-Tsur, K. Cohen, R. Dvash, D. Landsman-Milo, M.G.E.G. Bremer, S.M. Moghimi, D. Peer, Hyaluronan-coated nanoparticles: the influence of the molecular weight on CD44-hyaluronan interactions and on the immune response., J. Control. Release. 156 (2011) 231–238. doi:10.1016/j.jconrel.2011.06.031.

[38] M.P. Foster, C.A. McElroy, C.D. Amero, Solution NMR of Large Molecules and Assemblies, Biochemistry. 46 (2007) 331–340. doi:10.1021/bi0621314.

[39] A. Pensado, M. Martín-Pastor, G.K. Zorzi, E.S. Carvalho, A. Sanchez, Structural analysis of nanosystems: Solid Sorbitan esters Nanoparticles (SSN) as a case study, Eur. J. Pharm. Biopharm. 104 (2016) 189–199. doi:10.1016/j.ejpb.2016.05.002.

[40] M. Sznitowska, S. Janicki, E.A. Dabrowska, M. Gajewska, Physicochemical screening of antimicrobial agents as potential preservatives for submicron emulsions., Eur. J. Pharm. Sci. 15 (2002) 489–95.

[41] M.M. Hamawy, Molecular actions of calcineurin inhibitors, Drug News Perspect. 16 (2003) 277–82.

[42] L. Ramsden, C.C. Rider, Selective and differential binding of interleukin (IL)-1α, IL-1β, IL-2 and IL-6 to glycosaminoglycans, Eur. J. Immunol. 22 (1992) 3027–3031. doi:10.1002/eji.1830221139.

# *Chapter II*

## *Cyclosporine-loaded sorbitan ester nanoparticles (SENS) ameliorate signs of dry eye disease in TSP-1-deficient mice*

USC
UNIVERSIDADE
DE SANTIAGO
DE COMPOSTELA

**Abstract**

In this work, we evaluated the *in vivo* therapeutic efficacy of sorbitan ester nanoparticles (SENS). Cyclosporine (CsA)-loaded SENS showed a particle size of 176.9 nm, a zeta potential of +33.6 mV and a drug entrapment efficiency of 84.4%. The hyaluronic acid-coated version, i.e., SENS-HA, had a particle size of 188.2 ± 2.2 nm and a zeta potential of –24.5 ± 0.7. Both lyophilized nanoparticles (NPs) showed adequate stability when stored for 3 months at 4ºC or room temperature. SENS-HA were successfully sterilized by autoclaving without noticeable alterations in their physicochemical properties. We used a thrombospondin (TSP)-1-deficient mouse that spontaneously develops an ocular surface inflammatory status similar to that founded in Sjögren's syndrome-associated dry eye as a disease model. Topically applied CsA-loaded SENS did not improve the corneal barrier integrity but promoted goblet cell recovery and MUC5AC secretion in diseased animals. These NPs also reduced the levels of IL-6, IL-1β and TNF-α, which are increased in diseased animals. Topically applied CsA-loaded SENS-HA promoted corneal barrier reparation (CFS was reduced by –70.5%) as well as the recovery of conjunctival goblet cell number and MUC5AC secretion. CsA-loaded SENS-HA also diminished the levels of pro-inflammatory cytokines. Interestingly, blank SENS-HA exhibited some therapeutic activity as suggested by the recovery of goblet cell number and MUC5AC levels at the end of treatment.

USC
UNIVERSIDADE
DE SANTIAGO
DE COMPOSTELA

## 1. Introduction

Dry eye disease is a multifactorial and highly prevalent eye disorder that affects ocular surface structures and results in ocular discomfort and visual disturbances [1]. Conventionally, this pathology is divided in two subtypes, aqueous tear-deficient and evaporative dry eye. The first is characterized by a reduction in tear production due to lacrimal gland secretion failure and the second is characterized by tear hyperosmolarity due to excessive evaporative water loss. Nonetheless, both subtypes present a common pathological manifestation that is considered the core mechanism for this disorder: the presence of inflammation [2].

Dry eye therapeutic approaches are based on minimizing inflammation and restoring the physiological functionality of the tear film. For years, artificial tears (lipid- and gel-based) were the mainstay of therapy for maintaining patient comfort. However, tear substitutes do not control the underlying inflammatory status and the disease keeps evolving. Hence, a concomitant anti-inflammatory treatment is often necessary. Anti-inflammatory drugs such as corticosteroids, cyclosporine (CsA), antibiotics, polyunsaturated fatty acids, and the recently approved drug lifitegrast is used to reduce ocular surface inflammation [3]. CsA is a potent immunosuppressant that specifically inhibits lymphocyte T (T-cell) activation. This peptide forms a complex with cyclophilin present in the T-cell cytosol, specifically blocking the calcineurin pathway. This blocking results in the downregulation of interleukin (IL)-2 transcription and the subsequent suppression of T-cell replication and its mediated immune and inflammatory responses [4]. In dry eye, the specific immunomodulatory activity of CsA was first demonstrated in a spontaneous canine model of chronic *keratoconjunctivitis sicca* [5], in which topical CsA facilitated lymphocytic apoptosis and suppressed epithelial apoptosis, both of which are hallmarks in the etiology of this disease. Currently, topical CsA is the gold standard long-term treatment to control ocular surface inflammation and improve tear function in dry eye patients [6].

Topical ocular administration is the preferred route for ocular drug delivery because it provides local therapeutic effects in the eye and avoids systemic drug absorption. Different safety studies have demonstrated that topically applied CsA reached the blood in negligible concentrations and did not cause significant systemic effects [7,8]. However, the formulation of CsA in a simply aqueous vehicle can be a scientific challenge due to its low water solubility. Novel CsA delivery systems are focused both on the improvement of drug-related biopharmaceutical parameters (i.e., increasing

solubility and ocular bioavailability) and patient safety and acceptance (i.e., reducing dose and dosage frequency). Although multiple successful pharmaceutical approaches have been proposed from academic research, only few topical cyclosporine formulations have reached the market [9]. This might be explained because novel drug delivery systems, such as nanoparticles (NPs), are in early development stages and further studies regarding their technological viability and long-term safety are still necessary.

The present work explores the potential of the recently developed SENS as novel tools for the treatment of dry eye disease (Chapter I) [10]. These NPs previously showed the ability to solubilize high CsA concentrations without reducing *in vitro* biocompatibility. Taking into account that hyaluronic acid-coated SENS (SENS-HA) showed better biopharmaceutical properties than its uncoated version in a previous work (Chapter I) [10], throughout this work we aimed to confirm whether this difference also affects its therapeutic efficacy. As an experimental chronic ocular surface inflammation model, we used TSP-1-deficient mice [11,12], who spontaneously develop a chronic ocular surface inflammation as they age that is similar to Sjögren's syndrome-associated dry eye. The disease in TSP-1-deficient mice is characterized by alterations in the corneal epithelial barrier, secretory gland dysfunction and inflammation of the conjunctiva and lacrimal gland tissues [11,12].

Whereas available CsA ophthalmic treatments such as Restasis® need to be administered thrice daily [13], our aim in this work was to determine if the once-a-day administration of our NPs (using the same CsA dose) would be enough to diminish ocular surface inflammation and related dry eye signs.

## 2. Materials and methods

### 2.1. Materials

NP components including sorbitan monooleate (Span® 80), d-α-tocopheryl polyethylene glycol 1000 succinate (TPGS), cetyltrimethylammonium bromide (CTAB) and HA were purchased from Sigma-Aldrich (Madrid, Spain). CsA was obtained from LC Laboratories (Woburn, MA, USA). High-performance liquid chromatography (HPLC)-grade acetonitrile was from VWR (Barcelona, Spain). Sodium fluorescein was purchased from Sigma-Aldrich (St. Louis, MO, USA). The MUC5AC enzyme-linked immunosorbent assay (ELISA) kit was from TSZELISA (Waltham, MA, USA). Molecular biology reagents including TRizol®, the SuperScript® VILO™ cDNA

synthesis kit and SYBR™ Green PCR Master Mix were from Thermo Fisher Scientific (Madrid, Spain). The primer pairs used for RT-PCR were provided by Sigma-Aldrich (Madrid, Spain).

**2.2. NP preparation**

Cationic SENS were prepared using a previously reported method and composition (Chapter I). Briefly, an ethanolic phase containing all the NP components was constantly poured over an aqueous phase under continuous magnetic stirring. NPs formed spontaneously under these conditions. Ethanol was immediately removed using a rotating evaporator (Buchi® R-210, Massó Analítica, Barcelona) and the formulation was further concentrated rendering the following final composition (w/v): 2.00% Span® 80, 0.22% TPGS, 0.03% CTAB, and 0.65% CsA.

Anionic SENS-HA were prepared by coating the surface of the SENS with HA. Briefly, two volumes of SENS were mixed with one volume of HA (1,600 KDa) solution, giving a final HA concentration of 0.015%. For this purpose, the NPs were placed in an orbital shaker at 75 rpm for 20 minutes to allow total HA adsorption.

For the *in vivo* experiments, the NPs were diluted with a pH-adjusted isotonic sucrose solution to a final CsA concentration of 0.05% (w/v).

**2.3. Physicochemical characterization of the NPs**

The average size and the size distribution of the NPs were determined by dynamic light scattering (DLS). Samples were previously diluted with 0.1 mM KCl and analyses were performed at 25ºC with a detection angle of 173º. The zeta potential was determined by laser doppler anemometry (LDA). DLS and LDA analysis were performed with a Zetasizer® 3000HS (Malvern Instruments, Malvern, UK).

The CsA entrapment efficiency was determined as previously described (Chapter I) [10]. Briefly, non-entrapped CsA was removed by passing the NPs through a 0.22-µm filter. The resulting purified NPs were then disrupted, and the entrapped drug was extracted using acetonitrile. CsA was then quantified using a validated HPLC method (Chapter I) [10].

**2.4. NP lyophilization and the stability study for lyophilized NPs**

Three different sugars were evaluated as NP cryoprotectants during the freeze-drying process. Aqueous solutions of sucrose, glucose and trehalose were mixed with the NPs at a 1:1 (v/v) ratio to a final sugar concentration ranging from 5 to 20% (w/v). Lyophilization was performed with a Tesltar Lyoquest freeze dryer (Telstar, Barcelona,

Spain). The most appropriate cryoprotectant was selected for the posterior stability study.

For the stability study, each lyophilized sample was completely sealed to prevent humidification and stored at 4ºC, room temperature (RT) or 37ºC. Immediately after the freeze-drying process and after three months of storage, the lyophilized samples were rehydrated, and their physicochemical characteristics were determined. Three different samples were analyzed for each experimental condition.

**2.5. NP structural analysis by differential scanning calorimetry (DSC) and X-ray powder diffraction (XRD).**

The solid state of the lyophilized formulations was investigated using DSC and XRD techniques. DSC scans were performed using a DSC Q100 calorimeter (TA Instruments, Barcelona, Spain) in the range between -50 and 250ºC at 10ºC minutes$^{-1}$. XRD analysis was performed with a Philips PW1710 X-ray Diffraction Spectrometer using a cupper sealed tube as the radiation source. Diffractograms were obtained at an angular range between 2º and 50º, with a 0.02º step counting 2 seconds per step.

**2.6. NP sterilization by autoclaving**

For NP sterilization, 500 µL of formulations were placed inside 2-mL HPLC borosilicate glass vials (Agilent Technologies, Madrid, Spain) and subsequently autoclaved. Autoclaving was performed at 121ºC for 20 minutes using a Presoclave II autoclave (JP Selecta, Barcelona, Spain). The physicochemical characteristics of three different samples were monitored before and after the sterilization process.

**2.7. Animals**

TSP-1-deficient mice (C57BL/6 background) were purchased from Jackson Laboratory (Bar Harbor, MI, USA) and bred in a pathogen-free facility at Boston University (Boston, MA, USA). The protocol (AN-15400.2016.09) was approved by the Institutional Animal Care and Use Committee at Boston University School of Medicine. All animal experiments were performed following the Association for Research in Vision and Ophthalmology Statement for the Use of Animals in Ophthalmic and Vision Research.

**2.8. *In vivo* study of CsA-loaded SENS efficacy**

TSP-1-deficient mice (12-13 weeks old) were used to test the efficacy of the developed CsA formulations. Animals were divided into the following four different experimental groups: group 1 received CsA-loaded SENS (treatment 1), group 2 received blank SENS (control for treatment 1), group 3 received CsA-loaded SENS-HA

(treatment 2), and group 4 received blank SENS-HA (control for treatment 2). Treatments and controls were topically administered (5 µL/eye) once-a-day for three weeks. Four eyes were used (n = 4) for each treatment and control.

Treatment efficacy was evaluated by monitoring the main signs of ocular surface disease following the experimental setup depicted in **Figure 1**. The corneal integrity was assessed by corneal fluorescein staining and conjunctival secretory function by measuring the MUC5AC contents in tears. Both techniques were performed as previously described [11]. Briefly, for corneal fluorescein staining, 3 µL of 1% (w/v) sodium fluorescein were applied to eyes from previously isoflurane-sedated mice. After 3 minutes, the dye was removed from the ocular surface by several washes with PBS and corneal staining was immediately evaluated with a slit lamp biomicroscope using a cobalt blue light. The corneal fluorescein score (CFS) was recorded using the standardized National Eye Institute Grading System [14]. For tear collection, mice tearing was induced by the intraperitoneal injection of weight-dosed pilocarpine. Tear fluid (2 µL) was collected by placing a glass capillary tube in the tear meniscus at the canthus of each eye. Samples were subsequently maintained at -80ºC until further analysis. Tear samples were analyzed in quadruplicate to determine the MUC5AC content using a specific enzyme-linked immunosorbent assay kit (TSZ ELISA, Waltham, MA, USA). At the end of the study (week 3), the mice were euthanized, and eye tissues and cervical lymph nodes were collected for further histopathological and molecular analyses.

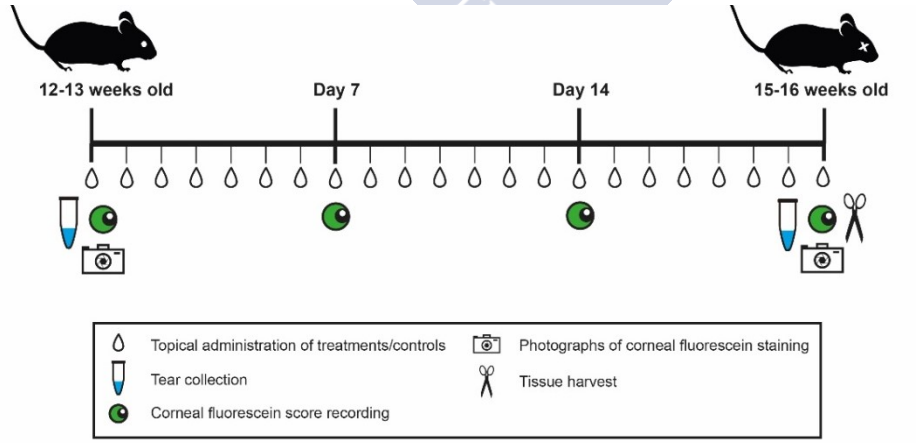


**Figure 1. Experimental setup for the treatment and control administration to TSP-1-deficient mice.** Disease evolution in mice was monitored during the three weeks they received treatment or control formulations by evaluating the corneal fluorescein score and MUC5AC content in tears. At the end of the treatment and after tissue harvest, a histological and molecular analysis was performed. Schematic created by Jesús Álvarez Trabado.

### 2.9. Tissue processing

Eyeballs with attached eyelids were harvested and fixed in a 4% paraformaldehyde-buffered solution. Then, the tissues were processed, embedded in paraffin for posterior microtome sectioning into sagittal 5-µm thick sections, and stained for histopathological evaluation.

Cervical lymph nodes were dissected and subsequently processed for RNA extraction and further cDNA analysis by real-time reverse transcription polymerase chain reaction (RT-PCR).

### 2.10. Histopathological study of ocular tissues

Tissue sections obtained from each eye were divided in two groups; one group was used for hematoxylin and eosin (H&E) staining and the other group was for periodic acid-Schiff and alcian blue (PAS/AB) staining.

H&E staining was used to evaluate the morphology of the ocular surface structures. The integrity of the corneal and conjunctival tissues was determined. Representative microphotographs were taken at 40x magnification.

PAS/AB staining was used to count goblet cells. Conjunctiva from sagittal sections of the center of the eye were used as representatives of the whole conjunctiva to control variations in goblet cell density over the ocular surface. Conjunctival goblet cells were counted in a masked fashion by two independent trained observers in the superior and inferior bulbar and tarsal conjunctiva for each eyeball analyzed. Considering that the superior or inferior tarsal conjunctiva were damaged in some samples, the goblet cell number was expressed as half the sum of goblet cells counted in the superior and inferior bulbar and tarsal conjunctiva. Representative microphotographs were taken at 40x magnification.

### 2.11. Real-time RT-PCR analysis of cervical lymph nodes

RNA was isolated from cervical lymph nodes using the TRizol® reagent and then converted into cDNA using the SuperScript® VILO™ cDNA synthesis kit. For RT-PCR analysis, the thermocycler conditions were as follows: one cycle of 95ºC for 600 s, followed by 40 cycles of 95ºC for 15 s and 60 cycles for 60 s, and a final cycle at 95ºC for 90 s. The PCR mix consisted of 20 ng of cDNA mixed with 1 µL of primers (**Table 1**) and 10 µL of SYBR™ Green PCR Master Mix to a final volume of 20 µL. For internal normalization, we used the glyceraldehyde-3-phosphate dehydrogenase (GAPDH) gene. Three independent experiments were performed in duplicate.

**Table 1. Sequences of the primers used for real time RT-PCR.**

| Gene | Forward primer sequence | Reverse primer sequence |
|---|---|---|
| IL-6 | 5′-AGTCAATTCCAGAAACCGCTATGA-3′ | 5′-TAGGGAAGGCCGTGGTTGT-3′ |
| IL-1β | 5′-TCTGAAGCAGCTATGGCAACTGTT-3′ | 5′-CATCTTTTGGGGTCCGTCAACT-3′ |
| TNF-α | 5′-GGCCTCCCTCTCATCAGTTCTATG-3′ | 5′-GTTTGCTACGACGTGGGCTACA-3′ |
| GAPDH | 5′-GAACGTGAAGGTCGGAGTCAAC-3′ | 5′-CGTGAAGATGGTGATGGGATTTC-3′ |

IL, interleukin; TNF-α, tumor necrosis factor-α; and GAPDH, glyceraldehyde-3-phosphate dehydrogenase.

### 2.12. Statistical Analysis

Data are expressed as the mean ± standard deviation (SD). Statistical comparisons between two groups were performed by Student's *t*-test. For more than two groups, statistically significant differences were evaluated by one-way analysis of variance followed by pairwise comparisons (Tukey test). Statistical significance was considered when $p \leq 0.05$.

## 3. Results and discussion

The main purpose of this work was to perform an *in vivo* proof-of-concept to validate the clinical potential of CsA-loaded SENS for the treatment of dry eye disease in a TSP-1-deficient mouse model. We also wanted to determine whether the HA-coating may positively influence the therapeutic efficacy of SENS. In these studies, the ethical precepts of the "Three Rs" [15] were present during all animal experiments, especially by using refined experimental procedures (e.g., invasive procedures were performed under isoflurane anesthesia) and by minimizing the number of animals needed to obtain sufficient data to answer the research question.

### 3.1. Physicochemical characteristics of the NPs

A schematic representation of the NPs is depicted in **Figure 2a**. After preparation, SENS had a particle size of 176.9 ± 5.3 nm, a zeta potential of +33.6 ± 1.1 mV and a CsA entrapment efficiency of 84.4 ± 4.1%. SENS-HA had a particle size of 188.2 ± 2.2 nm and a zeta potential of –24.5 ± 0.7. For the *in vivo* experiments, the formulations were isotonized and the pH was adjusted because the osmolarity and pH within

acceptable physiological ranges are crucial parameters to avoid potential biocompatibility issues [16]. The resulting diluted formulations displayed a milky appearance, with the SENS being the most translucent formulation due to its smaller particle size (**Figure 2b**).

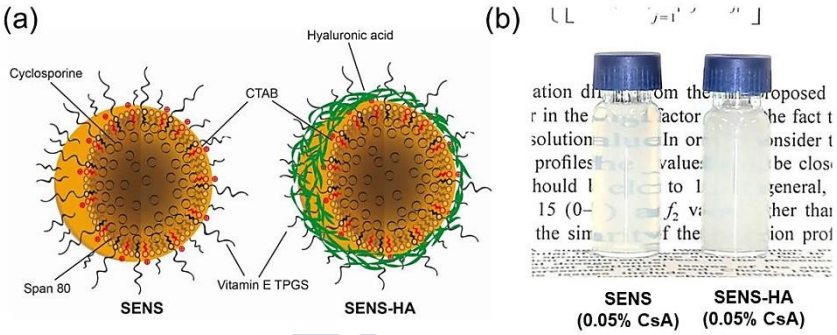


**Figure 2. NP formulations.** (a) Schematic representation of SENS and SENS-HA where the HA coating is shown in green. (b) After NP dilution to an equivalent CsA concentration of 0.05%, (w/v) SENS appeared more transparent than SENS-HA.

### 3.2. Screening of cryoprotectants and stability of the lyophilized NPs

Lyophilization is a commonly used procedure to remove water content from formulations with the objective of increasing their stability during long-term storage. Freeze-dried formulations avoid the risks of water-degradative reactions, drug leakage by diffusion or the growth of bacterial contamination [17]. Before starting a freezing process, the addition of cryoprotectant substances such as sugars [17–19] is usually necessary; this prevents the formation of crystals that may damage NPs. The selection of the most appropriate cryoprotectant is a critical step to minimize alterations in the final physicochemical properties of the NPs. As depicted in **Figure 3a**, sucrose was the cryoprotectant that offered the best results for our formulations, and the resulting lyophilized NPs could be water re-dispersed experiencing only minor (but statistically significant) variations in their physicochemical properties. After a 3-month study, the sucrose-cryoprotected NPs showed adequate stability when stored at 4ºC and room temperature, and only the NPs stored at 37ºC experienced a significant increase in particle size that could be attributed to an agglomeration phenomenon (**Figure 3b**).

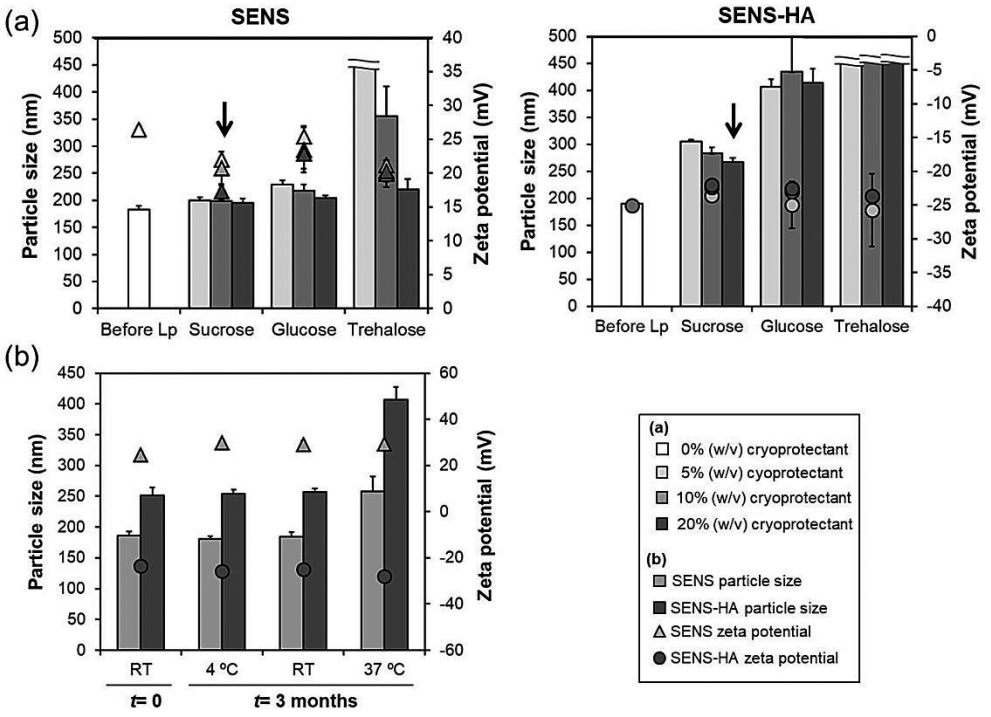


**Figure 3. Impact of cryoprotectants on NP lyophilization and a stability study on the lyophilized formulations.** (a) Sucrose-cryoprotected NPs showed the most adequate physicochemical properties after the freeze-drying process. Dark arrows highlight the most suitable sucrose concentrations for each type of NP. 10% (w/v) and 20% (w/v) sucrose concentrations were selected for further SENS and SENS-HA stability studies, respectively. (b) The stability study for the lyophilized formulations demonstrated that storage at 37ºC significantly modified the physicochemical properties of both NP types.

### 3.3. Analysis of drug distribution in the NPs after lyophilization.

We reported the structural characterization of the CsA-loaded NPs in the liquid state (Chapter I) [10]; the NMR results suggested that drug was dissolved at the molecular level in the nanoparticle matrix. In this case, we investigated the solid state of the NPs using DSC and XRD techniques. DSC profiles of the main NP components, blank NPs and CsA-loaded NPs are depicted in **Figure 4a**. The SENS profile was substantially modified after CsA incorporation, indicating a molecular interaction between the entrapped drug and NP components. For further clarification of the molecular status of CsA inside the NPs, we performed an XRD analysis. **Figure 4b** shows the diffractograms of crystalline sucrose (cryoprotectant), crystalline CsA, blank and CsA-loaded SENS. The characteristic spectrum peaks for crystalline CsA (6.81 and 9.20º) were absent in the drug-loaded formulation. The most visible peaks corresponded

to sucrose crystals. In view of these results, we can assume that drug was not in the crystalline state but dissolved at the molecular level in the NPs.

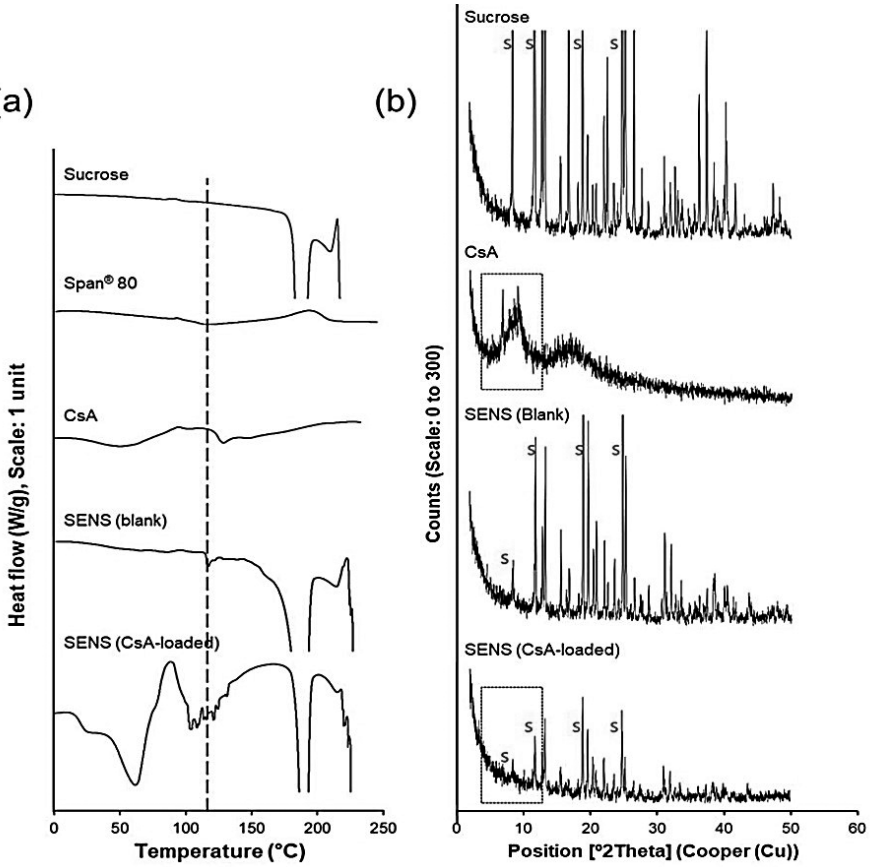


**Figure 4. Structural analysis of the NPs in the solid state.** (a) DSC profiles of the main NP components and two representative lyophilized NP formulations: blank SENS and CsA-loaded SENS. CsA entrapment by SENS translated into a visible change in the DSC spectrum shape. (b) XRD diffractograms of crystalline sucrose (cryoprotectant), crystalline CsA and two representative lyophilized NP formulations: blank SENS and CsA-loaded SENS. The characteristic CsA spectrum peaks were not visible in the drug-loaded formulation (highlighted area of spectra with rectangle). The most visible peaks corresponded to the sucrose crystals (S).

### 3.4. Physicochemical characteristics of the NPs after sterilization.

Sterility is a mandatory requirement for any ophthalmic formulation. Different methods have been proposed for NP sterilization including filtration, gamma or UV irradiation and autoclaving [20]. Although autoclaving is the most desirable method from an industrial perspective, the majority of nanosystems cannot be sterilized at high temperatures because of the occurrence of aggregation phenomena [20].

In this work, we observed (**Figure 5**) that SENS experienced significant particle growth (+18 nm; $p \leq 0.05$) and zeta potential reduction (–13 mV; $p \leq 0.001$) accompanied by a reduction in the entrapment efficiency (–26%; $p \leq 0.05$) after the autoclaving process. Considering our previous results (Chapter I) [10], these variations are indicative of drug leakage during the autoclaving process. On the other hand, SENS-HA were successfully sterilized by autoclaving without alterations to their physicochemical properties. Only the zeta potential experienced a slight reduction (–3.2 mV; $p \leq 0.001$), but we do not consider it of great technological relevance. These results suggest that the HA coating prevents NP destabilization at high temperatures, probably due to the additional steric effect provided by the HA chains.

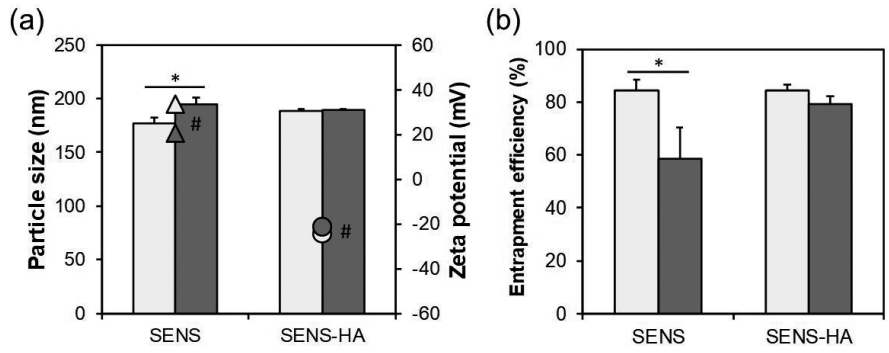


**Figure 5. Physicochemical properties of the NPs before (white bars) and after (gray bars) autoclaving.** (a) SENS experienced a significant particle size increase (* $p \leq 0.05$) and zeta potential reduction (# $p \leq 0.001$) while SENS-HA only experienced a minor zeta potential reduction (# $p \leq 0.001$). (b) EE (%) was significantly reduced for SENS (* $p \leq 0.05$) and was not affected for SENS-HA.

## 3.5. Therapeutic efficacy of topically applied CsA-loaded NPs in the treatment of dry eye disease in the TSP-1-deficient mouse model.

### 3.5.1. Monitoring of corneal integrity and secretory function of treated and control TSP-1-deficient mice.

We evaluated the corneal integrity after treatment with CsA-loaded NPs by analyzing the corneal fluorescein score (CFS). In the TSP-1-deficient mouse model, the CFS reached a maximum value (8 to 10) when mice are 12 weeks old and presents a well-established ocular surface disease that remains stable for additional weeks [21]. Based on these data, we studied the therapeutic effect of our two types of NPs to reduce this value.

**Figure 6a** shows that CFS evolved in a different way depending on the treatment applied. While SENS (either CsA-loaded or blank) did not significantly affect the evolution of CFS throughout the experiment, CsA-loaded SENS-HA significantly reduced CFS during the second ($p \leq 0.01$) and third ($p \leq 0.001$) weeks of treatment, reaching a CFS similar to that of non-treated healthy (wild type) mice (2~3) [21]. This difference was clearer when normalized values for the percentage of CFS reduction at the end of treatment were compared, where CsA-loaded SENS reduced the initial CFS score by –15.6% and SENS-HA by –70.5% ($p \leq 0.001$ between both treatments). Although it was not statistically significant, treatment with blank SENS-HA induced a visible reduction in the CFS (–26.0%). These results can be explained by a potential synergistic mechanism between the therapeutic properties of HA that promote corneal epithelial healing [22,23] and the immunosuppressant activity of CsA that reduces ocular surface inflammation [24,25]. Additionally, the higher corneal uptake of SENS-HA may contribute to its increased efficacy (Chapter I) [10]. **Figure 6b** shows representative fluorescein staining images at the beginning and at the end of treatment, in which SENS-HA visibly reduced the corneal staining compared with its uncoated version.

The secretory function of conjunctival goblet cells was monitored by measuring MUC5AC levels in tears. It is reported that the presence of ocular surface inflammation is related with goblet cell dysfunction and/or apoptosis and translates into lower levels of this mucin in tears [26,27]. In fact, clinical studies have demonstrated that tear MUC5AC levels are inversely correlated with the symptomatic severity of dry eye [28]. Our findings showed (**Figure 7**) that both types of CsA-loaded NPs increased MUC5AC levels in comparison with baseline levels ($p \leq 0.05$). Interestingly, blank SENS-HA significantly increased MUC5AC levels as well ($p \leq 0.05$), possibly due to the ability of HA to increase conjunctival goblet cell density [29].

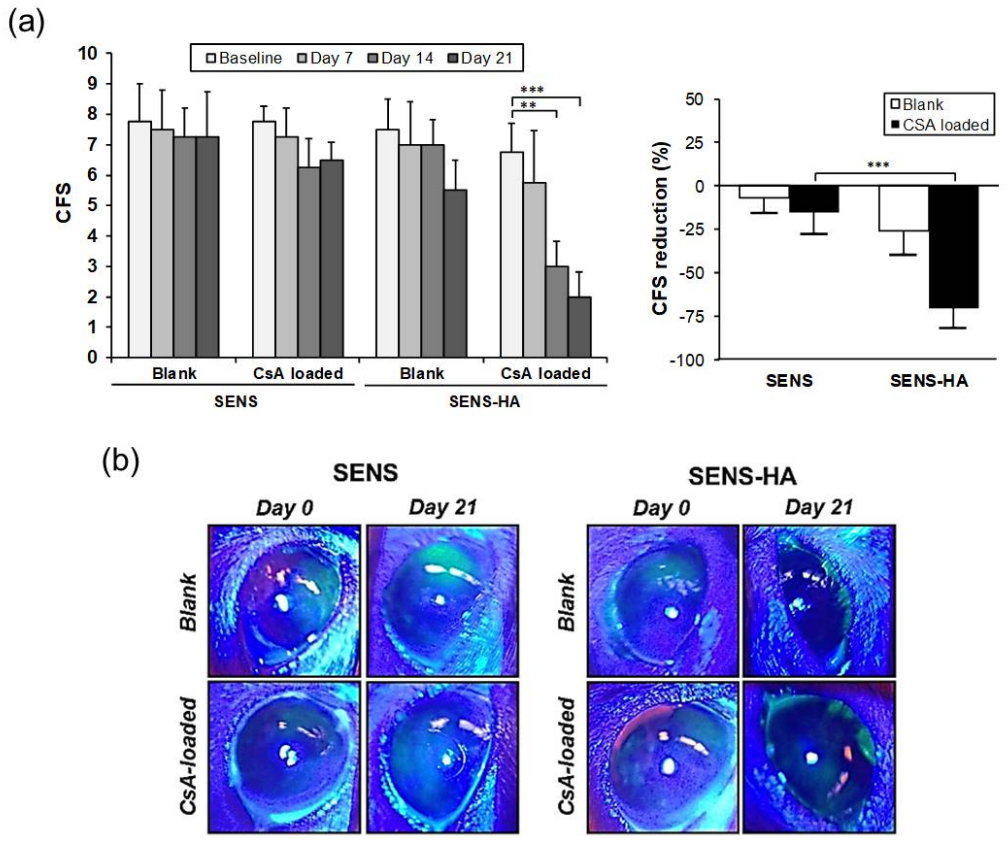


**Figure 6. Monitoring mouse corneal integrity.** (a) Corneal fluorescein score (CFS) evolution. CsA-loaded SENS-HA significantly reduced CFS during the second (** $p \leq 0.01$) and third week of treatment (*** $p \leq 0.001$). This latter reduction was 54.9% higher than that obtained with same uncoated NP formulation (*** $p \leq 0.001$). (b) Representative images of corneal fluorescein staining. The reduction in corneal fluorescein staining was most evident in the eyes treated with HA-containing NP formulations.

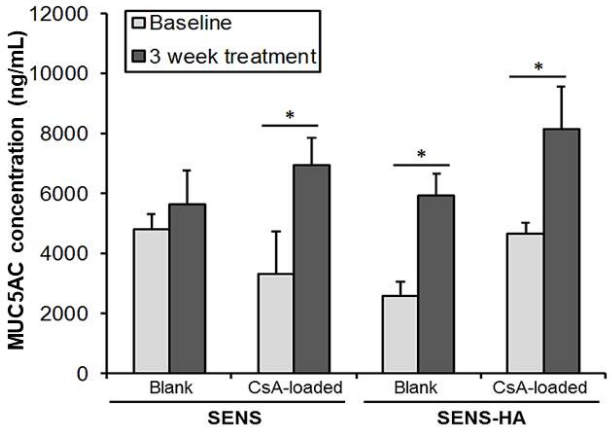


**Figure 7. Changes in MUC5AC levels in tears after treatment with blank and CsA-loaded NPs.** CsA-loaded NP formulations and blank SENS-HA significantly increased the levels of MUC5AC at the end of treatment (* $p \leq 0.05$).

### 3.5.2. Histopathology analysis of TSP-1-deficient mouse ocular tissues after treatment with blank and CsA-loaded NPs.

**Figure 8a** shows representative images of corneal and conjunctival tissue sections from control and treated TSP-1-deficient mice. No differences in corneal morphology were observed in the mice from any of the four experimental groups. The epithelial cell layers, cell morphology and stromal details remained the same among the groups, also showing no signs of tissue inflammation. The lack of morphological differences in the corneal tissues from mice treated with the blank and CsA-loaded NPs may be explained because dysfunctions in the corneal barrier were confined to changes in epithelial permeability, which cannot be observed by H&E staining, such as alterations in the structure and/or function of epithelial tight junctions [30,31]. The histological evaluation of the conjunctiva did not show alterations in the tissue integrity or the presence of inflammatory changes; however, it was observed that goblet cell numbers were higher for the CsA-loaded SENS, CsA-loaded SENS-HA and blank SENS-HA than for blank SENS (**Figure 8b**). These data correlate with the MUC5AC levels found in the tears indicating that the CsA-loaded and HA-coated blank formulations exerted beneficial effects in the recuperation of goblet cell density, consequently increasing MUC5AC secretion to the tear film.

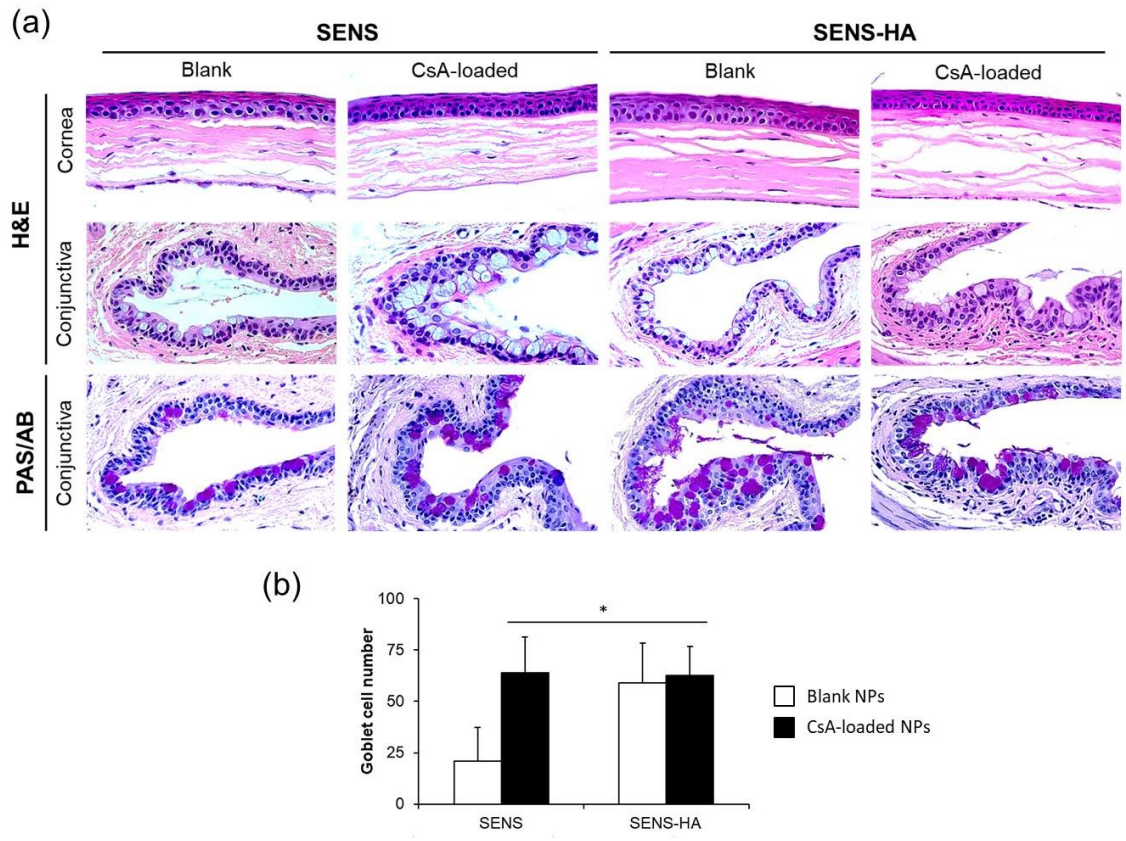


**Figure 8. Histopathology analysis of the control and treated TSP-1-deficient mouse ocular tissues.** (a) H&E- and PAS/AB-stained corneal and conjunctival tissues. There were no alterations in the cell layers, goblet cells, or other corneal and conjunctival tissue morphological details from either the blank or CsA-loaded NPs. Additionally, no inflammatory changes were observed. (b) However, significantly higher numbers of goblet cells were observed in the conjunctiva from CsA-loaded NP- and blank SENS-HA-treated mouse groups (* $p \leq 0.05$). H&E, hematoxylin and eosin; and PAS/AB, periodic acid-Schiff/Alcian blue.

### 3.5.3. Changes in pro-inflammatory cytokine levels after treatment with blank and CsA-loaded NPs.

For every disease, there are specific biomarkers whose levels are correlated with the progression of the disorder. In the case of dry eye, the presence of high levels of pro-inflammatory cytokines such as IL-6, IL-1β and TNF-α indicates a well-established ocular surface disease [28,32–34]. IL-6 is a key molecule in dry eye because it promotes the acquired immune response, favoring the perpetuation of the inflammatory condition [35]. IL-1β is related to alterations in the tight junctions present in the corneal epithelium that can lead to a weakening of the corneal barrier [36]. TNF-α causes goblet cell atrophy and apoptosis, and decreases MUC5AC secretion [27,37].

Cervical lymph nodes that drain from the ocular surface are involved in the generation of inflammatory effectors that sustain and further aggravate ocular surface inflammation [12]. Therefore, measuring cytokine levels in the cervical lymph nodes provides valuable information about the disease status and treatment efficacy. **Figure 9** shows the mRNA expression of IL-6, IL-1β and TNF-α in cervical lymph nodes obtained from TSP-1-deficient mice treated with either blank or CsA-loaded NPs. Both types of CsA-loaded NPs decreased the levels of the three pro-inflammatory cytokines compared with control formulations, revealing their anti-inflammatory efficacy. Particularly, the reduction in TNF-α levels may explain the positive effects on goblet cell recovery and MUC5AC secretion exhibited by the CsA-loaded NPs.

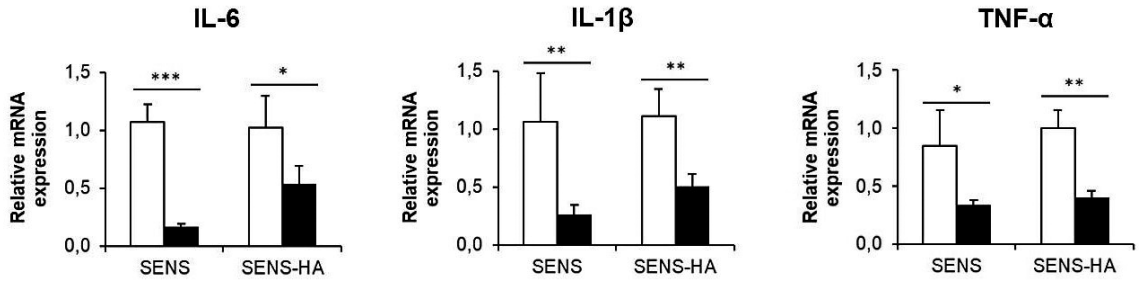


**Figure 9. Changes in relative mRNA expression for the three pro-inflammatory cytokines in cervical lymph nodes from control and treated TSP-1-deficient mice.** Both types of CsA-loaded NPs (black bars) significantly reduced IL-6, IL-1β and TNF-α mRNA expression compared with the controls (white bars) (* $p \leq 0.05$, ** $p \leq 0.01$, and *** $p \leq 0.001$).

## 4. Conclusions

In this work, we provide a proof-of-concept of the therapeutic efficacy of SENS in a mouse model of Sjögren's syndrome-associated dry eye. We also examined the influence of the HA coating on the technological viability and efficacy of SENS. Both SENS and SENS-HA exhibited reproducible physicochemical properties and adequate physical stability when lyophilized and stored at 4ºC or room temperature. Sterilization by autoclaving showed that HA exerted a beneficial effect on preserving SENS-HA from CsA leakage and aggregation at high temperatures.

*In vivo* studies showed that CsA-loaded SENS did not improve the corneal barrier integrity but promoted the recovery of conjunctival goblet cell density and MUC5AC secretion levels. This formulation also reduced the levels of main dry eye-associated pro-inflammatory cytokines. In contrast, CsA-loaded SENS-HA effectively promoted

corneal barrier reparation (from the second week treatment), the recovery of conjunctival goblet cell numbers and MUC5AC secretion levels as well as the recovery of the secretory function. CsA-loaded SENS-HA also diminished the levels of main dry eye-associated pro-inflammatory cytokines. Interestingly, the blank formulation exhibited some therapeutic activities, as suggested by the recovery in goblet cell numbers and its secretory function at the end of treatment. Overall, in this study, we demonstrated that SENS-HA potentially improves the efficacy of topically applied CsA in the treatment of experimental dry eye due to a synergistic mechanism between the anti-inflammatory efficacy of CsA and the benefits provided by HA. The mechanism by which this happens warrants further study.

## 5. Acknowledgments

This work was supported by grants from the Ministry of Economy and Competitiveness of Spain (MAT2013-47501-C02-R), Agencia Estatal y del Fondo Estrutural (FEDER), Xunta de Galicia (Competitive Reference Groups-FEDER Funds, Ref. 2017-PG101), FPI Scholarship Program (BES-2014-069437) and 2016 FPI grant for short stays (EEBB-I-17-12116). The authors would also like to thank Dr. Tatfong Ng for his assistance with the tissue processing experiments.

## References


[1] F. Stapleton, M. Alves, V.Y. Bunya, I. Jalbert, K. Lekhanont, F. Malet, K.-S. Na, D. Schaumberg, M. Uchino, J. Vehof, E. Viso, S. Vitale, L. Jones, TFOS DEWS II Epidemiology Report, Ocul. Surf. 15 (2017) 334–365. doi:10.1016/j.jtos.2017.05.003.

[2] Y. Wei, P.A. Asbell, The Core Mechanism of Dry Eye Disease Is Inflammation, Eye Contact Lens Sci. Clin. Pract. 40 (2014) 248–256. doi:10.1097/ICL.0000000000000042.

[3] P. Thulasi, A.R. Djalilian, Update in Current Diagnostics and Therapeutics of Dry Eye Disease., Ophthalmology. 124 (2017) S27–S33. doi:10.1016/j.ophtha.2017.07.022.

[4] C. Schultz, Safety and Efficacy of Cyclosporine in the Treatment of Chronic Dry Eye, Ophthalmol. Eye Dis. 6 (2014) 37–42. doi:10.4137/OED.S16067.

[5] J. Gao, T.A. Schwalb, J. V Addeo, C.R. Ghosn, M.E. Stern, The role of apoptosis in the pathogenesis of canine keratoconjunctivitis sicca: the effect of topical Cyclosporin A therapy, Cornea. 17 (1998) 654–63. http://www.ncbi.nlm.nih.gov/pubmed/9820947.

[6] S.N. Rao, Topical cyclosporine 0.05% for the prevention of dry eye disease progression., J. Ocul. Pharmacol. Ther. 26 (2010) 157–164. doi:10.1089/jop.2009.0091.

[7] D.S. Small, A. Acheampong, B. Reis, K. Stern, W. Stewart, G. Berdy, R. Epstein, R. Foerster, L. Forstot, D.D.-S. Tang-Liu, Blood Concentrations of Cyclosporin A During Long-Term Treatment With Cyclosporin A Ophthalmic Emulsions in Patients With Moderate to Severe Dry Eye Disease, J. Ocul. Pharmacol. Ther. 18 (2002) 411–418. doi:10.1089/10807680260362696.

[8] K. Sall, O.D. Stevenson, T.K. Mundorf, B.L. Reis, Two multicenter, randomized studies of the efficacy and safety of cyclosporine ophthalmic emulsion in moderate to severe dry eye disease. CsA Phase 3 Study Group., Ophthalmology. 107 (2000) 631–9. http://www.ncbi.nlm.nih.gov/pubmed/10768324.

[9] F. Lallemand, M. Schmitt, J.-L. Bourges, R. Gurny, S. Benita, J.-S. Garrigue, Cyclosporine A delivery to the eye: A comprehensive review of academic and industrial efforts, Eur. J. Pharm. Biopharm. 117 (2017) 14–28. doi:10.1016/j.ejpb.2017.03.006.

[10] J. Alvarez-Trabado, A. López-García, M. Martín-Pastor, Y. Diebold, A. Sanchez, Sorbitan ester nanoparticles (SENS) as a novel topical ocular drug delivery system: Design, optimization, and in vitro/ex vivo evaluation, Int. J. Pharm. 546 (2018) 20–30. doi:10.1016/j.ijpharm.2018.05.015.

[11] B. Turpie, T. Yoshimura, A. Gulati, J.D. Rios, D.A. Dartt, S. Masli, Sjögren's Syndrome-Like Ocular Surface Disease in Thrombospondin-1 Deficient Mice, Am. J. Pathol. 175 (2009) 1136–1147. doi:10.2353/ajpath.2009.081058.

[12] L. Contreras-Ruiz, B. Regenfuss, F.A. Mir, J. Kearns, S. Masli, Conjunctival Inflammation in Thrombospondin-1 Deficient Mouse Model of Sjögren's Syndrome, PLoS One. 8 (2013) e75937. doi:10.1371/journal.pone.0075937.

[13] S. Liu, M.D. Dozois, C.N. Chang, A. Ahmad, D.L.T. Ng, D. Hileeto, H. Liang, M.-M. Reyad, S. Boyd, L.W. Jones, F.X. Gu, Prolonged Ocular Retention of Mucoadhesive Nanoparticle Eye Drop Formulation Enables Treatment of Eye Diseases Using Significantly Reduced Dosage, Mol. Pharm. 13 (2016) 2897–2905. doi:10.1021/acs.molpharmaceut.6b00445.

[14] M.A. Lemp, Report of the National Eye Institute/Industry workshop on Clinical Trials in Dry Eyes, CLAO J. 21 (1995) 221–32. http://www.ncbi.nlm.nih.gov/pubmed/8565190.

[15] W.M.S. Russell, R.L. Burch, The principles of humane experimental technique, Univ. Fed. Anim. Welf. (1959).

[16] J. Alvarez-Trabado, Y. Diebold, A. Sanchez, Designing lipid nanoparticles for topical ocular drug delivery, Int. J. Pharm. 532 (2017). doi:10.1016/j.ijpharm.2017.09.017.

[17] C. Di Tommaso, C. Como, R. Gurny, M. Möller, Investigations on the lyophilisation of MPEG–hexPLA micelle based pharmaceutical formulations, Eur. J. Pharm. Sci. 40 (2010) 38–47. doi:10.1016/j.ejps.2010.02.006.

[18] P. Fonte, S. Soares, F. Sousa, A. Costa, V. Seabra, S. Reis, B. Sarmento, Stability Study Perspective of the Effect of Freeze-Drying Using Cryoprotectants on the Structure of Insulin Loaded into PLGA Nanoparticles, Biomacromolecules. 15 (2014) 3753–3765. doi:10.1021/bm5010383.

[19] A. Almalik, I. Alradwan, M.A. Kalam, A. Alshamsan, Effect of cryoprotection on particle size stability and preservation of chitosan nanoparticles with and without hyaluronate or alginate coating, Saudi Pharm. J. 25 (2017) 861–867. doi:10.1016/j.jsps.2016.12.008.

[20] M.A. Vetten, C.S. Yah, T. Singh, M. Gulumian, Challenges facing sterilization and depyrogenation of nanoparticles: Effects on structural stability and biomedical applications, Nanomedicine Nanotechnology, Biol. Med. 10 (2014) 1391–1399. doi:10.1016/j.nano.2014.03.017.

[21] L. Contreras-Ruiz, F.A. Mir, B. Turpie, A.H. Krauss, S. Masli, Sjögren's syndrome associated dry eye in a mouse model is ameliorated by topical application of integrin α4 antagonist GW559090, Exp. Eye Res. 143 (2016) 1–8. doi:10.1016/j.exer.2015.10.008.

[22] J.A.P. Gomes, R. Amankwah, A. Powell-Richards, H.S. Dua, Sodium hyaluronate (hyaluronic acid) promotes migration of human corneal epithelial cells in vitro., Br. J. Ophthalmol. 88 (2004) 821–5. doi:10.1136/bjo.2003.027573.

[23] J. Zhong, Y. Deng, B. Tian, B. Wang, Y. Sun, H. Huang, L. Chen, S. Ling, J. Yuan, Hyaluronate Acid-Dependent Protection and Enhanced Corneal Wound Healing against Oxidative Damage in Corneal Epithelial Cells, J. Ophthalmol. 2016 (2016) 1–10. doi:10.1155/2016/6538051.

[24] A. Ragam, A.M. Kolomeyer, J.S. Kim, N. V. Nayak, C. Fang, E. Kim, D.S. Chu, Topical Cyclosporine A 1% for the Treatment of Chronic Ocular Surface Inflammation, Eye Contact Lens Sci. Clin. Pract. 40 (2014) 283–288. doi:10.1097/ICL.0000000000000055.

[25] P. Hossain, Cyclosporine in ocular surface inflammation, Eye. 31 (2017) 665–667. doi:10.1038/eye.2017.5.

[26] L. Contreras Ruiz, F.A. Mir, B. Turpie, S. Masli, Thrombospondin-derived peptide attenuates Sjögren's syndrome-associated ocular surface inflammation in mice, Clin. Exp. Immunol. 188 (2017) 86–95. doi:10.1111/cei.12919.

[27] L. Contreras-Ruiz, A. Ghosh-Mitra, M.A. Shatos, D.A. Dartt, S. Masli, Modulation of Conjunctival Goblet Cell Function by Inflammatory Cytokines, Mediators Inflamm. 2013 (2013) 1–11. doi:10.1155/2013/636812.

[28] J. Zhang, X. Yan, H. Li, Analysis of the Correlations of Mucins, Inflammatory Markers, and Clinical Tests in Dry Eye, Cornea. 32 (2013) 928–932. doi:10.1097/ICO.0b013e3182801622.

[29] J.H. Choi, J.H. Kim, Z. Li, H.J. Oh, K.Y. Ahn, K.C. Yoon, Efficacy of the Mineral Oil and Hyaluronic Acid Mixture Eye Drops in Murine Dry Eye, Korean J. Ophthalmol. 29 (2015) 131. doi:10.3341/kjo.2015.29.2.131.

[30] S.C. Pflugfelder, Tear Dysfunction and the Cornea: LXVIII Edward Jackson

Memorial Lecture, Am. J. Ophthalmol. 152 (2011) 900–909.e1. doi:10.1016/j.ajo.2011.08.023.

[31] S.C. Pflugfelder, W. Farley, L. Luo, L.Z. Chen, C.S. de Paiva, L.C. Olmos, D.-Q. Li, M.E. Fini, Matrix Metalloproteinase-9 Knockout Confers Resistance to Corneal Epithelial Barrier Disruption in Experimental Dry Eye, Am. J. Pathol. 166 (2005) 61–71. doi:10.1016/S0002-9440(10)62232-8.

[32] L. Contreras-Ruiz, D.S. Ryan, R.K. Sia, K.S. Bower, D.A. Dartt, S. Masli, Polymorphism in THBS1 Gene Is Associated with Post-Refractive Surgery Chronic Ocular Surface Inflammation, Ophthalmology. 121 (2014) 1389–1397. doi:10.1016/j.ophtha.2014.01.033.

[33] M.L. Massingale, X. Li, M. Vallabhajosyula, D. Chen, Y. Wei, P.A. Asbell, Analysis of Inflammatory Cytokines in the Tears of Dry Eye Patients, Cornea. 28 (2009) 1023–1027. doi:10.1097/ICO.0b013e3181a16578.

[34] S.Y. Lee, S.J. Han, S.M. Nam, S.C. Yoon, J.M. Ahn, T.-I. Kim, E.K. Kim, K.Y. Seo, Analysis of Tear Cytokines and Clinical Correlations in Sjögren Syndrome Dry Eye Patients and Non–Sjögren Syndrome Dry Eye Patients, Am. J. Ophthalmol. 156 (2013) 247–253.e1. doi:10.1016/j.ajo.2013.04.003.

[35] S.A. Jones, Directing transition from innate to acquired immunity: defining a role for IL-6, J. Immunol. 175 (2005) 3463–8. http://www.ncbi.nlm.nih.gov/pubmed/16148087.

[36] K. Kimura, S. Teranishi, T. Nishida, Interleukin-1β–Induced Disruption of Barrier Function in Cultured Human Corneal Epithelial Cells, Investig. Opthalmology Vis. Sci. 50 (2009) 597. doi:10.1167/iovs.08-2606.

[37] Y.W. Ji, Y.J. Byun, W. Choi, E. Jeong, J.S. Kim, H. Noh, E.S. Kim, Y.J. Song, S.K. Park, H.K. Lee, Neutralization of Ocular Surface TNF-α Reduces Ocular Surface and Lacrimal Gland Inflammation Induced by In Vivo Dry Eye, Investig. Opthalmology Vis. Sci. 54 (2013) 7557. doi:10.1167/iovs.12-11515.

USC
UNIVERSIDADE
DE SANTIAGO
DE COMPOSTELA

# *Chapter III*

---

***Rapamycin-loaded sorbitan ester nanoparticles (SENS) as new tools for the treatment of corneal neovascularization: preliminary physicochemical characterization and in vitro antiangiogenic efficacy***

USC
UNIVERSIDADE
DE SANTIAGO
DE COMPOSTELA

**Abstract**

The aim of this work was to develop and characterize two types of rapamycin (Rapa)-loaded sorbitan ester nanoparticles (SENS) for topical therapy of corneal neovascularization (CN). Rapa-loaded SENS displayed a particle size of 173.8 nm, a zeta potential of +22.1 mV and a Rapa entrapment efficiency of 78.7%. The hyaluronic acid (HA)-coated version, i.e., Rapa-loaded SENS-HA, had a particle size of 178.0 nm and a zeta potential of –19.3 mV. Structural analysis of the formulations by differential scanning calorimetry and X-ray powder diffraction suggested that the drug was molecularly dissolved inside the NP matrix, accounting for a 600-fold increase with respect to the water solubility of this drug. The NPs were also characterized regarding their biocompatibility and antiangiogenic potential. Cell viability values for corneal and conjunctival cell lines showed a dose-dependent profile, with higher NP doses showing the most cytotoxic effects. Overall, the NP dose that we further evaluated for its antiangiogenic potential presented cell viability values above 75%, indicating appropriate biocompatibility. This NP dose also showed similar anti-VEGF activity to the Rapa solution used as a reference, confirming that the drug maintained its biological activity after entrapment inside the NP matrix.

USC
UNIVERSIDADE
DE SANTIAGO
DE COMPOSTELA

## 1. Introduction

The cornea is a highly organized structure that has the dual functions of protecting the inner structures of the eye and providing nearly two thirds of the eye's refractive power [1]. Due to its relevant role in vision, the cornea is an avascular and transparent tissue that allows the passage of light signals with minimum alterations. In some diseases or pathological circumstances, the corneal transparency is compromised because of the ingrowth of blood and lymph vessels from the pericorneal limbal plexus through a process known as corneal neovascularization (CN) [2]. Corneal injuries (chemical, thermal or mechanical), infectious keratitis, corneal allograft rejection, or extended contact lens wearing are often associated with pathological manifestations such as inflammation, hypoxia, or limbal dysfunction that may lead to CN [3].

Although many therapies have been used in the clinic to treat CN, such as corticosteroids, non-steroid anti-inflammatory drugs, laser photocoagulation or amniotic membrane transplantation, these treatments all have limited clinical efficacy and are often associated with undesirable side effects [4]. Understanding the pathophysiology of CN has led to the emergence of a new powerful targeted therapy, anti-VEGF therapy. Vascular endothelial growth factor (VEGF) is considered the key molecule in the pathophysiology of CN. This proangiogenic peptide favors vascular tube formation by promoting endothelial cell proliferation and migration [5]. It also enhances vascular permeability and promotes monocyte chemotaxis and B-cell production, indicating an active role in inflammation [6].

Anti-VEGF therapy is generally subdivided into the following two groups: neutralizing antibodies and kinase inhibitor-based therapies. Antibodies including bevacizumab, ranibizumab or aflibercept are currently used for the management of retinal pathologies such as neovascular age-related macular degeneration [4]. These proteins specifically bind VEGF molecules precluding its interaction with VEGF cell receptors and avoiding the triggering of the angiogenic cascade. Tyrosine kinase inhibitors, such as regorafenib, sunitib, trastuzumab, apatinib or midostaurin, impede the tyrosine kinase activity of VEGF receptors by preventing the intracellular transmission associated with angiogenic stimuli [4]. However, their inhibiting activity is not limited to VEGF-receptors; it can also affect tyrosine kinases from other proangiogenic receptors such as the platelet-derived growth factor receptor (PDGFR), thus increasing its antiangiogenic efficacy [7].

Immunomodulatory therapy is considered an effective alternative strategy for managing CN. Various immunosuppressant drugs have been tested for the treatment of CN including cyclosporine (CsA), tacrolimus and rapamycin (Rapa) [8]. Rapa, a natural macrolide that inhibits the so-called mammalian target of rapamycin (mTOR), is a potent immunosuppressant that also shows anti-VEGF effects [9,10]. It is reported that 0.05% Rapa showed greater antiangiogenic efficacy than 0.5% CsA and same efficacy as 0.1% dexamethasone in the treatment of CN secondary to stromal keratitis [11]. The combined immune-antiangiogenic effects of Rapa may also explain its efficacy in the prevention of allograft rejection without the appearance of CN [12].

In this work, we developed Rapa-loaded NPs specifically designed for topical ocular drug delivery. We used our patented sorbitan ester nanoparticles (SENS) that previously demonstrated its suitability for topical ocular CsA delivery as the drug vehicle both *in vitro* (Chapter I) [13] and *in vivo* (Chapter II). The developed nanoparticles (NPs) were preliminary characterized regarding their physicochemical properties, biocompatibility and antiangiogenic efficacy.

## 2. Materials and methods

### 2.1. Materials

Sorbitan monooleate (Span® 80), d-α-tocopheryl polyethylene glycol 1000 succinate (TPGS), cetyltrimethylammonium bromide (CTAB), hyaluronic acid (HA), benzalkonium chloride (BZK), and 2,3-bis[2-methoxy-4-nitro-5-sulfophenyl]-2H-tetrazolium-5-carboxyanilide inner salt (XTT) were obtained from Sigma-Aldrich (Madrid, Spain). Rapamycin (Rapa) was purchased from Apexbio (Boston, MA, USA). High-performance liquid chromatography (HPLC)-grade acetonitrile (ACN) was from VWR (Barcelona, Spain). Interleukin 1 beta (IL-1β) and tumor necrosis factor alpha (TNF-α) were from Peprotech (London, UK). The Pierce® BCA Protein Assay Kit was from Thermo Fisher Scientific (Waltham, MA, USA). The VEGF-A enzyme-linked immunosorbent assay (ELISA) kit was purchased from Diaclone (Besaçon, France) and Dulbecco's Modified Eagle Medium Nutrient Mixture F-12 (DMEM/F12) culture medium and other cell culture reagents were purchased from Invitrogen-Gibco (Inchinnan, UK).

## 3. Methods

### 3.1. Preparation of NPs

For SENS preparation, we followed a detailed previously described method (Chapter I) [13]. Briefly, all NP components including Span® 80, TPGS, and CTAB as well as Rapa – for the drug-loaded NPs – were dissolved in absolute ethanol. The organic phase was then added to an aqueous phase under continuous magnetic stirring (500 rpm, 15 minutes) leading to the spontaneous formation of NPs. The ethanol was immediately removed under reduced pressure with a rotatory evaporator (Buchi® R-210, Massó Analítica, Barcelona). The resulting concentrated formulation had the following nominal composition (w/v): 2.00% Span® 80, 0.22% TPGS, and 0.03% CTAB with 0.2% Rapa in the drug-loaded NPs.

HA-coated NPs (i.e., SENS-HA) were prepared by simply mixing two volumes of SENS with one volume of an aqueous solution of HA (1,600 KDa), giving a final polysaccharide concentration of 0.015% (w/v). To ensure total HA adsorption, the NPs were placed in an orbital shaker at 75 rpm for 20 minutes.

### 3.2. Physicochemical characterization of the NPs: particle size, zeta potential and entrapment efficiency.

The mean particle size (Z-average) and the size distribution (polydispersity index) of the NPs were determined by dynamic light scattering (DLS). In prior analyses, NP samples were properly diluted with 0.1 mM KCl. Analyses were performed at 25ºC with a detection angle of 173º. The zeta potential (mean electrophoretic mobility) was determined by laser doppler anemometry (LDA). Both analyses were performed with a Zetasizer® 3000HS (Malvern Instruments, Malvern, UK).

For the Rapa entrapment efficiency measurement, NPs were first passed through a 0.22-µm filter to remove any unentrapped drug crystals. The resulting purified NPs were then disrupted, and the drug content was extracted using ACN. Rapa was quantified by HPLC using a KromaPhase C18 reverse phase column (250×4.6 mm, 5 µm diameter). The HPLC system (Merck-Hitachi, Darmstadt, Germany) was composed of an L-6200 pump model, an AS-4000 automatic injector, an L-5025 column oven, and an L-4500 UV-detector coupled to a computer by a D-6000 interface. The HPLC method consisted of a mixture of ACN:ultrapure water at an 80:20 (w/v) ratio following an isocratic mode for 9 minutes. The temperature of the column oven was set at 60ºC. The flow rate was 1.2 mL/min and the injection volume was 20 µL. Rapa detection

occurred at 278 nm. The entrapment efficiency (EE%) was calculated with the following equation:

$$EE(\%) = \frac{Weight\ of\ Rapa\ recovered\ from\ nanoparticles}{Weight\ of\ Rapa\ initially\ added} \times 100$$

### 3.3. Analysis of NP morphology

The morphology of the NPs was examined by transmission electron microscopy (TEM) (CM 12 Philips, Eindhoven, Netherlands). For this purpose, NP samples were placed on Formvar®-coated cooper grids and subsequently stained with 2% (w/v) phosphotungstic acid solution. For each NP, representative microphotographs of two independent samples were acquired.

### 3.4. NP structural analysis by differential scanning calorimetry (DSC) and X-ray powder diffraction (XRD)

The structures of the lyophilized NPs were studied by DSC and XRD. DSC scans were performed with a DSC Q100 calorimeter (TA Instruments, Barcelona, Spain) at a temperature range between -50 and 250ºC with a heating rate of 10ºC/minute. The XRD studies were performed with a Philips PW1710 X-ray Diffraction Spectrometer (Philips Electronic Inst, Holland) using a sealed tube with copper solution as the radiation source. Diffractograms were recorded at an angular range from 2º and 50º with a 0.02º step.

### 3.5. Cell lines and culture conditions

Three cell types derived from ocular surface tissues were used. The human corneal epithelial cell line (HCE) [14] from passages 35-40 was cultured in DMEM/F-12 medium supplemented with 10% fetal bovine serum, 5000 U/mL penicillin/streptomycin, 10 ng/mL epidermal growth factor, and 5 µg/mL insulin. The IOBA–Normal Human Conjunctiva (IOBA-NHC) epithelial cell line [15] from passages 64-72 was cultured in DMEM/F-12 medium supplemented with 10% fetal bovine serum, 5000 U/mL penicillin/streptomycin, 2.5 µg/mL fungizone, 2 ng/mL epidermal growth factor, 1 µg/mL insulin, and 0.5 µg/mL hydrocortisone. Epithelial primary cultures (EPCs) were obtained from human bulbar conjunctiva using a previously described [16] and optimized [17] explant technique. The procedures were in accordance with the Tenets of the Declaration of Helsinki and Spanish Regulations concerning the use of human tissues for biomedical research and had the approval of the

Institutional Review Board of the University of Valladolid. Epithelial cells were cultured in IOBA-NHC medium substituting the fetal bovine serum supplement with human serum. All cell culture was maintained at 37ºC in a 5% $CO_2$ humidified atmosphere.

**3.6. Cell viability assay**

The effect of NPs on cell viability was assessed using the corneal and conjunctival epithelial cell lines. Cells were seeded onto 96-well plates ($2x10^4$ cells/well) and grown until confluence. The cells were then incubated with different NP concentrations prepared in phenol red-free DMEM. Additionally, two controls were used as references, including cells exposed to phenol red-free DMEM (negative control) and cells exposed to 0.01% (w/v) BZK (positive control). After 24 hours of incubation, all treatments were removed, and the cells washed with DPBS. The XTT cell viability assay was subsequently performed according to the manufacturer's instructions. The percentage of cell viability was calculated based on the negative control. Four independent experiments were completed at least in duplicate.

**3.7. *In vitro* antiangiogenic efficacy**

The antiangiogenic efficacy of the NPs was studied *in vitro* by measuring their anti-VEGF activity. Two functional assays were performed on stimulated EPCs and IOBA-NHC cells following the experimental setup depicted in **Figure 1**.

For EPCs, the cells were seeded onto 24 well-plates ($1x10^5$ cells/well) and grown in complete medium until they reached elevated confluence. The cells were then exposed to 50 ng/mL of the proangiogenic cytokine IL-6, which was prepared in EPC medium. After 24 hours of incubation, the IL-6-containing medium was replaced by the treatment dilutions. NP treatments including blank NPs, Rapa-loaded NPs and Rapa dissolved in DMSO were diluted to a Rapa concentration of 500 ng/mL [18] using fresh EPC medium. The concentration of blank NPs (7.5 µg/mL) was adjusted to that of the Rapa-loaded NPs. Two controls were used, including cells stimulated with the proangiogenic cytokine (positive control) and cells incubated with fresh EPC medium (negative control). After 24 hours of incubation, the medium containing secreted VEGF was removed and placed into Eppendorf tubes for storage until analysis. The 24-well plates containing the cell monolayers were washed with cold PBS and stored until protein analysis. VEGF expression was determined using a specific VEGF-A ELISA kit and the protein content by the Pierce® BCA Protein Assay Kit. The VEGF concentrations were

first normalized to the protein content from each well and then to the negative control. Three independent experiments were performed with 1-2 replicates each.

To determine the most adequate proangiogenic conditions for IOBA-NHC cells, the cells were exposed to different combinations of IL-1β and TNF-α [19], and the VEGF expression was quantified. For this purpose, cells were seeded onto 24-well plates ($3x10^5$ cells/well) and grown in complete medium until confluence. The cells were then synchronized for 5 hours by replacing the complete medium with pure serum-free DMEM. Then, appropriate mixtures of IL-1β and TNF-α (5-20 ng/mL) were added to the corresponding wells. After 24 hours of incubation, the medium containing the secreted VEGF was removed and stored until analysis using a specific VEGF-A ELISA kit. The same experimental procedure as described above was used to evaluate the anti-VEGF efficacy of the developed NPs. In this case, a cytokine mixture containing 10 ng/mL IL-1β and 10 ng/mL TNF-α was mixed with the NP treatments, including the blank NPs, Rapa-loaded NPs and Rapa dissolved in DMSO (500 ng/mL) [18]. The blank NP concentration (7.5 µg/mL) was adjusted to that of the Rapa-loaded NPs. Two controls were used, including cells stimulated with the proangiogenic combination (positive control) and cells incubated with pure DMEM (negative control). The VEGF concentrations were normalized to the negative control. The optimization of the experimental conditions and the functional assay with the NPs were performed in triplicate with 2 replicates each.

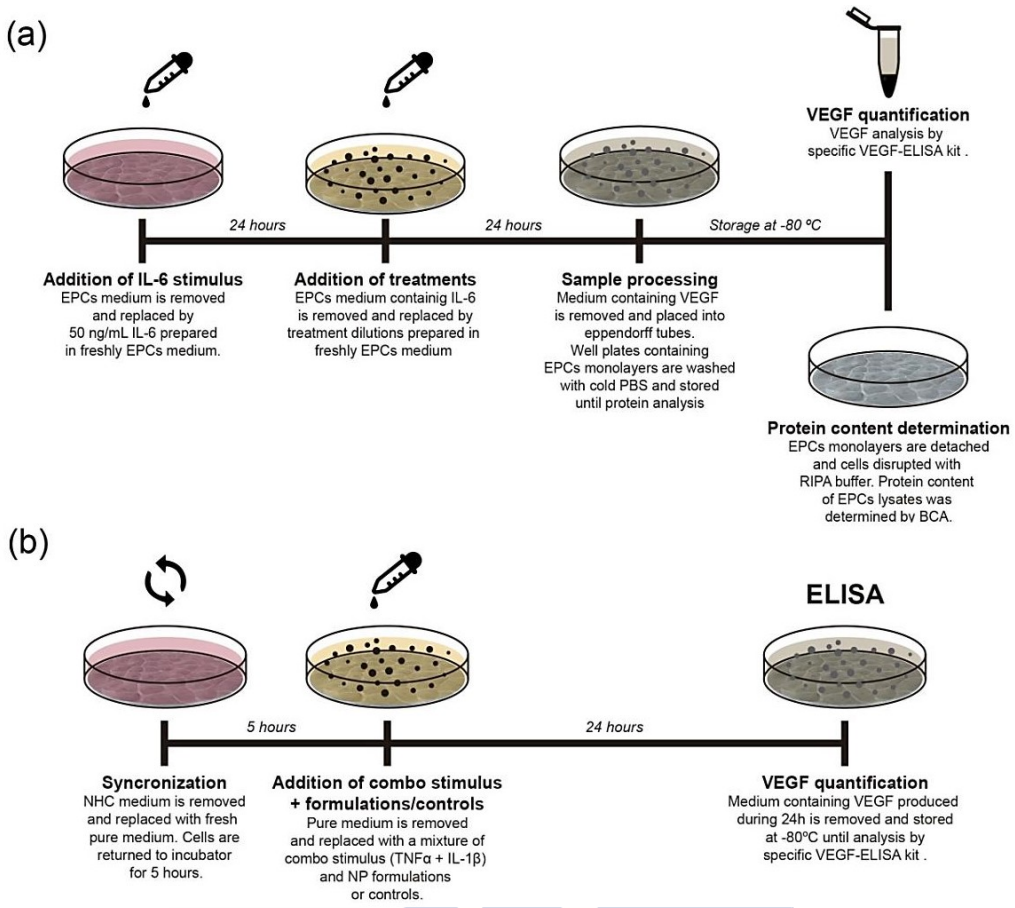


**Figure 1. Schematic representation of the two functional assays performed to evaluate the *in vitro* antiangiogenic efficacy of the developed NPs in (a) EPCs and (b) IOBA-NHC cells.** EPCs, epithelial primary cultures; RIPA, radioimmunoprecipitation assay buffer; and BCA, Pierce® BCA Protein Assay Kit. Schematic created by Jesús Álvarez Trabado.

To determine potential changes in cell morphology caused by the treatments, the IOBA-NHC cells were observed and photographed after the exposure period. A phase contrast microscope (Nikon Eclipse TS100, Tokyo, Japan) was used to acquire cell microphotographs. Duplicate images of each cell condition were acquired at 40x magnification.

### 3.8. Statistical analysis

All experimental measurements were expressed as the mean ± standard deviation (SD). The comparison of multiple data groups was completed by one-way ANOVA followed by pairwise comparisons (Tukey test) using the Statistical Procedures for the Social Sciences software (SPSS 20.0; SPSS Inc., Chicago, USA). Differences were considered significant when the *p*-value was $\leq 0.05$.

## 4. Results and discussion

For years, Rapa has been used in the clinic as a therapeutic alternative to systemic CsA immunosuppression because of its higher potency and lower incidence of adverse effects (i.e., absence of nephrotoxicity) [20,21]. In the ophthalmologic field, Rapa has had limited use, with only a few academic studies utilizing its anti-inflammatory [22] and antiangiogenic potential [11,12]. Among other reasons, this may be because this drug possesses very low water solubility [23], which seriously precludes its ophthalmic administration.

The objective of this work was to solubilize this drug in the form of a simple aqueous NP dispersion that can be easily administered topically. Furthermore, the developed Rapa-loaded NPs should be biocompatible with ocular surface cells and the entrapped drug should maintain its antiangiogenic efficacy.

### 4.1. Development and physicochemical characterization of the NPs.

The matrix composition of the NPs was selected from previously developed SENS-OPT and SENS-OPT-HA NPs (Chapter I) [13]. Those NPs were able to solubilize high amounts of cyclosporine (water insoluble drug) without compromising its biological activity. Both NPs also showed adequate biocompatibility profiles and excellent targeting ability, achieving higher values of cellular uptake and corneal penetration than using commercially available dosage forms of this drug.

In this case, although the therapeutic target is located in the pericorneal area -where angiogenesis begins- we considered the cornea as the main target for the Rapa-loaded NPs. The reason is that the corneal epithelium may act as a reservoir structure [24,25], enabling the sustained release of Rapa to the surrounding tissues over time.

**Table 1** shows main physicochemical characteristics of the developed NPs. Blank SENS showed a particle size in the nanometer range, low polydispersity and a positive zeta potential. Rapa entrapment (EE% = 78.7 ± 6.6%) did not significantly affect the particle size, suggesting that the drug was dissolved at the molecular level. Considering that Rapa solubility is 2.6 µg/mL [23], the solubilization effect caused by the NPs (up to 1.57 mg/mL) provoked a 600-fold increase compared with its aqueous solubility in the free form.

**Table 1. Summary of the main NP physicochemical characteristics.**

| Formulation | Particle size (nm) | Polydispersity (PdI) | Zeta Potential (mV) |
|---|---|---|---|
| Blank SENS | 176.1 ± 6.5 | 0.106 ± 0.005 | + 28.5 ± 0.9 |
| Rapa-loaded SENS | 173.8 ± 10.8 | 0.116 ± 0.058 | + 22.1 ± 5.2 |
| Blank SENS-HA | 185.6 ± 6.9 | 0.191 ± 0.009 | − 27.6 ± 0.2 |
| Rapa-loaded SENS-HA | 178.0 ± 6.7 | 0.146 ± 0.020 | − 19.3 ± 5.1 |

As expected, blank and Rapa-loaded SENS-HA had larger particle sizes and a negative zeta potential because of the HA adsorption. The size distribution plots (**Figure 2**) confirmed that the particle size and size distribution was not altered by the Rapa entrapment in both cases. As was observed in Chapter I [13], transmission electron microscopy microphotographs (**Figure 2**) showed the presence of a corona effect in the SENS-HA (both blank and Rapa-loaded), confirming the effective HA association.

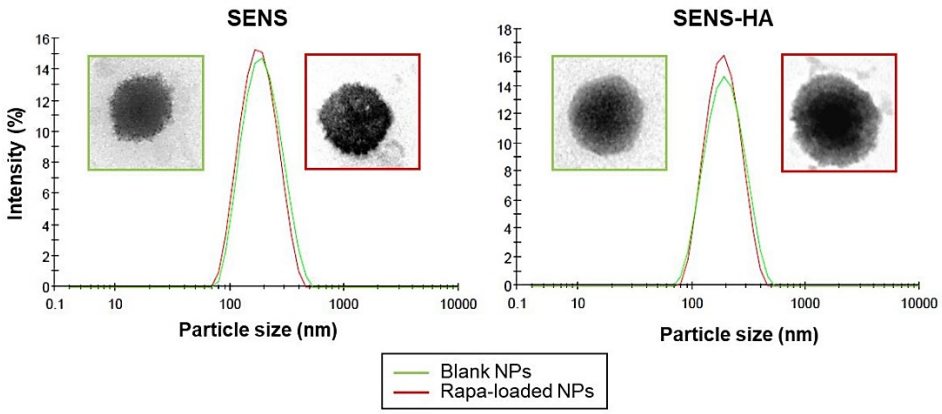


**Figure 2. Particle size distribution plots and transmission electron microphotographs of SENS and SENS-HA.** Both SENS and SENS-HA had homogeneous particle size distributions that were not altered by Rapa entrapment. The most visible difference in the morphologies of both types of NPs was the presence of the HA corona on the SENS-HA NPs.

To further characterize the physical state of Rapa inside the NPs, we used two complementary techniques, DSC and XRD. DSC thermal profiles of the lyophilized NPs are shown in **Figure 3a**. The thermal profile of sucrose (cryoprotectant), Span 80 (main NP matrix component), and Rapa (entrapped drug) were used as references. Drug

entrapment provoked a substantial alteration in the NP thermal profiles, which may be related to interactions between the drug and the NP matrix [26]. Additionally, the second melting peak of crystalline Rapa (198ºC) was not observable in the Rapa-loaded NPs, indicating the absence of the crystalline drug material in the NP formulation. XRD diffractograms of crystalline sucrose, crystalline Rapa and lyophilized NPs are depicted in **Figure 3b**. The most visible spectrum peaks in the NP formulations corresponded to sucrose due its high degree of crystallinity. Additionally, the characteristic spectrum peak of crystalline Rapa (7.23º) was not visible in the drug-loaded formulation. These results support that drug was not in the crystalline state but dissolved at the molecular level inside the NPs.

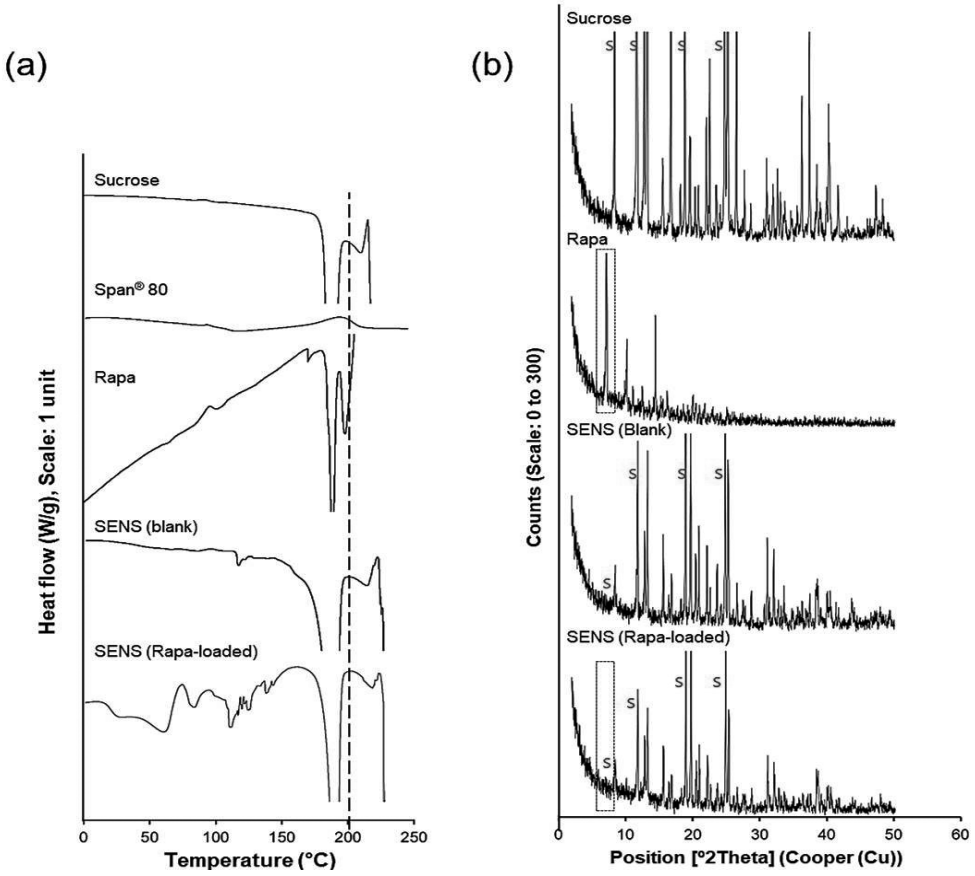


**Figure 3. Structural analysis of lyophilized NPs.** (a) DSC thermal profiles for the main NP components and two representative lyophilized NP formulations, including the blank SENS and Rapa-loaded SENS. Rapa entrapment by SENS caused visible alterations in their DSC thermal profiles. The second melting peak for crystalline Rapa (198ºC) –vertical dotted line facilitates peak colocalization- was not present in the drug-loaded formulation. (b) XRD diffractograms of crystalline sucrose, crystalline Rapa and two representative lyophilized NP formulations, including the blank SENS and Rapa-loaded SENS. The characteristic spectrum peak of crystalline Rapa (7.23º) was not observable in the drug-loaded formulation (highlighted area of spectra with rectangle). The most visible peaks corresponded to sucrose crystals (S).

### 4.2. *In vitro* evaluation of the biocompatibility of developed NPs.

Considering that the NPs were designed to be topically applied to the ocular surface, two representative ocular surface cell lines (i.e., corneal and conjunctival epithelial cell lines) were selected to assess their biocompatibility. Different concentrations of blank and Rapa-loaded NPs were tested. The concentration range of Rapa-loaded NPs (and its blank version) was established by considering the dose of Rapa that has been reported to show an *in vitro* antiangiogenic efficacy [18].

The cell viability results in **Figure 4** indicate different toxicity profiles depending on the NP type as well as the cell line used. The NPs generally showed less toxicity in the corneal cell line than in the conjunctival cell line, which may be explained by the higher sensitivity of conjunctival cells to damage [27]. There were clear differences between the toxicological profiles of the blank and drug-loaded NPs that were most evident at the highest NP dose. At this dose, Rapa-loaded NPs had 4-fold more cytotoxicity than the blank NPs ($p \leq 0.001$). This may be explained by a synergistic mechanism between the cytotoxicity of free CTAB once NPs are metabolized and the apoptosis-induced cell death caused by Rapa [28]. In general, the HA-coated NPs exhibited lower toxicity than their uncoated counterparts, which may be due to the presence of HA, as it exerts a cytoprotective effect [29,30]. This beneficial effect of HA was most obvious in the conjunctival line, where the Rapa-loaded SENS significantly reduced cell viability at the lower NP doses ($p \leq 0.001$), whereas the Rapa-loaded SENS-HA only showed a significant cytotoxic effect when the dose was 10-fold greater ($p \leq 0.05$). Overall, the NP dose we selected for further experiments was 7.5 µg/mL, which was equivalent to 0.5 µg/mL Rapa in the drug-loaded formulations. This concentration showed an adequate safety profile with cell viability values above 80% for both cell lines. Only conjunctival cells treated with Rapa-loaded SENS at this concentration showed a reduction in the percentage of living cells (77.2%).

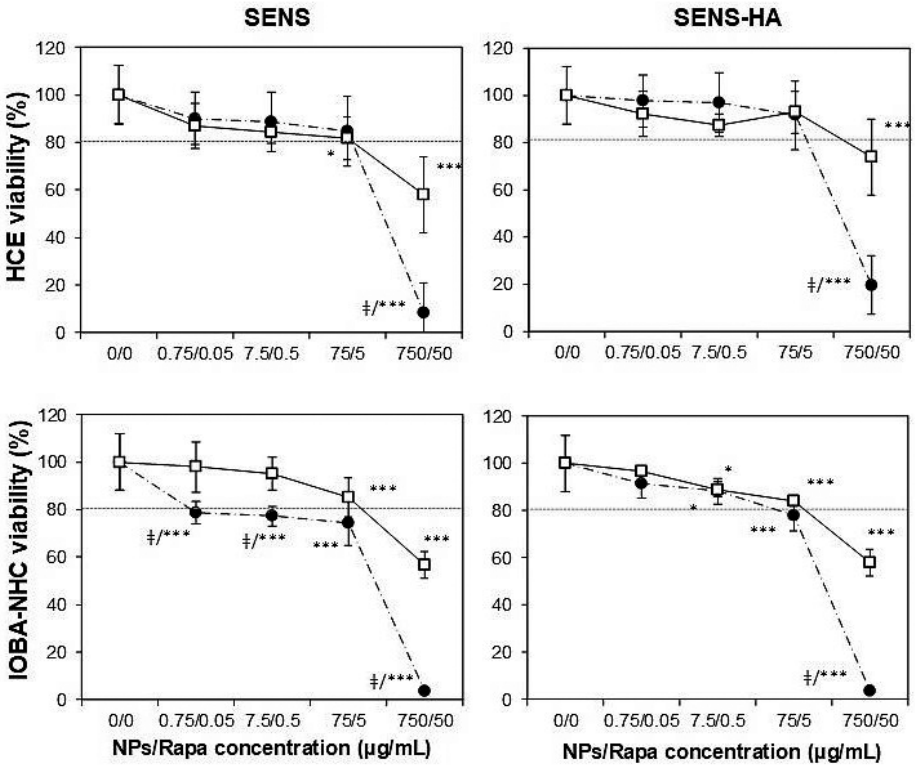


**Figure 4. Corneal and conjunctival cell line viability profiles upon treatment with the developed NPs.** The cell viability values show dose-dependent behaviors in both cell lines. In general, Rapa-loaded NPs (-●-) were more cytotoxic than the equivalent blank NPs (-□-) at high doses. HA-coated NPs showed lower cytotoxicity than the equivalent uncoated NPs. Significant differences with regard to the negative control are represented by * $p \leq 0.05$ and *** $p \leq 0.001$ and with regard to the equivalent concentration of blank NPs by ǂ $p \leq 0.001$. Note: The vertical axis represents the NP concentration and the equivalent Rapa concentration for the drug-loaded NPs.

### 4.3. *In vitro* evaluation of the antiangiogenic efficacy of the Rapa-loaded NPs.

As mentioned above, VEGF is a key molecule in the pathogenesis of CN. Some authors have reported that cytokines such as IL-6, TNF-α and IL-1β may stimulate the secretion of this proangiogenic protein [31][32][19]. Accordingly, we performed two functional assays on VEGF production using EPCs and an IOBA-NHC cell line. The anti-VEGF activities of the NPs were determined by measuring the relative VEGF production after incubation with proangiogenic stimuli and the NPs.

The results from the functional assay performed on EPCs are shown in **Figure 5**. Although not significant, VEGF secretion was slightly increased after incubation with IL-6. Both Rapa-loaded SENS and SENS-HA NPs decreased VEGF to levels that were similar to the reference Rapa solution ($p \leq 0.01$ and $p \leq 0.001$, respectively). This means that Rapa maintained its biological activity after incorporation into the NP matrix, and its efficacy was the same as the free Rapa. In the case of the blank NPs, both SENS and SENS-HA did not significantly affect the VEGF concentration.

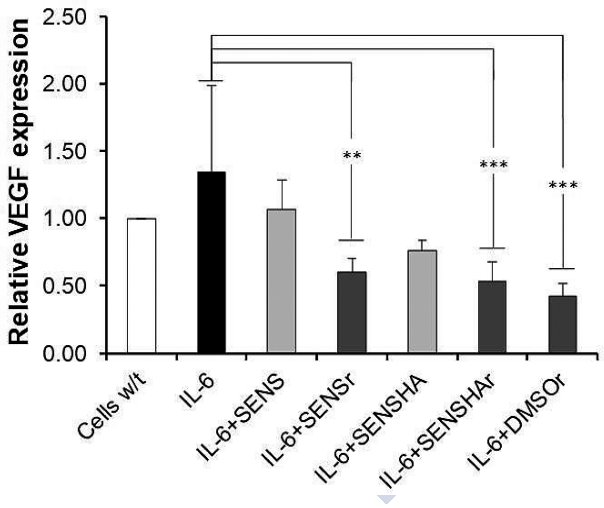


**Figure 5. Anti-VEGF efficacy of blank and Rapa-loaded NPs on EPC cells stimulated with IL-6.** Rapa-loaded NPs diminished VEGF secretion (** $p \leq 0.01$ and *** $p \leq 0.001$) to the same extent as the Rapa solution. W/t, without treatment and r, rapamycin.

Considering the technical and logistical limitations of working with primary cell cultures, we wanted to develop a simple and scalable functional assay using the IOBA-NHC cell line. The results from the functional assay on IOBA-NHC cells are depicted in **Figure 6**. In this case, we performed an initial experiment to determine the appropriate conditions. No significant differences in VEGF expression (**Figure 6a**) were observed after evaluating different concentrations of IL-1β and TNF-α (5-20

ng/mL). Taking this into account these results, we decided to use the intermediate concentrations of both cytokines (10 ng/mL), as it has been reported to show proangiogenic properties by others [19], with the objective of confirming the anti-VEGF efficacy of the NPs. The VEGF-A expression results from the IOBA-NHC cells (**Figure 6b**) are in agreement with the results previously observed in EPCs. The Rapa-loaded NPs decreased VEGF levels to a similar extent as the reference Rapa solution and the blank NPs did not affect the VEGF concentration. On the other hand, the NPs also did not affect IOBA-NHC cell morphology as reflected by the absence of morphological differences between the negative control (DMEM) and treated cells (**Figure 7**).

In view of these results, we assume that the NPs were effectively internalized and metabolized by the EPCs and IOBA-NHC cells causing Rapa release into the cytosol and provoking the downregulation of VEGF expression.

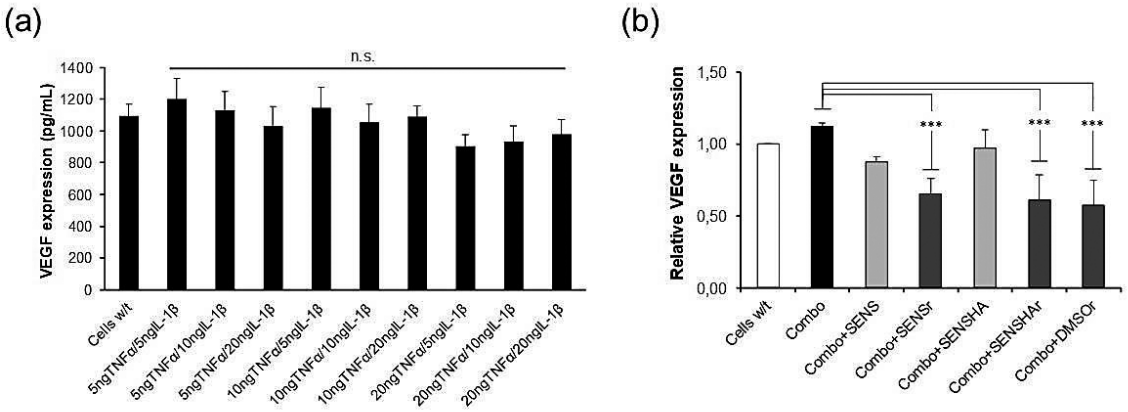


**Figure 6. Functional assay for VEGF expression and anti-VEGF efficacy in blank and Rapa-loaded NPs in IOBA-NHC cells stimulated with IL-1β and TNF-α.** (a) No significant differences were observed between the different IL-1β and TNF-α concentrations. (b) Rapa-loaded NPs diminished VEGF secretion (*** $p \leq 0.001$) to the same extent as the Rapa solution. W/t, without treatment; Combo, mixture of IL-1β and TNF-α at 10 ng/mL; and r, rapamycin.

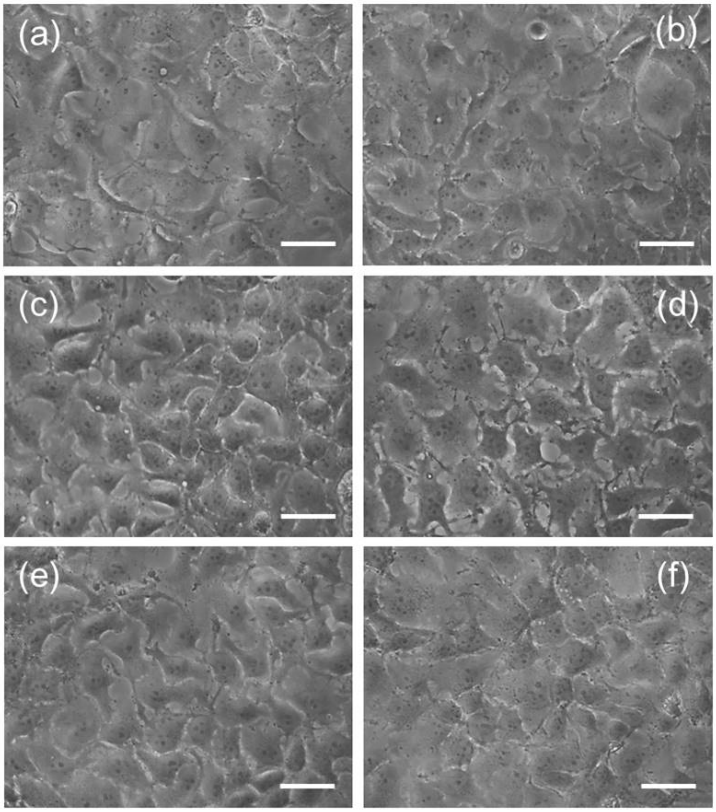


**Figure 7. Phase contrast microphotographs of the NHC cells after treatment.** (a) Cells incubated with supplement-free DMEM (negative control), (b) cells incubated with the proangiogenic combo (positive control), (c) cells incubated with the proangiogenic combo and blank SENS, (d) cells incubated with the proangiogenic combo and Rapa-loaded SENS, (e) cells incubated with the proangiogenic combo and blank SENS-HA and (f) cells incubated with the proangiogenic combo and Rapa-loaded SENS-HA. No morphological differences were observed between the treatments and the negative control. Scale bar = 20 µm.

## 5. Conclusions

In this work, we confirmed the suitability of our recently patented SENS as a vehicle for hydrophobic drugs such as Rapa. The Rapa entrapment by SENS caused an increase in the solubility of this antiangiogenic molecule equivalent to a 600-fold increase in its aqueous solubility as a free drug, and the resulting Rapa-loaded NPs maintained the same biological activity as the drug solution. Furthermore, the developed NPs were biocompatible with ocular surface cells in the concentration range where Rapa showed its antiangiogenic properties. Although further studies are necessary, we consider Rapa-loaded SENS and SENS-HA as promising tools that may help to treat CN.

## 6. Acknowledgments

This work was supported by grants from the Ministry of Economy and Competitiveness of Spain (MAT2013-47501-C02-R), Agencia Estatal y del Fondo Estrutural (FEDER), Xunta de Galicia (Competitive Reference Groups-FEDER Funds, Ref. 2017-PG101) and FPI Scholarship Program (BES-2014-069437).

**References**

[1] K.M. Meek, C. Knupp, Corneal structure and transparency, Prog. Retin. Eye Res. 49 (2015) 1–16. doi:10.1016/j.preteyeres.2015.07.001.

[2] C. Cursiefen, J. Colin, R. Dana, M. Diaz-Llopis, L.A. Faraj, S. Garcia-Delpech, G. Geerling, F.W. Price, L. Remeijer, B.T. Rouse, B. Seitz, P. Udaondo, D. Meller, H. Dua, Consensus statement on indications for anti-angiogenic therapy in the management of corneal diseases associated with neovascularisation: outcome of an expert roundtable, Br. J. Ophthalmol. 96 (2012) 3–9. doi:10.1136/bjo.2011.204701.

[3] P. Lee, C.C. Wang, A.P. Adamis, Ocular neovascularization: an epidemiologic review., Surv. Ophthalmol. 43 (1998) 245–69. http://www.ncbi.nlm.nih.gov/pubmed/9862312.

[4] S. Feizi, A.A. Azari, S. Safapour, Therapeutic approaches for corneal neovascularization, Eye Vis. 4 (2017) 28. doi:10.1186/s40662-017-0094-6.

[5] J.H. Chang, E.E. Gabison, T. Kato, D.T. Azar, Corneal neovascularization., Curr. Opin. Ophthalmol. 12 (2001) 242–9. http://www.ncbi.nlm.nih.gov/pubmed/11507336.

[6] J.-H. Chang, N.K. Garg, E. Lunde, K.-Y. Han, S. Jain, D.T. Azar, Corneal Neovascularization: An Anti-VEGF Therapy Review, Surv. Ophthalmol. 57 (2012) 415–429. doi:10.1016/j.survophthal.2012.01.007.

[7] J.J. Pérez-Santonja, E. Campos-Mollo, M. Lledó-Riquelme, J. Javaloy, J.L. Alió, Inhibition of Corneal Neovascularization by Topical Bevacizumab (Anti-VEGF) and Sunitinib (Anti-VEGF and Anti-PDGF) in an Animal Model, Am. J. Ophthalmol. 150 (2010) 519–528.e1. doi:10.1016/j.ajo.2010.04.024.

[8] X. Liu, S. Wang, X. Wang, J. Liang, Y. Zhang, Recent drug therapies for corneal neovascularization, Chem. Biol. Drug Des. 90 (2017) 653–664. doi:10.1111/cbdd.13018.

[9] Y.S. Kwon, J.C. Kim, Inhibition of corneal neovascularization by rapamycin, Exp. Mol. Med. 38 (2006) 173–179. doi:10.1038/emm.2006.21.

[10] Y.S. Kwon, H.S. Hong, J.C. Kim, J.S. Shin, Y. Son, Inhibitory Effect of

Rapamycin on Corneal Neovascularization In Vitro and In Vivo, Investig. Opthalmology Vis. Sci. 46 (2005) 454. doi:10.1167/iovs.04-0753.

[11] G. Zapata, L. Racca, J. Tau, A. Berra, Topical Use of Rapamycin in Herpetic Stromal Keratitis, Ocul. Immunol. Inflamm. 20 (2012) 354–359. doi:10.3109/09273948.2012.709575.

[12] W. Shi, H. Gao, L. Xie, S. Wang, Sustained Intraocular Rapamycin Delivery Effectively Prevents High-Risk Corneal Allograft Rejection and Neovascularization in Rabbits, Investig. Opthalmology Vis. Sci. 47 (2006) 3339. doi:10.1167/iovs.05-1425.

[13] J. Alvarez-Trabado, A. López-García, M. Martín-Pastor, Y. Diebold, A. Sanchez, Sorbitan ester nanoparticles (SENS) as a novel topical ocular drug delivery system: Design, optimization, and in vitro/ex vivo evaluation, Int. J. Pharm. 546 (2018) 20–30. doi:10.1016/j.ijpharm.2018.05.015.

[14] K. Araki-Sasaki, Y. Ohashi, T. Sasabe, K. Hayashi, H. Watanabe, Y. Tano, H. Handa, An SV40-immortalized human corneal epithelial cell line and its characterization., Invest. Ophthalmol. Vis. Sci. 36 (1995) 614–621.

[15] Y. Diebold, M. Calonge, A. Enríquez de Salamanca, A.E. de Salamanca, S. Callejo, R.M. Corrales, V. Sáez, K.F. Siemasko, M.E. Stern, Characterization of a spontaneously immortalized cell line (IOBA-NHC) from normal human conjunctiva., Invest. Ophthalmol. Vis. Sci. 44 (2003) 4263–74. http://www.ncbi.nlm.nih.gov/pubmed/14507870.

[16] Y. Diebold, M. Calonge, N. Fernández, M.C. Lázaro, S. Callejo, J.M. Herreras, J.C. Pastor, Characterization of epithelial primary cultures from human conjunctiva, Graefe's Arch. Clin. Exp. Ophthalmol. 235 (1997) 268–276. doi:10.1007/BF01739635.

[17] L. Garcia-Posadas, I. Arranz-Valsero, A. Lopez-Garcia, L. Soriano-Romani, Y. Diebold, A new human primary epithelial cell culture model to study conjunctival inflammation, Invest. Ophthalmol. Vis. Sci. 54 (2013) 7143–7152. doi:10.1167/iovs.13-12866.

[18] A. Stahl, L. Paschek, G. Martin, N.J. Gross, N. Feltgen, L.L. Hansen, H.T. Agostini, Rapamycin reduces VEGF expression in retinal pigment epithelium (RPE) and inhibits RPE-induced sprouting angiogenesis in vitro, FEBS Lett. 582 (2008) 3097–

3102. doi:10.1016/j.febslet.2008.08.005.

[19] C.N. Nagineni, A. William, A. Cherukuri, W. Samuel, J.J. Hooks, B. Detrick, Inflammatory cytokines regulate secretion of VEGF and chemokines by human conjunctival fibroblasts: Role in dysfunctional tear syndrome, Cytokine. 78 (2016) 16–19. doi:10.1016/j.cyto.2015.11.016.

[20] J. Salzmann, S. Lightman, The potential of newer immunomodulating drugs in the treatment of uveitis: a review., BioDrugs. 13 (2000) 397–408.

[21] E. Morelon, M. Mamzer-Bruneel, M. Peraldi, H. Kreis, Sirolimus: a new promising immunosuppressive drug. Towards a rationale for its use in renal transplantation, Nephrol. Dial. Transplant. 16 (2001) 18–20. doi:10.1093/ndt/16.1.18.

[22] W. Wu, Z. He, Z. Zhang, X. Yu, Z. Song, X. Li, Intravitreal injection of rapamycin-loaded polymeric micelles for inhibition of ocular inflammation in rat model, Int. J. Pharm. 513 (2016) 238–246. doi:10.1016/j.ijpharm.2016.09.013.

[23] P. Simamora, J.M. Alvarez, S.H. Yalkowsky, Solubilization of rapamycin, Int. J. Pharm. 213 (2001) 25–29. doi:10.1016/S0378-5173(00)00617-7.

[24] J.S. Mindel, H. Smith, M. Jacobs, A.B. Kharlamb, A.H. Friedman, Drug reservoirs in topical therapy, Invest. Ophthalmol. Vis. Sci. 25 (1984) 346. +.

[25] J.W. Sieg, J.R. Robinson, Mechanistic Studies on Transcorneal Permeation of Pilocarpine, J. Pharm. Sci. 65 (1976) 1816–1822. doi:10.1002/jps.2600651230.

[26] E. Prenner, M. Chiu, Differential scanning calorimetry: An invaluable tool for a detailed thermodynamic characterization of macromolecules and their interactions, J. Pharm. Bioallied Sci. 3 (2011) 39. doi:10.4103/0975-7406.76463.

[27] P. Pellinen, A. Huhtala, A. Tolonen, J. Lokkila, J. Maenpaa, H. Uusitalo, The cytotoxic effects of preserved and preservative-free prostaglandin analogs on human corneal and conjunctival epithelium in vitro and the distribution of benzalkonium chloride homologs in ocular surface tissues in vivo., Curr. Eye Res. 37 (2012) 145–154. doi:10.3109/02713683.2011.626909.

[28] Y. Liu, H. Xu, M. An, mTORC1 regulates apoptosis and cell proliferation in pterygium via targeting autophagy and FGFR3, Sci. Rep. 7 (2017) 7339.

doi:10.1038/s41598-017-07844-y.

[29] H. Wu, H. Zhang, C. Wang, Y. Wu, J. Xie, X. Jin, J. Yang, J. Ye, Genoprotective effect of hyaluronic acid against benzalkonium chloride-induced DNA damage in human corneal epithelial cells., Mol. Vis. 17 (2011) 3364–70. http://www.ncbi.nlm.nih.gov/pubmed/22219631.

[30] C. Debbasch, S. Bruneau De La Salle, F. Brignole, P. Rat, J.-M. Warnet, C. Baudouin, Cytoprotective effects of hyaluronic acid and Carbomer 934P in ocular surface epithelial cells, Invest. Ophthalmol. Vis. Sci. 43 (2002) 3409–3415.

[31] Q. Ebrahem, A. Minamoto, G. Hoppe, B. Anand-Apte, J.E. Sears, Triamcinolone Acetonide Inhibits IL-6– and VEGF-Induced Angiogenesis Downstream of the IL-6 and VEGF Receptors, Investig. Opthalmology Vis. Sci. 47 (2006) 4935. doi:10.1167/iovs.05-1651.

[32] N. Asano-Kato, K. Fukagawa, N. Okada, T. Kawakita, Y. Takano, M. Dogru, K. Tsubota, H. Fujishima, TGF-beta1, IL-1beta, and Th2 cytokines stimulate vascular endothelial growth factor production from conjunctival fibroblasts, Exp. Eye Res. 80 (2005) 555–560. doi:10.1016/j.exer.2004.11.006.

# *General discussion*

USC
UNIVERSIDADE
DE SANTIAGO
DE COMPOSTELA

## General discussion

In recent years, nanoparticles (NPs) have emerged as promising drug delivery systems (DDS) to enhance the ocular bioavailability and therapeutic efficacy of topically applied drugs. In addition to its controlled drug delivery potential, drug-loaded NPs ameliorate key drug biopharmaceutical properties such as the drug residence time at the ocular surface and its intraocular penetration. In this work, we developed and evaluated two types of NPs specifically designed for topical ocular drug delivery. Special attention was given to the influence of the NP surface properties on the final performance of the developed formulations.

This Doctoral Thesis report has been structured into three chapters. The first chapter covers the design and optimization of the NPs for topical ocular drug delivery, as well as their *in vitro* and *ex vivo* evaluation. The second chapter analyzes the *in vivo* therapeutic potential of the NPs for the treatment of dry eye disease. The last chapter focuses on the suitability of the NPs for the treatment of corneal neovascularization. For a better understanding of the developed work, the discussion section was structured in three blocks corresponding to 1) the development of NPs for topical ocular drug delivery; 2) the evaluation of their biocompatibility and targeting abilities; and 3) the evaluation of the therapeutic efficacy of the developed NPs.

### 1. Development of NPs for topical ocular drug delivery

### 1.1. Rational NP design

The first step in the formulation of NPs was the selection of the most adequate NP components. This selection was completed considering not only the technological properties of the components but also their biocompatibility and regulatory status.

The main NP component was sorbitan monooleate (Span® 80) (**Figure 1a**). We named these NPs after that component, as sorbitan ester nanoparticles (SENS). This non-ionic surfactant that has an FDA label as “generally recognized as safe” (GRAS) is widely used by food and pharmaceutical industries [1,2] It is also one of the cheapest pharmaceutical excipients available [3] that is reported to form solid nanostructures [4]. We used Span® 80 (HLB = 4.3) as the component for the NP matrix given its high affinity for hydrophobic compounds [5]. Considering that nearly 40% of available drugs and 70% of drugs under development are water insoluble molecules [6], we decided to focus our work on the delivery of hydrophobic drugs.

The second most abundant NP component is the vitamin E derivative d-α-tocopheryl polyethylene glycol 1000 succinate (TPGS) (**Figure 1b**), which is present in various commercialized ophthalmic formulations [7,8]. We selected this ingredient because of its polyvalence in drug delivery. Indeed, TPGS is a polyoxyethylated surfactant that increases the stability of different NP formulations by providing steric hindrance [9,10]. TPGS may also enhance drug bioavailability by increasing the permeability of biological membranes and by inhibiting the multidrug resistance associated with p-glycoprotein [11].

A less abundant but still important component was the cationic surfactant cetyltrimethylammonium bromide (CTAB) (**Figure 1c**). CTAB is a component in the topical antiseptic cetrimide, which is commonly used in ophthalmic formulations [12,13]. We included this cationic surfactant with the aim of providing the NPs a positive surface charge. It is generally accepted that cationic NPs may electrostatically interact with the negatively charged precorneal area, thus increasing the contact time with the ocular surface and ocular penetration [14–16]. Additionally, the rationale behind its incorporation was to provide positive surface charge for the NPs as a strategy to enable subsequent NP surface coating interactions with negatively charged polymers. In this respect, hyaluronic acid (HA) (**Figure 1d**), a natural and biocompatible polysaccharide widely used in the ophthalmologic field, was selected as a potential NP coating polymer, as our aim was to evaluate the influence of the HA coating on the pharmaceutical properties of NPs. HA-coated NPs may increase ocular drug bioavailability due to target receptor-mediated endocytosis by corneal cells [17,18]. In the present work, a 1,600 KDa HA was selected because high molecular weight HA has a higher receptor binding affinity than low molecular weight HA varieties [19,20].

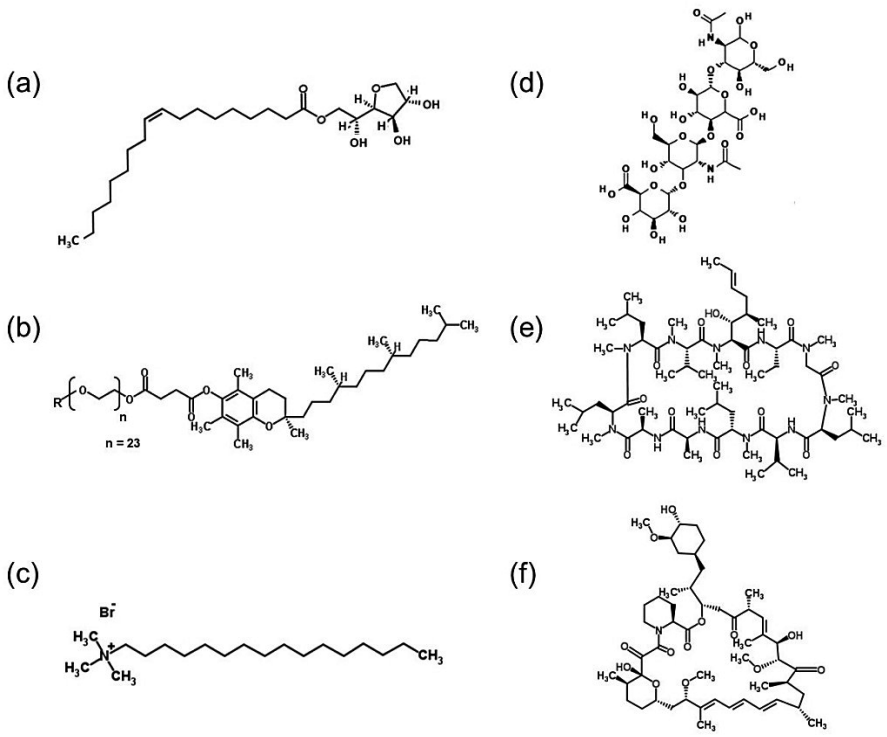


**Figure 1. Molecular structures of NP components.** (a) Span® 80, (b) TPGS, (c) CTAB, (d) HA, (e) CsA and (f) Rapa. The structures were obtained from the ChemSpider database [21][22][23][24][25] and PubChem database [26]. Permitted by ChemSpider and PubChem**.**

To validate the suitability of our NPs as a DDS, we used the following two drug models: cyclosporine A (CsA) (**Figure 1e**) and rapamycin (Rapa) (**Figure 1f**). CsA is an immunosuppressant drug that is commonly used at the ocular level for the treatment of inflammatory diseases affecting the ocular surface, such as dry eye disease [27]. Rapa is a non-nephrotoxic immunosuppressant drug [28] with antiangiogenic properties that has been used for the management of ocular diseases such as age-related neovascular macular degeneration [29] and corneal neovascularization [30]. From the technological point of view, CsA and Rapa have common physicochemical characteristics that make them perfect candidates for formulation with our NPs due to their neutral net charge and poor water solubility.

### 1.2. Elaboration and optimization of SENS

There are critical aspects that must be considered when developing a novel DDS, such as the cost-effectiveness relationship, technical feasibility, scale-up potential and batch-to-batch reproducibility [3,31]. These aspects might be enclosed in one key requirement: simplicity. Simple DDS designs and standardized elaboration methods

save production costs, facilitate scale-up and increase reproducibility, which ultimately allow for industrial translation [31].

In this work, we developed a novel type of NP-based DDS using an elaboration method that has been previously described in our patents [32]. This elaboration method, depicted in **Figure 2**, involves the following two consecutive steps: the spontaneous formation of NPs and evaporation of the residual organic solvent followed by the subsequent concentration of the formulation. The entire process takes place under mild conditions using conventional laboratory equipment, reflecting its simplicity and industrial suitability.

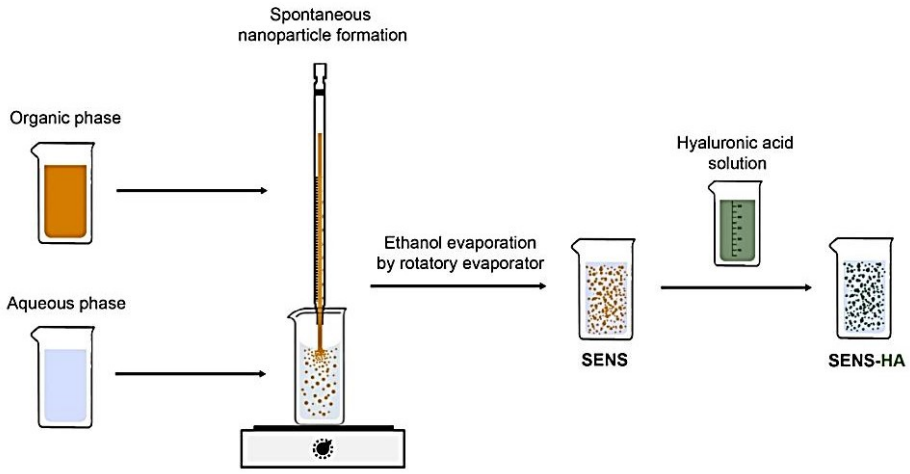


**Figure 2. Elaboration method used for NP preparation.** NPs are spontaneously formed after mixing the organic phase with the aqueous phase. Ethanol is then removed using a rotatory evaporator. For the NP coating, aqueous solutions of polymers (e.g., HA) are simply mixed with the NP dispersion. Schematic created by Jesús Álvarez Trabado.

Once the NP composition and elaboration method were selected, the next step was to obtain an optimized formulation with the most adequate physicochemical properties. To this end, we performed an extensive review, enclosed as Annex I, where we analyzed the main factors that affect topical ocular drug delivery [33]. We identified the particle size, zeta potential, drug entrapment efficiency and drug-loading as key factors. The smallest NP particle size (preferably below 200 nm) combined with a high positive zeta potential, entrapment efficiency and drug-loading were considered as the optimal physicochemical properties. We also evaluated the formulation variables that most affected the physicochemical properties. We identified the concentrations of Span® 80, TPGS and CsA as key variables.

Considering the large number of experimental runs needed to obtain a formulation that meets the optimal physicochemical properties and to avoid trial and error-based experiments, we performed a statistical approach using a Box-Behnken experimental design. The use of an experimental design methodology allows the for simultaneous testing of multiple factors, maximizing the quantity and quality of information obtained while minimizing the number of experimental runs [34].

Based on the results from the application of the aforementioned statistical approach, the resulting optimized sorbitan ester nanoparticles (SENS-OPT) (**Table 1**) had particle sizes under 200 nm, a positive zeta potential and a high entrapment efficiency. Special interest increased the high CsA payload (to nearly 20%), especially considering that one of the main limitations of NPs is low drug-loading [35]. This solubilizing effect of the optimized NPs resulted in a 200-fold increase in the aqueous solubility of CsA. For the preparation of the HA-coated NPs (i.e., SENS-OPT-HA), the SENS-OPT were simply incubated with a HA solution (**Figure 2**). Due to HA adsorption, the particle size significantly increased, and the zeta potential experienced an inversion from a positive to negative value (**Table 1**). The overall physicochemical results confirmed the suitability of both types of NPs for topical ophthalmic administration.

**Table 1. Summary of main NP physicochemical characteristics.**

| Formulation | Particle size (nm) | Polydispersity (PdI) | Zeta potential (mV) |
|---|---|---|---|
| Blank SENS | 176.1 ± 6.5 | 0.106 ± 0.005 | + 28.5 ± 0.9 |
| SENS-OPT | 170.5 ± 5.0 | 0.062 ± 0.006 | + 33.9 ± 0.5 |
| Rapa-loaded SENS | 173.8 ± 10.8 | 0.116 ± 0.058 | + 22.1 ± 5.2 |
| Blank SENS-HA | 185.6 ± 6.9 | 0.191 ± 0.009 | − 27.6 ± 0.2 |
| SENS-OPT-HA | 177.6 ± 5.1 | 0.096 ± 0.024 | − 20.6 ± 0.7 |
| Rapa-loaded SENS-HA | 178.0 ± 6.7 | 0.146 ± 0.020 | − 19.3 ± 5.1 |

For the preparation of Rapa-loaded NPs, we used the former optimized parameters with the exception of the Rapa concentration. In this case, we used a lower initial drug concentration given the high antiangiogenic potency of Rapa, which allowed a reduction in the drug dose [36]. The resulting NPs (**Table 1**) had a particle size similar to that of the CsA-loaded formulations, but the absolute value of their zeta potentials was slightly lower probably due to the decreased drug-loading. Nonetheless, the solubilizing effect

of the Rapa-loaded NPs provoked a 600-fold increase in the water solubility of this drug.

### 1.3. Morphological and structural characterization of the NPs

Transmission electron microscopy (TEM) is a simple imaging technique to evaluate the morphology of NPs. In our case, both CsA-loaded and Rapa-loaded NPs showed homogeneous NP populations with a spherical shape (**Figure 3**). The HA-coated NPs showed a less opaque corona, which can be attributed to the HA adsorption. No differences could be observed between the blank and drug-loaded formulations.

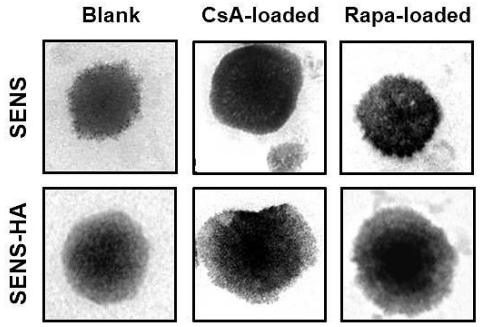


**Figure 3. TEM microphotographs of the developed NPs.** NPs displayed spherical shapes with the absence of differences between the blank and drug-loaded formulations. HA-coated NPs had a less opaque corona because of HA adsorption.

We performed an extensive structural analysis of the formulations using three complementary techniques. Nuclear magnetic resonance (NMR) was used to study the structure of the NPs in the liquid state (aqueous NP dispersion), and differential scanning calorimetry (DSC) and X-ray powder diffraction (XRD) were used to study the structure of the NPs in the solid state (lyophilized NPs). The results from the NMR study showed that all NP components formed solid nanostructures and the drug (CsA) was dissolved inside the NP matrix (Chapter I) [37]. The DSC study showed that there were molecular interactions between the NP components and the drugs (Chapters II and III). The XRD study revealed the absence of drug crystals in the drug-loaded NPs (Chapters II and III). Altogether, the analysis of the aforementioned studies indicates that the developed NPs are solid nanostructures containing the drug dissolved within the NP matrix at the molecular level, as depicted in **Figure 4**. This homogeneous drug distribution may not only increase the formulation stability but may also facilitate adequate drug dosage.

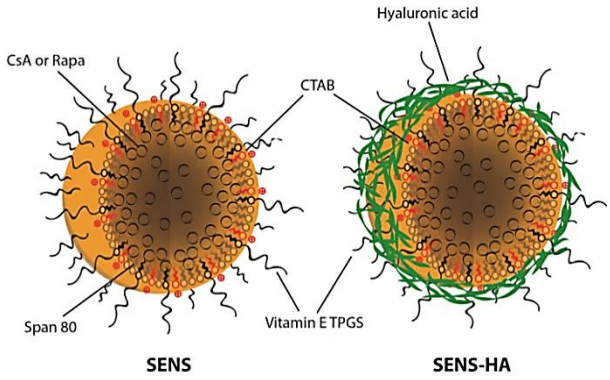


**Figure 4. Schematic representation of the developed NPs.** Schematic created by Jesús Álvarez Trabado.

### 1.4. NP stability

Stability is a mandatory requirement for the approval of any pharmaceutical product. Insufficient physical and chemical stability is often related to changes in the purity, potency and safety of formulations [38]. In this work, we focused on the physical stability of the formulations considering that this parameter is one of the major issues of colloidal systems, especially for highly loaded systems [39]. We evaluated the short-term stability of the aqueous and lyophilized CsA-loaded NP formulations by storing the formulations for three months under different temperature conditions. As shown **Figure 5a**, both types of aqueous CsA-loaded NP formulations showed adequate stability. The lyophilized NPs (**Figure 5b**) showed adequate stability when stored at 4ºC and room temperature but agglomerated when stored at 37ºC. These differences may be explained by different stabilization mechanisms. In the case of aqueous formulations, the presence of water favored the electrosteric stabilization of NPs, while for lyophilized formulations, only steric stabilization was available.

We also evaluated the biological stability of the NPs. The physicochemical properties of the NPs may change drastically after instillation due to interactions with tear film components, mainly proteins [40]. This phenomenon may not only affect the stability of the particle dispersion but also affect cellular uptake and biodistribution [41]. As shown **Figure 5c,** the developed CsA-loaded NPs demonstrated adequate biological stability after incubation with protein-enriched simulated lachrymal fluid. The slight increase in the SENS-OPT-HA particle size was attributed to protein opsonization processes.

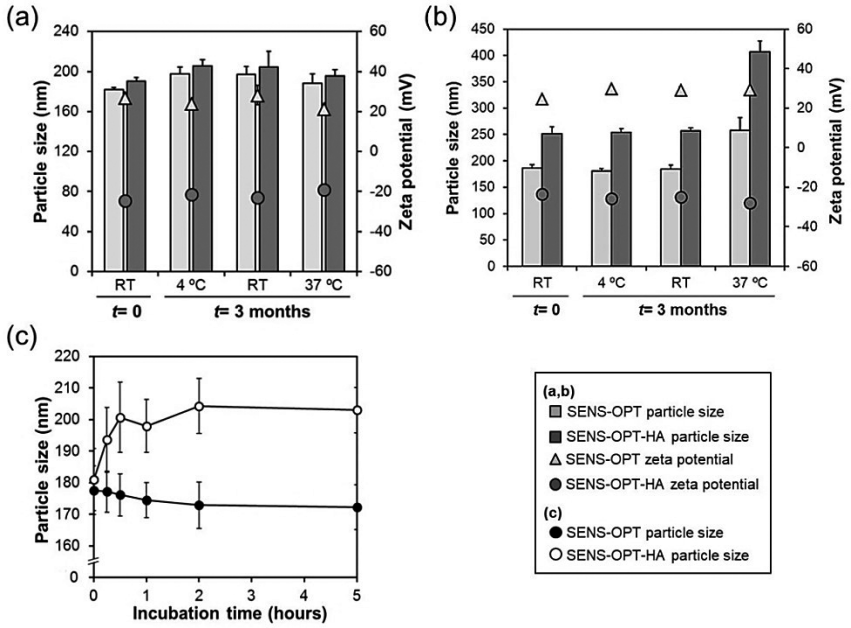


**Figure 5. Stability of CsA-loaded NPs.** (a) The physical stability of the aqueous NP dispersions. Both types of NPs exhibited minor variations in their size and zeta potential after 3 months ($p \leq 0.05$). (b) The physical stability of the lyophilized NPs. Storage at 37ºC significantly modified the particle size and zeta potential of both types of NPs. (c) The biological stability of the NPs. Only SENS-OPT-HA NPs experienced a minor but significant increase in their particle size after 2 hours of incubation ($p \leq 0.05$).

### 1.5. NP sterilization

Sterility is another mandatory requirement for any ophthalmic formulation. Different methods have been proposed for NP sterilization such as filtration, gamma irradiation and autoclaving [42,43]. From an industrial perspective, autoclaving is the most desirable technique because it allows for the processing of large volumes, which facilitates production scale-up. However, this technique cannot be implemented for all types of NPs due to the elevated temperatures used during the process. Changes in the physicochemical properties and biological activity of NPs are frequently reported [44,45]. Filtration is an alternative sterilization technique for thermally sensitive formulations. NPs with a particle size under 200 nm can be easily sterilized by passing the formulations through 0.22-µm pore size filters [46]. However, if particle size is close to or above the pore size, a clogging effect may occur, resulting in a decreased yield [44]. In this work, we regularly used a filtration method because the NP particle size was under 200 nm and the physicochemical properties of the NPs were not affected by this process (data not shown). Additionally, we also evaluated the autoclaving suitability of CsA-loaded NPs given the industrial interest in this sterilization technique (Chapter II). Our results showed that, in contrast to the uncoated NPs, the HA-coated

NPs did not experience any specific physicochemical alterations after autoclaving. We attributed these differences to the thermo-protective effect of the HA-coating, which provided an additional steric effect to increase the formulation stability of the NPs.

## 2. Evaluation of the biocompatibility and targeting ability of NPs

### 2.1. Influence of NPs on cell viability and proliferation

The next step after development and physicochemical characterization of the NPs was to evaluate their biocompatibility. Although all NP components were approved substances that are widely used in the pharmaceutical field, it is reported that NP cytotoxicity may differ from their raw materials [47]; thus, the NPs' effect on cell viability and proliferation should to be carefully evaluated. For this purpose, we used two different ocular surface epithelia-derived cell lines, including the human corneal epithelial (HCE) cell line and the IOBA–normal human conjunctiva (IOBA-NHC) epithelial cell line.

We performed two sets of experiments to evaluate the potential cytotoxicity of the NPs using the XTT assay. In one set of experiments, the HCE cells were exposed to blank and CsA-loaded NPs for 30 minutes. The cells showed high cell viability and there were no differences between the blank NPs and the corresponding CsA-loaded formulations (**Figure 6**). Only the highest concentration of SENS-OPT and SENS-OPT-HA reduced the cell viability by −30% and by −20%, respectively. The NP dose of 0.2% (w/v), which was equivalent to 0.05% (w/v) CsA for the drug-loaded NPs, did not show cytotoxicity. This dose was therefore used in further experiments.

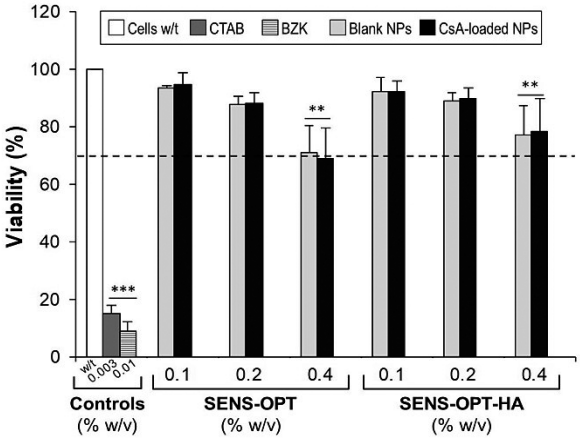


**Figure 6. HCE cell line viability results for SENS-OPT and SENS-OPT-HA.** Only the highest NP concentration significantly reduced (** $p \leq 0.01$) cell viability compared with the control cells without treatment (w/t). The positive controls cetyltrimethylammonium bromide (CTAB) and benzalkonium chloride (BZK) drastically reduced cell viability (*** $p \leq 0.001$).

In another set of experiments, the HCE and IOBA-NHC cells were exposed to blank and Rapa-loaded NPs for 24 hours. **Figure 7** shows the different cytotoxicity profiles depending both on the NP type and on the cell line used. We observed a Rapa concentration-dependent decrease in viability in both cell lines, which was more accentuated in the conjunctival epithelium cell line. The NP dose of 75 µg/mL, which was equivalent to 500 ng/mL Rapa for the drug-loaded NPs, did not reduce cell viability, and consequently, this dose was used in the additional efficacy experiments.

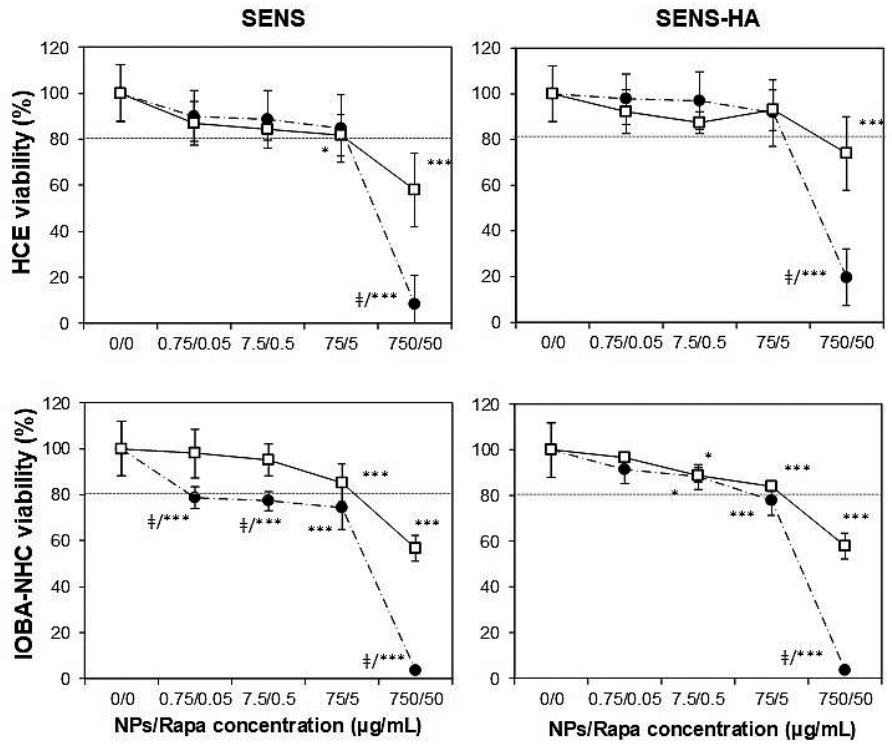


**Figure 7. Corneal and conjunctival cell line viability profiles upon treatment with the developed NPs.** The cell viability values show dose-dependent behaviors in both cell lines. In general, Rapa-loaded NPs (-●-) were more cytotoxic than the equivalent blank NPs (-□-) at high doses. HA-coated NPs showed lower cytotoxicity than the equivalent uncoated NPs. Significant differences with regard to the negative control are represented by * $p \leq 0.05$ and *** $p \leq 0.001$ and with regard to the equivalent concentration of blank NPs by ǂ $p \leq 0.001$. Note: The vertical axis represents the NP concentration and the equivalent Rapa concentration for the drug-loaded NPs.

Overall, from these two sets of experiments, it can be concluded that CsA- and Rapa-loaded NPs exhibited a dose-dependent relationship, with the highest NP dose producing the lowest cell viability percentages. Furthermore, the Rapa-loaded NPs reduced cell viability more than the CsA-loaded NPs. This may be attributed to 2

factors. One factor was the exposure time, which was extended from 30 minutes to 24 hours in the second set of experiments. Other factor was the inherent cytotoxicity of Rapa [48], which was shown by comparing the drug-loaded formulations with the equivalent blank formulations. It is interesting to note that, although it was not significant, the HA-coated NPs showed higher viability values than the uncoated NPs. We attributed these differences to the described cytoprotective effect of HA [49,50]. In any case, it should be emphasized that the concentrations of CsA- and Rapa-loaded NPs that we selected for the additional experiments maintained cell viability values above 70%, which is considered the limit to assert the absence of cytotoxicity [51].

In addition to the cell viability assays, we performed additional cell proliferation assays to determine if cell replication was compromised after NP exposure. To do this, HCE cells were exposed to blank and CsA-loaded NPs for 30 minutes. As shown in **Figure 8**, only the positive control irreversibly inhibited cell proliferation. The NPs did not affect cell recovery and proliferation. These results along with cell viability results confirmed the safety and biocompatibility of the CsA-loaded NPs for ophthalmic applications.

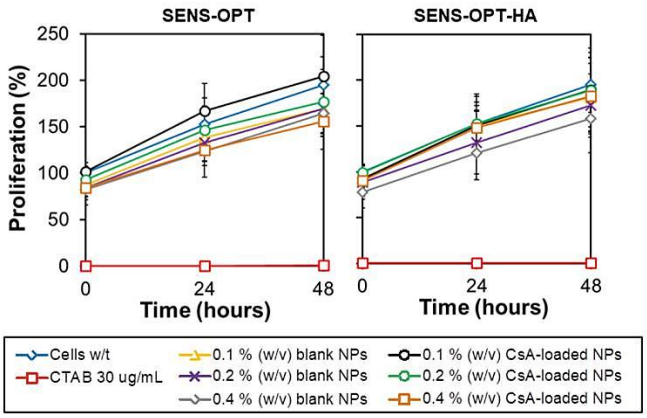


**Figure 8. HCE proliferation results for SENS-OPT and SENS-OPT-HA.** Only the positive control CTAB significantly inhibited cell proliferation (*** $p \leq 0.001$). There were no significant differences between the proliferation profiles for the cells without treatment and the cells treated with NPs.

## 2.2. Cellular uptake of NPs by corneal cells

The ability of developed nanosystems to target corneal cells was investigated in the HCE cell line. For this purpose, the drug was replaced by the fluorescent dye Nile Red during the elaboration of NPs. The relative cellular uptake, internalization mechanisms

and intracellular distribution of the Nile Red-loaded NPs were monitored using fluorescence techniques.

Although cellular uptake of NPs was effectively driven by energy-dependent mechanisms, as suggested by uptake inhibition at 4ºC, particular internalization mechanisms were observed for each type of NP. For the cationic NPs, the main cell uptake mechanism was caveolin-mediated endocytosis, as shown by inhibition with filipin. For the HA-coated NPs, the predominant mechanism was receptor-mediated endocytosis, as shown by inhibition with excess HA. This active targeting through HA receptors may explain the higher fluorescence signal observed in the corneal cells (**Figure 9**). It is reported that HA receptors, which are broadly distributed in corneal epithelial cells [52], promote and enhance NP internalization [17,53]. In contrast, the observed differences in the intracellular distribution of NPs may be related to their different net charges. The cationic NPs were mostly accumulated around the cell nucleus due to their electrostatic interactions with this negatively charged organelle, whereas the anionic HA-coated NPs were broadly distributed throughout the cytosol due to the opposite effect.

Overall, we demonstrated that although both types of NPs were effectively internalized by corneal epithelial cells, the HA-coated NPs showed higher cellular uptake and targeting efficacy than the uncoated NPs.

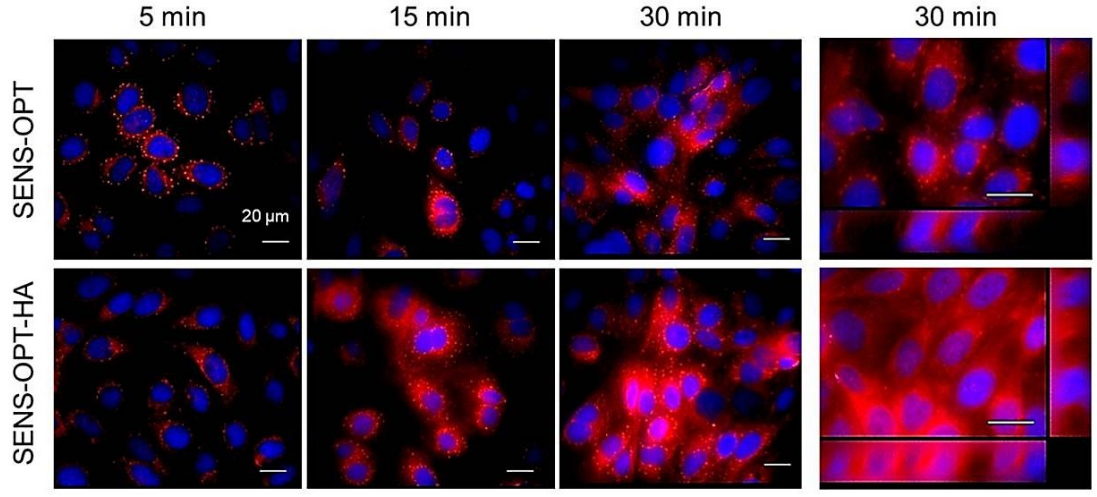


**Figure 9. Fluorescence microscopy images of HCE cells after exposure to Nile red-loaded NPs for 5, 15, and 30 minutes.** Cationic SENS-OPT NPs were mostly accumulated around the cell nuclei. In contrast, anionic SENS-OPT-HA NPs were broadly distributed in the cytosol. Both types of NPs were located inside cells as shown in the Z-scan images (upper and lower right panels) obtained after NP exposure for 30 minutes.

### 2.3. NP interactions with an *ex vivo* porcine cornea

The *ex vivo* porcine eye model is commonly used in vision sciences research, given the morphological similarity of the pig eye to the human eye [54]. We used *ex vivo* porcine corneal tissues to evaluate the corneal biodistribution of Nile Red- and CsA-loaded NPs.

Fluorescence microscopy images (**Figure 10**) showed that Nile Red-loaded NPs followed a corneal distribution pattern that agreed with that observed in the HCE cells. Cationic NPs (SENS-OPT) were mostly accumulated in the apical part of the epithelium and around the cell nuclei, probably due to the negative charge of both structures. In contrast, anionic HA-coated NPs (SENS-OPT-HA) were uniformly distributed throughout the epithelium and a small fraction of NPs reached the corneal stroma. In contrast, the results for the corneal CsA penetration (**Figure 11**) showed that SENS-OPT and SENS-OPT-HA promoted a 1.3- and 2.1-fold increase in CsA penetration, respectively, compared with the commercial formulation. Both studies along with the cellular uptake experiments suggest that the HA-coating increases the NP uptake by the corneal cells, ultimately enhancing the corneal drug penetration.

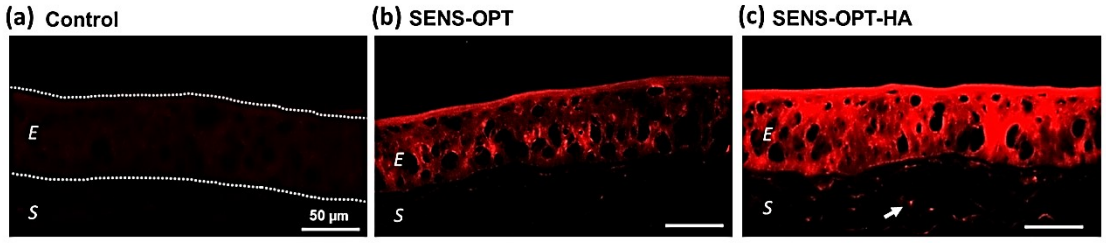


**Figure 10. Fluorescence microscopy images of the porcine cornea after topical application of Nile red dissolved in olive oil, Nile red-loaded SENS-OPT, and Nile red-loaded SENS-OPT-HA NPs.** (a) Nile red dissolved in olive oil had minimal penetration into the corneal epithelium. The corneal epithelium, which was nearly invisible due to the limited Nile red uptake, was highlighted with a dotted line at the anterior and posterior surfaces. (b) SENS-OPT NPs accumulated mostly in the apical part of the epithelium (E) and surrounding the cell nuclei. (c) SENS-OPT-HA NPs were broadly distributed throughout the epithelial layers and reached the corneal stroma (S) (white arrow).

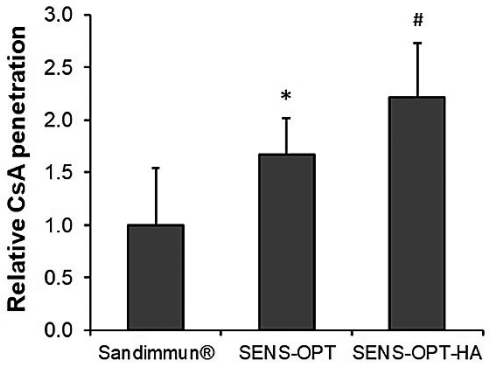


**Figure 11. Relative CsA penetration through excised pig cornea.** SENS-OPT and SENS-OPT-HA promoted a 1.3- and 2.1-fold increase, respectively, in drug penetration compared to the reference formulation Sandimmun®. SENS-OPT-HA promoted higher CsA penetration than the uncoated NPs. Significant differences are represented by $*p \leq 0.05$ compared to Sandimmun and SENS-OPT-HA and $\#p \leq 0.05$ compared to Sandimmun and SENS-OPT.

## 3. Evaluation of the therapeutic efficacy of the developed NPs.

### 3.1. *Ex vivo*/*in vitro* assessment of the biological activity of the NPs.

The immunosuppressive activity of the CsA-loaded NPs was evaluated using an *ex vivo* functional assay for lymphocyte activation. It has been reported that CsA specifically precludes lymphocyte activation and the subsequent production of pro-inflammatory cytokines such as IL-2 [55,56]. Bearing this in mind, we monitored IL-2 production from concanavalin A-activated human lymphocytes that were previously treated with the NP formulations. As depicted in **Figure 12**, both types of CsA-loaded NPs reduced IL-2 production similar to the commercial formulation Sandimmun®, indicating that CsA maintained its biological activity after entrapment inside NPs and its immunosuppressive effect was as high as that provided by the CsA commercial formulation.

The antiangiogenic effect of the Rapa-loaded NPs was evaluated using two *in vitro* functional assays focused on VEGF production. It has been reported that some pro-inflammatory cytokines such as IL-6, TNF-α and IL-1β are involved in VEGF production at the ocular surface [57–59]. Based on these data, we monitored the VEGF production of epithelial primary cultures (EPCs) from human conjunctiva stimulated with IL-6 and the human conjunctival epithelium-derived IOBA-NHC cell line after stimulation with TNF-α and IL-1β. As shown in **Figure 13**, both types of Rapa-loaded NPs lowered VEGF levels to the same extent as the commercial formulation in both cell types. Similar to our results with CsA-loaded NPs, these results suggest that Rapa

maintained its biological activity after entrapment inside NPs and its antiangiogenic efficacy was the same as that demonstrated by the drug solution.

Overall, we can conclude that the NP production process did not affect the biological activity of CsA and Rapa, and both drugs could be released in their bioactive forms from the NP matrix to exert their therapeutic effect.

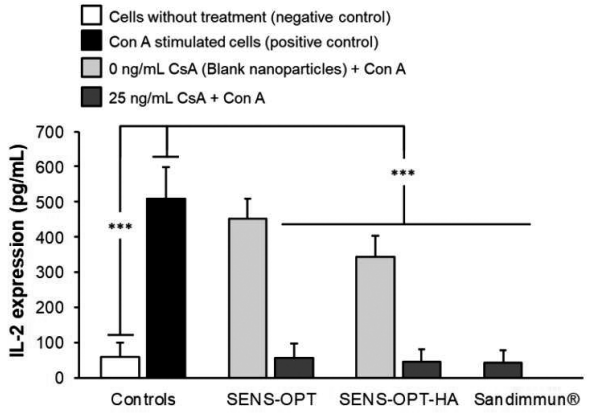


**Figure 12. Inhibitory effect of blank and CsA-loaded NPs on IL-2 production from freshly isolated human lymphocytes stimulated with concanavalin A.** IL-2 production was stimulated by the addition of concanavalin A. In cells previously treated with CsA-loaded SENS-OPT or SENS-OPT-HA NPs, the basal levels were maintained after concanavalin A exposure (***$p \leq 0.001$). This effect was the same as that observed for the commercial formulation Sandimmun®. The reduction in IL-2 induced by the blank SENS-OPT-HA was attributed to an experimental artifact.

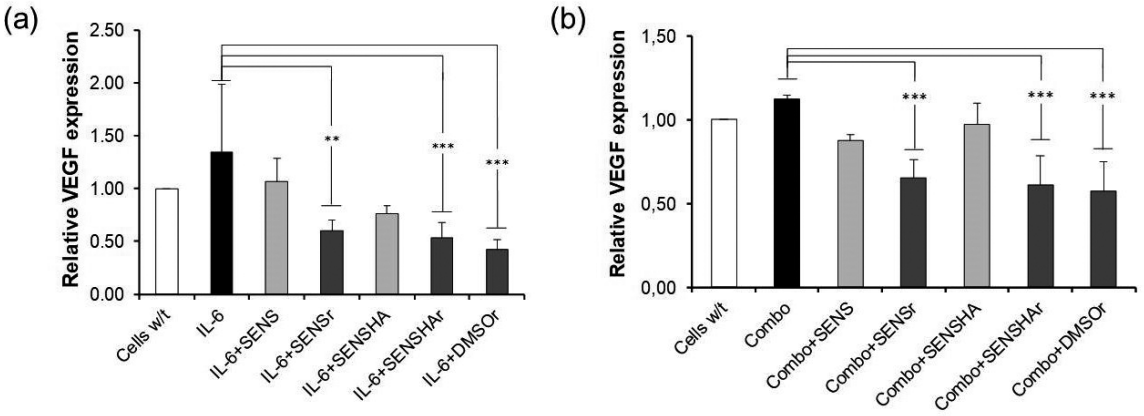


**Figure 13. Anti-VEGF efficacy of blank and Rapa-loaded NPs on EPCs and IOBA-NHC cells stimulated with proangiogenic cytokines.** (a) In EPCs, Rapa-loaded SENS and SENS-HA diminished VEGF secretion to the same extent as the Rapa solution (** $p \leq 0.01$ and *** $p \leq 0.01$). (b) In IOBA-NHC cells, Rapa-loaded NPs diminished VEGF secretion to the same extent as the Rapa solution (*** $p \leq 0.001$). W/t, without treatment; Combo, mixture of IL-1β and TNF-α at 10 ng/mL; and r, rapamycin.

### 3.2. Therapeutic efficacy of topically applied CsA-loaded NPs in the treatment of dry eye disease in a TSP-1-deficient mouse model.

The efficacy of the developed CsA formulations was tested in TSP-1-deficient mice. These animals spontaneously develop a chronic ocular surface inflammation with age that is similar to Sjögren's syndrome-associated dry eye [60,61]. NPs were topically administered and the main signs of ocular surface disease were monitored following the experimental setup depicted in **Figure 14**. Corneal integrity was assessed by corneal fluorescein staining and secretory function by measuring MUC5AC content in tears. At the end of the study, the mice were euthanized, and eye tissues and cervical lymph nodes were collected for further histopathological and molecular analysis.

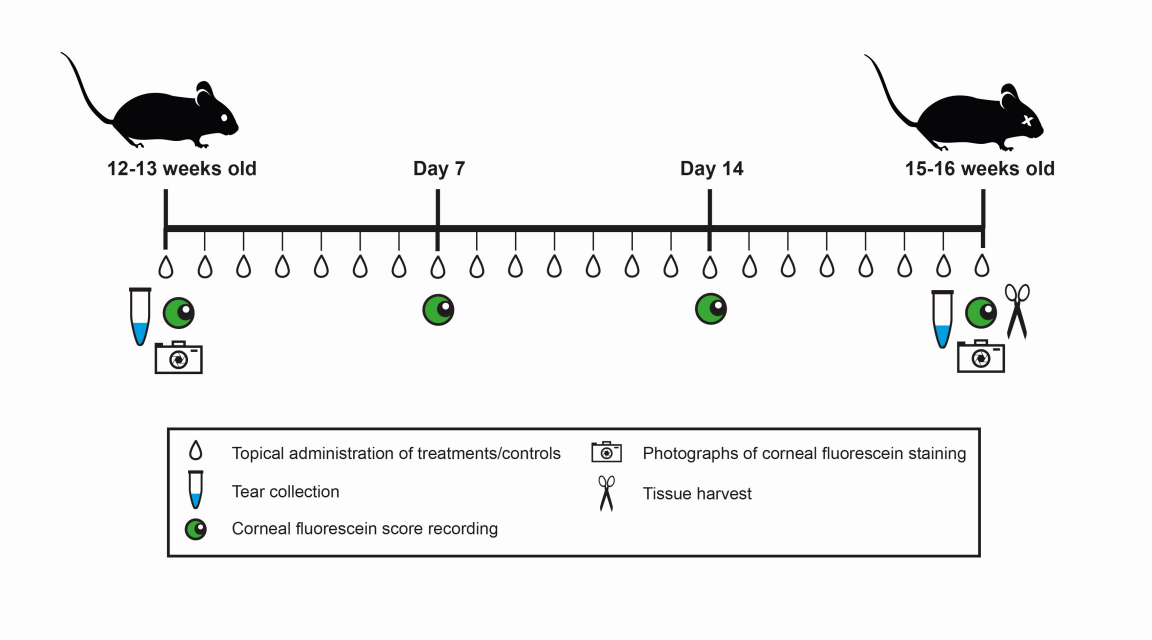


**Figure 14. Experimental setup for the treatment and control administration to TSP-1-deficient mice.** Disease evolution in mice was monitored during the three weeks they received treatment or control formulations by evaluating the corneal fluorescein score and MUC5AC content in tears. At the end of treatment and after tissue harvest, histological and molecular analyses were performed. Schematic created by Jesús Álvarez Trabado.

#### 3.2.1 Monitoring of corneal integrity and the secretory function in treated and control TSP-1-deficient mice.

The integrity of the corneal barrier was monitored by evaluating the corneal fluorescein staining score (CFS) [62]. In the TSP-1-deficient mice, the CFS reached the maximum value (8~10) when the mice showed a well-established ocular surface disease and remained stable for additional weeks [63]. Accordingly, we studied the effect of our NPs on the evolution of this disease indicator. As shown in **Figure 15a**, while SENS did

not affect CFS, CsA-loaded SENS-HA were able to reduce this parameter to values close to that of the healthy (wild-type) mice (2~3) [63]. These differences could also be observed in the corneal fluorescein staining images (**Figure 15b**). These results may be attributed to a combined or even possible synergistic therapeutic effect of HA, which promoted corneal epithelial healing [64,65], and the anti-inflammatory activity of CsA, which reduced ocular surface inflammation [27,66]. Additionally, the higher cellular uptake of SENS-HA (Chapter I) [37] may play a relevant role in their enhanced therapeutic efficacy.

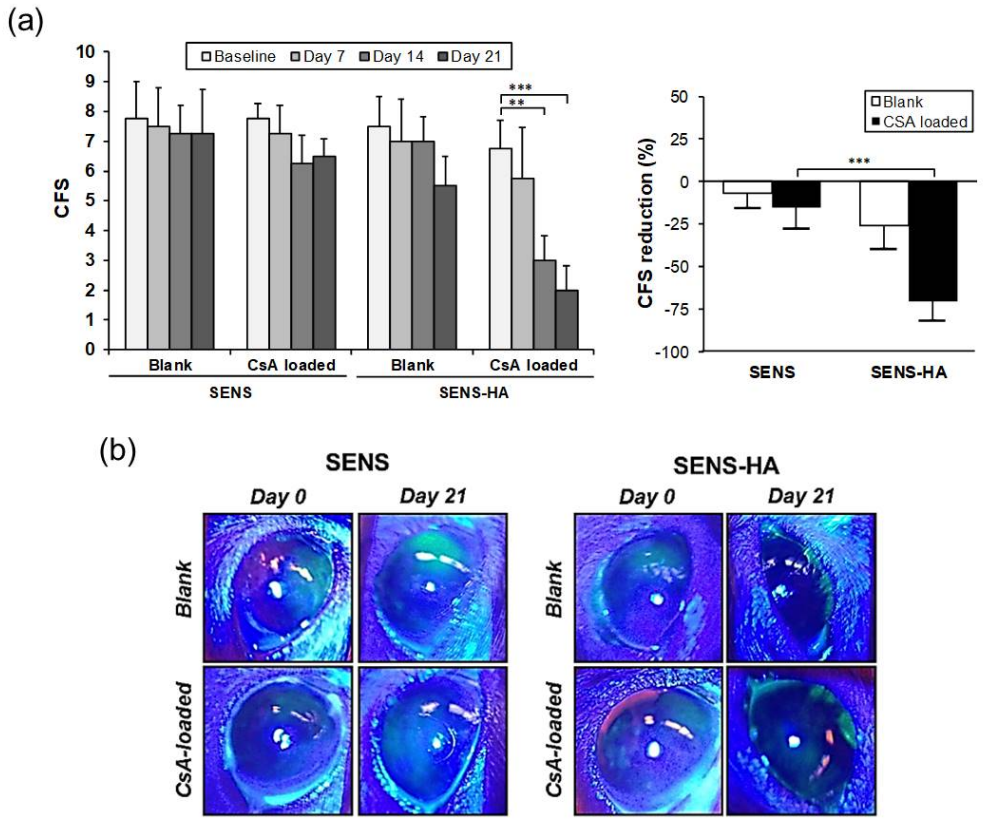


**Figure 15. Monitoring of mice corneal integrity.** (a) The corneal fluorescein score (CFS) evolution. CsA-loaded SENS-HA significantly reduced CFS during the second (** $p \leq 0.01$) and third weeks of treatment (*** $p \leq 0.001$). This latter reduction was 54.9% higher than that obtained with same uncoated NP formulation (*** $p \leq 0.001$). (b) Representative images of corneal fluorescein staining. The reduction in corneal fluorescein staining was most evident in the eyes treated with the HA-containing NP formulations.

The evaluation of the changes in the secretory function of TSP-1-deficient mice after NP treatment was evaluated by measuring MUC5AC levels in tears. The presence

of ocular surface inflammation is related to goblet cell dysfunction and/or apoptosis that translates into lower levels of MUC5AC in tears [63,67]. As shown **Figure 16**, both types of CsA-loaded NPs increased MUC5AC levels. This effect is most likely due to the anti-inflammatory activity of CsA. Interestingly, blank SENS-HA showed the same effect, which we considered to be related to a direct HA effect on goblet cell recovery [68].

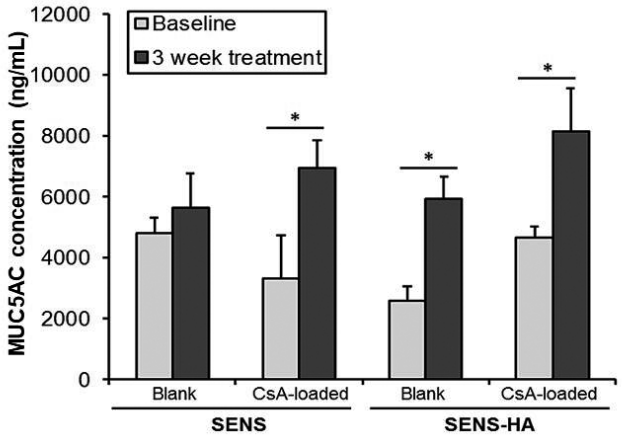


**Figure 16. Changes in MUC5AC levels in tears after treatment with blank and CsA-loaded NPs.** CsA-loaded NP formulations and blank SENS-HA significantly increased MUC5AC levels at the end of treatment (* $p \leq 0.05$).

### 3.2.1 Histopathology analysis in TSP-1-deficient mice ocular tissues after treatment with blank and CsA-loaded NPs.

H&E and AB/PAS staining were performed to evaluate the ocular surface structure morphology and conjunctival goblet cell count, respectively. Despite the differences observed in the CFS, no differences in the corneal morphology were observed in mice from any of the four experimental groups (**Figure 17a**). The lack of morphological differences in the corneal tissues from mice treated with blank or CsA-loaded NPs may be explained because alterations in the corneal barrier were confined to changes in the epithelial permeability that cannot be observed by H&E staining. The histological evaluation of the conjunctiva did not show differences regarding tissue integrity; however, the goblet cell density was higher after treatment with the CsA-loaded SENS, CsA-loaded SENS-HA and blank SENS-HA than the blank SENS (**Figure 17b**). These results are in agreement with MUC5AC levels found in tears, indicating that the CsA-loaded and HA-coated blank formulations exerted beneficial effects on goblet cell density recovery, and consequently increased MUC5AC secretion to the tear film.

### 3.2.1 Changes in pro-inflammatory cytokine levels after treatment with blank and CsA-loaded NPs.

Cervical lymph nodes that drain from the ocular surface are involved in the generation of inflammatory effectors that sustain and further aggravate ocular surface inflammation [61]. Therefore, measuring cytokine levels in the cervical lymph nodes provides valuable information about the disease status and treatment efficacy. Accordingly, we analyzed the mRNA expression of some of the most relevant pro-inflammatory cytokines involved in the pathology of dry eye, including IL-6, IL-1β and TNF-α [69–71]. The results depicted in **Figure 18** show that both types of CsA-loaded NPs decreased the levels of the three pro-inflammatory cytokines, revealing their therapeutic efficacy. Particularly, decreasing IL-6 may prevent the perpetuation of the inflammatory condition [72], decreasing IL-1β may contribute to corneal barrier recovery [73] and decreasing TNF-α may contribute to goblet cell recovery [74].

In summary, all the above discussed results indicate that CsA-loaded NPs possess a high potential for the treatment of dry eye disease, even though the HA-coated NPs showed higher therapeutic efficacy, which is probably due to the additional therapeutic effect provided by HA.

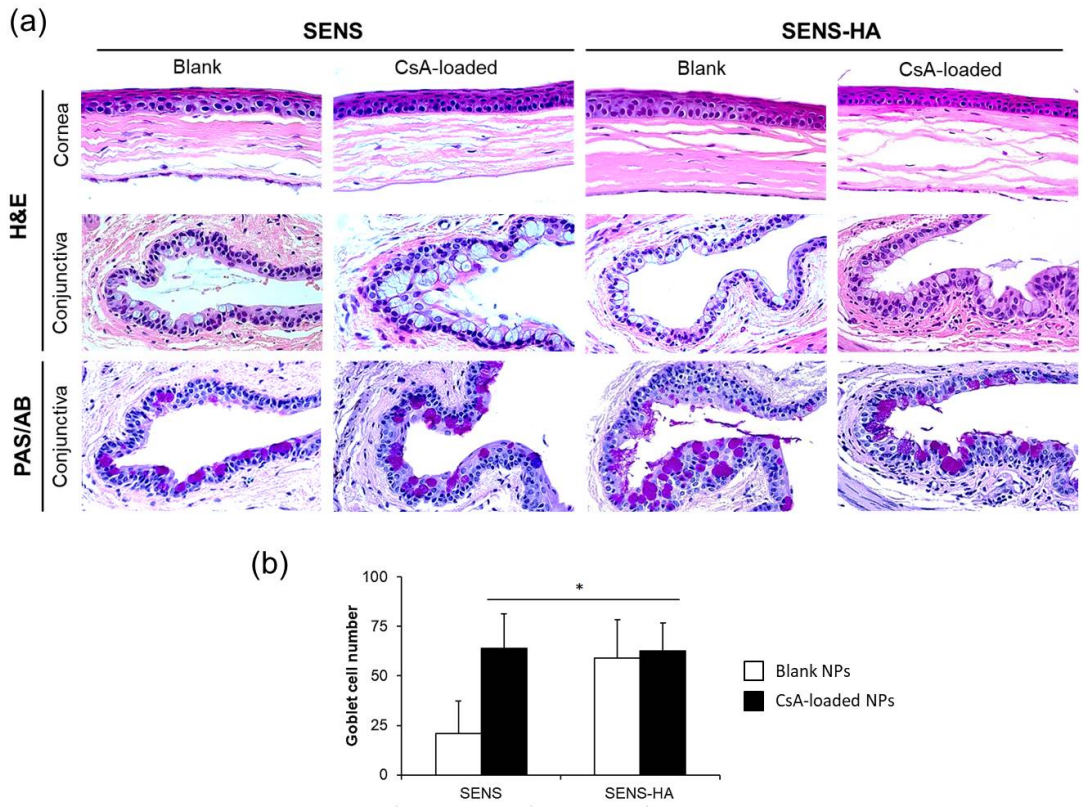


**Figure 17. Histopathology analysis of control and treated TSP-1-deficient mice ocular tissues.** (a) H&E- and PAS/AB-stained corneal and conjunctival tissues. There were no alterations in the cell layers, goblet cells, or other morphological details from the corneal and conjunctival tissues by either blank or CsA-loaded NPs. Additionally, no inflammatory changes were observed. (b) However, significantly higher numbers of goblet cells were observed in the conjunctiva in the CsA-loaded NP- and blank SENS-HA-treated mice groups (* $p \leq 0.05$). H&E, hematoxylin and eosin and PAS/AB, periodic acid-Schiff.

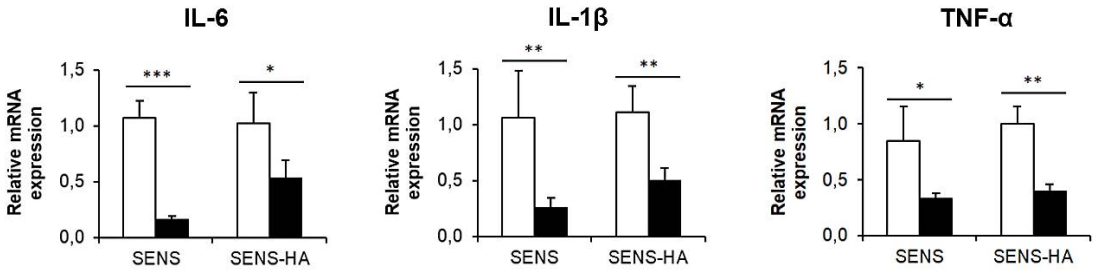


**Figure 18. Changes in relative mRNA expression of the three pro-inflammatory cytokines in cervical lymph nodes from control and treated TSP-1-deficient mice.** Both types of CsA-loaded NPs (black bars) significantly reduced IL-6, IL-1β and TNF-α mRNA expression compared with the controls (white bars) (* $p \leq 0.05$, ** $p \leq 0.01$, and *** $p \leq 0.001$).

**References**

[1] K. Kato, P. Walde, N. Koine, S. Ichikawa, T. Ishikawa, R. Nagahama, T. Ishihara, T. Tsujii, M. Shudou, Y. Omokawa, T. Kuroiwa, Temperature-Sensitive Nonionic Vesicles Prepared from Span 80 (Sorbitan Monooleate), Langmuir. 24 (2008) 10762–10770. doi:10.1021/la801581f.

[2] H. Nakata, T. Miyazaki, T. Iwasaki, A. Nakamura, T. Kidani, K. Sakayama, J. Masumoto, H. Miura, Development of tumor-specific caffeine-potentiated chemotherapy using a novel drug delivery system with Span 80 nano-vesicles, Oncol. Rep. 33 (2015) 1593–1598. doi:10.3892/or.2015.3761.

[3] A. Pensado, I. Fernandez-Piñeiro, B. Seijo, A. Sanchez, Anionic nanoparticles based on Span 80 as low-cost, simple and efficient non-viral gene-transfection systems, Int. J. Pharm. 476 (2014) 23–30. doi:10.1016/j.ijpharm.2014.09.032.

[4] A. Pensado, M. Martín-Pastor, G.K. Zorzi, E.S. Carvalho, A. Sanchez, Structural analysis of nanosystems: Solid Sorbitan esters Nanoparticles (SSN) as a case study, Eur. J. Pharm. Biopharm. 104 (2016) 189–199. doi:10.1016/j.ejpb.2016.05.002.

[5] A. Czajkowska-Kośnik, M. Sznitowska, Solubility of ocular therapeutic agents in self-emulsifying oils. I. Self-emulsifying oils for ocular drug delivery: solubility of indomethacin, aciclovir and hydrocortisone., Acta Pol. Pharm. 66 (2009) 709–13.

[6] K. Göke, T. Lorenz, A. Repanas, F. Schneider, D. Steiner, K. Baumann, H. Bunjes, A. Dietzel, J.H. Finke, B. Glasmacher, A. Kwade, Novel strategies for the formulation and processing of poorly water-soluble drugs, Eur. J. Pharm. Biopharm. 126 (2018) 40–56. doi:10.1016/j.ejpb.2017.05.008.

[7] A. Fernández-Ferreiro, M. Barcia, F. Otero-Espinar, M. Lamas, Lubricantes oculares en el tratamiento del ojo seco, Panor. Actual Del Medicam. 38 (2014) 350–356.

[8] K. Gumus, Topical Coenzyme Q10 Eye Drops as an Adjuvant Treatment in Challenging Refractory Corneal Ulcers: A Case Series and Literature Review., Eye Contact Lens. 43 (2017) 73–80. doi:10.1097/ICL.0000000000000229.

[9] W.S. Cheow, K. Hadinoto, Factors affecting drug encapsulation and stability of

lipid–polymer hybrid nanoparticles, Colloids Surfaces B Biointerfaces. 85 (2011) 214–220. doi:10.1016/j.colsurfb.2011.02.033.

[10] Z. Zhang, S. Tan, S.-S. Feng, Vitamin E TPGS as a molecular biomaterial for drug delivery, Biomaterials. 33 (2012) 4889–4906. doi:10.1016/j.biomaterials.2012.03.046.

[11] J. Jiao, Polyoxyethylated nonionic surfactants and their applications in topical ocular drug delivery, Adv. Drug Deliv. Rev. 60 (2008) 1663–1673. doi:10.1016/j.addr.2008.09.002.

[12] A.J. Bron, P. Daubas, R. Siou-Mermet, C. Trinquand, Comparison of the efficacy and safety of two eye gels in the treatment of dry eyes: Lacrinorm and Viscotears, Eye. 12 (1998) 839–847. doi:10.1038/eye.1998.215.

[13] M. Oechsner, S. Keipert, Polyacrylic acid/polyvinylpyrrolidone bipolymeric systems. I. Rheological and mucoadhesive properties of formulations potentially useful for the treatment of dry-eye-syndrome, Eur. J. Pharm. Biopharm. 47 (1999) 113–8.

[14] J.F. Fangueiro, A.C. Calpena, B. Clares, T. Andreani, M.A. Egea, F.J. Veiga, M.L. Garcia, A.M. Silva, E.B. Souto, Biopharmaceutical evaluation of epigallocatechin gallate-loaded cationic lipid nanoparticles (EGCG-LNs): In vivo, in vitro and ex vivo studies, Int. J. Pharm. 502 (2016) 161–169. doi:10.1016/j.ijpharm.2016.02.039.

[15] A. Leonardi, L. Crasci', A. Panico, R. Pignatello, Antioxidant activity of idebenone-loaded neutral and cationic solid-lipid nanoparticles., Pharm. Dev. Technol. 20 (2015) 716–723. doi:10.3109/10837450.2014.915572.

[16] A. Leonardi, C. Bucolo, F. Drago, S. Salomone, R. Pignatello, Cationic solid lipid nanoparticles enhance ocular hypotensive effect of melatonin in rabbit, Int. J. Pharm. 478 (2015) 180–186. doi:10.1016/j.ijpharm.2014.11.032.

[17] M.A. Kalam, Development of chitosan nanoparticles coated with hyaluronic acid for topical ocular delivery of dexamethasone, Int. J. Biol. Macromol. 89 (2016) 127–136. doi:10.1016/j.ijbiomac.2016.04.070.

[18] D. Liu, Y. Lian, Q. Fang, L. Liu, J. Zhang, J. Li, Hyaluronic-acid-modified lipid-polymer hybrid nanoparticles as an efficient ocular delivery platform for moxifloxacin

hydrochloride, Int. J. Biol. Macromol. 116 (2018) 1026–1036. doi:10.1016/j.ijbiomac.2018.05.113.

[19] S. Mizrahy, S.R. Raz, M. Hasgaard, H. Liu, N. Soffer-Tsur, K. Cohen, R. Dvash, D. Landsman-Milo, M.G.E.G. Bremer, S.M. Moghimi, D. Peer, Hyaluronan-coated nanoparticles: the influence of the molecular weight on CD44-hyaluronan interactions and on the immune response., J. Control. Release. 156 (2011) 231–238. doi:10.1016/j.jconrel.2011.06.031.

[20] H.S.S. Qhattal, X. Liu, Characterization of CD44-mediated cancer cell uptake and intracellular distribution of hyaluronan-grafted liposomes., Mol. Pharm. 8 (2011) 1233–1246. doi:10.1021/mp2000428.

[21] ChemSpider, Sorbitan monooleate structure, (n.d.). http://www.chemspider.com/Chemical-Structure.8095979.html?rid=eb1f34f8-8696-4fbc-8134-4816cbc43247&page_num=0 (accessed July 12, 2018).

[22] ChemSpider, Vitamin E TPGS structure, (n.d.). http://www.chemspider.com/Chemical-Structure.8113682.html?rid=086f9606-e288-4a4f-9db6-240c6a9aca03&page_num=0 (accessed July 12, 2018).

[23] ChemSpider, CTAB structure, (n.d.). http://www.chemspider.com/Chemical-Structure.5754.html?rid=772e731b-27a9-49fc-a37d-d7a13f960e97 (accessed July 12, 2018).

[24] ChemSpider, Cyclosporine A structure, (n.d.). http://www.chemspider.com/Chemical-Structure.4447449.html?rid=4c561f86-0f43-46fa-9b8c-fa0ab57d292b (accessed July 12, 2018).

[25] ChemSpider, Rapamycin (sirolimus) structure, (n.d.). http://www.chemspider.com/Chemical-Structure.10482078.html?rid=81678f16-f77f-41d3-b68d-69ab104c78b2 (accessed July 12, 2018).

[26] PubChem, Hyaluronic acid molecular structure, (n.d.). https://pubchem.ncbi.nlm.nih.gov/compound/24728612 (accessed July 10, 2018).

[27] P. Hossain, Cyclosporine in ocular surface inflammation, Eye. 31 (2017) 665–667. doi:10.1038/eye.2017.5.

[28] D.J.A.R. Moes, H.-J. Guchelaar, J.W. de Fijter, Sirolimus and everolimus in kidney transplantation, Drug Discov. Today. 20 (2015) 1243–1249. doi:10.1016/j.drudis.2015.05.006.

[29] M. Ishikawa, D. Jin, Y. Sawada, S. Abe, T. Yoshitomi, Future Therapies of Wet Age-Related Macular Degeneration, J. Ophthalmol. 2015 (2015). doi:10.1155/2015/138070.

[30] Y.S. Kwon, H.S. Hong, J.C. Kim, J.S. Shin, Y. Son, Inhibitory Effect of Rapamycin on Corneal Neovascularization In Vitro and In Vivo, Investig. Opthalmology Vis. Sci. 46 (2005) 454. doi:10.1167/iovs.04-0753.

[31] D. Liu, F. Yang, F. Xiong, N. Gu, The Smart Drug Delivery System and Its Clinical Potential, Theranostics. 6 (2016) 1306–1323. doi:10.7150/thno.14858.

[32] A. Sanchez, B. Seijo, G.K. Zorzi, E.S. Carvalho, A. Pensado, Nanoparticulate systems prepared from Sorbitan esters, WO2013068625 A1, 2013.

[33] J. Alvarez-Trabado, Y. Diebold, A. Sanchez, Designing lipid nanoparticles for topical ocular drug delivery, Int. J. Pharm. 532 (2017). doi:10.1016/j.ijpharm.2017.09.017.

[34] H. Ji, J. Tang, M. Li, J. Ren, N. Zheng, L. Wu, Curcumin-loaded solid lipid nanoparticles with Brij78 and TPGS improved in vivo oral bioavailability and in situ intestinal absorption of curcumin, Drug Deliv. 23 (2016) 459–470. doi:10.3109/10717544.2014.918677.

[35] J. Della Rocca, D. Liu, W. Lin, Are high drug loading nanoparticles the next step forward for chemotherapy?, Nanomedicine. 7 (2012) 303–305. doi:10.2217/nnm.11.191.

[36] G. Zapata, L. Racca, J. Tau, A. Berra, Topical Use of Rapamycin in Herpetic Stromal Keratitis, Ocul. Immunol. Inflamm. 20 (2012) 354–359. doi:10.3109/09273948.2012.709575.

[37] J. Alvarez-Trabado, A. López-García, M. Martín-Pastor, Y. Diebold, A. Sanchez, Sorbitan ester nanoparticles (SENS) as a novel topical ocular drug delivery system: Design, optimization, and in vitro/ex vivo evaluation, Int. J. Pharm. 546 (2018)

20–30. doi:10.1016/j.ijpharm.2018.05.015.

[38] P. Sengupta, B. Chatterjee, R.K. Tekade, Current regulatory requirements and practical approaches for stability analysis of pharmaceutical products: A comprehensive review, Int. J. Pharm. 543 (2018) 328–344. doi:10.1016/j.ijpharm.2018.04.007.

[39] C. Schwarz, Solid lipid nanoparticles (SLN) for controlled drug delivery II. drug incorporation and physicochemical characterization, J. Microencapsul. 16 (1999) 205–213. doi:10.1080/026520499289185.

[40] A.M. de Campos, Y. Diebold, E.L.S. Carvalho, A. Sanchez, M.J. Alonso, Chitosan nanoparticles as new ocular drug delivery systems: in vitro stability, in vivo fate, and cellular toxicity., Pharm. Res. 21 (2004) 803–810.

[41] E. Mahon, A. Salvati, F. Baldelli Bombelli, I. Lynch, K.A. Dawson, Designing the nanoparticle-biomolecule interface for "targeting and therapeutic delivery"., J. Control. Release. 161 (2012) 164–174. doi:10.1016/j.jconrel.2012.04.009.

[42] W. Mehnert, K. Mader, Solid lipid nanoparticles: production, characterization and applications., Adv. Drug Deliv. Rev. 47 (2001) 165–196.

[43] M.A. Vetten, C.S. Yah, T. Singh, M. Gulumian, Challenges facing sterilization and depyrogenation of nanoparticles: Effects on structural stability and biomedical applications, Nanomedicine Nanotechnology, Biol. Med. 10 (2014) 1391–1399. doi:10.1016/j.nano.2014.03.017.

[44] E. Memisoglu-Bilensoy, A.A. Hincal, Sterile, injectable cyclodextrin nanoparticles: Effects of gamma irradiation and autoclaving, Int. J. Pharm. 311 (2006) 203–208. doi:10.1016/j.ijpharm.2005.12.013.

[45] E.H. Gokce, G. Sandri, M.C. Bonferoni, S. Rossi, F. Ferrari, T. Güneri, C. Caramella, Cyclosporine A loaded SLNs: Evaluation of cellular uptake and corneal cytotoxicity, Int. J. Pharm. 364 (2008) 76–86. doi:10.1016/j.ijpharm.2008.07.028.

[46] Y.N. Konan, R. Cerny, J. Favet, M. Berton, R. Gurny, E. Allémann, Preparation and characterization of sterile sub-200 nm meso-tetra(4-hydroxylphenyl)porphyrin-loaded nanoparticles for photodynamic therapy., Eur. J. Pharm. Biopharm. 55 (2003) 115–24.

[47] C.W. How, A. Rasedee, R. Abbasalipourkabir, Characterization and Cytotoxicity of Nanostructured Lipid Carriers Formulated With Olive Oil, Hydrogenated Palm Oil, and Polysorbate 80, IEEE Trans. Nanobioscience. 12 (2013) 72–78. doi:10.1109/TNB.2012.2232937.

[48] Y. Liu, H. Xu, M. An, mTORC1 regulates apoptosis and cell proliferation in pterygium via targeting autophagy and FGFR3, Sci. Rep. 7 (2017) 7339. doi:10.1038/s41598-017-07844-y.

[49] C. Debbasch, S. Bruneau De La Salle, F. Brignole, P. Rat, J.-M. Warnet, C. Baudouin, Cytoprotective effects of hyaluronic acid and Carbomer 934P in ocular surface epithelial cells, Invest. Ophthalmol. Vis. Sci. 43 (2002) 3409–3415.

[50] H. Wu, H. Zhang, C. Wang, Y. Wu, J. Xie, X. Jin, J. Yang, J. Ye, Genoprotective effect of hyaluronic acid against benzalkonium chloride-induced DNA damage in human corneal epithelial cells., Mol. Vis. 17 (2011) 3364–70.

[51] S. Doktorovova, E.B. Souto, A.M. Silva, Nanotoxicology applied to solid lipid nanoparticles and nanostructured lipid carriers - a systematic review of in vitro data., Eur. J. Pharm. Biopharm. 87 (2014) 1–18. doi:10.1016/j.ejpb.2014.02.005.

[52] L. García-Posadas, L. Contreras-Ruiz, A. López-García, S. Villarón Álvarez, M.J. Maldonado, Y. Diebold, Hyaluronan receptors in the human ocular surface: a descriptive and comparative study of RHAMM and CD44 in tissues, cell lines and freshly collected samples, Histochem. Cell Biol. 137 (2012) 165–176. doi:10.1007/s00418-011-0878-z.

[53] L. Contreras-Ruiz, M. de la Fuente, J.E. Párraga, A. López-García, I. Fernández, B. Seijo, A. Sánchez, M. Calonge, Y. Diebold, Intracellular trafficking of hyaluronic acid-chitosan oligomer-based nanoparticles in cultured human ocular surface cells., Mol. Vis. 17 (2011) 279–90. http://www.ncbi.nlm.nih.gov/pubmed/21283563.

[54] I. Sanchez, R. Martin, F. Ussa, I. Fernandez-Bueno, The parameters of the porcine eyeball, Graefe's Arch. Clin. Exp. Ophthalmol. 249 (2011) 475–482. doi:10.1007/s00417-011-1617-9.

[55] G.M. Pereira, J.F. Miller, E.M. Shevach, Mechanism of action of cyclosporine A in vivo. II. T cell priming in vivo to alloantigen can be mediated by an IL-2-independent

cyclosporine A-resistant pathway., J. Immunol. 144 (1990) 2109–2116.

[56] M.M. Hamawy, Molecular actions of calcineurin inhibitors, Drug News Perspect. 16 (2003) 277–82.

[57] Q. Ebrahem, A. Minamoto, G. Hoppe, B. Anand-Apte, J.E. Sears, Triamcinolone Acetonide Inhibits IL-6– and VEGF-Induced Angiogenesis Downstream of the IL-6 and VEGF Receptors, Investig. Opthalmology Vis. Sci. 47 (2006) 4935. doi:10.1167/iovs.05-1651.

[58] N. Asano-Kato, K. Fukagawa, N. Okada, T. Kawakita, Y. Takano, M. Dogru, K. Tsubota, H. Fujishima, TGF-beta1, IL-1beta, and Th2 cytokines stimulate vascular endothelial growth factor production from conjunctival fibroblasts, Exp. Eye Res. 80 (2005) 555–560. doi:10.1016/j.exer.2004.11.006.

[59] C.N. Nagineni, A. William, A. Cherukuri, W. Samuel, J.J. Hooks, B. Detrick, Inflammatory cytokines regulate secretion of VEGF and chemokines by human conjunctival fibroblasts: Role in dysfunctional tear syndrome, Cytokine. 78 (2016) 16–19. doi:10.1016/j.cyto.2015.11.016.

[60] B. Turpie, T. Yoshimura, A. Gulati, J.D. Rios, D.A. Dartt, S. Masli, Sjögren's Syndrome-Like Ocular Surface Disease in Thrombospondin-1 Deficient Mice, Am. J. Pathol. 175 (2009) 1136–1147. doi:10.2353/ajpath.2009.081058.

[61] L. Contreras-Ruiz, B. Regenfuss, F.A. Mir, J. Kearns, S. Masli, Conjunctival Inflammation in Thrombospondin-1 Deficient Mouse Model of Sjögren's Syndrome, PLoS One. 8 (2013) e75937. doi:10.1371/journal.pone.0075937.

[62] M.A. Lemp, Report of the National Eye Institute/Industry workshop on Clinical Trials in Dry Eyes, CLAO J. 21 (1995) 221–32.

[63] L. Contreras-Ruiz, F.A. Mir, B. Turpie, A.H. Krauss, S. Masli, Sjögren's syndrome associated dry eye in a mouse model is ameliorated by topical application of integrin α4 antagonist GW559090, Exp. Eye Res. 143 (2016) 1–8. doi:10.1016/j.exer.2015.10.008.

[64] J.A.P. Gomes, R. Amankwah, A. Powell-Richards, H.S. Dua, Sodium hyaluronate (hyaluronic acid) promotes migration of human corneal epithelial cells in

vitro., Br. J. Ophthalmol. 88 (2004) 821–5. doi:10.1136/bjo.2003.027573.

[65] J. Zhong, Y. Deng, B. Tian, B. Wang, Y. Sun, H. Huang, L. Chen, S. Ling, J. Yuan, Hyaluronate Acid-Dependent Protection and Enhanced Corneal Wound Healing against Oxidative Damage in Corneal Epithelial Cells, J. Ophthalmol. 2016 (2016) 1–10. doi:10.1155/2016/6538051.

[66] A. Ragam, A.M. Kolomeyer, J.S. Kim, N. V. Nayak, C. Fang, E. Kim, D.S. Chu, Topical Cyclosporine A 1% for the Treatment of Chronic Ocular Surface Inflammation, Eye Contact Lens Sci. Clin. Pract. 40 (2014) 283–288. doi:10.1097/ICL.0000000000000055.

[67] L. Contreras-Ruiz, A. Ghosh-Mitra, M.A. Shatos, D.A. Dartt, S. Masli, Modulation of Conjunctival Goblet Cell Function by Inflammatory Cytokines, Mediators Inflamm. 2013 (2013) 1–11. doi:10.1155/2013/636812.

[68] J.H. Choi, J.H. Kim, Z. Li, H.J. Oh, K.Y. Ahn, K.C. Yoon, Efficacy of the Mineral Oil and Hyaluronic Acid Mixture Eye Drops in Murine Dry Eye, Korean J. Ophthalmol. 29 (2015) 131. doi:10.3341/kjo.2015.29.2.131.

[69] L. Contreras-Ruiz, D.S. Ryan, R.K. Sia, K.S. Bower, D.A. Dartt, S. Masli, Polymorphism in THBS1 Gene Is Associated with Post-Refractive Surgery Chronic Ocular Surface Inflammation, Ophthalmology. 121 (2014) 1389–1397. doi:10.1016/j.ophtha.2014.01.033.

[70] M.L. Massingale, X. Li, M. Vallabhajosyula, D. Chen, Y. Wei, P.A. Asbell, Analysis of Inflammatory Cytokines in the Tears of Dry Eye Patients, Cornea. 28 (2009) 1023–1027. doi:10.1097/ICO.0b013e3181a16578.

[71] S.Y. Lee, S.J. Han, S.M. Nam, S.C. Yoon, J.M. Ahn, T.-I. Kim, E.K. Kim, K.Y. Seo, Analysis of Tear Cytokines and Clinical Correlations in Sjögren Syndrome Dry Eye Patients and Non–Sjögren Syndrome Dry Eye Patients, Am. J. Ophthalmol. 156 (2013) 247–253.e1. doi:10.1016/j.ajo.2013.04.003.

[72] S.A. Jones, Directing transition from innate to acquired immunity: defining a role for IL-6, J. Immunol. 175 (2005) 3463–8.

[73] K. Kimura, S. Teranishi, T. Nishida, Interleukin-1β–Induced Disruption of

Barrier Function in Cultured Human Corneal Epithelial Cells, Investig. Opthalmology Vis. Sci. 50 (2009) 597. doi:10.1167/iovs.08-2606.

[74] Y.W. Ji, Y.J. Byun, W. Choi, E. Jeong, J.S. Kim, H. Noh, E.S. Kim, Y.J. Song, S.K. Park, H.K. Lee, Neutralization of Ocular Surface TNF-α Reduces Ocular Surface and Lacrimal Gland Inflammation Induced by In Vivo Dry Eye, Investig. Opthalmology Vis. Sci. 54 (2013) 7557. doi:10.1167/iovs.12-11515.

USC
UNIVERSIDADE
DE SANTIAGO
DE COMPOSTELA

# *Conclusions*

USC
UNIVERSIDADE
DE SANTIAGO
DE COMPOSTELA

## Conclusions

This Doctoral Thesis was focused on the development of a nanoparticle-based therapeutic alternative to existing treatments for ocular surface diseases such as dry eye disease and corneal neovascularization.

Considering all the results presented in this report, we conclude the following.

1. We demonstrated that SENS can be successfully developed and optimized as a topical ocular drug delivery system. The nanoparticles can also be surface-decorated with hyaluronic acid for specific targeting purposes.

2. The developed nanoparticles showed adequate physicochemical properties for topical ocular administration. Particularly, the elevated cyclosporine loading, which caused a remarkable increase in the water solubility of this drug, did not compromise the physical stability of the aqueous nanoparticle dispersion.

3. The developed nanoparticles showed an adequate safety profile in corneal and conjunctival cell lines. The hyaluronic acid-coated nanoparticles showed higher targeting ability to the cornea compared with the uncoated nanoparticles both *in vitro* and *ex vivo*.

4. The nanoparticle production process did not affect the biological activity of cyclosporine and rapamycin, and both drugs could be released in their bioactive forms from the nanoparticle matrix to exert their therapeutic effects.

5. We demonstrated that the hyaluronic acid-coated nanoparticles enhanced the therapeutic efficacy of topically applied cyclosporine in the treatment of experimental dry eye; these results are probably due to a synergistic mechanism between the anti-inflammatory efficacy of CsA and the benefits provided by HA. This proof-of-concept may aid in the design of more efficient topically applied nanoparticle-based drug delivery systems.

USC
UNIVERSIDADE
DE SANTIAGO
DE COMPOSTELA

# *Annex I*

---

## *Designing lipid nanoparticles for topical ocular drug delivery*

USC
UNIVERSIDADE
DE SANTIAGO
DE COMPOSTELA

**Abstract**

Topically-applied dosage forms, such eye drops, are the most used formulations in the treatment of ocular diseases. Nonetheless, because of the special protection of the eye associated with the ocular surface, drug bioavailability and subsequent therapeutic efficiency obtained with these conventional dosage forms are very low. Recently, novel drug delivery systems have been proposed to solve the main drawbacks of conventional formulations. Nanotechnology, and more specifically lipid nanoparticles, have emerged as promising "modified eyedrops" with the purpose of improving therapeutic efficiency without compromising drug safety and patient compliance. The purpose of this review is to offer an overview of lipid nanoparticles as feasible alternatives to the conventional topically-applied dosage forms. We discuss the main limitations of topical ocular drug delivery and describe how correctly designed lipid nanoparticles can be highly valuable tools to overcome the constraints imposed by the ocular surface. Special emphasis is placed on the description of production methods and bulk materials used in the development of lipid nanoparticles for ophthalmic use and how both issues will determine the physicochemical and biopharmaceutical properties of the developed nanosystems.

USC
UNIVERSIDADE
DE SANTIAGO
DE COMPOSTELA

## 1. Introduction

Ocular drug delivery (ODD) includes multiple pharmaceutical strategies to reach a therapeutic target in the eye through a variety of different routes. Topical administration, because of its simplicity, non-invasiveness, and high patient compliance, is the conventional and preferred route to achieve the therapeutic goal. In fact, topical formulations such as eyedrops represent 90% of the marketed dosage forms used in eye care [1]. The purpose for topical ODD is two-fold. One is to treat anterior segment diseases affecting the ocular surface (OS), such as conjunctivitis, blepharitis, and keratoconjunctivitis sicca. The other purpose is to penetrate through the cornea to treat intraocular pathologies, such as glaucoma and uveitis [2]. Nevertheless, traditional drug therapies based on conventional dosage forms, i.e., eyedrops and ointments, typically have a low clinical success rate. This is attributed in part to the unfavorable physicochemical properties, i.e., low water solubility, of the active substances such as anti-infective agents, anti-inflammatories, and immunosuppressants, which are typically included in these formulations. Additionally, the highly impermeable milieu of the eye, especially the OS, limits the bioavailability and subsequent efficacy of the active agents. For this reason, high doses of drugs and frequent administration are necessary to maintain sufficiently high therapeutic levels at the site of action.

Multiple ODD systems have been proposed to overcome these limitations. These include hydrogels [3], polymeric nanoparticles [4], polymeric micelles [5], nanosuspensions [6], and lipid-based nanocarriers [7]. Lipid-based nanocarriers, a broad category comprised of liposomes, niosomes, cubosomes, nanoemulsions, nanomicelles, and lipid nanoparticles (LNs) have attracted enormous interest in recent years [7]. These types of colloidal systems offer several advantages, including solubility enhancement of hydrophobic drugs, accurate adjustment of pharmacokinetic parameters, and drug protection from enzymatic degradation, all of which ultimately improve bioavailability [8].

The market of lipid colloidal systems for ODD is growing continuously. Since the approval of Restasis (2002; Allergan, Irvine, CA, USA), an anionic nanoemulsion for the treatment of severe dry eye syndrome, and the marketing authorization of Ikervis (2015; Santen Inc., Emeryville, CA, USA), a cationic nanoemulsion for the treatment of severe keratitis in adult patients with dry eye disease, other lipidic formulations have been developed [9]. However, LN-based formulations are currently limited to research applications, and none are available for commercial use because they are in early

developmental stages. Further investigation is necessary, both regarding the technological feasibility and safety after chronic exposure.

In this review, we analyze different elaboration methods and bulk materials commonly employed in the production of LNs for ODD, focusing on how they may influence the physicochemical and biopharmaceutical properties of the final formulation. We also describe different approaches to optimize these properties. Finally, as a case study, we summarize the available literature regarding the use of LNs in the topical administration of the immunosuppressant drug cyclosporine.

## 2. The OS as a barrier

Designing a formulation for topical ODD constitutes a pharmaceutical challenge for scientists due to the special protection of the eye against penetration of foreign substances. The anatomical barriers and physiological conditions of this organ limit the therapeutic efficacy of promising drugs if formulated as conventional dosage forms like eyedrops [1]. Moreover, most therapeutic molecules have unfavorable physicochemical properties that prevent absorption and distribution through the ocular tissues, decreasing dramatically the fraction of drug that reaches the target tissue. Thus, the bioavailability in the anterior chamber is expected to be less than 5% for lipophilic substances and less than 0.5% for hydrophilic ones [10]. To follow a rational design in the formulation of novel dosage forms, it is necessary to understand the constraints that limit drug bioavailability once the drug contacts with the OS. These constraints, depicted in **Figure 1**, can be divided in two categories: precorneal factors and the corneal barrier.

### 2.1 Precorneal factors

Immediately after instillation, the administered drug is exposed to various physiological mechanisms of the eye that lead to a partial loss of the administered dose. Under normal conditions, the tear film is renewed at a rate of 16% per minute [11]; thus, only a few minutes are needed for a complete removal of the formulation from the OS. Furthermore, tear production is increased in the presence of irritating substances that are contained in some formulations [12]. The normal tear volume is only 7 µL and the maximum capacity of the precorneal tear film when the eye is not blinking is 30 µL, which is reduced to 10 µL during blinking. This results in a limited retention capacity of the instilled volume, which usually is about 50 µL for the conventional dosage forms. The excess formulation is quickly drained from the eye through the nasolacrimal duct, potentially leading to undesirable systemic effects [13].

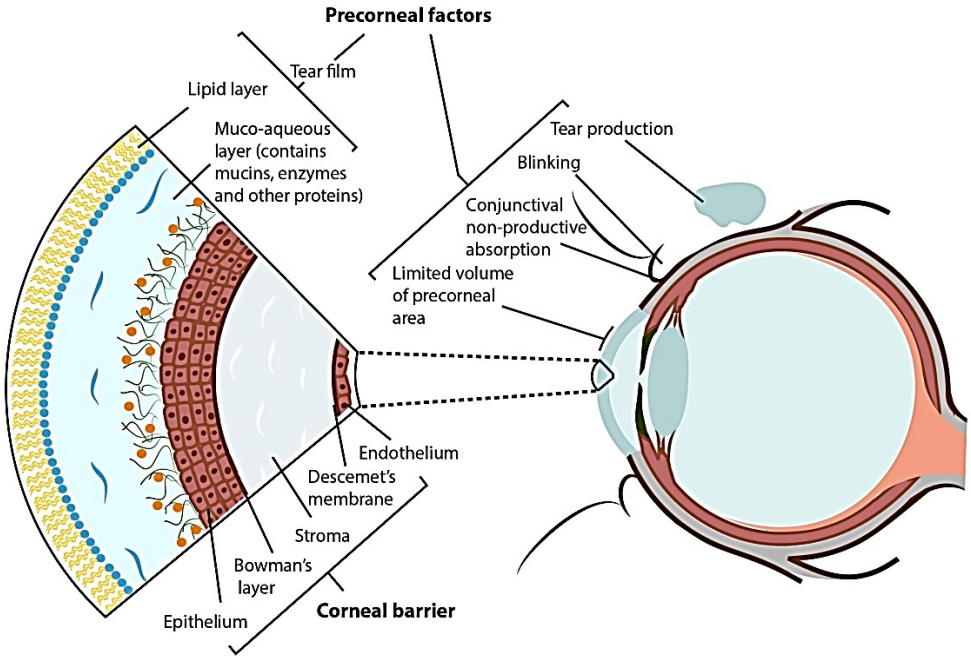


**Figure 1. Representation of the main ocular factors and barriers that any delivery system must overcome to access the therapeutic target after topical administration.**

Tears contain about 0.7% protein under normal conditions [14], but this percentage can increase during disease. This aspect is of particular interest for two reasons. First, many drugs are metabolized by the action of certain enzymes such as cytochrome P-450, esterases, and peptidases [15]. Second, drug-protein complexes can be formed that reduce the fraction of free drug available for absorption [14]. In addition, drugs are absorbed by other tissues aside from the cornea. For instance the conjunctiva, which has a larger surface than the cornea, has 2-30 times higher permeability than the cornea [16]. This non-productive absorption leads not only to a reduction in drug therapeutic efficacy, but also to an increase in the systemic absorption with associated undesirable effects [17].

### 2.2 The corneal barrier

One of the most important functions of the cornea is the protection of intraocular structures against penetration of harmful entities such as infective agents or chemical substances. For this reason, the cornea is a highly-organized structure composed mainly of three layers, i.e., epithelium, stroma, and endothelium, all of which act as selective barriers. The *epithelium* is the outermost structure of the cornea and is formed by about six cell layers. The apical or free surface is covered by a complex glycocalyx composed of glycoproteins such as mucins [18]. The presence of acid moieties in the mucins, such

as sialic acids (pKa=2.6), gives the epithelium a negative charge at physiological pH [19]. The main characteristic of the epithelium is the presence of intercellular tight junctions (*zonula occludens*) that prevent the diffusion of hydrophilic macromolecules with size >100 Da through the paracellular route [20]. In contrast, lipophilic substances, which readily diffuse through the lipid-based cell membranes, can pass through the epithelium via a transcellular route. The epithelial cells then act as reservoirs that slowly release these substances to the corneal stroma [21]. Another important feature of the corneal epithelium is the presence of efflux transporters such as P-glycoproteins that are involved in drug resistance [22].

The corneal *stroma* constitutes about 90% of the thickness of the cornea, starting in Bowman's layer, annexed to the basal surface of the epithelium, and ending in Descemet's membrane, an acellular layer in direct contact with endothelium. The stroma is a highly hydrophilic structure, composed mainly of collagen fibrils and mucopolysaccharides. Unlike the epithelium, only hydrophilic substances can diffuse across the stroma because of the high water content. The open structure of the collagen fibrils and inter-fibril content allows the diffusion of large molecules with sizes up to 500 kDa [23].

The corneal *endothelium* is the innermost part of the cornea and is constituted by a porous, single cell layer. It shares features with both the epithelium and the stroma. Similar to the epithelium, lipophilic substances can diffuse more easily than hydrophilic ones, while the open cell network structure allows diffusion of large molecules with sizes up to 70 kDa [24].

Based on these observations, the ideal formulation for topical ODD would be able to (i) increase the drug residence time at the ocular surface, (ii) protect the drug from degradation occurring in the presence of tear enzymes, (iii) provide targeted drug delivery to the site of action, increasing bioavailability and minimizing the non-productive absorption, and (iv) promote drug penetration through the cornea, enabling it to act as a controlled release system, thus reducing the dosing frequency. Clearly the materials used in any ODD system must be biocompatible, biodegradable, and non-irritating. In this context, LNs have emerged as promising tools in ODD with the possibility of fulfilling these requirements.

## 3. General considerations regarding LNs

LNs are colloidal structures that are submicrometer in size, usually between 50 and 400 nm. They are made of biocompatible and biodegradable lipids, including glycerides, fatty acids, steroids, waxes, and derivatives thereof, that are stabilized by surfactants and co-surfactants, if required [8,25]. The first generation of LNs, solid lipid nanoparticles (SLNs, **Figure 2-1**), were the result of the technological evolution of oil-in-water nanoemulsions, replacing the liquid lipid of the emulsion droplets by lipids that are solid at room temperature [26]. These nanosystems had more physical stability than nanoemulsions due to the solid structure formed by a rigid core surrounded by a stabilizing surfactant layer. Moreover, surfactants were used at a concentration much lower than used in nanoemulsion preparations, which resulted in less toxicity and a better biocompatibility profile. Nevertheless, SLNs had some drawbacks as a consequence of the rigid crystalline matrix. Two of these limitations were low drug loading and substantial drug leakage during storage [27].

To circumvent these technological limitations, scientists developed a second generation of LNs, known as nanostructured lipid carriers (NLCs, **Figure 2-2**). These lipid nanosystems were also composed of solid lipid matrices, but a spatially incompatible liquid lipid was added with the intention of increasing the molecular disorganization of the lipid lattice. This innovation increased the payload and prevented drug expulsion during storage [28]. Even though the resulting structure usually contained up to 30% of liquid lipids, the solid state was maintained in the absence of crystalline formation in the lipid matrix. Muller et al. described three different types of NLCs according the lipid nanostructure: imperfect type, structureless type, and multiple type [28]. Imperfect NLCs were prepared by mixing solid lipids with small amounts of liquid lipids (oils) to prevent crystallization. In the second type, structureless NLCs, the lipid matrix was formed by a solid lipid, such as hydroxyoctacosanylhydroxystearate, that had an amorphous structure after solidification. Multiple NLCs are prepared using high amounts of liquid lipids blended with solid lipids. This incompatible mixture generated tiny oil nanovacuoles within the solid lipid matrix, allowing the incorporation of high amounts of drugs. However, the second generation of LNs was unable to address one of the main technological limitations of lipid nanocarriers: low drug loading, usually below 0.5%, for hydrophilic substances [29].

For this reason, a third approach to LN construction was developed under the name of lipid-drug conjugates (LDCs, **Figure 2-3**). In this case, the hydrophilic drug was

modified by salt formation with fatty acids (e.g., oleic acid) or by covalent bonding with esters or ethers, transforming the drug into a lipid-soluble substance. This resulted in an improved drug payload, with drug loading above 30% [29].

LNs offer several pharmaceutical advantages compared with other lipid-based nanocarriers. Some of them are: excellent biocompatibility and biodegradability thanks to the use of generally recognized as safe (GRAS) substances [30]; high physical stability during storage [31]; high biological stability in environments with intense enzymatic activity [32]; ease to modulate its physicochemical characteristics depending on requirements [33]; production through solvent-free methods and possibility of sterilization by autoclaving. All together, these characteristics make LNs very attractive for industry.

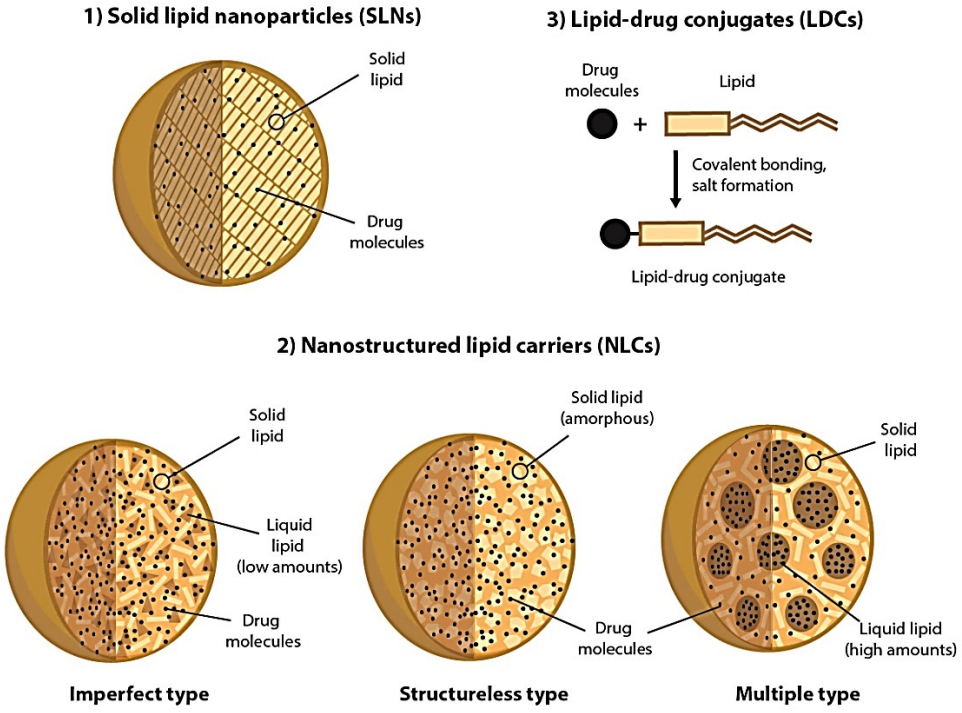


**Figure 2. Schematic representation of different types of lipid nanoparticles used in drug delivery.**

## 4. LNs and the concept of "modified eyedrops"

As described above, for reasons of simplicity and patient compliance, eyedrops are the most often used formulations in ODD. Even so, they have important pharmaceutical limitations such as low drug bioavailability, impossibility of drug targeting to specific ocular structures, and drug binding/inactivation by tear proteins. In this context, the

concept of "modified eyedrops" refers to ophthalmic formulations that are based on nanotechnology, such as LNs, that intend to circumvent the limitations of conventional eyedrops without affecting patient usability and compliance [34]. LNs are postulated to be promising prototypes of "modified eyedrops" for different reasons:

a. *Drug solubility enhancement:* The oil-in-water (O/W) biphasic composition of LNs allows them to solubilize high amounts of water insoluble drugs in a dispersed aqueous formulation that can be administered drop-wise [35]. This technological property is very helpful because drugs commonly used in ocular therapies, such as non-steroidal anti-inflammatory drugs (NSAIDs), immunosuppressants, and corticoids are poorly soluble in water. Potta et al., using stearic acid and trilaurin as solid lipids, developed two types of SLNs that were loaded with cyclosporine in final concentrations ranging from 1 to 2% [36]. To measure the effective drug solubilization caused by the nanoparticles, they analyzed the *in vitro* dissolution profile of the SLNs compared with that of the SLN-free drug suspension. After 150 min, they observed that more than 80% of cyclosporine was present in the release medium from both types of SLNs, and less than 10% was recovered from the drug suspension.
b. *Drug bioavailability improvement:* LNs can improve ocular drug bioavailability in two complementary ways. First, LNs maximize the nanoparticle interaction with the OS due to their high specific surface area and their formulation components, partially avoiding drug washout caused by tear turnover. The result is an increase in the formulation residence time in the precorneal area, acting as a depot system that releases the drug in a controlled manner. For this feature, different materials are included in the nanoparticle composition, such as cationic lipids [37,38] or mucoadhesive coating polymers, such as chitosan [39,40]. On the other hand, LNs enhance transcorneal penetration due to the nanometric size of the particles [41]. They also improve penetration due to formulation components such as polyoxyethylated non-ionic surfactants (i.e., Tween® 20, 40, 80) that inhibit drug efflux by P-glycoproteins and increase the transcellular permeability of the epithelium [42]. Li et al. developed a novel cationic NLC composed of Gelucire 44/14 as the solid lipid, Transcutol P as the permeability enhancer, and stearylamine as the cationizing agent [43]. They demonstrated *in vivo* improvement of both preocular retention and transcorneal penetration of ibuprofen

compared with commercial eyedrops. This combined effect resulted in a four-fold improvement of bioavailability compared with conventional ibuprofen eyedrops.

c. *Targeted drug delivery:* The possibility of active targeting to specific tissues, even to specific intracellular compartments, has attracted enormous interest in recent years because novel therapeutic molecules, as proteins or nucleic acids, can have low *in vivo* stability and poor cellular uptake. Although there are fewer reports in the literature compared to other nanosystems, such as polymeric nanoparticles, [44,45], LNs are versatile constructs that have the potential to target specific ocular structures. Using Wistar rats, Delgado et al. measured the *in vivo* transfection efficiency of SLNs conjugated with protamine, dextran, and two plasmids coding for enhanced green fluorescent protein (EGFP) [46]. The formulation was administered intravitreally, subretinally, and topically onto the eyes. The SLN formulation substantially increased the expression of EGFP in the retina for both the intravitreal and subretinal administrations, and in the cornea for the topical administration. They attributed the success to the careful selection of nanoparticle components, especially the presence of dextran in SLN-protamine-DNA complexes, which allowed targeted internalization through clathrin-mediated endocytosis, something fundamental for the uptake of protamine-DNA conjugates.

## 5. LN elaboration methods

Since the discovery of LNs in the 1990's, different elaboration methods have been used for LN production. Mehnert and Mäder described four production procedures [47]: high shear homogenization and ultrasound [48], high pressure homogenization [49,50], solvent emulsification/evaporation [40,51], and microemulsion method [52,53]. In addition, Yousry and co-workers described a water-in-oil-in-water (W/O/W) double emulsion method for the preparation of vancomycin-loaded SLNs [54]. Recently, a quasi-emulsion solvent diffusion technique was utilized by Leonardi et al. to prepare cationic SLNs loaded with the antioxidant drug idebenone [55]. Other approaches not used as often for LN elaboration include coacervation, super-critical fluids, membrane contactor, spray-drying, and electro-spray [56,57]. In the following sub-sections, we described in depth each of these procedures.

### 5.1 High shear homogenization and ultrasound

High shear homogenization is an easy-to-handle dispersal technique suitable for LN production. However, the quality of the final product is compromised by the presence of

microparticles. In addition, metal contamination can be present if ultrasound is used. Recently, Üstündağ et al. used this technique to develop a cationic NLC formulation for topical ocular administration of ofloxacin [48]. The resulting formulation presented appropriate physicochemical and biopharmaceutical properties for the intended topical use.

### 5.2 High pressure homogenization (HPH)

HPH is the most widely employed method for LN production due to its technical feasibility. The pharmaceutical industry has years of experience with HPH as it was first used for preparation of nanoemulsions for parenteral nutrition and later implemented for SLN production. The main advantage of this technique is the ease to scale up for large productions. Homogenizers that can produce 11,000 L/h are commercially available [58]. The main drawback is related to the mechanical and thermodynamic stress to which the formulation is subjected during the process. HPH fundamentally consists of a compartment containing the pressurized preformulation (100-2000 bar) that is forced through a micrometer-sized narrow gap. Under these conditions, the pre-formulation is exposed to very high shear and cavitation forces, generating particles in the submicrometer size [47]. Two different approaches have been proposed for LN production: hot and cold homogenization. In both cases, there are preparatory steps in which drug is mixed (dissolved or dispersed) with the melted bulk lipid.

#### 5.2.1. Hot homogenization

In hot homogenization, the drug-loaded lipid is heated above the melting point and poured to mix under continuous stirring with a hot aqueous surfactant solution. After that, the resulting dispersion is homogenized using a high-shear force mixing device to form a pre-emulsion. During the following HPH, the temperature is maintained above the melting point of the bulk lipid with the intention of lowering the viscosity of the inner phase, which ultimately results in a nanoemulsion with smaller particle size [59]. The HPH step can be repeated as required, but the forces involved in each HPH cycle increase the total system temperature. This can be a limitation for entrapment of certain thermolabile drugs commonly used in ocular therapies, such as proteins or peptides. The final LN formulation is obtained after cooling the nanoemulsion to room temperature or temperatures below the lipid melting point. Gonzalez-Mira et al. used this process to elaborate flurbiprofen-loaded NLCs for topical ocular administration [50]. They identified the proportion of liquid lipid/solid lipid, the surfactant concentration, and the

drug concentration as key factors that determine the nanoparticle physicochemical properties.

### 5.2.2. Cold homogenization

In cold homogenization, the issue related to the excessive temperature during nanoparticle production is partially, but not completely, avoided because the preparatory drug-lipid melting step remains necessary. In this approach, the drug-loaded lipid is cooled and solidified using liquid nitrogen or dry ice, and subsequently milled to render a powder with particle sizes ranging 50-100 μm [47]. In the following step, this powder is dispersed under stirring into a cold aqueous surfactant solution. The resulting pre-suspension is subjected to various HPH cycles, maintaining the system temperature at or below room temperature. In general, LNs obtained by this technique present particle size and polydispersity that is higher than that of LNs obtained by hot homogenization [47].

## 5.3 Solvent emulsification/evaporation

LNs elaborated by solvent emulsification/evaporation are prepared by precipitation of an O/W emulsion in an aqueous medium. The bulk lipid is dissolved in a water-immiscible organic solvent and then emulsified in an aqueous phase. Immediately after solvent evaporation, nanoparticles are formed by precipitation of the lipid in the remaining aqueous phase. In 1992, Sjöström and Bergenståhl used this technique for preparing cholesterol acetate-loaded nanoparticles [60]. They used a mixture of lecithin and sodium glycolate as a stabilizing agent, and the nanoparticles produced by the procedure were around 25 nm. A few years later, Westesen reproduced this technique and prepared nanoparticles of tripalmitin [61]. The mean particle size, in the range of 30-100 nm, was affected by the nature of the surfactant and co-surfactant and the lipid concentration. Thus, smaller nanoparticles were produced using bile salts as co-surfactants and low lipid concentration (5%). More recently, del Pozo-Rodríguez et al. developed a cationic SLN for retinal gene therapy [51]. Nanoparticles were composed of the solid lipid Precirol® ATO 5, the cationic lipid DOTAP, and the surfactant Tween 80. SLNs, which were nanometric in size (281 nm) with a positive surface charge (+30 mV), had high transfection efficiency in the HEK293 cell line. The main advantage of this procedure is the avoidance of thermal stress during the whole process; nonetheless, the use of organic solvents that can remain in the final formulation is a clear limitation.

### 5.4 Microemulsion method

Microemulsion method is an easy technique for LN production, which avoids the use of organic solvents. Nonetheless, the drug is exposed to high temperatures during the process, which can be an issue for thermolabile substances. The first step of this technique consists of melting the bulk lipid (10ºC above the melting point) and solubilizing the drug in it. Then, the melted phase is placed into a hot aqueous phase containing surfactant and co-surfactants (if required) under mechanical agitation to form an O/W microemulsion. After that, the O/W microemulsion is rapidly cooled to 2-3ºC, with agitation, using an ice bath [52] or dispersing the emulsion droplets, drop wise, into a cold aqueous phase [53]. This sudden change in temperature allows lipid crystallization and subsequent LN formation. In fact, high-temperature gradients are preferred because they facilitate a rapid lipid crystallization and prevent LN aggregation [47,62]. Khare and co-workers observed that LN sizes increase with a higher lipid concentration due to increased viscosity of dispersed phase [53]. Marengo et al. showed that increasing the rate of addition of the hot emulsion into the cold aqueous phase diminished particle size and polydispersity [62].

### 5.5 W/O/W double emulsion

The W/O/W double emulsion is a method commonly used to encapsulate hydrophilic substances which has been proved effective in the formulation of lipid nanoparticles [63]. As in solvent emulsification/evaporation, thermal stress is avoided, making the procedure suitable for thermolabile substances such as peptides [64] or proteins [65]. However, the procedure uses organic solvents, which is a disadvantage. W/O/W double emulsions are prepared by a two-step process. In the first step, which forms the primary water-in-oil (W/O) emulsion, the drug is dissolved in water and then emulsified by sonication in an organic phase containing the lipids solubilized in a suitable solvent. In the second step, the primary W/O emulsion is transferred to an aqueous solution containing the surfactant, and mechanically emulsified by sonication to form the water-in-oil-in-water (W/O/W) emulsion. That emulsion is then stirred to allow organic solvent evaporation, leading to nanoparticle formation.

The final quality of the product can be optimized by identifying the variables that condition the physicochemical properties, such as the sonication time. Yousry et al. developed an optimized SLN for topical ophthalmic administration of vancomycin [54]. They utilized two consecutive full factorial designs to study the effect of different

variables on the properties of the SLNs. Results showed that sonication time significantly affected particle size, polydispersity, and zeta potential.

### 5.6 Quasi-emulsion solvent diffusion (QESD)

The fundamental principle of this method is based on the miscibility of certain organic solvents (i.e., acetone, ethanol) with water. Leonardi et al. described the procedure to elaborate neutral and cationic SLNs loaded with an antioxidant substance for ODD [55]. First, the bulk lipid (didecyldimethylammonium bromide, DDAB) and the drug (idebenone) were solubilized in a 1:1 mixture of ethanol:acetone. Then, the resulting solution was slowly injected into an aqueous phase containing the surfactant (Tween® 80) and kept at 0ºC under constant agitation with a high-shear force device. After 15 min stirring, the dispersion was sonicated for 4 min. At this point, the water-soluble dissolvents diffuse to the aqueous medium, causing lipid precipitation and SLN formation. Finally, the formulation was placed at room temperature under magnetic stirring for 24 h to allow the complete evaporation of organic solvents. The physicochemical properties of the final formulation depend on different variables, such as the sonication technique or the composition of the aqueous phase, but in general, satisfactory physicochemical properties are obtained using this method.

## 6. Bulk materials used for preparation of LNs

Adequate selection of bulk materials has an enormous impact in the final physicochemical and biopharmaceutical properties of each formulation. For example, Seyfoddin et al. showed an increase in the entrapment efficiency of acyclovir-loaded NLC from 37.85% to 91.64% depending on the type of liquid lipid used in the formulation [66]. **Table 1** summarizes the main bulk materials and properties associated with the formulations.

**Table 1. Commonly used materials in the elaboration of lipid nanoparticles for ocular drug delivery and the resulting physicochemical and biopharmaceutical properties of the formulation.**

| Materials | | Properties | | Ref |
|---|---|---|---|---|
| | | Physicochemical | Biopharmaceutical | |
| Solid lipids | Triglycerides *Dynasan® 116 (Tripalmitin)* | The SLNs had an appropriate size (248 nm) and zeta potential (+50.3 mV) for topical application. The nanocarrier exhibited sustained cyclosporine release over 48 h and good stability after 6 months of storage. | Cyclosporine was detectable *in vivo* in the aqueous and vitreous humors of sheep eyes for 48 hours. The authors attributed these results to the controlled and prolonged release of cyclosporine secondary to the enhanced residence time of the cationic SLNs in the eye. | [35] |
| | Partial glycerides *Compritol® (Glyceryl behenate)* | Compritol® was used in the formulation of voriconazole-loaded SLNs. The optimized formulation had an appropriate range of size and sustained release (60% drug released after 12 h). | The *ex vivo* studies revealed better corneal permeation of SLNs than the drug suspension. The *in vivo* studies showed that bioavailability of voriconazol in the aqueous humor of rabbit eyes was significantly superior to the drug suspension | [67] |
| | Fatty acids *Stearic acid* | Stearic acid was used to formulate levofloxacin-loaded SLNs. The optimized formulation provides a particle size of 237.82 nm and showed an entrapment efficiency of 78.71%. Both DSC and X-ray diffraction analysis revealed low degree of crystallinity in the lipid matrix and an amorphous state of the incorporated drug. | The developed SLNs exhibited good ability to diffuse across the goat cornea (69.54 µg/cm2 of levofloxacin in 4 h) without compromising corneal integrity. The antibacterial activity of the formulation was similar to the commercial eyedrops | [68] |
| Liquid lipids | Mygliol® *(Caprylic/ Capric Triglyceride)* | Mygliol® was selected as the liquid lipid because of good ocular biocompatibility and the ability to improve mangiferin loading and sustained release. The optimized NLCs presented a particle size of 51 nm and zeta potential of -36.5 mV. Entrapment efficiency was high (88.10%) and drug release was prolonged over 12 h (86.98% released). | Mangiferin-loaded NLCs promoted higher corneal penetration (4.31-fold increase in Papp) and significantly higher drug bioavailability in aqueous humor (5.69-fold increase in AUC) in comparison with drug solution. | [69] |

| | | | | |
|---|---|---|---|---|
| Cationic lipids | CTAB/DDAB | The *in vivo* transcorneal and transcleral penetration of two cationic LNs containing CTAB or DDAB as cationic lipids were evaluated. The entrapped drug was the hydrophilic molecule epigallocatechin. Both nanosystems exhibited a particle size under 150 nm and positive zeta potential, showing similarities in the drug release behavior | Both formulations reached the anterior and posterior segments of the eye after topical administration. CTAB-LNs were more appropriate for drug delivery to the anterior segment and DDAB-LNs for drug delivery to the posterior of the eye. Two formulations showed good ocular tolerance, confirmed by HET-CAM test and Draize test | [70] |
| Surfactants | Ionic *Sodium taurocholate* | Sodium taurocholate, in combination with Epikuron (amphoteric surfactant) was used to stabilize a dispersion of tobramycin-loaded SLNs. The particle size was under 100 nm showing a narrow size distribution (polydispersity index <0.2). The final drug content was as high as 2.5%. | The formulation had a 4-fold increase in the aqueous humor bioavailability of tobramycin (AUC) in comparison with reference eyedrops. The effect was associated with the small particle size and the corneal penetration enhancement attributed to surfactants. | [71] |
| | Non-ionic *Tween 80® (Polysorbate 80)* | Tween 80® was selected to stabilize cyclosporine-loaded SLNs. The increased surfactant concentration in drug-loaded SLNs resulted in smaller particle sizes and reduced zeta potential (absolute value). Also, Tween 80® conferred a protective effect against particle size growth during heat sterilization. Drug release was dependent on enzymatic degradation of SLNs. | The *in vitro* studies on RCE cells revealed significant toxicity of formulations after sterilization, probably due the partial leakage of Tween 80® from the nanostructure. The cyclosporine penetration through excised pig cornea after 2 h was 2-fold in comparison with drug suspension. | [72] |
| | Amphoteric *Phospholipon ® 90G (Phosphatidyl choline)* | The addition of Phospholipon to SLNs improved several physicochemical properties: diminished particle size (from ~180 nm to ~40 nm), increased timolol entrapment efficiency (from 36% to 44%), and provided sustained release with absence of burst effect | The modified SLNs provided a significantly higher sustained release of timolol through a bioengineered cornea, in comparison with the reference timolol solution | [73] |
| Surface modifiers | Chitosan | NLCs coated with chitosan oligosaccharides (3,000-6,000 kDa) demonstrated improved efficiency in the delivery of flurbiprofen to the eye. A range of chitosan coating concentrations from 0% to 0.8% was evaluated. The increasing in chitosan concentration results in higher particle size, ranging from 55.4 to 169.9 nm; and higher zeta potential ranging from -0.446 to +20 mV. | The presence of chitosan coating increased 7.7-fold drug bioavailability (AUC) and 2.4-fold drug permeability (Papp) in eye rabbits in comparison with un-coated NLCs. The changes were attributed to increased residence time due the bioadhesive properties and to improved drug penetration through cornea. | [74] |

### 6.1 Lipids

Mehnert et al. summarized the influence of ingredient composition on the final quality of the LNs [47]. Lipid type and properties, namely hydrophobicity, crystallization behavior, and shape of the lipid crystals are critical parameters for nanoparticle formation [47]. Other variables affecting properties of LNs include lipid concentration [53,61] and the physical state of the lipid [75].

#### 6.1.1 Solid lipids

Solid lipids used in the elaboration of LNs include triglycerides, partial glycerides, fatty acids, steroids, and waxes [47]. Triglycerides are esters derived from glycerol and three fatty acids (e.g., palmitic acid), and they are differentiated by the hydrocarbon chain length of the fatty acid. Many triglycerides have been used in the preparation of LNs, such as tricarpin, trilaurin (Dynasan® 112), trimyristin (Dynasan® 114), tripalmitin (Dynasan® 116), and tristearin (Dynasan® 118) [8,76]. In general, longer hydrocarbon chain lengths are associated with high melting points and greater nanoparticle stability. However, experts recommend using a combination of lipids with different chain lengths to improve drug loading and prevent abnormal lipid crystallization. It is important to note that the behavior of colloidal nanosystems can greatly differ from the lipid bulk material [76]. Therefore, the type of lipid should be carefully selected based on the properties desired for the final product.

Partial glycerides (e.g., Compritol®, Gelucire®, Precirol®) are mixtures of mono-, di-, and triglycerides commonly used to formulate SLNs loaded with drugs with poor solubility [67]. The combination of different types of glycerides increases SLN drug loading and prevents lipid re-crystallization.

Stearic acid is a fatty acid widely used for preparation of SLNs for ODD [68,71,77]. Kalam et al. showed that for nanoparticle preparation, a lipid mixture of stearic acid with Compritol® is preferred instead of the fatty acid alone [77]. They observed that SLN formed by the combination of both lipids presented low crystallinity and subsequent high drug loading and better stability.

Cholesterol, a steroid commonly used in the formulation of liposomes, has also been used in the elaboration of LNs [78]. The developed formulation showed adequate physicochemical properties and the absence of tissue damage after contact with ocular structures.

Jenning et al. showed that SLNs formulated with waxes presented better physical stability but lower drug entrapment than those formulated with glycerides [79]. They

related these outcomes with the high degree of crystallinity of waxes after particle solidification, in contrast to the disordered lattices of SLN-elaborated with glycerides.

### 6.1.2. Liquid lipids

Liquid lipids are oils composed of medium to short hydrocarbon chains with a melting point less than body temperature. Solid lipids are mixed with liquid lipids at ratios from 70:30 up to 99.9:0.1 to form NLCs [80]. Some examples of liquid lipids used in the formulation of NLCs for ODD are oleic acid [48], castor oil [50], squalene [81], Mygliol® [50,69,82], and mixtures thereof [50]. Gonzalez-Mira used a mixture of Mygliol® and castor oil (ratio 70:30) to produce NLCs for topical ophthalmic use [50]. They selected these liquid lipids based on safety concerns for ocular administration and on the capacity for drug solubilization. Furthermore, this lipid combination allowed the formation of NLCs with small particle size even when the total lipid content reached 10%.

### 6.1.3 Cationic lipids

The structure of cationic lipids consists of a positively charged head group and one or two hydrocarbon chains or steroid structures (Pensado et al., 2014). Cationic lipids, such as DDAB or DOTAP (1,2-dioleoyl-3-trimethylammoniumpropane) are frequently used in topical ODD. The presence of cationic moieties at the nanosystem surface gives the LNs a positive charge that can establish electrostatic interactions with the negatively charged corneal epithelium. Leonardi et al. showed that by using the cationic lipid DDAB in the formulation of melatonin-loaded SLNs, both mucoadhesion and preocular retention were enhanced in rabbit eyes. In fact, the hypotensive effect of the drug was maintained up to 24 h after a single topical administration [37]. Cationic lipids also are present in several formulations for ocular gene delivery [46,83,84]. In these cases, the function of the lipid is twofold. First, it facilitates the adsorption of the negatively charged genetic material onto the nanoparticle surface, protecting it from enzymatic degradation. Second, the positive charge of the LN-genetic complex allows the interaction with the corneal epithelium, increasing the residence time and transfection efficiency. Other examples of cationic lipids approved for ophthalmic use are quaternary ammoniums such as cetyl trimethylammonium bromide (CTAB), benzalkonium chloride, cetylpyridinium chloride, and benzethonium chloride [85].

## 6.2 Surfactants

Surfactants are amphiphilic molecules (polar head and nonpolar tail) for which the main role is stabilizing formulations by reducing the surface tension between the

different phases. Selection of adequate surfactants (and co-surfactants if required) is a crucial step in the design of LNs for ocular administration. The type of surfactant not only determines the physicochemical properties of the nanosystem, but it also conditions the biocompatibility [8]. Importantly, the cytotoxicity of LNs is more dependent on the nature of the surfactant than on the nature of the lipids that form them [86]. Thus, the adequate selection of surfactant type and concentration should be a compromise between stability and toxicity.

According to the charge, surfactants can be classified as ionic, non-ionic, and amphoteric [87]. Non-ionic surfactants, such as sorbitan esters (e.g., Span 80) or polysorbates (e.g., Tween® 80) present lower toxicity and irritancy than ionic ones. Pensado et al. developed a novel type of solid nanoparticle for ocular gene therapy using Span 80 and oleylamine. In this case the function of Span 80 was not to act as a surfactant, but rather as the main component of the nanoparticle (Pensado et al., 2014). The nanosystem showed excellent biocompatibility and high transfection efficiency. Other commonly used surfactants in ODD are poloxamers, cremophors, tyloxapol, and vitamin E TPGS (D-α-tocopherol polyethylene glycol 1000 succinate) [85].

### 6.3 Surface modifiers

Different approaches had been proposed by scientists to increase nanoparticle residence time in the precorneal area, such as the use of viscosity enhancers [89], *in situ* gelling polymers [90], and nanoparticle surface modifiers [91]. The main purpose of surface modifiers is to maximize the interaction of the LNs with OS structures and/or promote nanoparticle penetration. The most used surface modifiers are described below.

#### 6.3.1. Chitosan

Chitosan (CS) is a biocompatible cationic polysaccharide obtained by the deacetylation of chitin from crustacean and insect shells. Chitosan acts not only as a mucoadhesive polymer [92], but it also increases drug penetration by reversibly opening the tight junctions present between the corneal epithelial cells [93]. The main limitation of this polymer is low solubility at physiological pH. A commonly used technique to ameliorate this problem is to decrease the molecular weight of the polymer, obtaining chitosan oligosaccharides (COS). Cationic LNs can be obtained by using CS [40,52] or COS [48,74] as surface modifiers. These decorated nanoparticles can electrostatically interact with the negatively charged corneal epithelium (**Figure 3-1**), resulting in an extended residence time on the ocular surface. This, along with the penetration

enhancement effect, leads to a significant improvement of drug bioavailability, as seen with the anti-inflammatory drug flurbiprofen [74].

### 6.3.2. Hyaluronic acid

Hyaluronic acid (HA) is a biocompatible and biodegradable non-sulfated glycosaminoglycan composed of repeating disaccharides of (β, 1–4)-glucuronic acid and (β, 1-3)-N-acetyl glucosamine. This polymer is naturally present in the extracellular matrix of many soft connective tissues, which, along with other structural macromolecules, contributes to the maintenance of tissue structural integrity [94]. Also, HA plays a regulatory function through binding to HA cell receptors. HA cell surface receptors, namely CD44 and the receptor for hyaluronan-mediated motility (RHAMM), are distributed throughout different body tissues, including the ocular surface epithelia (mainly corneal epithelium), where they control cell regeneration and migration [95]. The presence of these receptors in therapeutic targets such as the cornea can be precisely exploited if LNs are functionalized with HA to obtain a targeted drug delivery system [96]. Nanoparticle interaction with HA receptors facilitates cell internalization of the therapeutic agent (**Figure 3-2**), improving delivery efficacy [97]. Interestingly, formulation parameters such as the molecular weight of the HA component of the nanoparticles determines receptor binding affinity [98] and degree of bioadhesion [99]. Apaolaoza et al. developed and evaluated *in vitro* a HA-SLN complex for ocular gene therapy [83]. In this case, the function exerted by HA was twofold. The presence of HA directed the SLN to the CD44 receptors, maximizing particle uptake. It also facilitated the release of genetic material to the nuclei of the epithelial cells, improving transfection efficiency.

### 6.3.3. Polyethylene glycol

Polyethylene glycol (PEG) is a hydrophilic and non-ionic polymer with high chain flexibility. Surface coating of nanoparticles with this polymer is termed *pegylation.* Pegylation is a commonly used strategy to increase nanosystem residence time in biological fluids, resulting in better drug delivery efficiency. The rationale behind this increase is that PEG chains act as a shield that covers the nanoparticle surface, avoiding opsonization by surrounding proteins and thereby preventing macrophage clearance [100]. The prevention of opsonization by pegylation is sometimes referred to as the *stealth effect*. Curiously, if the concentration of stealth agents is excessive, pegylation can reduce drug efficacy because it can inhibit phagocytic uptake in target cells. Despite this, PEG coating offers helpful advantages when coating nanocarriers for topical

ophthalmic administration. These advantages include physical stabilization of formulations by steric hindrance and thus the prevention of aggregate formation [101], increased biological stability of colloidal dispersions in the presence of body fluids [102], and enhanced particle penetration through the mucus layer (**Figure 3-3**) [103,104]. Interestingly, surfactants such as poloxamers, polysorbates (i.e., Tween® 80), and vitamin E TPGS that contain PEG chains can be easily incorporated during LN elaboration due to its amphipathic nature, obtaining formulations with the aforementioned advantages [105]. Olbrich et al. reported that the steric effect attributed to the PEG chains of Poloxamer 407 and Tween® 80 partially hinders the degradation of SLNs by lipases, making these surfactants very useful for controlling the degradation rate of LNs and subsequent drug release [106].

**6.3.4. Thiolated polymers**

To improve bioadhesion, polymers such as chitosan, hyaluronic acid, and polyethylene glycol can be chemically modified to incorporate thiol groups. These moieties can interact through covalent bonding with cysteine-rich subdomains present in corneal mucins (**Figure 3-4**). The resulting disulfide bonds are much stronger and more stable than non-covalent bonds (hydrogen bonds, ionic interactions, etc.) or physical entanglements formed with unmodified polymers [107]. Furthermore, thiolated polymers possess permeation enhancing properties associated with the opening of tight junctions between epithelial cells [107]. Li et al. compared topically applied LNs coated with three different types of chitosan derivatives, including a thiolated form [108]. The formulation coated with thiolated chitosan had higher retention and an 18.8-fold increase in the apparent permeability coefficient in comparison with control eyedrops. Shen et al. studied the distribution of a thiolated-PEG NLC containing cyclosporine after topical administration to rabbit eyes [109]. The nanocarrier prolonged drug pre-corneal residence time up to 6 h and delivered significantly higher cyclosporine levels to anterior segment tissues compared with those of the NLC without thiol modification.

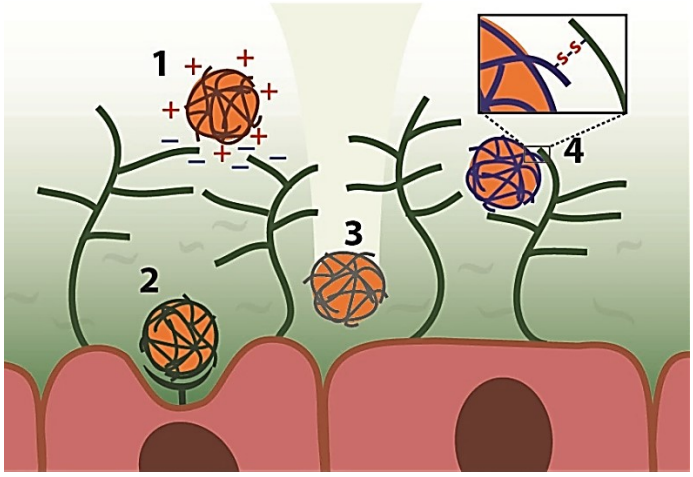


**Figure 3. Influence of surface modifiers on lipid nanoparticle interactions with the ocular surface.** (1) electrostatic interaction between sialic groups of corneal mucins and chitosan-coated lipid nanoparticles; (2) HA receptor-mediated endocytosis of HA-coated lipid nanoparticles; (3) PEG coating favors mucus penetration by lipid nanoparticles; (4) thiolated polymers establish disulfide bonding with corneal mucins.

## 7. Optimization of LNs for topical ocular drug delivery

An essential step in the development of any formulation is the optimization of the technological parameters according to the route of administration and the therapeutic objective. In this case, different physicochemical characteristics of LNs must to be considered such as particle size, surface charge, entrapment efficiency, drug loading, drug release, physicochemical stability, and stability in the biological media. Furthermore, all formulations developed for ODD must comply with other quality specifications, including requirements for sterility, osmolality, pH, viscosity and surface tension properties [147].

### 7.1 Particle size

It is generally accepted that nanoparticles with smaller sizes are more suitable for topical administration than larger ones [110]. From a biopharmaceutical point of view, this can be attributed to the fact that small size facilitates a faster travel of nanoparticles through the mucus layer of the tear film [103] and favors corneal uptake by epithelial cells [111]. From a technological perspective, smaller particle size increases the stability of the dispersion during storage, avoiding the formation of aggregates [112]. Additionally, LNs smaller than 0.2 μm can be easily sterilized by filtration [47], an important issue when other sterilization techniques cannot be applied due to particle instability or by encapsulating labile drugs. Numerous factors can condition the particle

size of LNs. For instance, increasing the liquid lipid proportion results in a lower particle size due to inhibition of solid lipid recrystallization phenomena upon solidification [113]. Another critical issue is the adequate selection of surfactant(s). Cavalli et al. showed that using a combination of different surfactants results in a smaller sized particle, compared with those produced using only one surfactant [114]. Also, ionic surfactants rendered the smallest particles, in comparison with non-ionic ones [114]. Certain parameters of the production methods, such as sonication time [54], and parameters of the post-production processes, such as temperature of sterilization [72], can also significantly alter the final particle diameter.

### 7.2 Zeta potential

Along with size, particle surface charge, measured as the zeta potential, is the most studied characteristic of nanoparticles because of its relevance in critical aspects such as formulation stability and nanosystem interaction with biological matrices. Regarding formulation stability, an absolute value of |30| mV is sufficient for full electrostatic stabilization of particle dispersion. Whereas, for LNs coated with surfactants with steric properties (i.e., Vitamin E TPGS), the zeta potential value required to make a stable formulation is smaller [112]. As mentioned before, one of the main objectives of topical LNs is to maximize the interactions with the OS structures to increase the residence time in the precorneal area. In this respect, the majority of scientists in our community agree that positive zeta potential values are preferable to promote the electrostatic interaction with the negatively charged sialic acid residues of corneal mucins [37,70,74,83]. Zeta potential can be influenced by different parameters affecting particle surface, such as surfactant composition [115], drug distribution into the nanoparticle [116], and post-production processes such as sterilization and freeze drying [87].

### 7.3 Entrapment efficiency and drug loading

Optimization of drug-related parameters is critical to develop a nanosystem that is feasible for clinical use. High values of entrapment efficiency are desired because this means that the drug can be successfully incorporated into the nanosystem, avoiding the waste of drug during elaboration. Also, it is necessary to consider the drug payload of the formulation. Increased drug loading enables the production of formulations with high doses, thereby reducing the content of the excipients, which improves the biocompatibility profile [117]. Lipid composition and drug solubility are critical factors that determine drug incorporation into LNs. As described above, for hydrophobic drugs, mixtures of solid lipids of different chain lengths with liquid lipids are preferred

because of the ability to accommodate a greater number of drug molecules in the spaces created between the carbon chains, improving both the entrapment efficiency and the drug loading [28]. When slightly water soluble drugs need to be encapsulated, lower temperatures during the production process are recommended, with the purpose of reducing drug solubility in water and preventing drug partitioning into the aqueous phase [28]. In the case of hydrophilic drugs, the most studied approach is to convert the drug in a fat-soluble lipid-drug conjugates. By employing this technique, drug payload can reach values up to 33% [29]. Nonetheless, careful evaluation of the structure of the final drug-loaded nanocarrier, i.e., by nuclear magnetic resonance spectroscopy, is recommended. It is important to document effective particle solidification because an excessive payload can induce supercooled melts instead of a solid structure [112].

### 7.4 Drug release

Another relevant aspect in the development of any formulation is the control of the drug liberation kinetics to the biological environment. This is necessary to keep the drug concentration in the therapeutic range. To achieve proper liberation kinetics, optimization is focused on obtaining LNs with controlled and prolonged drug release. Drug release is a parameter strongly linked with drug distribution in the LNs. Depending on different factors, such as particle composition or production method, the drug can be homogenously dispersed within each nanoparticle or, in contrast, it may form drug-enriched zones within each nanoparticle [118]. In the first case, which is the ideal situation, the drug is slowly released from the LNs, obtaining a sustained liberation over time. In the second case, the drug is quickly released (*burst* effect) because of its disposition in the outer layers of LN. If the drug-enriched zone is placed in the core of the LNs, drug diffusion is governed by surrounding the lipids that form the outer layers of nanoparticles and effectively act as a membrane [118]. The burst effect can also be minimized with the incorporation of phospholipids in the outer layers of the LNs [73] or using surface modifiers such as thiolated PEG-stearate [119]. Another factor that greatly conditions drug release from the LNs is the type of surfactant employed. Surfactants influence drug release either by particle size reduction [120] or by preventing particle degradation by biological enzymes [106].

### 7.5 Physicochemical and biological stability

Despite the demonstrated safety of LNs with respect to the component biocompatible lipids, alterations in the physicochemical stability can occur and lead to toxicity issues. Problems such as the sedimentation of LNs during storage result in poor

drug homogeneity in the instilled formulation, making it impossible to know if the dosage is correct. Problems affecting the physicochemical stability of LNs have been reviewed by Shah et al. [87]. According to these authors, lipid stability plays a crucial role in the stability of the whole formulation. Because lipids are the main constituents of LNs, minor alterations in the lipid matrix can drastically change the entire structure of the nanosystem. An example of such a change is the modification in lipid crystallinity that can occur by a shift in the polymorphic state, causing an unstable organization (α polymorph) to become more stable (ß'/ß polymorphs) [87]. The subsequent molecular reorganization of the LN inner structure is frequently associated with drug leakage, which negatively affects drug loading capacity and drug release kinetics. A common approach to prevent this phenomenon is the use of liquid lipids to increase molecular mobility and prevent the transition to the crystalline state [87].

Other frequent stability issues are related to modifications in LN dispersion such as particle growth (Ostwald ripening phenomenon), flocculation, and creaming/sedimentation. Changes in particle size and zeta potential during storage can be good predictors of these instability problems [87]. To avoid particle dispersion problems, the appropriate selection of surfactant is essential. The combination of surfactants that provide electrostatic (ionic surfactants) and steric stabilization (e.g., PEG-containing surfactants) is recognized as an efficient approach to ensure dispersion stability [121].

Chemical stability of LNs is another aspect that is necessary to consider because the aqueous environment surrounding LNs is propitious for the appearance of degradative hydrolytic processes. For this reason, different techniques in which water is eliminated from the formulation, such as spray-drying [122] or freeze-drying [123], can be applied.

Few reports have studied the stability of LNs after they come into contact with biological fluids [102,124]. Nonetheless, this issue is of great relevance because the physicochemical properties of nanoparticles may change drastically due to interfacial interactions with surrounding biomolecules [125]. The resulting nanoparticle-biomolecule complex will not only condition the stability of the particle dispersion, but also affect cellular uptake and biodistribution [125]. Thus, some molecules present in the tear film, such as mucins and lactoferrin, can influence nanoparticle zeta potential [126] and drug release [127].

### 7.6 Other quality specifications

When ocular administration of LNs is sought, parameters such as sterility, pH, isotonicity, viscosity, and surface tension properties should be considered.

Sterility is a basic requirement for any parenteral or ophthalmic formulation. Because aseptic elaboration is usually too expensive, different techniques had been implemented for the sterilization of the final formulation, including heating, gamma-irradiation, and filtration [47]. Clearly, some sterilization procedures, such as elevated temperatures, can seriously affect the final physicochemical characteristics of the LNs [72]; hence, a careful selection of the sterilization technique is essential.

Any LN formulation should have a pH closer to physiological values, which range between 6.9 and 7.5 [128]. Although the buffering capacity of tears can quickly accommodate the instillation of a solution with a pH of 5.5 [129], an appropriate pH range for ODD is considered to be between 6.8 and 8.2 [130]. Regarding tonicity, the eye can tolerate osmolality values ranging from 150 to 320 mOsm/L without causing great discomfort [131]. Nonetheless, isotonic formulations of around 290 mOsm/L are preferred.

Thickening agents, such as poloxamers [90] or carbomers [132], are frequently included in the preparation of topical ocular formulations. The purpose of these agents is to increase formulation residence time on the OS and to reduce physiological drug drainage. Viscosity values ranging from 1-15 mPa·s improve drug delivery efficiency, with the optimal being around 12-15 mPa·s [133]. Higher viscosity may induce OS irritation, resulting in reflex blinking and lacrimation.

In addition to the above requirements, the developed formulation needs to have appropriate surface tension properties. The optimum formulation should have a low contact angle between the instilled droplet and the ocular surface, which means a suitable spreading coefficient and an adequate degree of "wettability" [7], which ultimately improve the residence time. This contact angle may decrease if appropriate surfactants are selected. Cationic surfactants are preferred rather than anionic, because the former reduce the contact angle due to their electrostatic interaction with negatively charged corneal epithelium [7].

## 8. Biocompatibility of LNs

An essential step in the development of a novel drug delivery system is to evaluate its biocompatibility in order to demonstrate preclinical safety. As mentioned above, ocular safety of LNs is primarily conditioned by adequate selection of bulk materials.

In this regard, the lipid-core material of LNs is composed by physiological lipids and/or GRAS substances which are considered safe. Nonetheless, Doktorovova et al. found contradictory data about safety of commonly used lipids [134]. Doktorovova states that whereas there are authors reporting absence of cytotoxicity of LNs containing 1 mg/mL stearic acid, other reported a high cytotoxic effect at this level of concentration (2.2% cell viability). They attributed these discrepancies to the different *in vitro* models used for evaluating cell viability, and to the absence of adequate controls studying the cytotoxicity of raw materials *per se*.

However, main biocompatibility concerns are due to presence of surfactants or cationic lipids in the formulation. Leonardi et al. deepened evaluated the *in vivo* ocular tolerance of six surfactants commonly used in the preparation of LNs for ODD [135]. For this end, they prepared various batches of LNs using Dynasan® 114 as the lipid matrix stabilized by different surfactant concentrations. The biocompatibility of nanosystems was evaluated in rabbit eyes using the Draize test. They found that LNs elaborated with the non-ionic surfactant Kolliphor® P188 were well tolerated by the ocular surface without any detectable irritant sign even up to a surfactant concentration of 0.4% (w/v). In contrast, for those LNs elaborated with the non-ionic surfactants Tween® 80 or Kolliphor® HS 15, the maximum surfactant concentration that could be considered safe was 0.05% (w/v).

Some cationic lipids, such as quaternary ammonium derivatives were widely used in the field of ODD because of its antimicrobial properties. These cationic substances interact with the negatively charged surface of bacteria disrupting their cell membranes. However, this cytotoxic mechanism is not only limited to microorganisms but it also can damage corneal epithelial cells after chronic exposures [136]. Interestingly, in 2002, Sznitowska documented that cytotoxicity of quaternary ammonium derivatives was diminished or neutralized in the presence of emulsions [137]. This was attributed to the fact that cationic lipids were attached to the droplets of the emulsion and only a minor fraction thereof was free in the aqueous phase to exert the cytotoxic effect. Probably this was one of the reasons of the good ocular biocompatibility showed by the LNs formulated with these cationic substances [70].

## 9. Case study: topical ocular delivery of cyclosporine using LNs

Cyclosporine is a natural immunosuppressant drug isolated from the fungus *Tolypocladium inflatum*. This cyclic undecapeptide is effective in the treatment of ocular diseases involving the activation of immune system, such as vernal

conjunctivitis, dry eye syndrome, and in the prevention of corneal allograft rejection [138]. Nonetheless, administration of this drug constitutes a pharmaceutical challenge due to its physicochemical properties. Cyclosporine is a lipophilic compound practically insoluble in aqueous media (6.6 μg/mL) [139], and therefore it cannot be formulated as conventional eyedrops. Historically, when topical administration was considered, cyclosporine was dissolved and administered in lipid matrices, typically vegetable oils. However, vegetable oils, such as olive oil, are not well tolerated by ocular surface structures, and they cause a burning sensation on the conjunctiva [140,141]. Furthermore, these oil-based media are incapable of delivering high concentrations of any drug to the therapeutic target [142]. In recent decades, scientists developed different types of drug delivery systems to overcome problems associated with traditional oil-based formulations [143]. In a recent work, Sánchez-López et al. extensively reviewed the potential of LNs for the treatment of different ocular pathologies [144].

LNs are promising modified eyedrops because they can facilitate the topical administration of drugs like cyclosporine that have less favorable biopharmaceutical properties. Understanding of the association between LN physicochemical properties and the important biopharmaceutical properties is essential to design an efficient drug delivery system. In the development of a NLC for topical ocular administration of cyclosporine, Shen et al. studied the incorporation of a liquid lipid (Mygliol®) on the physicochemical and biopharmaceutical properties of nanosystems [113]. The addition of Mygliol® not only increased the LN drug loading due to an inhibition of recrystallization of the lipid matrix, but it also improved the *vitro* cellular uptake. Also, the liquid lipid gave the nanostructure more flexibility, favoring LN penetration through the mucus layer and increasing the contact time with the OS. The developed nanosystem exhibited good ocular biocompatibility, confirmed *in vitro* by a cell viability tests and *in vivo* by an ocular tolerance assay.

Another parameter that greatly affects LN interaction with the ocular structures is the surface charge. Battaglia and colleagues studied the effect of surface charge on the distribution of cyclosporine-loaded LNs throughout the ocular tissues [145]. Using a coacervation technique, they prepared three types of SLNs: non-ionic, anionic, and cationic. The solid lipid was stearic acid, and the surface modifiers were arabic gum (for anionic SLNs) and chitosan hydrochloride (for cationic SLNs). They evaluated the accumulation and penetration of the drug through *ex vivo* excised rabbit corneas, using a fluorescent-labelled version of cyclosporine (isocyclosporine A-FMOC). They found

significantly higher penetration of all three SLNs in comparison with controls (drug suspension and emulsion). Nonetheless, only the cationic nanosytem provided higher drug accumulation values than those obtained with drug suspension, possibly due to the enhancement in nanoparticle cell uptake attributed to chitosan coating. None of the developed formulations showed *in vivo* corneal irritation, making them appropriate for ODD.

Sandri et al. evaluated the suitability of two types of cationic SLNs for the topical administration of cyclosporine [146]. Both types of nanoparticles were produced by the high shear homogenization and ultrasound technique. The solid lipids were Compritol® and Precirol®, and the surface modifier was chitosan hydrochloride. The optimized formulations showed appropriate physicochemical properties for ophthalmic administration, including the size below 200 nm for each nanoparticle and zeta potentials of +27.9 mV for Compritol-SLN and +30.1 mV for Precirol-SLN. In addition, entrapment efficiencies were quite high, 94% and 81%, respectively. Regarding formulation stability, Compritol-SLN had good physical stability up to 3 months of storage at 4ºC for both the cyclosporine-loaded and unloaded formulations. In contrast, the Precirol-SLNs drastically increased particle size after 30 days of storage in the same conditions. They used *in vitro* (rabbit corneal endothelial cell cultures) and *ex vivo* (excised pig corneas) studies to evaluate the interaction of the SLNs with biological structures. Both types of SLNs had better cyclosporine penetration and permeation than the drug suspension alone, although Compritol-SLN had higher values than Precirol-SLNs for both parameters. Furthermore, both nanosystems were biocompatible, having cell viability values close to 100% after 1 and 2 h of exposure.

## 10. Conclusions

The main purpose of this work was to offer help to any researcher who is beginning scientific labor in the field of LNs for ODD. The design of novel topical ODD systems is focused to overcome the main eye barriers and improve the therapeutic efficiency without compromising safety and patient compliance. In recent decades, LNs have been designed and studied as ODD systems to provide alternatives to the conventional dosage forms. Throughout these studies, the ocular tolerance and biocompatibility of LNs have been demonstrated, showing promising results in terms of their physicochemical and biopharmaceutical properties.

In this review we analyzed, from a technical perspective, the available literature of LNs use for topical ODD. The influence of different technological parameters in the final properties of LNs was presented. Finally, commonly used approaches to optimize these parameters were discussed.

**Acknowledgements:**

This work was supported by grants from the Ministry of Economy and Competitiveness of Spain (MAT2013-47501-C02-R), Xunta de Galicia (Competitive Reference Groups, FEDER Funds, Ref. 2014/043), and FPI Scholarship Program (BES-2014-069437)

**References**


[1] A. Patel, K. Cholkar, V. Agrahari, A.K. Mitra, Ocular drug delivery systems: An overview, World J. Pharmacol. 2 (2013) 47–64. doi:10.5497/wjp.v2.i2.47 [doi].

[2] J. Araujo, E. Gonzalez, M.A. Egea, M.L. Garcia, E.B. Souto, Nanomedicines for ocular NSAIDs: safety on drug delivery, Nanomedicine. 5 (2009) 394–401. doi:10.1016/j.nano.2009.02.003 [doi].

[3] S. Kirchhof, A.M. Goepferich, F.P. Brandl, Hydrogels in ophthalmic applications., Eur. J. Pharm. Biopharm. 95 (2015) 227–238. doi:10.1016/j.ejpb.2015.05.016.

[4] H. Almeida, M.H. Amaral, P. Lobao, C. Frigerio, J.M. Sousa Lobo, Nanoparticles in Ocular Drug Delivery Systems for Topical Administration: Promises and Challenges., Curr. Pharm. Des. 21 (2015) 5212–5224.

[5] A. Mandal, R. Bisht, I.D. Rupenthal, A.K. Mitra, Polymeric micelles for ocular drug delivery: From structural frameworks to recent preclinical studies, J. Control. RELEASE. 248 (2017) 96–116. doi:10.1016/j.jconrel.2017.01.012.

[6] X. Wang, S. Wang, Y. Zhang, Advance of the application of nano-controlled release system in ophthalmic drug delivery, DRUG Deliv. 23 (2016) 2897–2901. doi:10.3109/10717544.2015.1116025.

[7] L. Gan, J. Wang, M. Jiang, H. Bartlett, D. Ouyang, F. Eperjesi, J. Liu, Y. Gan, Recent advances in topical ophthalmic drug delivery with lipid-based nanocarriers., Drug Discov. Today. 18 (2013) 290–297. doi:10.1016/j.drudis.2012.10.005.

[8] E.B. Souto, S. Doktorovova, E. Gonzalez-Mira, M.A. Egea, M.L. Garcia, Feasibility of lipid nanoparticles for ocular delivery of anti-inflammatory drugs., Curr. Eye Res. 35 (2010) 537–52. doi:10.3109/02713681003760168.

[9] R. Pignatello, C. Carbone, C. Puglia, A. Offerta, F.P. Bonina, G. Puglisi, Ophthalmic applications of lipid-based drug nanocarriers: an update of research and patenting activity., Ther. Deliv. 6 (2015) 1297–1318. doi:10.4155/tde.15.73.

[10] W. Zhang, M.R. Prausnitz, A. Edwards, Model of transient drug diffusion across cornea, J. Control. Release. 99 (2004) 241–258. doi:10.1016/j.jconrel.2004.07.001 [doi].

[11] S. Mishima, A. Gasset, S.D. Klyce, J.L. Baum, Determination of tear volume and tear flow., Invest. Ophthalmol. 5 (1966) 264–76. http://www.ncbi.nlm.nih.gov/pubmed/5947945.

[12] Loftssona, Jarvinen, Cyclodextrins in ophthalmic drug delivery., Adv. Drug Deliv. Rev. 36 (1999) 59–79. doi:10.1016/S0169-409X(98)00055-6.

[13] A. Urtti, L. Salminen, Minimizing systemic absorption of topically administered ophthalmic drugs., Surv. Ophthalmol. 37 (1993) 435–456. doi:10.1016/0039-6257(93)90141-S.

[14] T.J. Mikkelson, S.S. Chrai, J.R. Robinson, Altered bioavailability of drugs in the eye due to drug-protein interaction., J. Pharm. Sci. 62 (1973) 1648–1653. doi:10.1002/jps.2600621014.

[15] S. Duvvuri, S. Majumdar, A.K. Mitra, Role of metabolism in ocular drug delivery., Curr. Drug Metab. 5 (2004) 507–515. doi:10.2174/1389200043335342.

[16] W. Wang, H. Sasaki, D.S. Chien, V.H. Lee, Lipophilicity influence on conjunctival drug penetration in the pigmented rabbit: a comparison with corneal penetration., Curr. Eye Res. 10 (1991) 571–579. doi:10.3109/02713689109001766.

[17] A. Urtti, H. Rouhiainen, T. Kaila, V. Saano, Controlled ocular timolol delivery: systemic absorption and intraocular pressure effects in humans., Pharm. Res. 11 (1994) 1278–1282. doi:10.1023/A:1018938310628.

[18] B. Yanez-Soto, M.J. Mannis, I.R. Schwab, J.Y. Li, B.C. Leonard, N.L. Abbott, C.J. Murphy, Interfacial phenomena and the ocular surface., Ocul. Surf. 12 (2014) 178–201. doi:10.1016/j.jtos.2014.01.004.

[19] Y. Zambito, G. Di, Polysaccharides as Excipients for Ocular Topical Formulations, in: Biomater. Appl. Nanomedicine, InTech, 2011. doi:10.5772/24430.

[20] M. Malhotra, D.K. Majumdar, Permeation through cornea., Indian J. Exp. Biol. 39 (2001) 11–24. http://www.ncbi.nlm.nih.gov/pubmed/11349520.

[21] J.W. Sieg, J.R. Robinson, Mechanistic Studies on Transcorneal Permeation of Pilocarpine, J. Pharm. Sci. 65 (1976) 1816–1822. doi:10.1002/jps.2600651230.

[22] R. Gaudana, H.K. Ananthula, A. Parenky, A.K. Mitra, Ocular Drug Delivery, AAPS J. 12 (2010) 348–360. doi:10.1208/s12248-010-9183-3.

[23] L. Battaglia, L. Serpe, F. Foglietta, E. Muntoni, M. Gallarate, A. Del Pozo Rodriguez, M.A. Solinis Aspiazu, Application of lipid nanoparticles to ocular drug delivery, Expert Opin. Drug Deliv. 5247 (2016) 17425247.2016.1201059. doi:10.1080/17425247.2016.1201059.

[24] J.H. Kim, K. Green, M. Martinez, D. Paton, Solute permeability of the corneal

endothelium and Descemet's membrane., Exp. Eye Res. 12 (1971) 231–8. doi:10.1016/0014-4835(71)90143-6.

[25] A. Seyfoddin, J. Shaw, R. Al-Kassas, Solid lipid nanoparticles for ocular drug delivery., Drug Deliv. 17 (2010) 467–489. doi:10.3109/10717544.2010.483257.

[26] R.H. Müller, K. Mäder, S. Gohla, Solid lipid nanoparticles (SLN) for controlled drug delivery – a review of the state of the art, Eur. J. Pharm. Biopharm. 50 (2000) 161–177. doi:10.1016/S0939-6411(00)00087-4.

[27] K. Westesen, H. Bunjes, M.H.. Koch, Physicochemical characterization of lipid nanoparticles and evaluation of their drug loading capacity and sustained release potential, J. Control. Release. 48 (1997) 223–236. doi:10.1016/S0168-3659(97)00046-1.

[28] R.. Müller, M. Radtke, S.. A. Wissing, R.H. Muller, M. Radtke, S.. A. Wissing, Nanostructured lipid matrices for improved microencapsulation of drugs., Int. J. Pharm. 242 (2002) 121–128. doi:10.1016/S0378-5173(02)00180-1.

[29] C. Olbrich, A. Gessner, O. Kayser, R.H. Müller, Lipid-Drug-Conjugate (LDC) Nanoparticles as Novel Carrier System for the Hydrophilic Antitrypanosomal Drug Diminazenediaceturate, J. Drug Target. 10 (2002) 387–396. doi:10.1080/1061186021000001832.

[30] C. Puglia, A. Offerta, C. Carbone, F. Bonina, R. Pignatello, G. Puglisi, Lipid Nanocarriers (LNC) and their Applications in Ocular Drug Delivery, Curr. Med. Chem. 22 (2015) 1589–1602. doi:10.2174/0929867322666150209152259.

[31] S. Gao, D.J. McClements, Formation and stability of solid lipid nanoparticles fabricated using phase inversion temperature method, Colloids Surfaces A Physicochem. Eng. Asp. 499 (2016) 79–87. doi:10.1016/j.colsurfa.2016.03.065.

[32] M. García-Fuentes, D. Torres, M.. Alonso, Design of lipid nanoparticles for the oral delivery of hydrophilic macromolecules, Colloids Surfaces B Biointerfaces. 27 (2003) 159–168. doi:10.1016/S0927-7765(02)00053-X.

[33] J. Hao, X. Fang, Y. Zhou, J. Wang, F. Guo, F. Li, X. Peng, Development and optimization of solid lipid nanoparticle formulation for ophthalmic delivery of chloramphenicol using a Box-Behnken design., Int. J. Nanomedicine. 6 (2011) 683–692. doi:10.2147/IJN.S17386.

[34] R.C. Nagarwal, S. Kant, P.N. Singh, P. Maiti, J.K. Pandit, Polymeric nanoparticulate system: a potential approach for ocular drug delivery., J. Control. Release. 136 (2009) 2–13. doi:10.1016/j.jconrel.2008.12.018.

[35] E. Basaran, M. Demirel, B. Sirmagul, Y. Yazan, Cyclosporine-A incorporated cationic solid lipid nanoparticles for ocular delivery., J. Microencapsul. 27 (2010) 37–47. doi:10.3109/02652040902846883.

[36] S.G. Potta, S. Minemi, R.K. Nukala, C. Peinado, D.A. Lamprou, A. Urquhart, D. Douroumis, Development of solid lipid nanoparticles for enhanced solubility of poorly soluble drugs., J. Biomed. Nanotechnol. 6 (2010) 634–640.

[37] A. Leonardi, C. Bucolo, F. Drago, S. Salomone, R. Pignatello, Cationic solid lipid nanoparticles enhance ocular hypotensive effect of melatonin in rabbit, Int. J. Pharm. 478 (2015) 180–186. doi:10.1016/j.ijpharm.2014.11.032.

[38] J.F. Fangueiro, T. Andreani, L. Fernandes, M.L. Garcia, M.A. Egea, A.M. Silva, E.B. Souto, Physicochemical characterization of epigallocatechin gallate lipid nanoparticles (EGCG-LNs) for ocular instillation., Colloids Surf. B. Biointerfaces. 123 (2014) 452–460. doi:10.1016/j.colsurfb.2014.09.042.

[39] T. Fu, J. Yi, S. Lv, B. Zhang, Ocular amphotericin B delivery by chitosan-modified nanostructured lipid carriers for fungal keratitis-targeted therapy., J. Liposome Res. (2016) 1–6. doi:10.1080/08982104.2016.1224899.

[40] F. Wang, L. Chen, D. Zhang, S. Jiang, K. Shi, Y. Huang, R. Li, Q. Xu, Methazolamide-loaded solid lipid nanoparticles modified with low-molecular weight chitosan for the treatment of glaucoma: vitro and vivo study., J. Drug Target. 22 (2014) 849–858. doi:10.3109/1061186X.2014.939983.

[41] K. Baba, Y. Tanaka, A. Kubota, H. Kasai, S. Yokokura, H. Nakanishi, K. Nishida, A method for enhancing the ocular penetration of eye drops using nanoparticles of hydrolyzable dye, J. Control. Release. 153 (2011) 278–287. doi:10.1016/j.jconrel.2011.04.019.

[42] J. Jiao, Polyoxyethylated nonionic surfactants and their applications in topical ocular drug delivery, Adv. Drug Deliv. Rev. 60 (2008) 1663–1673. doi:10.1016/j.addr.2008.09.002.

[43] X. Li, S. Nie, J. Kong, N. Li, C. Ju, W. Pan, A controlled-release ocular delivery system for ibuprofen based on nanostructured lipid carriers., Int. J. Pharm. 363 (2008) 177–182. doi:10.1016/j.ijpharm.2008.07.017.

[44] U.B. Kompella, S. Sundaram, S. Raghava, E.R. Escobar, Luteinizing hormone-releasing hormone agonist and transferrin functionalizations enhance nanoparticle delivery in a novel bovine ex vivo eye model., Mol. Vis. 12 (2006) 1185–98. http://www.ncbi.nlm.nih.gov/pubmed/17102798.

[45] W.-L.L. Suen, Y. Chau, Specific uptake of folate-decorated triamcinolone-encapsulating nanoparticles by retinal pigment epithelium cells enhances and prolongs antiangiogenic activity., J. Control. Release. 167 (2013) 21–28. doi:10.1016/j.jconrel.2013.01.004.

[46] D. Delgado, A. del Pozo-Rodriguez, M.A. Solinis, M. Aviles-Triqueros, B.H.F. Weber, E. Fernandez, A.R. Gascon, Dextran and protamine-based solid lipid nanoparticles as potential vectors for the treatment of X-linked juvenile retinoschisis., Hum. Gene Ther. 23 (2012) 345–355. doi:10.1089/hum.2011.115.

[47] W. Mehnert, K. Mader, Solid lipid nanoparticles: production, characterization and applications., Adv. Drug Deliv. Rev. 47 (2001) 165–196.

[48] N. Üstündağ-Okur, E.H. Gökçe, D.İ. Bozbıyık, S. Eğrilmez, Ö. Özer, G. Ertan, Preparation and in vitro–in vivo evaluation of ofloxacin loaded ophthalmic nano structured lipid carriers modified with chitosan oligosaccharide lactate for the treatment of bacterial keratitis, Eur. J. Pharm. Sci. 63 (2014) 204–215. doi:10.1016/j.ejps.2014.07.013.

[49] S. Kakkar, S.M. Karuppayil, J.S. Raut, F. Giansanti, L. Papucci, N. Schiavone, I.P. Kaur, Lipid-polyethylene glycol based nano-ocular formulation of ketoconazole., Int. J. Pharm. 495 (2015) 276–289. doi:10.1016/j.ijpharm.2015.08.088.

[50] E. Gonzalez-Mira, M.A. Egea, E.B. Souto, A.C. Calpena, M.L. García, Optimizing flurbiprofen-loaded NLC by central composite factorial design for ocular delivery, Nanotechnology. 22 (2011) 045101. doi:10.1088/0957-4484/22/4/045101.

[51] A. del Pozo-Rodríguez, D. Delgado, M.A. Solinís, A.R. Gascón, J.L. Pedraz, Solid lipid nanoparticles for retinal gene therapy: Transfection and intracellular trafficking in RPE cells, Int. J. Pharm. 360 (2008) 177–183. doi:10.1016/j.ijpharm.2008.04.023.

[52] A. Seyfoddin, T. Sherwin, D. Patel, C. McGhee, I. Rupenthal, J. Taylor, R. Al-Kassas, Ex vivo and In vivo Evaluation of Chitosan Coated Nanostructured Lipid Carriers for Ocular Delivery of Acyclovir, Curr. Drug Deliv. 13 (2016) 923–934. doi:10.2174/1567201813666151116142752.

[53] A. Khare, I. Singh, P. Pawar, K. Grover, Design and Evaluation of Voriconazole Loaded Solid Lipid Nanoparticles for Ophthalmic Application, J. Drug Deliv. 2016 (2016) 1–11. doi:10.1155/2016/6590361.

[54] C. Yousry, R.H. Fahmy, T. Essam, H.M. El-Laithy, S.A. Elkheshen, Nanoparticles as tool for enhanced ophthalmic delivery of vancomycin: a multidistrict-based microbiological study, solid lipid nanoparticles formulation and evaluation., Drug Dev. Ind. Pharm. 42 (2016) 1752–1762. doi:10.3109/03639045.2016.1171335.

[55] A. Leonardi, L. Crasci', A. Panico, R. Pignatello, Antioxidant activity of idebenone-loaded neutral and cationic solid-lipid nanoparticles., Pharm. Dev. Technol. 20 (2015) 716–723. doi:10.3109/10837450.2014.915572.

[56] A. Pensado, B. Seijo, A. Sanchez, Current strategies for DNA therapy based on lipid nanocarriers., Expert Opin. Drug Deliv. 11 (2014) 1721–1731. doi:10.1517/17425247.2014.935337.

[57] A. del Pozo-Rodriguez, D. Delgado, A.R. Gascon, M. Angeles Solinis, Lipid Nanoparticles as Drug/Gene Delivery Systems to the Retina, J. Ocul. Pharmacol. Ther. 29 (2013) 173–188. doi:10.1089/jop.2012.0128.

[58] R.H. Muller, R. Shegokar, C.M. Keck, 20 years of lipid nanoparticles (SLN and NLC): present state of development and industrial applications., Curr. Drug Discov. Technol. 8 (2011) 207–227.

[59] R. Lander, W. Manger, M. Scouloudis, A. Ku, C. Davis, A. Lee, Gaulin homogenization: a mechanistic study., Biotechnol. Prog. 16 (2000) 80–85. doi:10.1021/bp990135c.

[60] B. Sjöström, B. Bergenståhl, Preparation of submicron drug particles in lecithin-stabilized o/w emulsions I. Model studies of the precipitation of cholesteryl acetate, Int. J. Pharm. 88 (1992) 53–62. doi:10.1016/0378-5173(92)90303-J.

[61] B. Siekmann, K. Westesen, Investigations on solid lipid nanoparticles prepared by precipitation in o/w emulsions, Eur. J. Pharm. Biopharm. 42 (1996) 104–109.

[62] E. Marengo, R. Cavalli, O. Caputo, L. Rodriguez, M.R. Gasco, Scale-up of the preparation process of solid lipid nanospheres. Part I., Int. J. Pharm. 205 (2000) 3–13.

[63] M.J. Ansari, M.K. Anwer, S. Jamil, R. Al-Shdefat, B.E. Ali, M.M. Ahmad, M.N. Ansari, Enhanced oral bioavailability of insulin-loaded solid lipid nanoparticles: pharmacokinetic bioavailability of insulin-loaded solid lipid nanoparticles in diabetic rats, DRUG Deliv. 23 (2016) 1972–1979. doi:10.3109/10717544.2015.1039666.

[64] X. Qi, L. Wang, J. Zhu, Water-In-Oil-In-Water Double Emulsions: An Excellent

Delivery System for Improving the Oral Bioavailability of Pidotimod in Rats, J. Pharm. Sci. 100 (2011) 2203–2211. doi:10.1002/jps.22443.

[65] S.-I. Ahn, Y.-K. Lee, H.-S. Kwak, Optimization of water-in-oil-in-water microencapsulated beta-galactosidase by response surface methodology, J. Microencapsul. 30 (2013) 460–469. doi:10.3109/02652048.2012.752534.

[66] A. Seyfoddin, R. Al-Kassas, Development of solid lipid nanoparticles and nanostructured lipid carriers for improving ocular delivery of acyclovir., Drug Dev. Ind. Pharm. 39 (2013) 508–519. doi:10.3109/03639045.2012.665460.

[67] R. Kumar, V.R. Sinha, Solid lipid nanoparticle: an efficient carrier for improved ocular permeation of voriconazole., Drug Dev. Ind. Pharm. 42 (2016) 1956–1967. doi:10.1080/03639045.2016.1185437.

[68] M.S. Baig, A. Ahad, M. Aslam, S.S. Imam, M. Aqil, A. Ali, Application of Box-Behnken design for preparation of levofloxacin-loaded stearic acid solid lipid nanoparticles for ocular delivery: Optimization, in vitro release, ocular tolerance, and antibacterial activity., Int. J. Biol. Macromol. 85 (2016) 258–270. doi:10.1016/j.ijbiomac.2015.12.077.

[69] R. Liu, Z. Liu, C. Zhang, B. Zhang, Nanostructured lipid carriers as novel ophthalmic delivery system for mangiferin: improving in vivo ocular bioavailability., J. Pharm. Sci. 101 (2012) 3833–3844. doi:10.1002/jps.23251.

[70] J.F. Fangueiro, A.C. Calpena, B. Clares, T. Andreani, M.A. Egea, F.J. Veiga, M.L. Garcia, A.M. Silva, E.B. Souto, Biopharmaceutical evaluation of epigallocatechin gallate-loaded cationic lipid nanoparticles (EGCG-LNs): In vivo, in vitro and ex vivo studies, Int. J. Pharm. 502 (2016) 161–169. doi:10.1016/j.ijpharm.2016.02.039.

[71] R. Cavalli, M.R. Gasco, P. Chetoni, S. Burgalassi, M.F. Saettone, Solid lipid nanoparticles (SLN) as ocular delivery system for tobramycin., Int. J. Pharm. 238 (2002) 241–245.

[72] E.H. Gokce, G. Sandri, M.C. Bonferoni, S. Rossi, F. Ferrari, T. Güneri, C. Caramella, Cyclosporine A loaded SLNs: Evaluation of cellular uptake and corneal cytotoxicity, Int. J. Pharm. 364 (2008) 76–86. doi:10.1016/j.ijpharm.2008.07.028.

[73] A.A. Attama, S. Reichl, C.C. Muller-Goymann, Sustained release and permeation of timolol from surface-modified solid lipid nanoparticles through bioengineered human cornea., Curr. Eye Res. 34 (2009) 698–705.

[74] Q. Luo, J. Zhao, X. Zhang, W. Pan, Nanostructured lipid carrier (NLC) coated with Chitosan Oligosaccharides and its potential use in ocular drug delivery system., Int. J. Pharm. 403 (2011) 185–191. doi:10.1016/j.ijpharm.2010.10.013.

[75] K. Westesen, H. Bunjes, Do nanoparticles prepared from lipids solid at room temperature always possess a solid lipid matrix?, Int. J. Pharm. 115 (1995) 129–131. doi:http://dx.doi.org/10.1016/0378-5173(94)00347-8.

[76] H. Bunjes, K. Westesen, M.H.J. Koch, Crystallization tendency and polymorphic transitions in triglyceride nanoparticles, Int. J. Pharm. 129 (1996) 159–173. doi:10.1016/0378-5173(95)04286-5.

[77] M.A. Kalam, Y. Sultana, A. Ali, M. Aqil, A.K. Mishra, K. Chuttani, Preparation, characterization, and evaluation of gatifloxacin loaded solid lipid nanoparticles as colloidal ocular drug delivery system., J. Drug Target. 18 (2010) 191–204. doi:10.3109/10611860903338462.

[78] D. Pandurangan, P. Bodagala, V. Palanirajan, S. Govindaraj, Formulation and evaluation of voriconazole ophthalmic solid lipid nanoparticles in situ gel, Int. J. Pharm. Investig. 6 (2016) 56. doi:10.4103/2230-973X.176488.

[79] V. Jenning, S. Gohla, Comparison of wax and glyceride solid lipid nanoparticles (SLN®), Int. J. Pharm. 196 (2000) 219–222. doi:http://dx.doi.org/10.1016/S0378-5173(99)00426-3.

[80] D. Patel, S. Dasgupta, S. Dey, Y.R. Ramani, S. Ray, B. Mazumder, Nanostructured Lipid Carriers (NLC)-Based Gel for the Topical Delivery of Aceclofenac: Preparation, Characterization, and In Vivo Evaluation., Sci. Pharm. 80 (2012) 749–764. doi:10.3797/scipharm.1202-12.

[81] J. Araújo, E. Gonzalez-Mira, M.A. Egea, M.L. Garcia, E.B. Souto, Optimization and physicochemical characterization of a triamcinolone acetonide-loaded NLC for ocular antiangiogenic applications, Int. J. Pharm. 393 (2010) 168–176. doi:10.1016/j.ijpharm.2010.03.034.

[82] W. Pan, W. Zhang, X. Li, T. Ye, F. Chen, S. Yu, J. Chen, X. Yang, N. Yang, J. Zhang, J. Liu, J. Kong, Nanostructured lipid carrier surface modified with Eudragit RS 100 and its potential ophthalmic functions, Int. J. Nanomedicine. 9 (2014) 4305. doi:10.2147/IJN.S63414.

[83] P.S. Apaolaza, D. Delgado, A. del Pozo-Rodriguez, A.R. Gascon, M.A. Solinis, A novel gene therapy vector based on hyaluronic acid and solid lipid nanoparticles for ocular diseases., Int. J. Pharm. 465 (2014) 413–426.

doi:10.1016/j.ijpharm.2014.02.038.

[84] M.R. Gasco, Lipid nanoparticles as vehicles for nucleic acids, process for their preparation and use, US 20080206341 A1, 2008. https://www.google.com/patents/WO2005120469A1?cl=enAn.

[85] F. Lallemand, P. Daull, S. Benita, R. Buggage, J.-S. Garrigue, Successfully improving ocular drug delivery using the cationic nanoemulsion, novasorb., J. Drug Deliv. 2012 (2012) 604204. doi:10.1155/2012/604204.

[86] C. Olbrich, N. Scholer, K. Tabatt, O. Kayser, R.H. Muller, Cytotoxicity studies of Dynasan 114 solid lipid nanoparticles (SLN) on RAW 264.7 macrophages-impact of phagocytosis on viability and cytokine production., J. Pharm. Pharmacol. 56 (2004) 883–891. doi:10.1211/0022357023754.

[87] R. Shah, D. Eldridge, E. Palombo, I. Harding, Lipid Nanoparticles: Production, Characterization and Stability, in: SpringerBriefs Pharm. Sci. Drug Dev., Springer, 2015: pp. 75–97. doi:10.1007/978-3-319-10711-0_5.

[88] A. Pensado, I. Fernandez-Piñeiro, B. Seijo, A. Sanchez, Anionic nanoparticles based on Span 80 as low-cost, simple and efficient non-viral gene-transfection systems, Int. J. Pharm. 476 (2014) 23–30. doi:10.1016/j.ijpharm.2014.09.032.

[89] A.K. Zimmer, P. Chetoni, M.F. Saettone, H. Zerbe, J. Kreuter, Evaluation of pilocarpine-loaded albumin particles as controlled drug delivery systems for the eye. II. Co-administration with bioadhesive and viscous polymers, J. Control. Release. 33 (1995) 31–46. doi:10.1016/0168-3659(94)00059-4.

[90] H. Almeida, P. Lobao, C. Frigerio, J. Fonseca, R. Silva, P. Quaresma, J.M. Sousa Lobo, M.H. Amaral, Development of mucoadhesive and thermosensitive eyedrops to improve the ophthalmic bioavailability of ibuprofen, J. Drug Deliv. Sci. Technol. 35 (2016) 69–80. doi:10.1016/j.epsr.2016.04.010.

[91] D. Liu, J. Li, H. Pan, F. He, Z. Liu, Q. Wu, C. Bai, S. Yu, X. Yang, Potential advantages of a novel chitosan-N-acetylcysteine surface modified nanostructured lipid carrier on the performance of ophthalmic delivery of curcumin, Sci. Rep. 6 (2016). doi:10.1038/srep28796.

[92] N. Li, C. Zhuang, M. Wang, X. Sun, S. Nie, W. Pan, Liposome coated with low molecular weight chitosan and its potential use in ocular drug delivery, Int. J. Pharm. 379 (2009) 131–138. doi:http://dx.doi.org/10.1016/j.ijpharm.2009.06.020.

[93] D. Vllasaliu, R. Exposito-Harris, A. Heras, L. Casettari, M. Garnett, L. Illum, S.

Stolnik, Tight junction modulation by chitosan nanoparticles: comparison with chitosan solution., Int. J. Pharm. 400 (2010) 183–193. doi:10.1016/j.ijpharm.2010.08.020.

[94] X. Xu, A.K. Jha, D.A. Harrington, M.C. Farach-Carson, X. Jia, Hyaluronic Acid-Based Hydrogels: from a Natural Polysaccharide to Complex Networks., Soft Matter. 8 (2012) 3280–3294. doi:10.1039/C2SM06463D.

[95] S.N. Zhu, B. Nolle, G. Duncker, Expression of adhesion molecule CD44 on human corneas., Br. J. Ophthalmol. 81 (1997) 80–84.

[96] L. Contreras-Ruiz, M. de la Fuente, J.E. Párraga, A. López-García, I. Fernández, B. Seijo, A. Sánchez, M. Calonge, Y. Diebold, Intracellular trafficking of hyaluronic acid-chitosan oligomer-based nanoparticles in cultured human ocular surface cells., Mol. Vis. 17 (2011) 279–90. http://www.ncbi.nlm.nih.gov/pubmed/21283563.

[97] M. Ruponen, S. Ronkko, P. Honkakoski, J. Pelkonen, M. Tammi, A. Urtti, Extracellular glycosaminoglycans modify cellular trafficking of lipoplexes and polyplexes., J. Biol. Chem. 276 (2001) 33875–33880. doi:10.1074/jbc.M011553200.

[98] S. Mizrahy, S.R. Raz, M. Hasgaard, H. Liu, N. Soffer-Tsur, K. Cohen, R. Dvash, D. Landsman-Milo, M.G.E.G. Bremer, S.M. Moghimi, D. Peer, Hyaluronan-coated nanoparticles: the influence of the molecular weight on CD44-hyaluronan interactions and on the immune response., J. Control. Release. 156 (2011) 231–238. doi:10.1016/j.jconrel.2011.06.031.

[99] A.M. Durrani, S.J. Farr, I.W. Kellaway, Influence of molecular weight and formulation pH on the precorneal clearance rate of hyaluronic acid in the rabbit eye, Int. J. Pharm. 118 (1995) 243–250. doi:http://dx.doi.org/10.1016/0378-5173(94)00389-M.

[100] J.S. Suk, Q. Xu, N. Kim, J. Hanes, L.M. Ensign, PEGylation as a strategy for improving nanoparticle-based drug and gene delivery., Adv. Drug Deliv. Rev. 99 (2016) 28–51. doi:10.1016/j.addr.2015.09.012.

[101] J.-Q. Su, Z. Wen, Y.-A. Wen, W.-N. Xiao, J. Lin, Z.-K. Zheng, Modification and stabilizing effects of PEG on resveratrol-loaded solid lipid nanoparticles, J. Iran. Chem. Soc. 13 (2016) 881–890. doi:10.1007/s13738-015-0803-9.

[102] M. Garcia-Fuentes, C. Prego, D. Torres, M.J. Alonso, A comparative study of the potential of solid triglyceride nanostructures coated with chitosan or

poly(ethylene glycol) as carriers for oral calcitonin delivery., Eur. J. Pharm. Sci. 25 (2005) 133–143. doi:10.1016/j.ejps.2005.02.008.

[103] S.K. Lai, Y.-Y. Wang, J. Hanes, Mucus-penetrating nanoparticles for drug and gene delivery to mucosal tissues, Adv. Drug Deliv. Rev. 61 (2009) 158–171. doi:http://dx.doi.org/10.1016/j.addr.2008.11.002.

[104] A. De Campos, The effect of a PEG versus a chitosan coating on the interaction of drug colloidal carriers with the ocular mucosa, Eur. J. Pharm. Sci. 20 (2003) 73–81. doi:10.1016/S0928-0987(03)00178-7.

[105] Z. Zhang, S. Tan, S.-S. Feng, Vitamin E TPGS as a molecular biomaterial for drug delivery, Biomaterials. 33 (2012) 4889–4906. doi:10.1016/j.biomaterials.2012.03.046.

[106] C. Olbrich, R.H. Muller, Enzymatic degradation of SLN-effect of surfactant and surfactant mixtures., Int. J. Pharm. 180 (1999) 31–39.

[107] A. LUDWIG, The use of mucoadhesive polymers in ocular drug delivery, Adv. Drug Deliv. Rev. 57 (2005) 1595–1639. doi:10.1016/j.addr.2005.07.005.

[108] J. Li, D. Liu, G. Tan, Z. Zhao, X. Yang, W. Pan, A comparative study on the efficiency of chitosan-N-acetylcysteine, chitosan oligosaccharides or carboxymethyl chitosan surface modified nanostructured lipid carrier for ophthalmic delivery of curcumin, Carbohydr. Polym. 146 (2016) 435–444. doi:http://dx.doi.org/10.1016/j.carbpol.2016.03.079.

[109] J. Shen, Y. Wang, Q. Ping, Y. Xiao, X. Huang, Mucoadhesive effect of thiolated PEG stearate and its modified NLC for ocular drug delivery., J. Control. Release. 137 (2009) 217–223. doi:10.1016/j.jconrel.2009.04.021.

[110] S.K. Sahoo, F. Dilnawaz, S. Krishnakumar, Nanotechnology in ocular drug delivery, Drug Discov. Today. 13 (2008) 144–151. doi:http://dx.doi.org/10.1016/j.drudis.2007.10.021.

[111] J.-H. Park, H. Jeong, J. Hong, M. Chang, M. Kim, R.S. Chuck, J.K. Lee, C.-Y. Park, The Effect of Silica Nanoparticles on Human Corneal Epithelial Cells, Sci. Rep. 6 (2016) 37762. http://dx.doi.org/10.1038/srep37762.

[112] B. Heurtault, P. Saulnier, B. Pech, J.-E. Proust, J.-P. Benoit, Physico-chemical stability of colloidal lipid particles, Biomaterials. 24 (2003) 4283–4300. doi:http://dx.doi.org/10.1016/S0142-9612(03)00331-4.

[113] J. Shen, M. Sun, Q. Ping, Z. Ying, W. Liu, Incorporation of liquid lipid in lipid nanoparticles for ocular drug delivery enhancement., Nanotechnology. 21 (2010)

25101. doi:10.1088/0957-4484/21/2/025101.

[114] R. Cavalli, O. Caputo, E. Marengo, F. Pattarino, M.R. Gasco, The effect of the components of microemulsions on both size and crystalline structure of solid lipid nanoparticles (SLN) containing a series of model molecules, PHARMAZIE. 53 (1998) 392–396.

[115] A.B. Kovačević, R.H. Müller, S.D. Savić, G.M. Vuleta, C.M. Keck, Solid lipid nanoparticles (SLN) stabilized with polyhydroxy surfactants: Preparation, characterization and physical stability investigation, Colloids Surfaces A Physicochem. Eng. Asp. 444 (2014) 15–25. doi:http://dx.doi.org/10.1016/j.colsurfa.2013.12.023.

[116] Z. Urban-Morlan, A. Ganem-Rondero, L.M. Melgoza-Contreras, J.J. Escobar-Chavez, M.G. Nava-Arzaluz, D. Quintanar-Guerrero, Preparation and characterization of solid lipid nanoparticles containing cyclosporine by the emulsification-diffusion method., Int. J. Nanomedicine. 5 (2010) 611–620. doi:10.2147/IJN.S12125.

[117] K.S. Chu, A.N. Schorzman, M.C. Finniss, C.J. Bowerman, L. Peng, J.C. Luft, A.J. Madden, A.Z. Wang, W.C. Zamboni, J.M. DeSimone, Nanoparticle drug loading as a design parameter to improve docetaxel pharmacokinetics and efficacy., Biomaterials. 34 (2013) 8424–8429. doi:10.1016/j.biomaterials.2013.07.038.

[118] M. Uner, G. Yener, Importance of solid lipid nanoparticles (SLN) in various administration routes and future perspectives., Int. J. Nanomedicine. 2 (2007) 289–300.

[119] J. Shen, Y. Deng, X. Jin, Q. Ping, Z. Su, L. Li, Thiolated nanostructured lipid carriers as a potential ocular drug delivery system for cyclosporine A: Improving in vivo ocular distribution, Int. J. Pharm. 402 (2010) 248–253. doi:10.1016/j.ijpharm.2010.10.008.

[120] H.A. Ebrahimi, Y. Javadzadeh, M. Hamidi, M.B. Jalali, Repaglinide-loaded solid lipid nanoparticles: effect of using different surfactants/stabilizers on physicochemical properties of nanoparticles., Daru. 23 (2015) 46. doi:10.1186/s40199-015-0128-3.

[121] K. Karn-Orachai, S.M. Smith, S. Saesoo, A. Treethong, S. Puttipipatkhachorn, S. Pratontep, U.R. Ruktanonchai, Surfactant effect on the physicochemical characteristics of gamma-oryanol-containing solid lipid nanoparticles,

COLLOIDS SURFACES A-PHYSICOCHEMICAL Eng. Asp. 488 (2016) 118–128. doi:10.1016/j.colsurfa.2015.10.011.

[122] P. Blasi, A. Schoubben, G.V. Romano, S. Giovagnoli, A. Di Michele, M. Ricci, Lipid nanoparticles for brain targeting II. Technological characterization, Colloids Surfaces B Biointerfaces. 110 (2013) 130–137. doi:10.1016/j.colsurfb.2013.04.021.

[123] S. Soares, P. Fonte, A. Costa, J. Andrade, V. Seabra, D. Ferreira, S. Reis, B. Sarmento, Effect of freeze-drying, cryoprotectants and storage conditions on the stability of secondary structure of insulin-loaded solid lipid nanoparticles., Int. J. Pharm. 456 (2013) 370–381. doi:10.1016/j.ijpharm.2013.08.076.

[124] H. Yuan, C.-Y. Chen, G.-H. Chai, Y.-Z. Du, F.-Q. Hu, Improved transport and absorption through gastrointestinal tract by PEGylated solid lipid nanoparticles., Mol. Pharm. 10 (2013) 1865–1873. doi:10.1021/mp300649z.

[125] E. Mahon, A. Salvati, F. Baldelli Bombelli, I. Lynch, K.A. Dawson, Designing the nanoparticle-biomolecule interface for "targeting and therapeutic delivery"., J. Control. Release. 161 (2012) 164–174. doi:10.1016/j.jconrel.2012.04.009.

[126] A.M. de Campos, Y. Diebold, E.L.S. Carvalho, A. Sanchez, M.J. Alonso, Chitosan nanoparticles as new ocular drug delivery systems: in vitro stability, in vivo fate, and cellular toxicity., Pharm. Res. 21 (2004) 803–810.

[127] M.R. Jafari, A.B. Jones, A.H. Hikal, J.S. Williamson, C.M. Wyandt, Characterization of drug release from liposomal formulations in ocular fluid., Drug Deliv. 5 (1998) 227–238. doi:10.3109/10717549809065752.

[128] M.S. Norn, Tear fluid pH in normals, contact lens wearers, and pathological cases., Acta Ophthalmol. 66 (1988) 485–9. http://www.ncbi.nlm.nih.gov/pubmed/3218470.

[129] M. Yamada, M. Kawai, H. Mochizuki, Y. Hata, Y. Mashima, Fluorophotometric measurement of the buffering action of human tears in vivo., Curr. Eye Res. 17 (1998) 1005–1009.

[130] N. Bodor, P. Buchwald, Ophthalmic drug design based on the metabolic activity of the eye: Soft drugs and chemical delivery systems, AAPS J. 7 (2005) E820–E833. doi:10.1208/aapsj070479.

[131] M. Vicario-de-la-Torre, J.M. Benítez-del-Castillo, E. Vico, M. Guzmán, B. de-las-Heras, R. Herrero-Vanrell, I.T. Molina-Martínez, Design and Characterization of an Ocular Topical Liposomal Preparation to Replenish the

Lipids of the Tear FilmOcular Topical Liposomal Preparation, Invest. Ophthalmol. Vis. Sci. 55 (2014) 7839. doi:10.1167/iovs.14-14700.

[132] E. Gonzalez-Mira, S. Nikolic, A.C. Calpena, M. Antonia Egea, E.B. Souto, M. Luisa Garcia, Improved and safe transcorneal delivery of flurbiprofen by NLC and NLC-based hydrogels, J. Pharm. Sci. 101 (2012) 707–725. doi:10.1002/jps.22784.

[133] T.F. Patton, J.R. Robinson, Ocular evaluation of polyvinyl alcohol vehicle in rabbits., J. Pharm. Sci. 64 (1975) 1312–1316.

[134] S. Doktorovova, E.B. Souto, A.M. Silva, Nanotoxicology applied to solid lipid nanoparticles and nanostructured lipid carriers - a systematic review of in vitro data., Eur. J. Pharm. Biopharm. 87 (2014) 1–18. doi:10.1016/j.ejpb.2014.02.005.

[135] A. Leonardi, C. Bucolo, G.L. Romano, C.B.M. Platania, F. Drago, G. Puglisi, R. Pignatello, Influence of different surfactants on the technological properties and in vivo ocular tolerability of lipid nanoparticles., Int. J. Pharm. 470 (2014) 133–140. doi:10.1016/j.ijpharm.2014.04.061.

[136] D.A. Ammar, R.J. Noecker, M.Y. Kahook, Effects of benzalkonium chloride-preserved, polyquad-preserved, and sofZia-preserved topical glaucoma medications on human ocular epithelial cells, Adv. Ther. 27 (2010) 837–845. doi:10.1007/s12325-010-0070-1.

[137] M. Sznitowska, S. Janicki, E.A. Dabrowska, M. Gajewska, Physicochemical screening of antimicrobial agents as potential preservatives for submicron emulsions., Eur. J. Pharm. Sci. 15 (2002) 489–95. http://www.ncbi.nlm.nih.gov/pubmed/12036725.

[138] F. Lallemand, O. Felt-Baeyens, K. Besseghir, F. Behar-Cohen, R. Gurny, Cyclosporine A delivery to the eye: a pharmaceutical challenge., Eur. J. Pharm. Biopharm. 56 (2003) 307–318.

[139] S.D. Mithani, V. Bakatselou, C.N. TenHoor, J.B. Dressman, Estimation of the increase in solubility of drugs as a function of bile salt concentration., Pharm. Res. 13 (1996) 163–167.

[140] P. Ames, A. Galor, Cyclosporine ophthalmic emulsions for the treatment of dry eye: a review of the clinical evidence, Clin. Investig. (Lond). 5 (2015) 267–285. doi:10.4155/cli.14.135.

[141] D.L. Williams, A comparative approach to topical cyclosporine therapy, Eye. 11 (1997) 453–464. doi:10.1038/eye.1997.126.

[142] M. Kuwano, H. Ibuki, N. Morikawa, A. Ota, Y. Kawashima, Cyclosporine A formulation affects its ocular distribution in rabbits., Pharm. Res. 19 (2002) 108–111.

[143] P. Agarwal, I.D. Rupenthal, Modern approaches to the ocular delivery of cyclosporine A, Drug Discov. Today. 21 (2016) 977–988. doi:10.1016/j.drudis.2016.04.002.

[144] E. Sanchez-Lopez, M. Espina, S. Doktorovova, E.B. Souto, M.L. Garcia, Lipid nanoparticles (SLN, NLC): Overcoming the anatomical and physiological barriers of the eye - Part II - Ocular drug-loaded lipid nanoparticles., Eur. J. Pharm. Biopharm. 110 (2017) 58–69. doi:10.1016/j.ejpb.2016.10.013.

[145] L. Battaglia, I. D'Addino, E. Peira, M. Trotta, M. Gallarate, Solid lipid nanoparticles prepared by coacervation method as vehicles for ocular cyclosporine, J. Drug Deliv. Sci. Technol. 22 (2012) 125–130. doi:http://dx.doi.org/10.1016/S1773-2247(12)50016-X.

[146] G. Sandri, M.C. Bonferoni, E.H. Gokce, F. Ferrari, S. Rossi, M. Patrini, C. Caramella, Chitosan-associated SLN: in vitro and ex vivo characterization of cyclosporine A loaded ophthalmic systems., J. Microencapsul. 27 (2010) 735–746. doi:10.3109/02652048.2010.517854.

Web references:

[147] Dale S. Aldrich, Cynthia M. Bach, William Brown, Wiley Chambers, Jeffrey Fleitman, Desmond Hunt, Margareth R. C. Marques, Yana Mille, Ashim K. Mitra, Stacey M. latzer, Tom Tice, George W. Tin, 2013. Ophthalmic Preparations. US Pharmacopeial Convention.

Recovered from:

*http://www.usp.org/sites/default/files/usp_pdf/EN/meetings/workshops/ophthalmi preparations.pdf (accessed 29.05.17)*

USC
UNIVERSIDADE
DE SANTIAGO
DE COMPOSTELA



In this work, we developed a new nanoparticle-based therapeutic strategy for the treatment of ocular surface diseases. Two types of sorbitan ester nanoparticles (SENS) for topical ocular administration, including a cationic nanosystem and its hyaluronic acid-coated version, were developed and optimized. Both types of nanoparticles were physicochemically characterized and evaluated in terms of biocompatibility, targeting ability and therapeutic efficacy. Moreover, the therapeutic potential of developed nanoparticles to treat dry eye disease was demonstrated in an in vivo disease model.